National Library of Canada
Acquisitions and Bibliographic Services Branch
395 Wellington Street
Ottawa, Ontario
K1A 0N4

Bibliothèque nationale du Canada
Direction des acquisitions et des services bibliographiques
395, rue Wellington
Ottawa (Ontario)
K1A 0N4

Your file Votre référence

Our file Notre référence

NOTICE

The quality of this microform is heavily dependent upon the quality of the original thesis submitted for microfilming. Every effort has been made to ensure the highest quality of reproduction possible.

If pages are missing, contact the university which granted the degree.

Some pages may have indistinct print especially if the original pages were typed with a poor typewriter ribbon or if the university sent us an inferior photocopy.

Reproduction in full or in part of this microform is governed by the Canadian Copyright Act, R.S.C. 1970, c. C-30, and subsequent amendments.

AVIS

La qualité de cette microforme dépend grandement de la qualité de la thèse soumise au microfilmage. Nous avons tout fait pour assurer une qualité supérieure de reproduction.

S'il manque des pages, veuillez communiquer avec l'université qui a conféré le grade.

La qualité d'impression de certaines pages peut laisser à désirer, surtout si les pages originales ont été dactylographiées à l'aide d'un ruban usé ou si l'université nous a fait parvenir une photocopie de qualité inférieure.

La reproduction, même partielle, de cette microforme est soumise à la Loi canadienne sur le droit d'auteur, SRC 1970, c. C-30, et ses amendements subséquents.

Canada

MAGMATIC - HYDROTHERMAL SYSTEMS AND ASSOCIATED MAGNETITE-APATITE-ACTINOLITE DEPOSITS, ECHO BAY, NORTHWEST TERRITORIES

by

Nancy Catherine Reardon

A thesis submitted to the School of Graduate Studies in partial fulfillment of the requirement for the degree of Master of Science in Geology

University of Ottawa
Ottawa - Carleton Geoscience Centre
Ottawa, Canada, 1992

ISBN 0-315-82547-2

UNIVERSITÉ D'OTTAWA
UNIVERSITY OF OTTAWA

Master of Science
(Geology)

University of Ottawa
Ottawa, Ontario

TITLE: Magmatic - Hydrothermal Systems And Associated Magnetite-Apatite-Actinolite Deposits, Echo Bay, Northwest Territories

AUTHOR: Nancy Catherine Reardon

SUPERVISOR: Bruce E. Taylor

EXAMINING COMMITTEE: André E. Lalonde

Richard P. Taylor

Abstract

Magnetite-apatite-actinolite deposits occur as pervasive replacement, veins, pods and breccias within wall rocks to the plutons of the Mystery Island intrusive suite at Echo Bay, Northwest Territories. The plutons and their altered wall rocks host previously-mined pitchblende, native Ag, Ni-Co arsenide veins. Although numerous studies were carried out on the pitchblende, native Ag, Ni-Co arsenide veins, the origin of the altered rocks which host them remains uncertain.

The plutons of the Mystery Island intrusive suite intrude a complex of andesitic stratovolcanoes of the LaBine Group, within the 1.87 Ga Great Bear magmatic zone of Wopmay orogen. The plutons are compositionally heterogeneous, sheet-like bodies of intermediate composition and were emplaced at a depth of 2 to 3 km. At 1.84 Ga the stratovolcanoes and plutons were folded such that the tops and bottoms of the plutons are exposed. After 1.84 Ga, the area was cut by northeast-trending transcurrent faults and mafic dykes and sills.

All of the plutons of the Mystery Island intrusive suite are metasomatically altered. The plutons have haloes of altered wall rock characterized by three zones with characteristic mineral assemblages: 1) an inner zone of albite; 2) an intermediate zone of magnetite-apatite-actinolite; and 3) an outer zone of disseminated sulphides. Albite occurs as fine-grained crystals which replace the plutons and the wallrocks. Magnetite, apatite and actinolite occur as disseminated crystals, in veins, pods, and breccias above the plutons, and locally, within and below the plutons. Hydrothermal breccias occur locally, near pluton contacts. The pyrite zone is characterized by the presence of disseminated pyrite crystals or pods up to several centimeters in diameter which form visible rusty patches on weathered outcrop surfaces, or extensive gossans where pyrite is locally abundant. Chalcopyrite occurs locally.

Altered andesites with higher K_2O contents are enriched in Ba, Sr, Rb, Zr, and Al_2O_3 and depleted in FeO, MgO, MnO and REEs. Na-rich rocks are depleted in FeO, MgO, MnO, Ba, and Rb, and enriched in REEs. Na_2O and K_2O contents do not correlate. The plutons are both K-metasomatized and Na-metasomatized.

Whole-rock $\delta^{18}O$ and δD values of altered rocks range from +5.7 to +12.3 and -70 to -57‰, respectively, for the plutons, without apparent zoning. $\delta^{18}O$ and δD values range from +5.3 to +11.7 and -92 to -56‰, respectively, for altered andesitic lavas, cogenetic andesitic porphyries, and volcaniclastic rocks. Most $\delta^{18}O$ and δD values are higher than +6 and -70‰, respectively, consistent with alteration by magmatic fluids. Lower values suggest involvement of a minor component of evolved meteoric water, evolved seawater, or connate water. Based on stable isotopic data from whole-rock samples and mineral separates, the magnetite-apatite-actinolite (MAA) deposits formed from fluids of a dominantly magmatic origin, having $\delta^{18}O$ values of about +7.0 to +11.0‰ and δD values of -45 to -20‰.

The effects of the hydrothermal system which deposited the pitchblende, native Ag, Ni-Co arsenide-bearing veins on the isotopic composition of the altered rocks associated with the Mystery Island intrusive suite are difficult to evaluate, since fluids responsible for formation of the quartz veins may have ranged in time from lighter than, to the same as, those which formed the MAA zone alteration. However, no large-scale zoning of $\delta^{18}O$ or δD values occurs around the veins.

Overall, the formation of magnetite-apatite-actinolite veins, pervasive replacement of rocks by albite and magnetite-apatite-actinolite, and hydrothermal brecciation by magmatic fluids is consistent with geologic and isotopic data. Thus, it is inferred that these deposits formed by replacement in a hydrothermal system dominated by magmatic fluids exsolved by cooling epizonal plutons of the Mystery Island intrusive suite.

ACKNOWLEDGEMENTS

Robert Hildebrand and Bruce Taylor are thanked for initiating the project, and for their patient guidance and instruction. André Lalonde (University of Ottawa) and Richard Taylor (Carleton University) critically reviewed the thesis. John Henderson critically reviewed the map and made several suggestions to improve its content and appearance. Many thanks to the Geological Survey of Canada, especially Richard Lancaster, Guy D'Arcy, Gerry Gagnon, Ron Christie, Pat Lavergne, Robert Laramée and Steve Frewen for their assistance; Andrew Roberts performed X-ray diffraction analyses. John Sekerka is thanked for mass spectrometer analyses and many oxygen and hydrogen extractions, and Jean Louis Bouvier performed ferric/ferrous iron analyses of actinolite samples. Thanks to Gilles St. Jean and Margaret McLaren (University of Ottawa) for assistance with isotopic extractions, and mass spectrometer work. Glen Poirier (McGill University) is thanked for assistance with microprobe analyses. Stéphane Lagacé assisted in mapping in 1988 and 1989. CEGB provided use of their Beaver airplane, some great meals, and interesting dinner conversation.

Funding for field work and technical support was provided by the Geological Survey of Canada through Project 86002 (R. S. Hildebrand), and Project C1.1.5 of the Northwest Territories - Canada Mineral Development Agreement. Support for graduate studies at the University of Ottawa was provided by an NSERC research grant # OGP24815 to Bruce Taylor.

TABLE OF CONTENTS

Abstract iii
Acknowledgements v
Table of Contents vi
List of Tables viii
List of Figures ix

I. INTRODUCTION 1
Location 1
Previous work 4
Geology of the Echo Bay - Camsell River area 4
Kiruna-type deposits 7
Pitchblende, native Ag, Ni-Co arsenide vein deposits 9
Current work: objectives and methods 10

II. GEOLOGIC SETTING 13
Regional geology 13
Wopmay orogen 13
Great Bear magmatic zone 13
General geology: lithologies 14
LaBine Group 15
Port Radium Formation 15
Echo Bay Formation 18
Cameron Bay Formation 18
Mystery Island intrusive suite 19
Bertrand Lake pluton 20
McLeod Lake pluton 21
Contact Lake pluton 22
Glacier Lake pluton 23
Tut pluton 26
Richardson pluton 26
General geology: structures 27
Folds 27
Faults 27
Mineral deposits 28
Pitchblende, native Ag, Ni-Co arsenide vein deposits 28
Mineralogy and paragenesis 28
Distribution and geometry 29
Age relationships 30
Magnetite-apatite-actinolite replacement and veins 32

III. PETROGRAPHY AND GEOCHEMISTRY OF ALTERED AND MINERALIZED ROCKS 33
Albite zone 33
Magnetite-apatite-actinolite zone 36
Pyrite zone 48
Distribution of alteration 50
Bertrand Lake pluton 50
McLeod Lake pluton 54
Contact Lake pluton 54
Glacier Lake pluton 55
Tut pluton 55

Whole-rock geochemical analyses 56
Andesite 56
Plutons 63

IV. STABLE ISOTOPE GEOCHEMISTRY 70
Plutons and wall rocks 70
Oxygen and Hydrogen 70
Port Radium Formation 70
Echo Bay Formation 75
Mystery Island intrusive suite 75
Cameron Bay Formation 75
Richardson pluton 76
Carbon 76
Magnetite-apatite-actinolite zone 76
Oxygen 76
Hydrogen 78
Fluid inclusions 78
Pyrite zone 79
Sulphur 79
Quartz-carbonate veins 80
Oxygen and carbon 80
Sulphur 81
Fluid inclusions 81

V. DISCUSSION: EVIDENCE FOR A HYDROTHERMAL ORIGIN OF MAGNETITE -APATITE-ACTINOLITE DEPOSITS 89

VI. SUMMARY AND CONCLUSIONS 95

REFERENCES 98

APPENDICES:
A. Electron microprobe data 120
B. Whole-rock geochemical analyses 126
C. Stable isotope analyses 126
D. Sample descriptions and petrographic summaries 127

PLATE: Geologic map of the distribution of altered rocks associated with the Mystery Island intrusive suite in the Echo Bay area with sample locations in pocket

List of Tables

Table 1.	Schematic stratigraphic section, with descriptions, LaBine Group	16
Table 2.	Major, minor and trace element analyses: Echo Bay Formation and Mystery Island intrusive suite	57
Table 3.	Whole-rock $\delta^{18}O$, δD and water content data: LaBine Group, Mystery Island intrusive suite and Richardson pluton	71
Table 4.	$\delta^{18}O$ and δD values, and calculated isotopic fluid compositions for silicate and oxide minerals from magnetite-apatite-actinolite veins and pervasively altered rocks from the magnetite-apatite-actinolite zone	77
Table 5.	$\delta^{34}S$ of pyrite and chalcopyrite from the pyrite zone.	82
Table 6.	a) $\delta^{18}O$ and $\delta^{13}C$ of calcite and siderite from quartz-carbonate-sulphide veins; b) $\delta^{34}S$ of chalcopyrite from quartz-carbonate-sulphide veins	83

List of Figures

Figure 1. General geology of the northwestern Canadian Shield. 2

Figure 2. Geology of the northern Great Bear magmatic zone. 3

Figure 3. General geology of the Echo Bay and Camsell River areas with mine locations. 6

Figure 4. General geology of the Echo Bay area showing the plutons of the Mystery Island intrusive suite. 11

Figure 5. Simplified geology and distribution of altered rocks in the Bertrand Lake pluton area. 17

Figure 6. Simplified geology and distribution of altered rocks in the Contact Lake pluton and northern Mcleod Lake pluton areas. 22

Figure 7. Simplified geology and distribution of altered rocks in the area of the southern portion of the Glacier Lake pluton. 24

Figure 8. Simplified geology and distribution of altered rocks in the Port Radium area, southern Tut pluton and the northern part of the Glacier Lake pluton. 25

Figure 9. Photograph of coarse albite replacing an andesitic lava flow. 34

Figure 10. Photomicrograph of an albitized andesitic lava flow. 35

Figure 11. Secondary riebeckite in the Glacier Lake pluton. 37

Figure 12. Photograph of pervasively altered volcanogenic arkose cut by actinolite-magnetite veins, Port Radium. 38

Figure 13. Paragenetic sequence of alteration minerals in veins and pervasively altered rocks from the magnetite-apatite-actinolite zone. 40

Figure 14. Euhedral actinolite and subhedral magnetite replacing albitized andesitic lava flow. 41

Figure 15. Photomicrograph of feldspar and actinolite replacing laminations in sandstone, Port Radium. 42

Figure 16. Rose diagram of strike orientations for MAA veins in the Echo Bay area. 43

Figure 17. Photomicrograph of a magnetite-apatite-actinolite vein in intrusive porphyritic andesite. 45

Figure 18. Photograph of hydrothermal breccia with magnetite matrix in intrusive porphyritic andesite, Port Radium. 46

Figure 19. Plot of Ca-Mg-Fe_{TOT} for actinolites from magnetite-apatite-actinolite veins and pervasively altered rocks in the Echo Bay area. 47

Figure 20. Histogram of TiO_2 for magnetites from magnetite-apatite-actinolite veins and pervasively altered rocks. 49

Figure 21. Photograph of a pyrite vein cutting magnetite-apatite-actinolite rock in andesitic lava flow. 51

Figure 22. Photomicrograph of pyrite growing on magnetite in a pervasively altered andesitic lava flow. 52

Figure 23. Photomicrograph of hematite replacing pyrite in a pervasively altered andesitic lava flow. 53

Figure 24. a) Plots of K_2O vs. MgO, Al_2O_3, MnO, FeO, Rb, Sr, Zr, Ba, Ce, Eu, Gd, and Dy for andesitic lava flows above the southern part of the Glacier Lake pluton. 60

Figure 24. b) Plots of Na_2O vs. MnO, FeO, Rb, Sr, Zr, Ba, Ce, Eu, Gd, and Dy for andesitic lava flows above the southern part of the Glacier Lake pluton. 62

Figure 25. Plots of a) CaO vs. SiO_2 ; b) K_2O vs. SiO_2; and c) Na_2O vs. SiO_2 for the Tut, Bertrand Lake, Glacier Lake, Contact Lake and McLeod Lake plutons. 64

Figure 26. a) Plot of Na_2O vs. K_2O for the Glacier Lake and Contact Lake plutons. 65

Figure 26. b) Plot of Na_2O vs. V, Fe_{TOT}, Cr, P_2O_5 and V vs. P_2O_5 and K_2O for the Glacier Lake and Contact Lake plutons. 66

Figure 27. a) SiO_2, K_2O and Na_2O vs. relative height in the southern part of the Glacier Lake pluton. 68

Figure 27. b) SiO_2, K_2O and Na_2O vs. relative height in the Contact Lake pluton. 69

Figure 28. Histogram of $\delta^{18}O$ data for altered andesitic lava flows, cogenetic intrusive porphyritic andesite and plutons of the Mystery Island intrusive suite. 73

Figure 29. Histogram of δD data for altered andesitic lava flows, cogenetic intrusive porphyritic andesite and plutons of the Mystery Island intrusive suite. 74

Figure 30. Plot of whole-rock values of $\delta^{18}O$ vs. δD for altered andesitic lava flows, cogenetic intrusive porphyritic andesite and plutons of the Mystery Island intrusive suite and for waters in equilibrium with these rocks. 85

Figure 31. a) Plot of $\delta^{18}O$ vs. δD for actinolites from veins, pods and pervasively altered rocks in the magnetite-apatite-actinolite zone, and for waters in equilibrium with these minerals at 300°C; b) Plot of $\delta^{18}O$ vs. δD for actinolites from veins, pods and pervasively altered rocks in the magnetite-apatite-actinolite zone, and for waters in equilibrium with these minerals at 400°C. 87

I. INTRODUCTION

The Echo Bay and Camsell River areas are best known for their rich pitchblende, native Ag, Ni-Co arsenide vein deposits. These veins occur within the alteration haloes of several sill-like plutons of intermediate composition known as the Mystery Island intrusive suite, and, in one location, within one of the plutons. Despite a large number of studies of the pitchblende, native Ag, Ni-Co arsenide veins in the Echo Bay and Camsell River areas, few workers have examined the plutons of the Mystery Island intrusive suite or their altered wall rocks and magnetite-apatite-actinolite (MAA) deposits.

Badham and Morton (1976) carried out a study of the magnetite-apatite-actinolite deposits which form part of the alteration haloes associated with plutons similar to the Mystery Island intrusive suite in the Camsell River area. They concluded that the deposits formed by the injection of immiscible iron-phosphate melts separated from a magma of intermediate composition. However, based on detailed geological, petrographical and geochemical data, Hildebrand (1986) concluded that magnetite-apatite-actinolite deposits in the Camsell River area were formed by deuteric-hydrothermal processes. A geological, petrographical, geochemical and stable isotopic study was undertaken in the Echo Bay area to determine the distribution of altered rocks, their relationship to the plutons of the Mystery Island intrusive suite, and the source of the fluids responsible for their formation. These deposits are similar to the well-known Kiruna deposits, and the results of this study may apply to Kiruna-type deposits in general.

Location

Echo Bay is located on the eastern shore of Great Bear Lake, Northwest Territories, 270 km north-northwest of Yellowknife (Figs. 1 and 2). The Echo Bay study area is within the Canadian National Topographic System map sheets 86L/1 (Echo Bay), 86K/4 (Vance

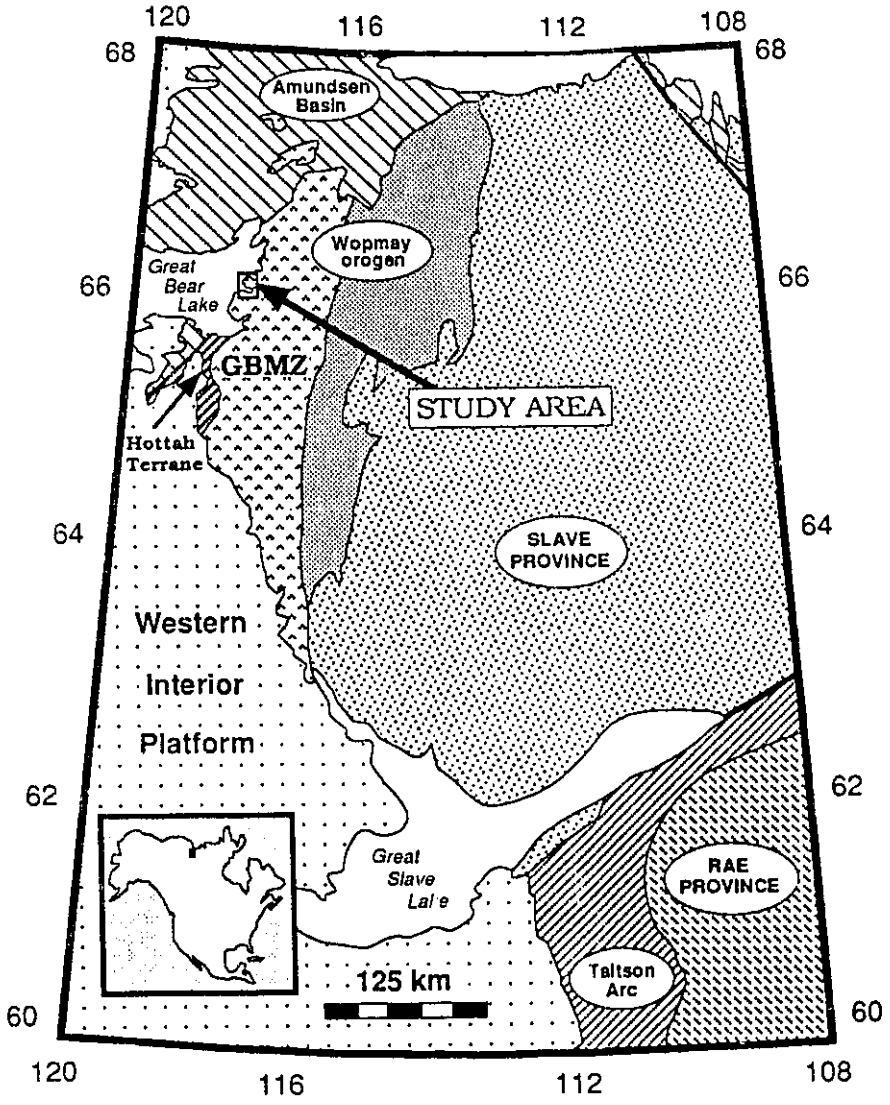

Figure 1. Generalized geology of the northwestern Canadian Shield (modified from Hoffman, 1989) showing major structural provinces and the study area of this report.

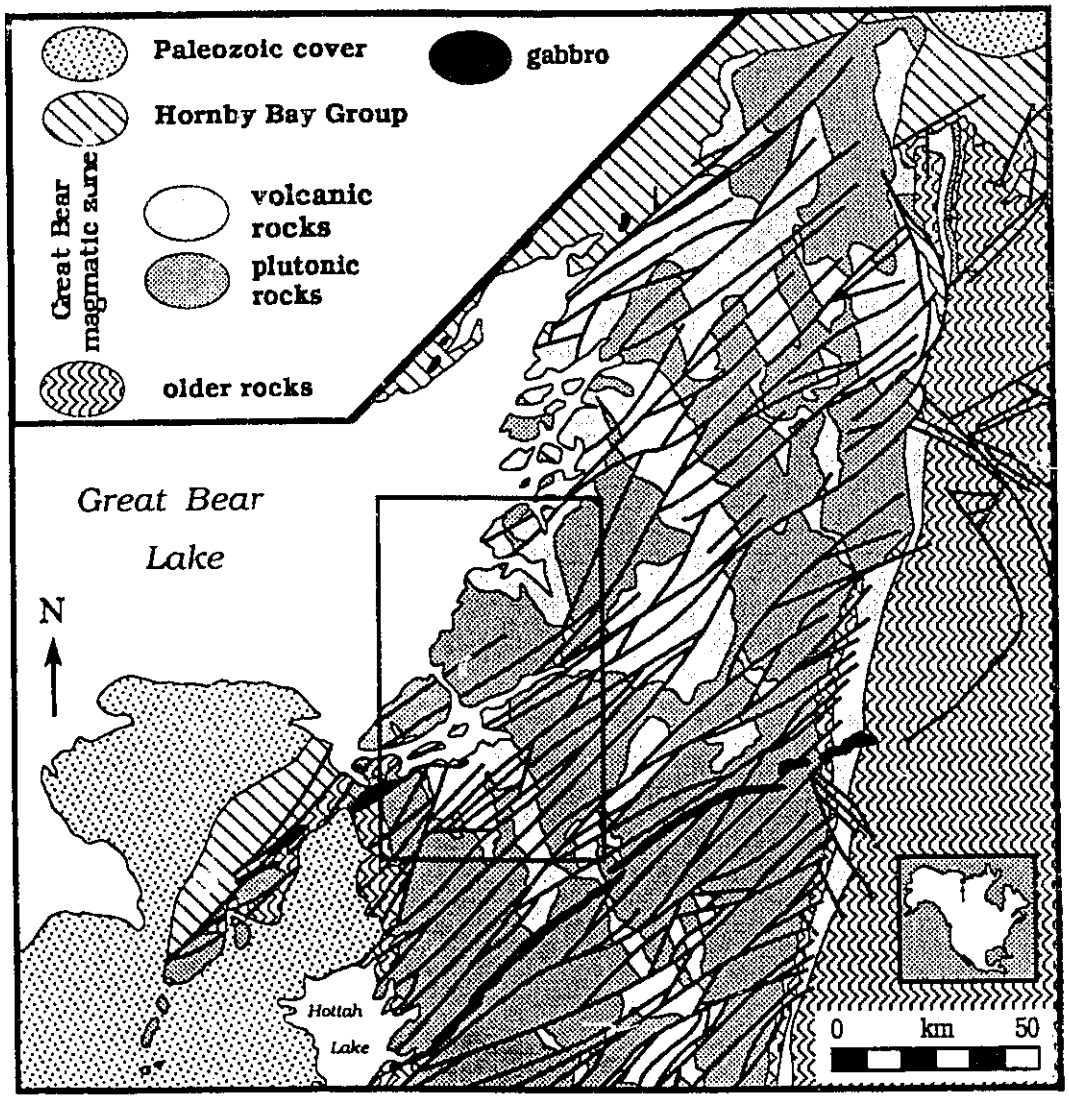

Figure 2. Geology of the northern Great Bear magmatic zone, after Hildebrand, 1986. The box outlines the area shown in Figure 3.

Peninsula), and 86F/13 (Moody Lake), and includes the abandoned townsite of Port Radium.

Previous work

Geology of the Echo Bay - Camsell River area

Evidence of mineralization in the Echo Bay area was first recorded by J.M. Bell in 1900 (Bell, 1901), who noted the presence of "*cobalt bloom and copper green stain*". In 1929, Gilbert LaBine visited Echo Bay with E.G. St. Paul and located several minor occurrences of copper, cobalt and bismuth (The Staff, Eldorado, 1946). The following year, LaBine returned to the area and discovered the pitchblende and silver deposit which he called Eldorado. Eldorado began production three years later, and was the only known occurrence of pitchblende in Canada at that time (The Staff, Eldorado, 1946).

Numerous studies of Eldorado and related deposits in the Echo Bay and Camsell River areas were subsequently carried out, the most comprehensive by Kidd (1932) and Furnival (1935; 1939a, b), who studied the general geology of the area as well as the mineralogy, texture and paragenesis of the mineralized veins. Large-scale mapping of the Echo Bay area was completed by Robinson (1933), Riley (1935), Feniak (1947) and Furnival (1939a).

In 1944, the Eldorado mine was taken over by the Canadian government and the Port Radium/Echo Bay area was mapped at the 1:4800 scale by Joliffe and Bateman (1944), Thurber (1946), Feniak (1947) and Fortier (1948), all of the Geological Survey of Canada. Mursky (1973) compiled large-scale maps of the Port Radium area produced during the 1940's and 50's. More recently, Hoffman and Bell (1975), Hoffman et al. (1976), Hoffman (1978) and Hildebrand (1983a) mapped the lithologies of the Echo Bay area. More detailed mapping was carried out in the Camsell River area by Shegelski and Murphy (1973),

Padgham et al. (1974) and Hildebrand (1983b). Robinson and Morton (1972) attempted to date rocks of the Port Radium and Echo Bay formations by K-Ar and Rb-Sr methods, but were unsuccessful due to thermal resetting at about 1400 Ma

The first study of intermediate plutons of the Mystery Island intrusive suite in the Echo Bay area was that of Furnival (1939a; b), who provided a detailed description of the mineralogy, alteration, structure, stratigraphy and age relationships of one of the plutons. More recently, Cherer (1988) studied the petrology and geochemistry of three of the plutons of the Mystery Island intrusive suite in the Echo Bay area. In the Camsell River area (Fig. 3), Tirrul (1976) mapped mineralogical and compositional zoning within, and altered wall rocks above, one of two intermediate composition plutons similar to the plutons of the Mystery Island intrusive suite. Hildebrand (1983b; 1984b; 1986) mapped and studied in detail the geology, petrography and geochemistry of these plutons and associated magnetite-apatite-actinolite deposits in the Camsell River.

The origin of the magnetite-apatite-actinolite deposits at Great Bear Lake was first investigated by Badham and Morton (1976), who completed a geological and geochemical study of the deposits near Camsell River. They concluded that the magnetite-apatite-actinolite bodies were formed as immiscible liquids separated from intermediate silicate melts, and were intruded as a volatile-rich "crystal mush" at about 600°C. Hildebrand (1982; 1983b; 1986) mapped plutons and associated altered and mineralized rocks in the Camsell River area and recognized zoned alteration haloes within, and adjacent to, the plutons. He divided altered rocks into three zones: 1) an inner zone of albite; 2) an intermediate zone of magnetite-apatite-actinolite; and 3) an outer zone of pyrite. Hildebrand (1986) concluded that the mineralization process was one of replacement and brecciation of the country rocks by high-temperature, highly acidic, chlorine-dominated fluids derived from epizonal plutons.

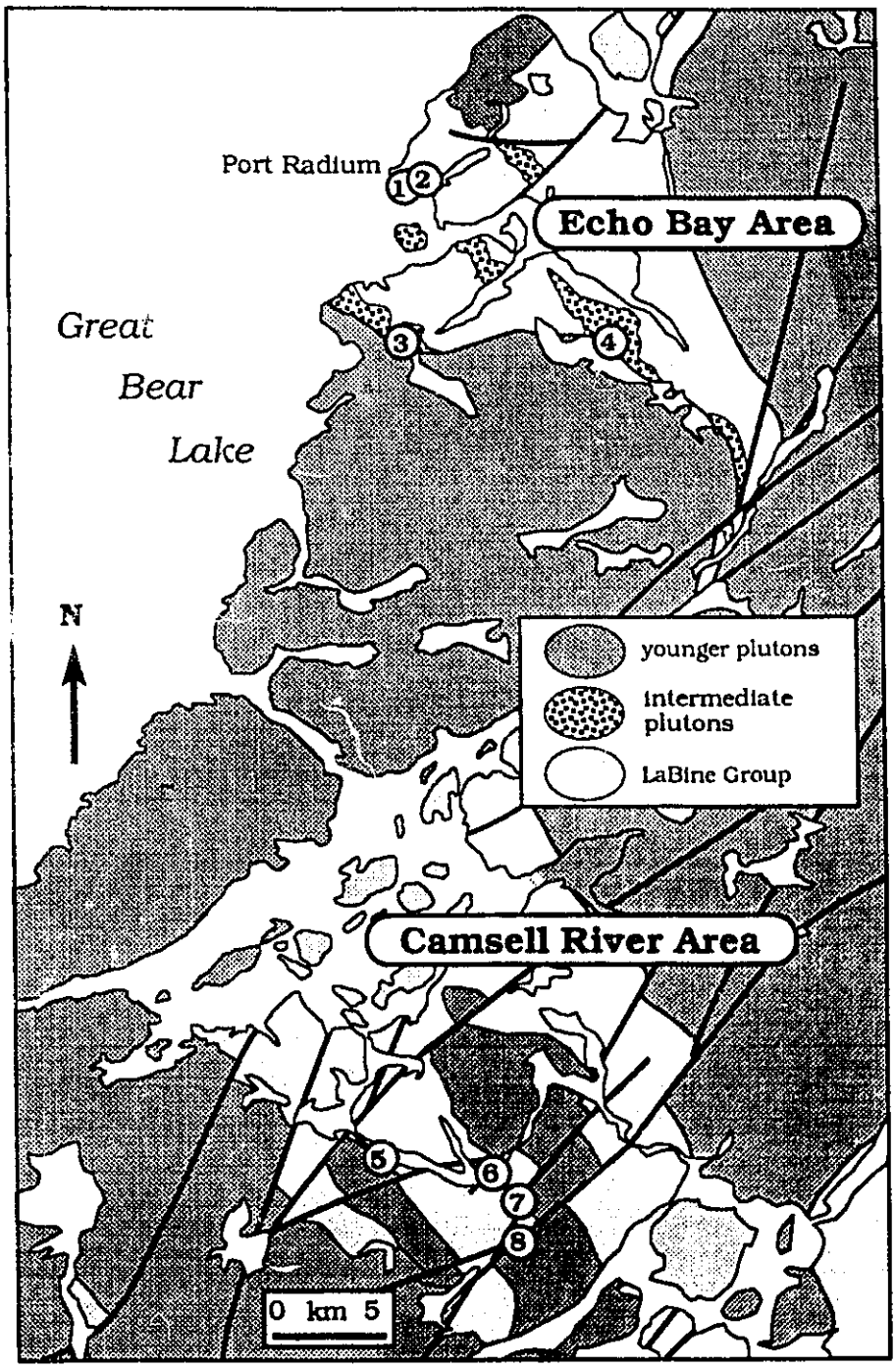

Figure 3. General geology of the Echo Bay and Camsell River areas with previous mine locations. 1 = Eldorado, 2 = Echo Bay, 3 = El Bonanza and Bonanza, 4 = Contact Lake, 5 = Terra, 6 = Northrim, 7 = Norex, 8 = Smallwood (after Changkakoti et al., 1986a).

Kiruna-type deposits

Kiruna-type iron deposits are characterized by ore consisting of magnetite and/or hematite with amphibole and apatite as the principal gangue minerals. These deposits were first described in northern Sweden, where the type deposit is located. Despite the large number of studies of Kiruna-type deposits worldwide, the origin of the deposits is still poorly understood. Geijer (1911; 1915; 1930) and Geiger and Odman (1974) proposed that Kiruna-type deposits form from "a magmatic differentiate rich in volatiles", based primarily on the presence of "dikes and veins of ore-forming minerals". Snyder (1969), Park (1972), and Frietsch (1978) also considered the deposits to be "magmatic segregations".

Daly (1915) proposed that liquid immiscibility led to the separation of a volatile-rich, immiscible iron liquid from a silicate melt. Textural relations, principally "globular and spherical magnetite and actinolite concentrations", (Lundberg and Smellie, 1979; Smellie,1980) and the presence of "magnetite dikes" (Badham and Morton,1976), were used to further support this model. Philpotts (1967) supported the immiscibility model with experimental evidence for immiscible liquids above 1400°C for mixtures of synthetic magnetite and apatite with diorite. However, Hildebrand (1986) demonstrated that magnetite-apatite-actinolite samples did not melt completely after 48 hours at 1150°C under dry conditions at 1 atmosphere.

Hegemann and Albrecht (1954) ascribed the iron deposits at Kiruna to sedimentary exhalative processes. Parák (1973, 1975, 1985) compared the genesis of these deposits to that of massive sulphide deposits. Graded beds and crossbedding in the apatite-rich ores, and "erosion phenomena" in the hanging wall contact at Kiruna were used as definitive evidence to support the exhalative hypothesis. According to this model, organic phosphorus in these ores was remobilized from older phosphorus-rich sedimentary rocks, and iron and rare earth elements were leached from greenstones (Landergren, 1948; Park

1961, 1972; Frutos and Oyarzún, 1975). Parák considered veins and breccias of magnetite-apatite-actinolite to form by the remobilization of sedimentary ore into fracture systems. The exhalative-sedimentary model is supported by Forsell (1987).

Other studies have concluded that magnetite-apatite-actinolite deposits are formed by hydrothermal processes. Ruiz et al. (1968) proposed a deuteric alteration model for the iron deposits of Chile, and Bookström (1977) similarily attributed magnetite-apatite-actinolite deposits associated with diorite at El Romeral, Chile, to hydrothermal replacement related to the intrusion of plutons. Vidal et al. (1990) attributed apatite and actinolite-bearing Cu-Fe skarns in Peru deposits to hydrothermal processes. Ménard (1986) supported the hydrothermal replacement model, and demonstrated the formation of magnetite-apatite-actinolite by hydrothermal replacement within and adjacent to intermediate plutons at El Algarrobo, Chile. Ménard also calculated mass balances for the major elements and phosphorus, and concluded that mass transfer by hydrothermal fluids was sufficient to explain the concentration of iron in the orebodies. Mackin (1968), in one of the best studies of its type, proposed a metasomatic origin for the iron skarn deposits of the Iron Springs district, Utah, which occur within and adjacent to intermediate plutons, and concluded that sufficient iron was leached from the altered rocks to produce the deposits. Panno and Hood (1983) attributed the Pilot Knob magnetite and hematite deposits of Missouri to hydrothermal replacement, but did not rule out possible magmatic injection to explain the breccias found there.

An extensive geological and mineralogical study of Meso-Cenozoic iron deposits in the middle-lower Yangtze valley by an iron deposit research group in China (Research Group of Porphyrite Iron Ore of the Middle-lower Yangtze Valley, 1977) demonstrated the genetic relationship between intermediate to mafic, sill-like, subvolcanic plutons and zoned alteration haloes. The altered rocks are divided into three zones of about 250 m

thickness each, based on surficial mapping and drill core: 1) an inner albite zone, 2) an intermediate zone of pyroxene-(actinolite)-apatite-magnetite, and 3) an outer zone of sulphides. They proposed that the deposits formed as a continuum of processes related to the intrusion and cooling of the magmas, occurring from about 450° to 200°C. A time sequence of overlapping alteration within the magnetite-apatite-actinolite zone from anhydrous ferromagnesian silicates and albitization to hydrous silicates, propylitization, magnetite-apatite-actinolite replacement and pyritization and finally silicification and martitization of magnetite was recognized. The geologic and mineralogic features described from various other MAA deposits elsewhere are observed within a single system, at various depths and distances from the plutons, and within various rock types. The deposits were divided into genetic types and attributed to volcanic-sedimentary (early, stratified, hematite-quartz-barite deposits) and hydrothermal processes. A magmatic ("ore magma") origin was considered for some of the massive, high-temperature deposits.

Pitchblende, Ag, Ni-Co arsenide vein deposits

Numerous geological, geochemical, and isotopic studies were carried out on the silver and pitchblende veins at Echo Bay and Camsell River (Kidd, 1932; Riley, 1935; Furnival, 1935, 1939a, 1939b; Campbell, 1955; Badham, 1972, 1973a, 1973b, 1975; Jory, 1964). The veins were dated by Jory (1964), who determined a U-Pb model age for pitchblende of 1429 ± 29 Ma Thorpe (1971;1974) determined a Pb-Pb model age of 1625 Ma for galenas and a U-Pb model age of 1445 Ma for pitchblende, and attributed the discrepancy to resetting of the pitchblende ages. Miller (1982) determined a U-Pb model age of 1500 ± 10 Ma to 1424 ± 29 Ma for pitchblende.

Robinson (1971) carried out geochemical and fluid inclusion studies of the veins. Robinson and Ohmoto (1973) presented data on mineralogy, fluid inclusions, $\delta^{18}O$ and $\delta^{13}C$

of vein carbonates, and $\delta^{18}O$ for quartz and hematite. They concluded that the veins were deposited in seven stages by seawater at temperatures of 200° to 95°C. Robinson and Badham (1974) determined the $\delta^{18}O$ and $\delta^{13}C$ of carbonates and $\delta^{34}S$ of sulphides from the veins, and concluded that the veins were formed by seawater at 200°C. More recently, Changkakoti et al. (1986a) determined $\delta^{18}O$ and $\delta^{13}C$ of carbonates, $\delta^{18}O$ of quartz, and δD of fluid inclusions in quartz, dolomite and calcite. They concluded that the veins were deposited by magmatic fluids with increasing input of meteoric water towards the final stages. Shegelski (1973), Shegelski and Scott (1975) and Changkakoti et al. (1986b) carried out detailed fluid inclusion studies of the veins, and concluded that they were deposited by boiling saline fluids from 450° to 90°C.

Current work: objectives and methods

This study presents the results of a detailed mapping, petrographic and stable isotopic study of the plutons of the Mystery Island intrusive suite and associated altered and mineralized rocks in the Echo Bay area (Fig. 4). The objective of this study was to understand the genesis of the alteration haloes, the origin of the magnetite-apatite-actinolite mineralization, and their relationship to the plutons of the Mystery Island intrusive suite. Excellent exposure of the plutons and their altered wall rocks in oblique cross-section allowed a unique assessment of geologic and geochemical variations with depth and distance from plutonic contacts.

The plutons of the Mystery Island intrusive suite and their altered wall rocks in the Echo Bay area were mapped at 1:15 000 scale to determine: 1) the distribution of altered rocks; 2) age relationships between the plutons and the alteration haloes; 3) compositional variation within the haloes; and 4) the paragenesis of magnetite-apatite-actinolite vein and replacement minerals. Outcrop in the area is excellent, up to 80 percent. Most outcrops

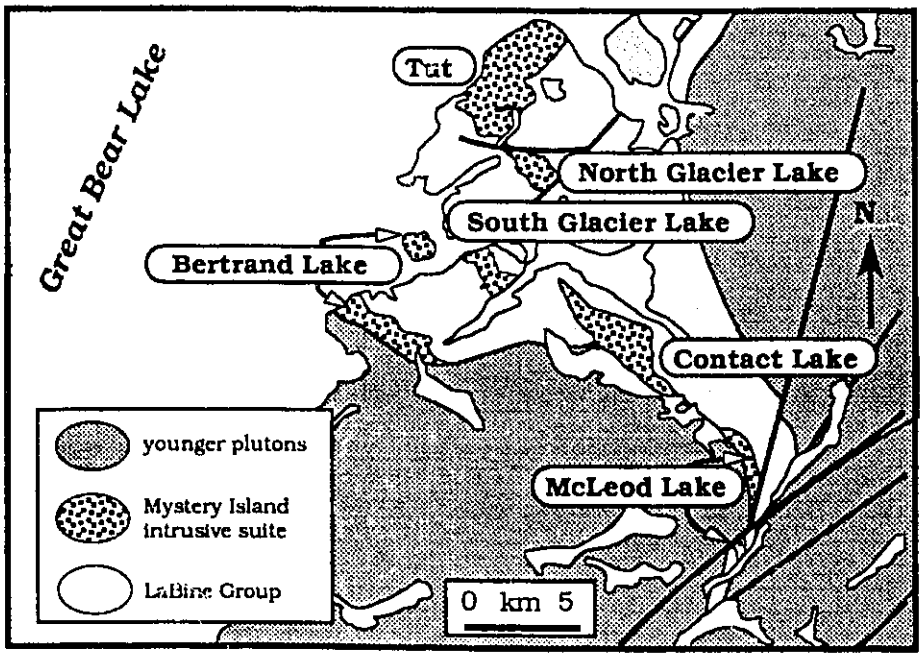

Figure 4. General geology of the Echo Bay area showing the plutons of the Mystery Island intrusive suite.

were examined throughout the alteration zones, and in some areas, all outcrops were examined. Locally, detailed mapping at the outcrop scale was carried out to document relationships between rocks pervasively replaced by magnetite-apatite-actinolite and veins and pods of these minerals.

Petrographic examination and chemical analysis of the altered rocks were used to determine mineralogical and chemical variations within the plutons and their altered wallrocks. Stable isotopic analysis of the plutons, their wallrocks, and minerals from the magnetite-apatite-actinolite bodies and pyrite zones were carried out to determine the isotopic composition of the fluids responsible for alteration.

II. GEOLOGIC SETTING

Regional geology

Wopmay orogen

The Mystery Island intrusive suite and associated magnetite-apatite-actinolite deposits are located within the Great Bear magmatic zone of the Wopmay orogen (Hoffman, 1980, Hoffman and Bowring, 1984), an early Proterozoic orogenic belt located in the northwesternmost part of the Canadian Shield (Fig. 1). The Great Bear magmatic zone is the youngest magmatic belt within Wopmay orogen. Wopmay orogen formed as the Hottah terrane, an exotic microcontinent, collided with the western margin of the Archean Slave craton at 1.89 Ga (Hildebrand and Bowring, 1991) during the Calderian orogeny (Hildebrand and Bowring, 1991). The collision thrust shelf-rise and overlying foredeep rocks deposited on the Slave craton, and 2.0 to 2.55 Ga gneissic rocks and 1.90 Ga volcanic and sedimentary cover of the Grant-Akaitcho groups (Hildebrand et al., 1991) eastward to produce a thrust-fold belt (Tirrul, 1983; King, 1986; Hoffman, 1987; Hoffman et al., 1988). Continued eastward subduction following the collision led to continental *a* magmatism of the Great Bear magmatic zone from 1.88 to 1.84 Ga (Bowring, 1984).

Great Bear magmatic zone

The Great Bear magmatic zone (Figs. 1 and 2) is a northerly-trending belt of continental arc rocks about 100 km across and 900 km in length (Hildebrand and Bowring, 1984; Hildebrand et al., 1987). The zone crops out for 450 km along strike. Deformed rocks of the Hottah terrane form the basement beneath most of the Great Bear magmatic zone. The Great Bear magmatic zone comprises minor amounts of tholeiitic basalt, mafic to felsic calc-alkaline volcanic rocks, caldera-related ignimbrites, lesser volcanogenic sedimentary rocks, and related intermediate composition plutons (Hoffman and McGlynn,

1977; Hoffman, 1972, 1982; Hildebrand, 1981, 1984; Hildebrand et al., 1987). Intermediate composition rocks are dominant. The Great Bear magmatic zone is synclinal, such that the oldest rocks crop out in the east and west (Hoffman and McGlynn, 1977; Hildebrand and Bowring, 1984; Hildebrand et al., 1987).

Rocks of the Great Bear magmatic zone were intruded by a suite of biotite- and hornblende-bearing granitic plutons at about 1.843 Ga (Bowring, 1984). Cessation of arc magmatism in the Great Bear magmatic zone was followed by folding about northwest-trending axes during a period of dextral transpression, possibly due to ridge subduction (Hildebrand et al., 1987). Subsequent erosion exposed oblique cross-sections through the crust. In the western part of the zone, large andesitic stratovolcanoes up to 3 km thick and synvolcanic epizonal plutons are exposed (Hildebrand, 1984a, b).

Large syenogranitic plutons intruded the Great Bear magmatic zone after folding (Hildebrand et al., 1987), and all of the rocks were then cut by northeast-trending conjugate transcurrent faults (Fig. 2) (Hoffman, 1984; Tirrul, 1983). East-west-trending diabase dykes of the Cleaver dykes (Hoffman, 1982) postdate transcurrent faulting. The Cleaver dykes are themselves cut by gabbroic sheets of several ages known as the Western Channel diabase.

General Geology: Lithologies

Excellent exposure of the rocks in the Echo Bay area has allowed a thorough understanding of the geology in the area. Much of the area is mapped in detail, particularly within previous mining camps. The following geological descriptions are based largely on the accumulated results of previous workers in the Echo Bay area.

Labine Group

Host rocks to the Mystery Island intrusive suite in the Echo Bay area belong to the LaBine Group, a succession of silicious to intermediate lava flows, pyroclastic rocks, and related sedimentary rocks (Hoffman and McGlynn, 1977). Rocks of the LaBine Group (Figs. 3 and 4; Table 1) crop out on the western margin of the Great Bear magmatic zone. They unconformably overly rocks of the Bell Island Group (Hildebrand and Roots, 1985), which represent a pre-Calderian cover sequence on Hottah terrane (Hildebrand et al., 1990). The LaBine Group was probably deposited in a continental to marginal marine environment, as indicated by rare marine sedimentary rocks and features such as mud cracks, ripple marks and herringbone cross-beds (Hildebrand, 1981; 1984a). In the Echo Bay area, the LaBine group comprises the Port Radium, Echo Bay and Cameron Bay formations, and is described in detail by Hildebrand (1981; 1984b).

Port Radium Formation

The Port Radium Formation (Table 1) is the oldest unit of the LaBine Group in the Echo Bay area. It consists of at least 1 200 m of fine- to coarse-grained sedimentary rocks (Hildebrand, 1981). The base of the formation is truncated by the Richardson pluton (Fig 5). In general, the sequence coarsens upwards, from fine-grained sedimentary facies to subaerial conglomerates and air-fall tuff (Hoffman and Bell, 1975). However, the dominant rock type is laminated to thinly bedded, gray siltstone to fine sandstone. Graded beds and cross-bedding are present locally. The Port Radium Formation is conformably overlain by the Echo Bay Formation.

Table 1. Schematic stratigraphic section, with descriptions, LaBine Group.

LaBine Group	Cameron Bay Fm	Planar and crossbedded, volcanic-lithic and feldspathic sandstone and gritstone; ripple laminated siltstone and mudstone with mudcracks; hematitic polymictic conglomerate of mainly volcano-plutonic provenance; thin beds and erosional remnants of ashstone; local talus and explosion breccias; cauldron collapse breccias interfingered with ash flow tuff. The formation is divided into 12 members which are described in detail by Hildebrand (1984a, 1984b).
	Echo Bay Fm	**Sparkplug Lake Member:** porphyritic andesite flows and breccia. This member distinguished only by its stratigraphic position above the Mackenzie Tuff.
		Surprise Lake Member: porphyritic (hornblende-augite-plagioclase) andesite flows and breccia; many flows are trachytic; some flows are oxidized to a brick-red colour; also thin sedimentary beds and minor laharic breccia.
		Cobalt Porphyry Member: intrusive hornblende-plagioclase porphyry and microdiorite.
		Mile Lake Member: porphyritic lava flows with intrbedded volcanogenic sandstone and conglomerate; andesitic lapilli tuff and ashstone.
	Port Radium Fm	Thin-bedded, fine grained sandstone and siltstone with at least two carbonate beds less than 1 m thick; all exposures are within the alteration halos of the Mystery Island intrusive suite.

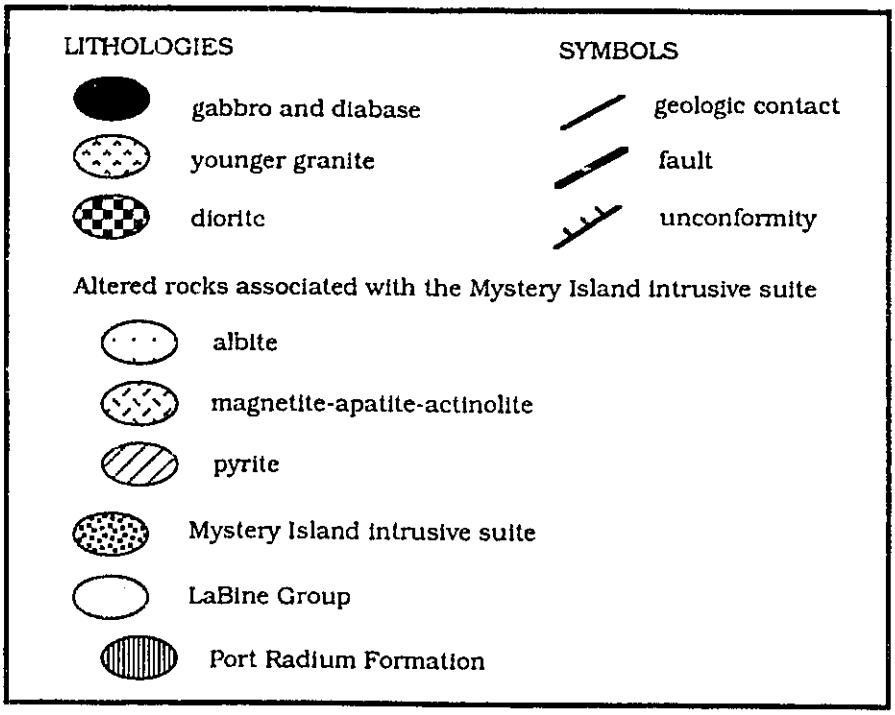

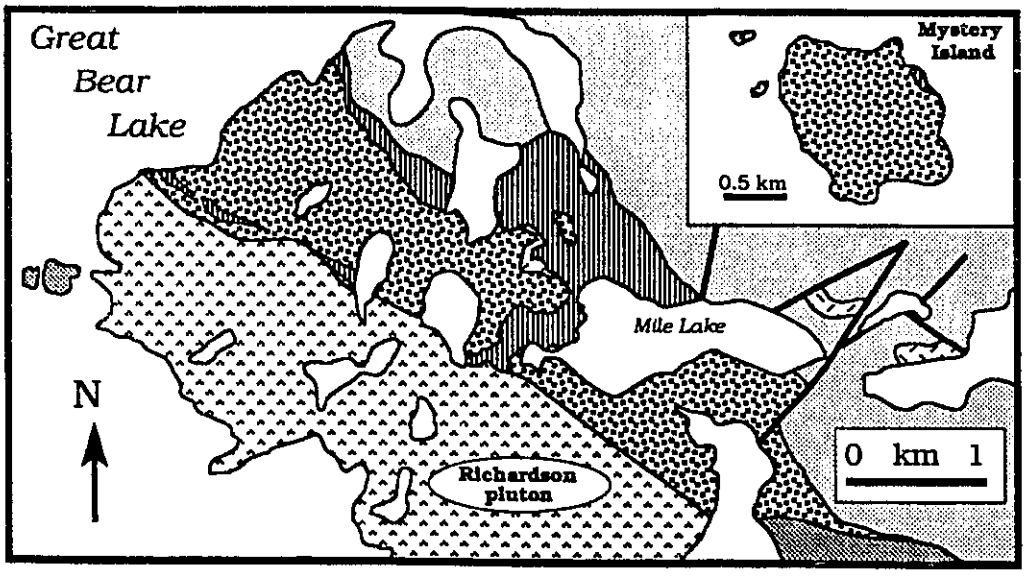

Figure 5. Simplified geology and distribution of altered rocks in the Bertrand Lake pluton area and legend for figures 5 to 8.

Echo Bay Formation

The Echo Bay Formation (Table 1) consists of subaerial, plagioclase porphyritic and amygdaloidal, hornblende- and augite-bearing andesitic lava flows, rare rhyodacite flows, epiclastic rocks and breccias (Hildebrand, 1981; 1984). The exposed section of the Echo Bay Formation in the Echo Bay area is nearly 3000 m thick, and lies conformably upon the Port Radium Formation. The lower 400 m of the formation consists of intercalated epiclastic rocks and lava flows, whereas the upper part of the formation is composed mostly of lava flows with minor amounts of epiclastic rocks (Hildebrand, 1981).

Epiclastic rocks of the Echo Bay Formation consist of volcanogenic sandstone, conglomerate, debris flow deposits, and reworked tuffs (Hildebrand, 1981). The lava flows which comprise most of the Echo Bay Formation are plagioclase porphyritic, and contain from 5 to 45% subhedral to euhedral, platy plagioclase phenocrysts up to 6 mm in length. Minor amounts of hornblende, and less commonly, augite, are also found as subhedral to euhedral phenocrysts up to 5 mm in length. Some of the flows contain up to 20 % quartz-filled amygdules up to 1 cm in diameter, which locally contain chlorite and calcite. Some flows have flow-top breccias.

Cameron Bay Formation

The Cameron Bay Formation (Table 1) consists of at least 4000 m of volcanic rocks and fine- to coarse-grained sedimentary rocks of volcanic and plutonic provenance (Hildebrand, 1981; 1982; 1983a). The volcanic rocks are dominantly tuffs, with lesser amounts of lava flows. Rocks of the Cameron Bay Formation also interfinger with andesites of the Echo Bay Formation (Hoffman and Bell, 1975; Hildebrand, 1983a). The Cameron Bay Formation is separated from the underlying Echo Bay Formation by local unconformities formed during synvolcanic erosion, and characterized by highly

ferruginous conglomerate. Boulders of similar composition to plutons of the Mystery Island intrusive suite are found in a conglomerate in the Echo Bay area (Hildebrand, 1981). A conglomerate mapped above the Contact Lake pluton contains fragments of altered andesite, some of which contain abundant magnetite, as well as abundant vitreous quartz grains (Reardon, 1990). Thus, the altered rocks above the Contact Lake pluton were eroded and at least one of the plutons was probably exposed before the termination of volcanism of the Echo Bay Formation. A small intrusive body similar to the plutons of the Mystery Island intrusive suite cuts the Cameron Bay Formation near Cameron Bay (Hildebrand, 1984a). The Cameron Bay Formation is overlain by volcanic and sedimentary rocks of the Feniak Formation and the Sloan Group (Hoffman and Bell, 1975; Hoffman, 1978).

Mystery Island intrusive suite

The Mystery Island intrusive suite (Hildebrand, 1981) comprises five semi-concordant, epizonal plutons: the Bertrand Lake, McLeod Lake, Contact Lake, Glacier Lake and Tut plutons (Figs 3 and 4). Two synvolcanic plutons similar in composition to the plutons of the Mystery Island intrusive suite occur in the Camsell River area (Fig. 3). Although the stratigraphy of the hostrocks of these plutons is not directly correlative between the Echo Bay and Camsell River areas, similar U-Pb ages, rock types and regional stratigraphic positions suggest that volcanism in both areas was roughly contemporaneous (Hildebrand, 1986).

The plutons of the Mystery Island intrusive suite are sill-like in cross-section, up to 10 km across, and up to 2 km thick. The plutons were emplaced at two distinct stratigraphic levels within the LaBine Group (Hildebrand, 1984a). The Bertrand Lake pluton (Figs. 4 and 5) was emplaced within the Port Radium Formation and the lowermost part of the conformably overlying Echo Bay Formation. The other plutons intrude

approximately 1 km above the Bertrand Lake pluton. Younger granitic plutons of the Great Bear batholith truncate some of the plutons.

Plutons of the Mystery Island intrusive suite are intermediate in composition, consisting of fine- to medium-grained, seriate rocks varying from diorite to quartz monzonite (IUGS, Streckeisen, 1973). Locally, the plutons contain sufficient quartz to be classified as granodiorite or granite (Cherer, 1988).

All of the plutons contain 30 to 50% subhedral to euhedral, seriate plagioclase phenocrysts. Interstitial, cloudy, anhedral alkali feldspar up to 3 mm in length comprises 10 to 30% of the rock. Quartz occurs as 1 to 4 mm interstitial, anhedral grains and comprises 5 to 25% of the rock. Hornblende (20 to 30%) and biotite (5 to 15%) are the primary mafic minerals. Minor euhedral to subhedral 1 to 2 mm clinopyroxene phenocrysts are present near plutonic margins. Very fine-grained (<1 mm) magnetite and very fine-grained euhedral apatite and subhedral zircon are ubiquitous accessory minerals.

The plutons are weakly to moderately altered throughout. Plagioclase phenocrysts are weakly to very strongly sericitized and locally epidotized. Hornblende and biotite and are partially to completely altered to chlorite. Some biotite is altered to magnetite along cleavage planes. Most of the plutons contain minor amounts of riebeckite. Pods and veins of tourmaline are present locally. Quartz, calcite and chlorite veinlets occur throughout the plutons.

Bertrand Lake pluton

The Bertrand Lake pluton crops out from the shore of Great Bear Lake eastward beyond Mile Lake, and on a displaced section on Mystery Island (Figs. 4 and 5). The upper

contact of this pluton is sharp, generally conformable to bedding within the Port Radium and Echo Bay Formations. The lower contact is truncated by the Richardson pluton.

Internally, the pluton is compositionally heterogeneous, consisting of fine- to medium-grained diorite to quartz diorite to the west, and monzonite to the east. It comprises about 50% subhedral plagioclase phenocrysts and 15 to 35% anhedral alkali feldspar. The pluton contains 5 to 12% fine-grained, anhedral quartz. The mafic minerals are dominantly subhedral hornblende with lesser biotite, and constitute 15 to 20% of the rock, but up to 40% near the lower contact. Accessory minerals are magnetite (approximately 2%), trace zircon and apatite (up to 2% near the lower contact). Minor riebeckite occurs near the center of the pluton. All samples examined are strongly altered; plagioclase is strongly sericitized and the mafic minerals are completely chloritized. The upper border phase contains 60% plagioclase phenocrysts and minor clinopyroxene. Locally, adjacent to the lower contact, the pluton contains up to 20% epidote.

McLeod Lake pluton

The McLeod Lake pluton crops out in at least three fault-bounded segments between Contact Lake and McLeod Lake (Figs. 4 and 6). The upper contact is sharp and regular, and the lower contact is completely truncated by the Richardson pluton. Only the northernmost part of the pluton was mapped during this study.

The pluton is homogeneous and consists of moderately altered, medium-grained quartz monzonite, containing 35% partially sericitized, subhedral plagioclase, 20 to 30% anhedral potassium feldspar, 10 to 20% anhedral quartz and minor granophyre. Mafic minerals, mostly hornblende and lesser biotite, comprise 15 to 30%, are strongly chloritized, and are more abundant towards the bottom of the pluton. Accessory phases are magnetite, apatite, titanite, epidote and riebeckite.

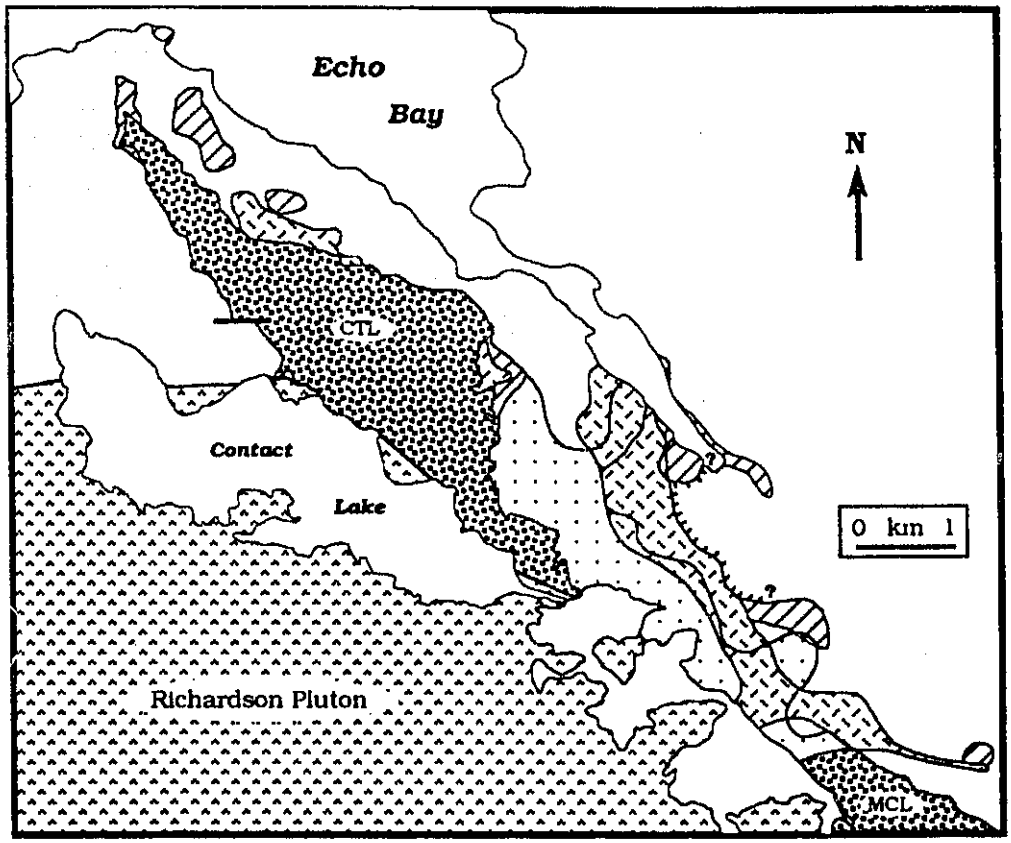

Figure 6. Geology of the Contact Lake pluton showing the distribution of altered rocks. Alteration is more extensive above the southern part of the pluton, between the Contact Lake and McLeod Lake plutons. Note the unconformity ( ) which truncates the alteration zones at the southeastern end of Echo Bay. "?" indicates that the continuation of the unconformity beyond this point is uncertain.

Contact Lake pluton

The Contact Lake pluton crops out along the north side of Contact Lake (Figs. 4 and 6). The upper contact is sharp and locally irregular. The lower contact is sharp where exposed, but it is mostly truncated by the intrusion of the Richardson pluton. The pluton is zoned internally, consisting of fine- to medium-grained seriate quartz monzodiorite to quartz monzonite, and granite towards the lower part of the pluton, near Contact Lake (Cherer, 1988). This may represent normal zoning from a more mafic rim to a felsic core, however, the mafic rim at the lower contact has been truncated. The pluton comprises of 35 to 45% weakly to strongly sericitized and epidotized, subhedral plagioclase, 15 to 35% anhedral potassium feldspar, and 10 to 25% quartz. Mafic minerals consist of 10 to 20% subhedral, chloritized hornblende, less than 5% chloritized biotite, and minor clinopyroxene locally. The pluton contains 1 to 3% magnetite, up to 3.5% epidote and 1.6% calcite locally (Cherer, 1988), minor granophyre, and trace apatite, titanite, zircon, and riebeckite.

Glacier Lake pluton

The Glacier Lake pluton outcrops in two areas separated by a right-lateral transcurrent fault with greater than 2 km separation. Outcrops occur at Echo Bay (Figs. 4 and 7) and southeast of Glacier Lake (Fig. 8). Both the upper and lower contacts of the pluton are sharp.

A fine-grained, clinopyroxene-bearing border phase occurs at the lower contact. The pluton consists of fine- to medium-grained, seriate quartz monzodiorite to monzogranite comprised of 40% weakly to strongly sericitized plagioclase, 30% potassium feldspar, 15 to 25% quartz, and 10 to 15% chloritized hornblende and biotite. Granophyre occurs locally. The pluton contains minor magnetite, up to 2.5% riebeckite, up to 1%

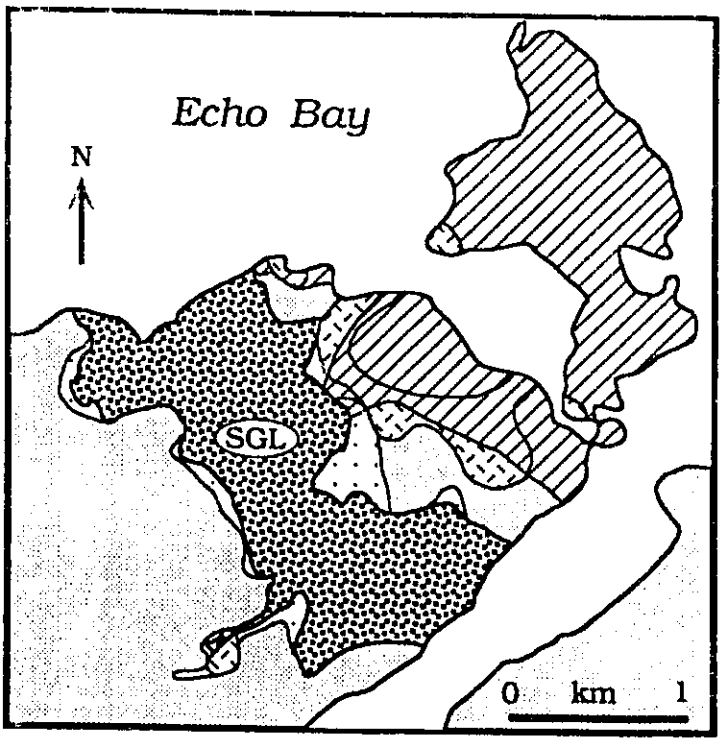

Figure 7. Geology of the southern part of the Glacier Lake pluton showing the distribution of altered rocks. Magnetite-apatite-actinolite occurs beneath the pluton adjacent to a narrow extension perpendicular to the bottom of the pluton.

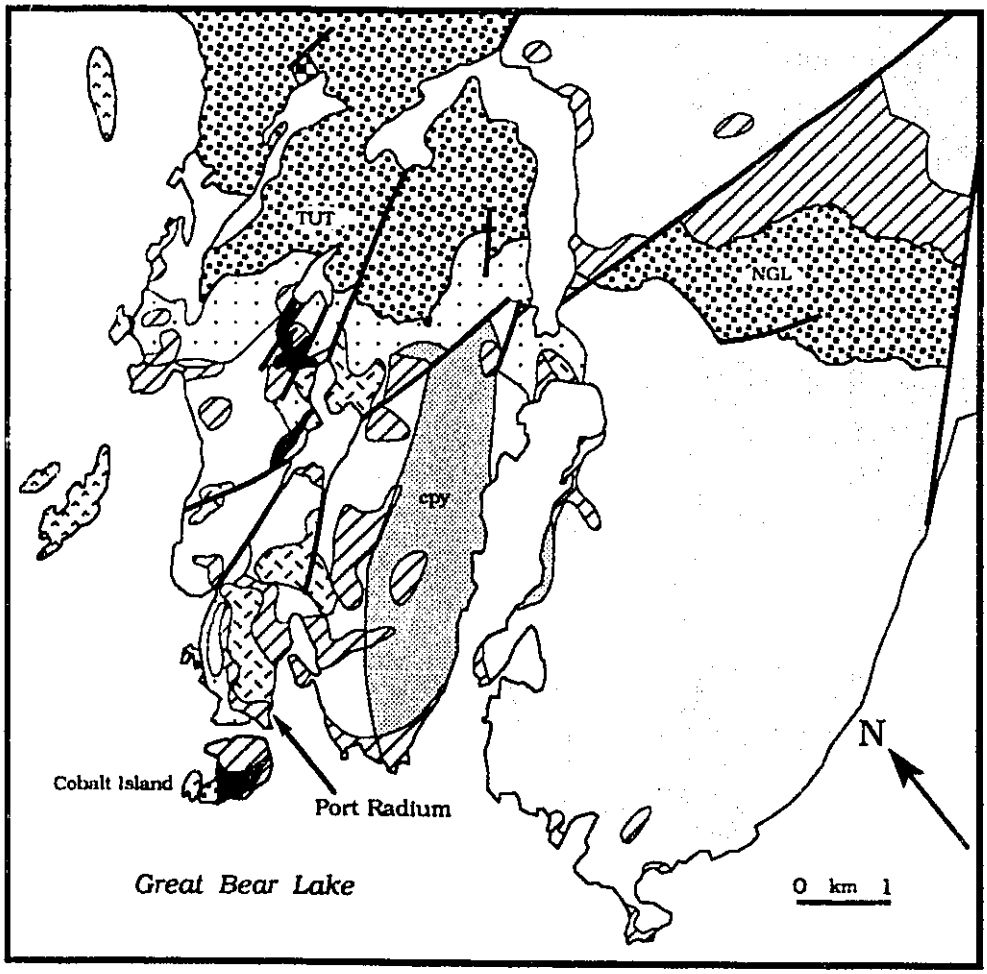

Figure 8. Geology of the Port Radium area, southern Tut pluton and the northern part of the Glacier Lake pluton showing simplified alteration zones. Note the fault-bounded portion of an intermediate pluton, possibly of the Mystery Island intrusive suite, which outcrops on Cobalt Island. Zones of altered rocks are subparallel to the shoreline of Great Bear Lake north of Port Radium. Note the displacement of the plutons and alteration zones along faults.

apatite, titanite, zircon, calcite and epidote. Mineralogical and chemical discontinuities near the center of the pluton may indicate that the pluton consists of two intrusions (Cherer, 1988).

Tut pluton

The Tut pluton (Figs. 4 and 8) is exposed over 18 km^2 on the shore of Great Bear Lake and occupies the core of a syncline (Hildebrand, 1984a). The upper and lower contacts are, therefore, not extensively exposed. Where they are exposed, the contacts are sharp.

The pluton consists of seriate to porphyritic, fine- to medium-grained, quartz monzodiorite to granodiorite, and at least one small diorite body in sharp contact with the main body of the pluton. The pluton comprises 30 to 40% moderately to strongly sericitized, subhedral plagioclase phenocrysts, 20 to 30% anhedral alkali feldspar, 15 to 30% anhedral quartz, less than 2 to 4% chloritized biotite, 5 to 25% chloritized hornblende, 1 to 2% magnetite, and trace apatite, titanite, calcite, zircon. Rare, discontinous veins of specular hematite up to 3 cm wide occur locally.

Richardson pluton

The 1.84 Ga Richardson pluton (Figs. 5 and 6) (Bowring, 1984) is a coarse-grained, biotite syenogranite of the Great Bear batholith. It comprises the southwestern portion of the map area and truncates the lower contacts of the Bertrand Lake and Contact Lake plutons. The pluton has sharp contacts and shows no visible evidence of extensive alteration within the pluton itself or within the adjacent wall rocks.

General geology: structures

Folds

Rocks in the Echo Bay area underwent two periods of compressive deformation and a later period of extension. Dextral transpression folded the rocks about northwest-trending, gently plunging axes (Hoffman and McGlynn, 1977; Hildebrand and Bowring, 1991). The folds are asymmetrical and have wavelengths of 1 to 15 km (Hildebrand, 1984b). Northeasterly-dipping limbs are longer, and expose large parts of the Great Bear magmatic zone in oblique cross-section. The plutons of the Mystery Island intrusive suite in the Echo Bay area are exposed on the southern limb of a fold, except the Tut pluton, which occurs in a syncline (Hildebrand, 1981; 1984a). Locally, at Port Radium, siltstones are openly folded on the scale of meters, with some smaller, tight folds and chevron folds. There is no megascopically visible penetrative cleavage associated with folding.

Faults

Numerous northeast-trending, vertical transcurrent faults cut the Great Bear magmatic zone (Fig. 2); (Hoffman, 1984; Tirrul, 1983). The faults have right-lateral separation of up to several km, and are commonly joined to each other by northwest-trending sinistral and east-trending faults which have smaller separations and are less numerous than the northeast-trending faults (Tirrul, 1983).

Within the Echo Bay area, the transcurrent faults have right-lateral separation of up to 2 km (Fig. 4). Two major sets of faults related to regional transcurrent faulting are present in the Port Radium area, one striking about 045° and a second striking at about 005°. Numerous smaller fault- and fracture-filling veins occur at various orientations.

The transcurrent faults were reactivated, and have undergone several periods of movement, as indicated by multiple generations of breccias (Furnival, 1939). The most

recent movement along these faults was dip-slip, and occurred during a period of extension (Furnival, 1935; Hoffman et al., 1976; Hoffman and McGlynn, 1977), which may be contemporaneous with the pitchblende, native Ag and Ni-Co arsenide veins (Campbell, 1955; Hildebrand, 1988b; Bowring et al., 1989). West-side down normal faulting is recognized within rocks of the Hornby Bay Group, which unconformbly overlie the Great Bear magmatic zone (Hoffman and McGlynn, 1977; Kerans et al., 1981).

Mineral deposits

Pitchblende, native Ag, Ni-Co arsenide vein deposits

The Echo Bay area is best known for its silver and uranium deposits. Several mines (Fig. 3) have operated in the area, and produced more than 15 million ounces of silver and over 14 million pounds of U_3O_8 (McNiven, 1967). However, the origin of the mineralized veins remains obscure. These deposits are classified as Ag - sulpharsenide deposits (Bastin, 1939), and are similar to those of the Cobalt-Gowganda camp (Andrews et al., 1982); Jáchymov, Czechoslovakia (Mrna, 1963), Kongsberg district, Norway (Neumann, 1944); Khovou, in former U.S.S.R (Kroutov, 1972); Chalanches, France (Ypma, 1972); and Saxony (Rosler and Bauman, 1970).

Mineralogy and paragenesis

Quartz-carbonate veins, many of which contain sulphides, are found throughout the study area. The principal minerals of these non-economic veins in the Echo Bay area are quartz, calcite, siderite, chalcopyrite, hematite and pyrite. Minor amounts of nickel-cobalt arsenides are present locally. Most of the veins contain strongly chloritized, or, less commonly, hematized fragments of country rock. The veins are divided into several types according to their mineralogy: 1) quartz (± carbonate), 2) quartz + hematite (± carbonate),

and 3) quartz (± carbonate) + chalcopyrite (± pyrite) (Reardon, 1990). In all veins observed, quartz was deposited first, followed by hematite or sulphides. Most of the veins contain carbonate, usually siderite, which is younger than quartz. Where carbonate and sulphide minerals are both present, the sulphides are found within the carbonate. Veins of calcite and siderite are common and many contain chalcopyrite. Locally, veins of siderite cut quartz-siderite-sulphide veins.

The mineralogy and paragenesis of veins of economic importance in the Echo Bay area were studied by numerous workers (see "Previous work - pitchblende, Ag, Ni-Co arsenide vein deposits"), and therefore will not be discussed in detail. Based on fluid inclusion work, the veins were deposited during at least five stages of hydrothermal activity from saline fluids containing from 15 to 35 wt.% NaCl equivalent, at temperatures of 90°to 450°C (Changkakoti et al., 1986b). Calculated estimates of $\delta^{18}O$ of the fluids range from +0.47‰ to +9.12‰ (Changkakoti et al., 1986b).

Distribution and geometry

The vein system within the Echo Bay area is complex. Quartz and quartz-carbonate veins are present throughout the study area, but are more abundant in the Port Radium area than elsewhere. Kidd (1932) described two sets of faults in the Port Radium area, one striking at about 045° and a second about 005°, as well as narrower veins oriented in various directions. The quartz-carbonate veins dip steeply to the northwest, are up to 15 m wide, and extend up to 450 m along strike.

Furnival (1935; 1939a; 1939b) described the structural geology of the Contact Lake area (Figs. 4 and 6). In this area, the dominant trend of the veins is 075°, and they dip steeply to the southeast. Furnival (1939b) noted that pitchblende, Ag, Ni-Co arsenide veins in the Contact Lake pluton followed older, altered zones which contain chlorite, garnet,

epidote, actinolite, pyrite, magnetite, hematite and arsenopyrite, cut by veins of magnetite and hematite. Since the U-Ag-Ni-Co veins pass from altered granodiorite into unaltered granodiorite, and displace the magnetite-hematite veins, the altered zones cannot be related to the pitchblende, Ag, Ni-Co arsenide veins. Elsewhere in the Echo Bay and Camsell River areas, the pitchblende, Ag, Ni-Co arsenide veins occur within the magnetite-apatite-actinolite and pyrite zones (Hildebrand, 1988b; Reardon, 1989). The spatial association between pitchblende, native Ag, Ni-Co arsenide vein mineralization and MAA/pyrite altered rocks suggests that the veins may be localized by interaction of hydrothermal fluids with the altered wall rocks of the Mystery Island intrusive suite, as suggested by Hildebrand (1988b).

Age relationships

Kidd (1932) noted that the pitchblende, Ag, Ni-Co arsenide veins at Port Radium were subjected to repeated fracturing. Furnival (1935) recognized two major periods of movement: one which predates and one which postdates the 1.7 Ga Hornby Bay Group. Campbell (1955) argued that many of the veins filled faults and tension fractures related to the NE-trending transcurrent faults, and proposed that a major period of fracturing was followed by three periods of extension, the last involving a dip-slip movement contemporaneous with mineralization.

Jory (1964) described a diabase dyke in the Eldorado mine (Fig. 3) at Port Radium which intersects and is diverted by quartz veins. The dyke is brecciated by later movement on the veins and healed by vein mineralization. Jory (1964) also reported that a diabase sill in the mine is not offset by quartz veins, but is affected by late mineralization. Robinson (1971) concluded that diabase dykes in the Eldorado mine are younger than the initial development of the vein structures but older than most of the vein minerals. In

agreement with Jory, Robinson (1971) concluded that a diabase sill in the mine cut all but the latest stages of mineralization. The cross-cutting relationships of the veins and diabase dykes and sills described by Jory (1964) and Robinson (1971) suggest that faulting and vein formation at Port Radium took place before and after the emplacement of the dykes, and that the youngest period of vein formation is contemporaneous with mineralization.

Since most mineralized veins strike northeast, it might seem reasonable to relate them to northeasterly-striking transcurrent faults. However, the largest transcurrent faults in the area are not known to be mineralized, although they contain quartz stockworks up to 30 m wide (Furnival, 1935). Whereas strike-slip faults only develop dilatant zones at bends (Crowell, 1974), it is difficult to explain how mineralized veins, up to 1.5 km long and with features characteristic of extension, would be generated along such faults.

Along the western side of the Great Bear magmatic zone, a number of workers have identified west-side-down normal faults which juxtapose rocks of the lower Hornby Bay Group against rocks of Wopmay orogen (Kerans et al., 1981; Hildebrand, 1982; Hoffman, 1984; McGrath and Hildebrand, 1984a; Ross and Kerans, 1989). The presence of pitchblende, Ag, Ni-Co arsenide mineralization in northeasterly-striking fault zones may be explained by relating the timing of mineral deposition to west-side-down normal faulting, as proposed by Campbell (1955) and later supported by Hildebrand (1988b). The hydrothermal cells which were responsible for mineralization may have been driven by 1663 $^{+/-}$8 Ma (Bowring and Ross, 1985) magmatism of the lower Hornby Bay Group (Hildebrand, 1988b).

Robinson and Ohmoto (1973) argued that diabase dykes and sills, actinolite-magnetite veins and pitchblende, native Ag, Ni-Co arsenide veins are closely related in

time, and were formed at about 1450-1400 Ma based on: K-Ar ages of 1400 Ma (1405 Ma new standardized age, Steiger and Jager, 1978) for a diabase sill in the Port Radium area (Wanless et al., 1970), and 1420 Ma (1425 Ma new standardized age) for actinolite-magnetite veins in the Echo Bay mine (Robinson and Morton, 1972); a U-Pb age of 1450 Ma on pitchblende from mineralized veins at Port Radium (Jory, 1964); and cross-cutting relationships, as described above. Thorpe (1971) reported a Pb-Pb age for galena in mineralized veins of 1625 Ma.

Magnetite-apatite-actinolite replacement and veins

Magnetite-apatite-actinolite replacement and veins occur throughout the Echo Bay and Camsell River areas. Although the deposits are sub-economic, they are very similar to Kiruna-type deposits and iron deposits of the Andes. The geology and geochemistry of these deposits in the Echo Bay area is discussed in detail in the following chapters.

III. PETROGRAPHY AND GEOCHEMISTRY OF ALTERED AND MINERALIZED ROCKS

Although regional metamorphism in the Great Bear magmatic zone is subgreenschist facies, all of the wall rocks of the Mystery Island intrusive suite are moderately to very strongly altered. Zonation of altered rocks associated with intermediate composition plutons in the Camsell River area (Fig. 3) was first mapped by Hildebrand (1986), who recognized three zones above and within the plutons: 1) an albite zone, present within and adjacent to the plutons; 2) a magnetite-apatite-actinolite zone, beyond the albite zone; and 3) an outer pyrite zone. All three zones also are present around plutons of the Mystery Island intrusive suite, and were mapped in the Echo Bay area.

Albite zone

The albite zone is characterized by pervasive replacement of the host rock by albite; albitized rocks are red-brown to pale pink. Extensively altered rocks, found in close proximity to the plutons, are white both on the fresh and weathered surfaces. Replacement of the rocks by coarse albite (Fig. 9), and veins and pods of albite are present in some highly-altered areas. Albitized rocks generally occur within 100 m of the roofs of the plutons, but locally are found up to 1 km above the plutons. Locally, the plutons themselves are albitized, near their contacts. In some areas, the upper contacts of the plutons are obliterated by intense albitization of both the pluton and the adjacent wallrocks. The albite zone commonly overlaps with the magnetite-apatite-actinolite and pyrite zones.

In thin section, rocks from within the albite zone are replaced by fine-grained, equant albite up to 4 mm, but typically less than 0.5 mm. In strongly altered andesitic lavas, the groundmass is replaced, and plagioclase phenocrysts are partially recrystallized at crystal margins (Fig 10). Extremely altered rocks contain very fine-grained, polygonal albite with

Figure 9. Photograph of coarse albite in andesitic lava flow, Glacier Bay.


TAMRON

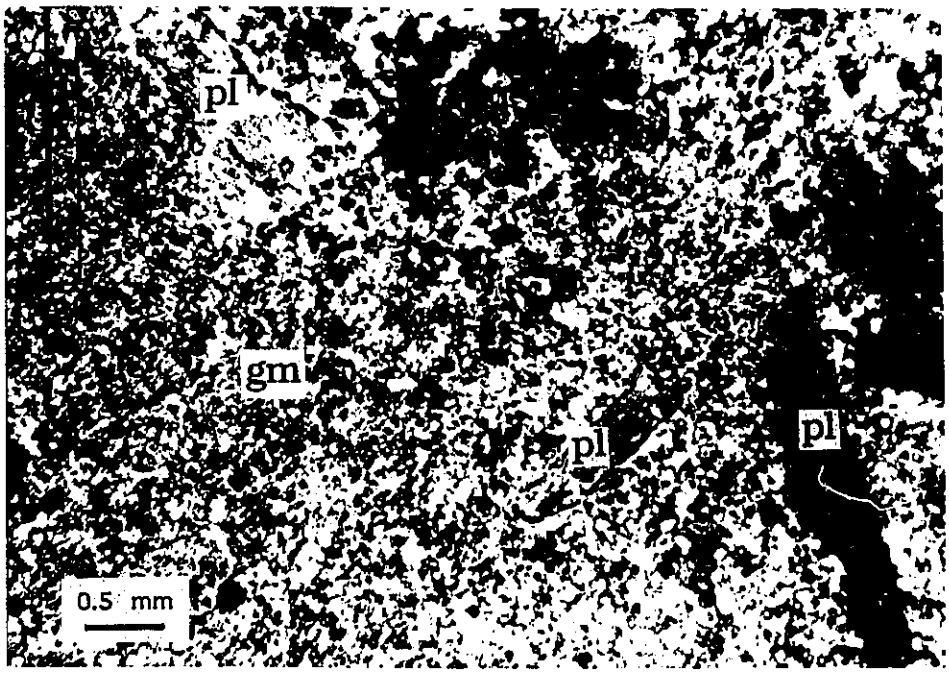

Figure 10. Photomicrograph of albitized andesitic lava flow. The groundmass (gm) consists primarily of very fine-grained albite. Plagioclase phenocrysts (pl) are partially recrystallized. The irregular, dark patch near the top of the photo is an amygdule which consists of quartz and chlorite. Scale: 1 cm = .5 mm. (Sample 89-404).

minor disseminated chlorite. This secondary feldspar is clear and unaltered as compared to primary feldspar, which is turbid. Chlorite is ubiquitous, and comprises up to 15% of albitized andesitic lava flows. Up to 15% very fine-grained, anhedral epidote is also present in most samples. Minor magnetite occurs as corroded crystals or ragged patches with anhedral titanite. One andesitic lava flow in the albite zone contains riebeckite within plagioclase phenocrysts, and riebeckite occurs in small amounts within all of the plutons (Fig. 11). In sedimentary rocks, very fine-grained, anhedral to subhedral albite preferentially replaces individual beds. Albitized plutonic rocks contain very fine-grained, anhedral to subhedral, unaltered albite on the margins of strongly sericitized plagioclase (labradorite to andesine) phenocrysts.

Magnetite-apatite-actinolite zone

The magnetite-apatite-actinolite (MAA) zone is defined by the presence of at least two of the three minerals: magnetite, apatite or actinolite. These minerals also occur as disseminated crystals, veins, pods, and breccias above the plutons, and locally, within and below them. The most common assemblages of these alteration minerals, in decreasing order of abundance, are: 1) actinolite + magnetite; 2) actinolite + apatite; and 3) magnetite + apatite + actinolite. The mode of occurrence of magnetite, apatite and actinolite varies with original lithology. In andesitic lava flows, these minerals are disseminated, and constitute up to 45% of the rock. In sedimentary rocks, albite, actinolite, apatite and magnetite replace individual beds. Some pervasively altered andesite flows and sedimentary rocks are cut by veins of magnetite-apatite-actinolite or magnetite-actinolite (Fig. 12). In the plutons, actinolite or actinolite-apatite occur only as veins near the upper contacts, and no magnetite was observed in veins within the plutons.

Figure 11. Photomicrograph of secondary riebeckite (rb) in plagioclase (pl), Glacier Lake pluton. Scale: 1 cm = 0.25 mm. (Sample 89-593).

Figure 12. Photograph of pervasively altered volcanogenic arkose, replaced albite, actinolite and minor magnetite, and cut by veins of (magnetite)-apatite-actinolite, Port Radium.

38a

The paragenetic sequence of alteration minerals in the MAA zone is given in Figure 13, and is the same in both volcanic and sedimentary rocks. In pervasively altered rocks, where the albite zone and MAA zone overlap, turbid albite is an early mineral. Albite is replaced by actinolite, epidote and ragged magnetite.

Actinolite is the most common mineral within the MAA zone and comprises up to 45% of the rock. Locally, calcite replaces actinolite, and commonly occurs with secondary titanite. Andesite flows partially replaced by MAA contain fine-grained, anhedral to euhedral secondary actinolite up to 3 mm in length within the groundmass (Fig. 14), and as overgrowths on primary hornblende. Hornblende is moderately to strongly chloritized, whereas the actinolite is typically unaltered. Magnetite and minor subhedral titanite occur within actinolite. Locally, fine-grained epidote comprises up to 25% of the rock. Apatite occurs as subhedral to euhedral crystals less than 1 mm in diameter in the groundmass and within secondary actinolite, and comprises up to 3% of the rock. Magnetite occurs within feldspar, epidote and actinolite as finely-disseminated grains or subhedral crystals to 4 mm, and comprises up to 15% of the rock. The magnetite is hematized on rims and along cleavage planes. In sedimentary rocks, beds are preferentially replaced by albite, actinolite or magnetite (Fig. 15). Limy beds at Port Radium are replaced by very fine-grained, massive magnetite.

Veins of MAA up to 80 cm wide are discontinuous and generally exposed along strike for less than 1 m. The veins have various orientations, but generally strike NE and SW (Fig. 16) and are steeply dipping. Thus, the majority of the veins are oriented either perpendicular or parallel to the contacts of the plutons. Pods are generally less than 1 cm in diameter, but many are up to several decimeters across. Actinolite is the most abundant mineral and occurs as laths up to 5 cm in length. Magnetite crystals are subhedral to euhedral, up to 8 cm in diameter, but generally less than 1 cm. Fluorapatite occurs as dark

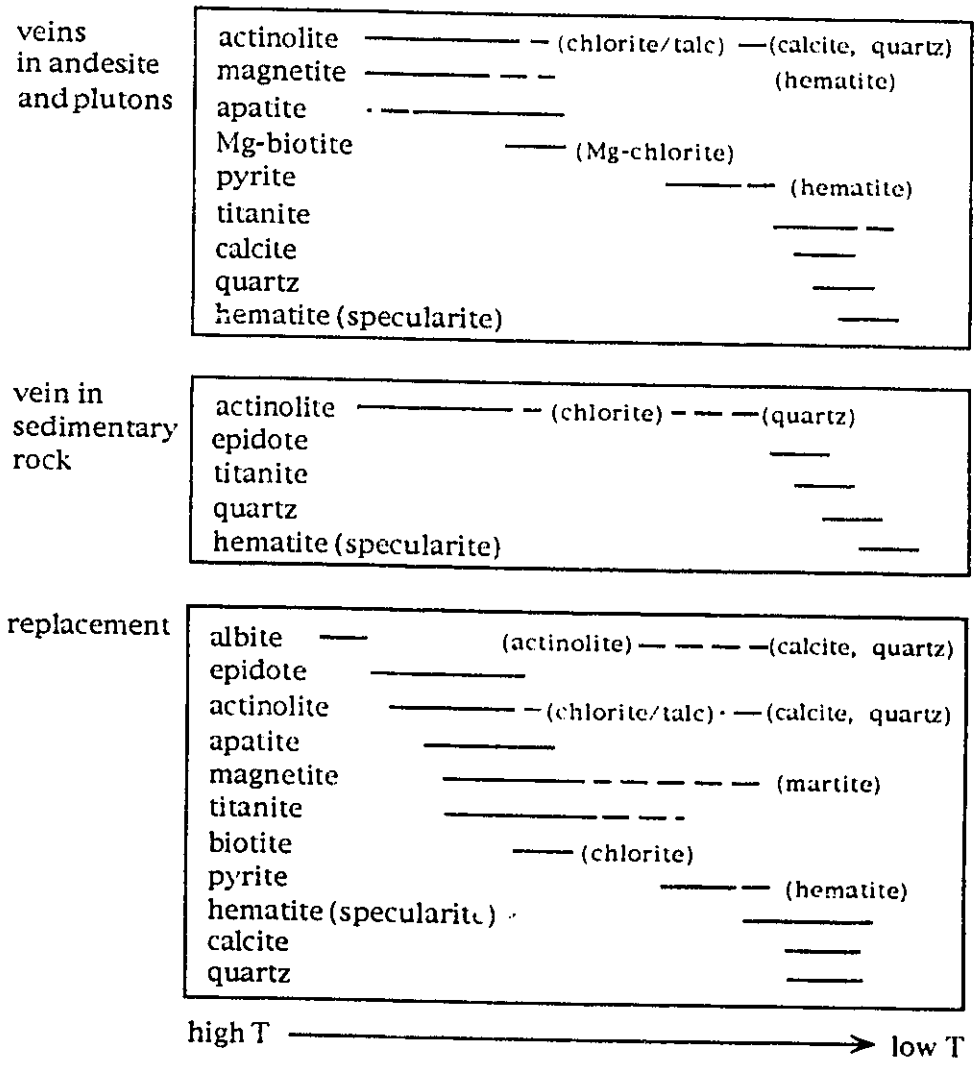

Figure 13. Paragenetic sequence of alteration minerals in veins and pervasively altered rocks from the magnetite-apatite-actinolite zone.

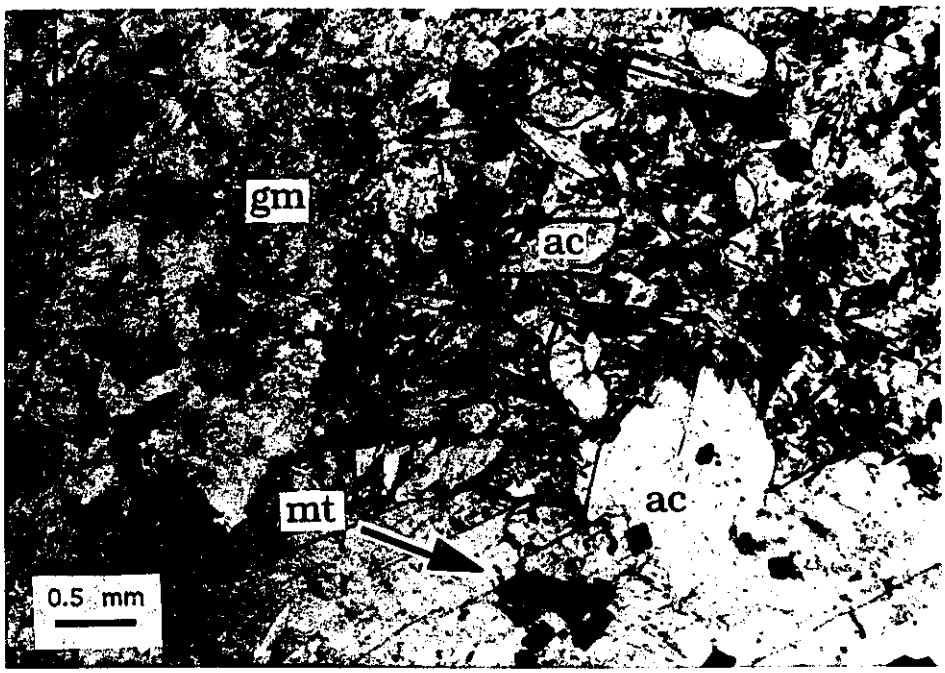

Figure 14. Photomicrograph of euhedral actinolite (ac) and subhedral magnetite (mt) replacing albitized andesitic lava flow; gm = groundmass. Scale: 1 cm = 0.5 mm. (Sample 89-153).

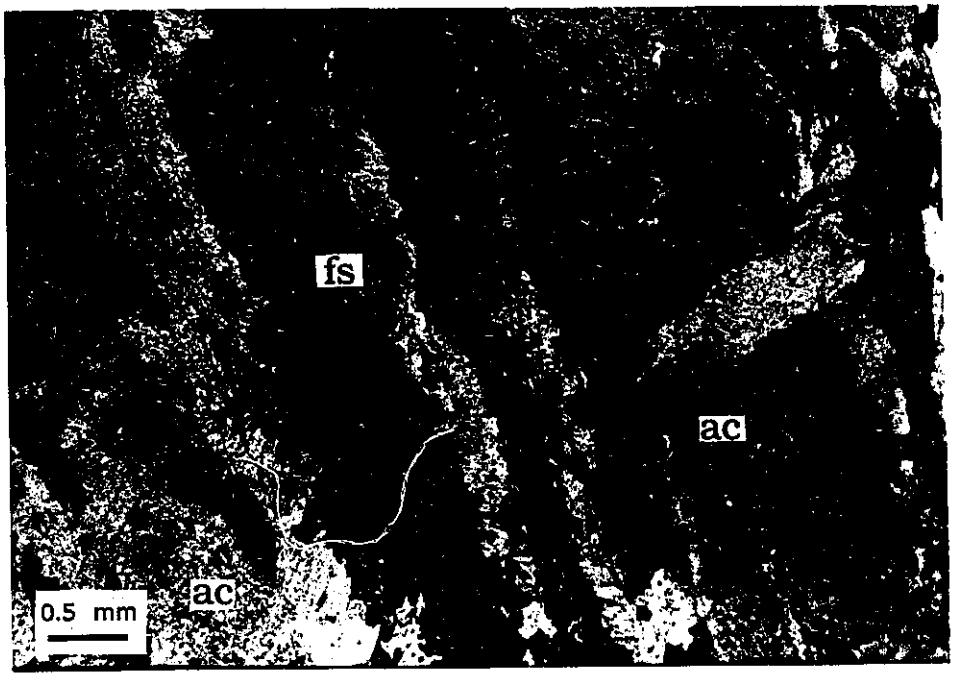

Figure 15. Photomicrograph of feldspar (albite?) (fs) and actinolite (ac) replacing laminations in sandstone. The dark colour of the feldspar is due to hematization. Scale: 1 cm = 0.5 mm. (Sample 89-600b). This thin section is from the outcrop shown in Figure 12.

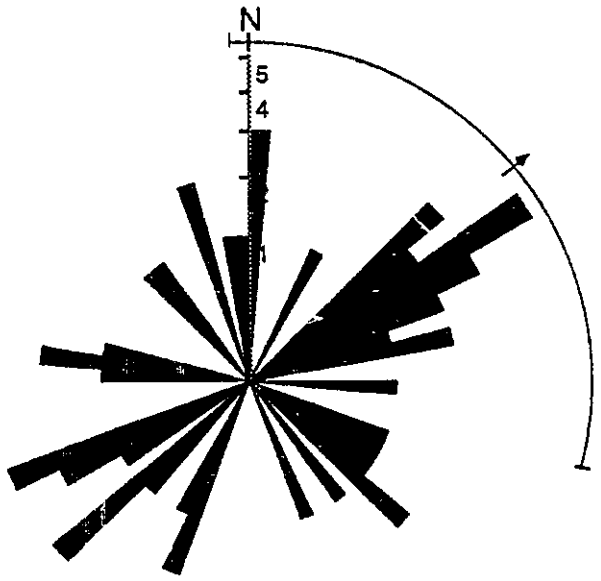

Figure 16. Rose diagram of strike orientations for 54 MAA veins in the Echo Bay area. The mode of their orientations is 060°; each interval represents 5°. Most veins are oriented NE-SW or NW-SE, and are therefore perpendicular and parallel to the plutons contacts, which generally trend NW-SE.

pink to mauve, subhedral to euhedral crystals up to 5 cm in length. The apatite occurs within magnetite or interstitial to magnetite and actinolite (Fig. 17). Actinolite veins with apatite cores also occur. Fluorine-rich chlorite and biotite are present in some veins. Fluorine-rich talc occurs in a specularite- and pyrite-bearing magnetite-actinolite vein above the southern part of the Glacier Lake pluton, and replaces actinolite in an actinolite vein within the Tut pluton. A vein within the Port Radium Formation above the Bertrand Lake pluton contains chloritized actinolite, epidote, quartz and hematite-lined vesicles less than 4 mm in diameter. Minor amounts of titanite and carbonate are present in all veins and replaced rocks studied in thin section. Minor pyrite is present in some veins.

MAA breccias, typically present near the contacts of the plutons, comprise angular to sub-rounded fragments of country rock up to 1 m in diameter in a matrix of medium- to coarse-grained magnetite (± pyrite, chalcopyrite), actinolite, apatite, epidote and albite (Fig. 18). Actinolite-rich breccias, which occur as pink (albitized?) fragments in a dark, actinolite-magnetite matrix, are also found near pluton contacts.

Chemical analyses of mineral phases from veins and pervasively altered rocks were obtained using the Cameca Camebax microprobe at McGill University (Appendix A). Actinolite (after the classification of Leake, 1978) contains from 0.02 to 1.34 wt% fluorine, 1.34 to 2.6% H_2O, and trace amounts of chlorine. A plot of Ca-Mg-Fe_{TOT} for actinolites from the Echo Bay area is given in Figure 19. The composition of the actinolite overlaps that of actinolites from skarns and actinolite schists (data from Leake, 1968). Titanium-rich Mg-biotite (4.32 wt.% TiO_2) occurs in a magnetite-poor, actinolite-rich altered andesite flow south of the Tut pluton. Fluorine-rich Mg-biotite (2.76 wt% F) occurs in siltstone of the Port Radium Formation which is replaced by MAA. Apatite from four samples of

Figure 17. Photomicrograph of a apatite (ap) - actinolite (ac) vein in intrusive porphyritic andesite; fs = secondary feldspar (albite?); gm = groundmass. Scale: 1 cm = 0.5 mm. (Sample 88-248).

Figure 18. Photograph of hydrothermal breccia with magnetite matrix in intrusive porphyritic andesite, Port Radium. Fragments up to several decimeters across are angular and have altered (albitized?) rims. The matrix is mostly magnetite; epidote, albite, pyrite, chalcopyrite and minor bornite occur within the same outcrop. The pen is 15 cm long.

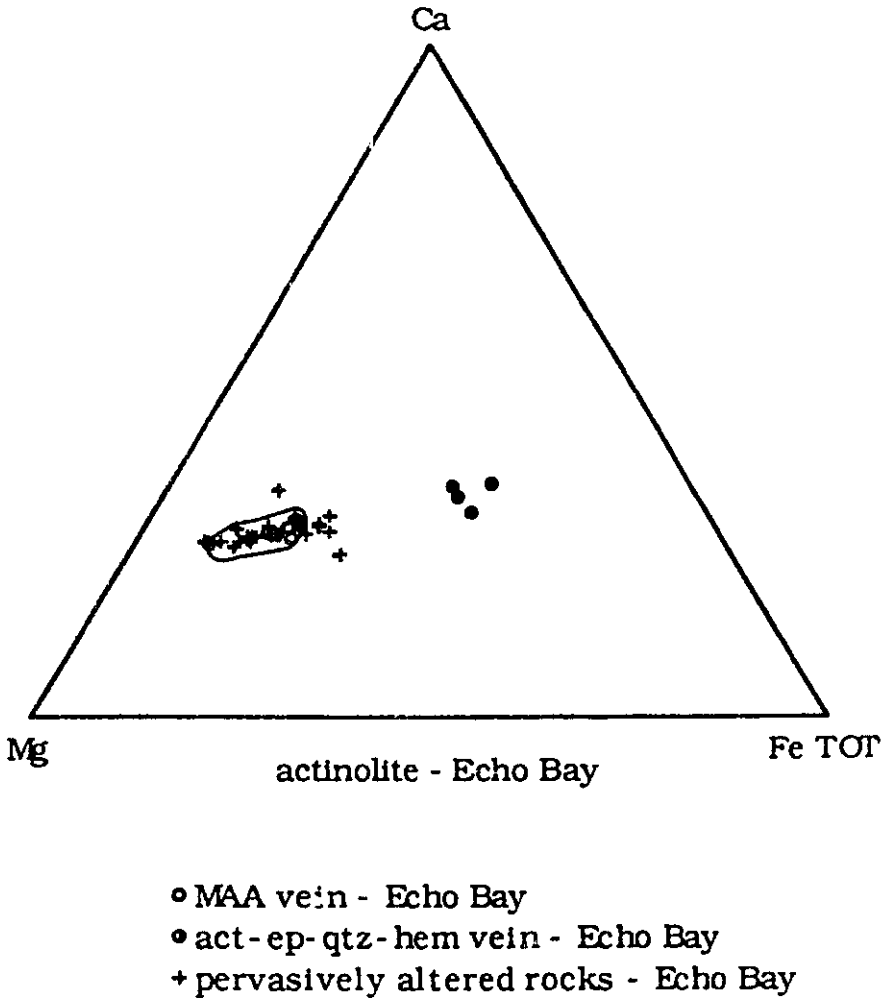

Figure 19. Plot of Ca-Mg-Fe_{TOT} for actinolites from magnetite-apatite-actinolite veins and pervasively altered rocks in the Echo Bay area. All samples, except actinolite from a actinolite-epidote-quartz-hematite vein plot within the field of actinolites from skarns.

pervasively replaced andesitic lava flows and MAA veins has fluorine contents of about three percent, similar to the fluorapatites in the Camsell River area (Hildebrand, 1986), and of those at Iron Mountain, Missouri and in northern Sweden (Parák, 1973). All magnetite in the MAA zone is characterized by low titanium (Fig. 20), low Cr_2O_3, and about 0.5 wt.% V_2O_5. Badham and Morton (1976) reported average values for magnetites from the Camsell River area of 0.12 ±0.03 wt.% V and 0.55 ±0.03 wt.% Ti from wet chemical analyses. The titanium content of the magnetites is similar to that in magnetites of other Kiruna-type ores, where it rarely exceeds 1% in the Kiruna ores and 0.5% in Chilean deposits. These values are lower than Ti contents of magnetites from volcanic or plutonic rocks. All vein magnetite is partially altered to hematite (martite) on rims and along cleavage planes. Primary hematite (specularite) also occurs in some of the veins, and is similar in composition to the martite. A single occurrence of ilmenite from an actinolitized andesite flow is manganese-rich (6.4 wt.% MnO). A titanium-manganese-iron mineral, possibly pyrophanite, occurs in trace amounts in two samples of magnetite- and actinolite-rich altered andesite flows.

Pyrite zone

The pyrite zone is characterized by the presence of disseminated pyrite crystals or pods up to several centimeters in diameter which form visible rusty patches on weathered outcrop surfaces, or extensive gossans where pyrite is locally abundant. Veins of massive pyrite up to 1 cm wide also occur. The pyrite zone occurs principally above the plutons, but locally within and below them. The zone is irregular and discontinuous, and is generally found at some distance above the roofs of the plutons. However, one gossan, more than 1 km across, is present directly above the northern portion of the Glacier Lake pluton. The

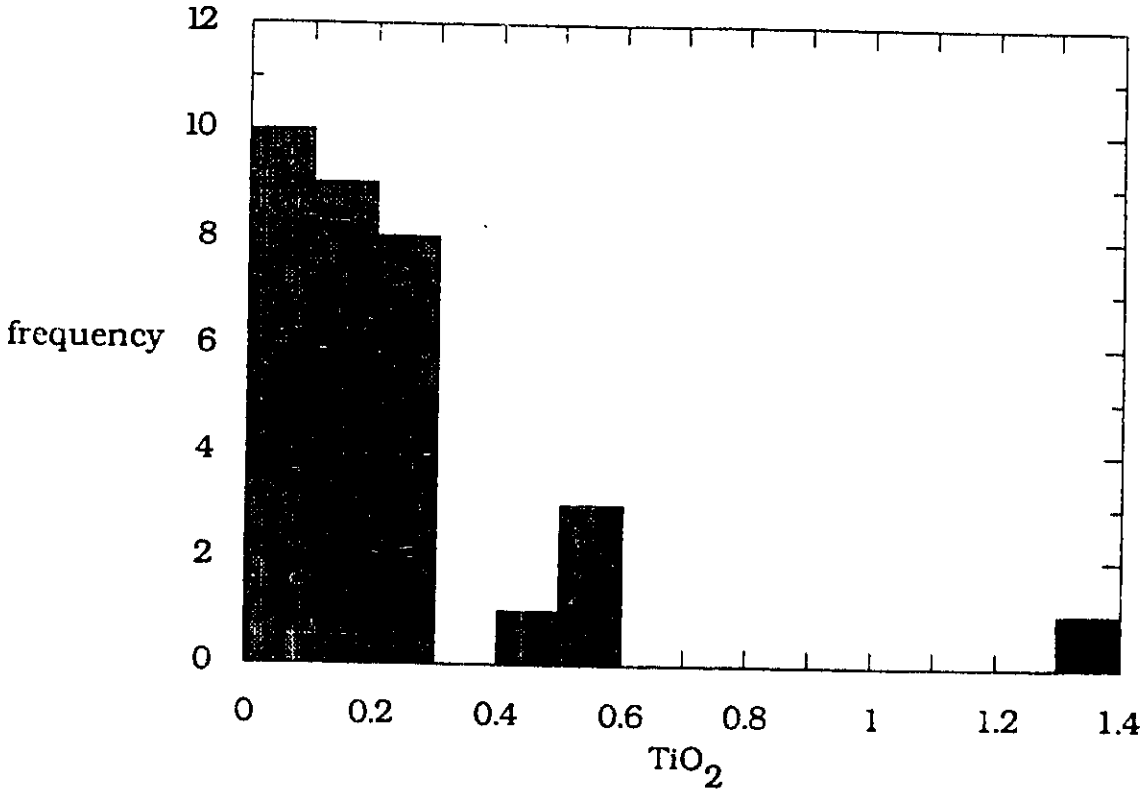

Figure 20. Histogram of TiO_2 for magnetites magnetite-apatite-actinolite veins and pervasively altered rocks in the Echo Bay area.

pyrite zone commonly overlaps the MAA zone, and in one outcrop north of Port Radium, pyrite is disseminated throughout magnetite-apatite-actinolite rock which is cut by a pyrite vein (Fig. 21), which indicates that the deposition of the sulphide zone occurred after formation of the MAA zone.

In thin section, pyrite occurs as finely disseminated, subhedral to euhedral crystals less than 0.5 mm across. Titanite is commonly present in rocks of the pyrite zone as anhedral crystals adjacent to pyrite and magnetite. One sample is cut by a 0.1 mm-wide pyrite-titanite veinlet. Pyrite also replaces magnetite within the MAA zone locally (Fig. 22), and is itself replaced by hematite (Fig. 23).

A possible subzone of the pyrite zone east of Port Radium (Fig. 8) is characterized by the presence of finely-disseminated chalcopyrite within the groundmass and within amygdules in andesitic lava flows. The zone is subparallel to stratigraphy. Higher concentrations of pyrite and chalcopyrite are present in sedimentary rocks than in andesitic lavas and porphyries. This may be due to differences in permeability and/or composition of the two host lithologies.

Distribution of alteration

All of the plutons of the Mystery Island intrusive suite have associated zoned alteration haloes, although the zones are somewhat irregular and discontinuous. The type and distribution of alteration varies slightly with each pluton, and detailed descriptions of the alteration facies associated with each of the plutons are given below (see Plate 1).

Bertrand Lake pluton

Altered rocks adjacent to the Bertrand Lake pluton (Fig. 5) are albitized and sedimentary rocks of the Port Radium Formation are replaced by actinolite along bedding

Figure 21. Photograph of a pyrite vein cutting magnetite-apatite-actinolite rock in an andesitic lava flow.

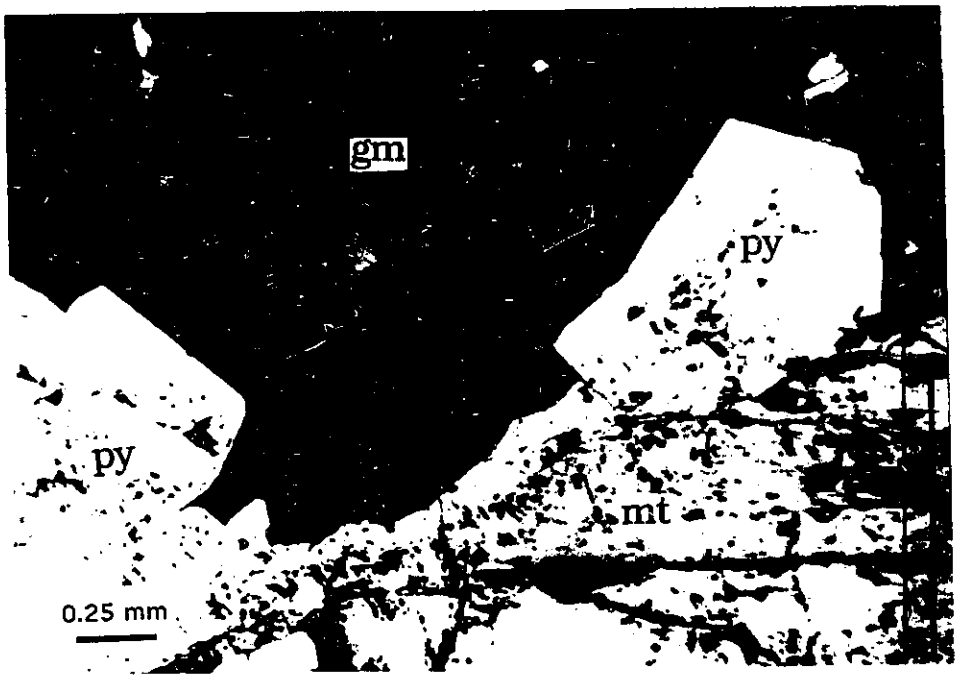

Figure 22. Photomicrograph (reflected light) of pyrite growing on magnetite in pervasively altered andesitic lava flow; py = pyrite, hm = hematite, gm = groundmass. Scale: 1 cm = 0.25 mm. (Sample 88-135).

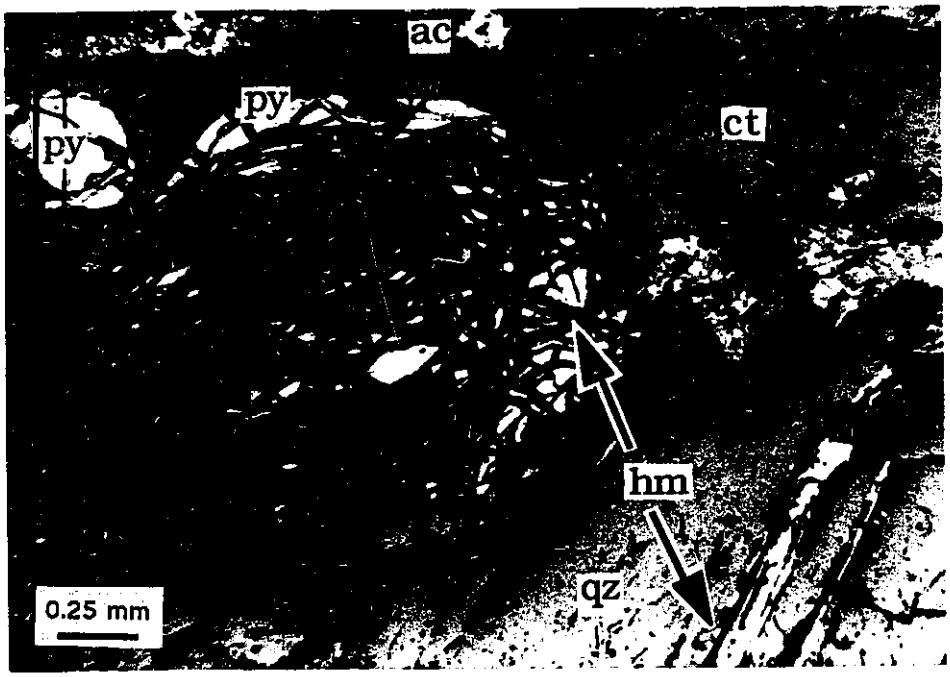

Figure 23. Photomicrograph (reflected light) of hematite replacing pyrite in pervasively altered andesitic lava flow; py = pyrite, hm = hematite, qz = quartz, ac = actinolite. Scale: 1 cm = 0.25 mm. (Sample 89-495).

planes. Andesitic lava flows of the Echo Bay Formation are cut by small veinlets and disseminations of actinolite, and, less commonly, actinolite-magnetite. Apatite was observed, but is uncommon. Numerous small veins of actinolite, apatite, actinolite-magnetite and actinolite-magnetite-apatite cut the pluton near the upper contact, and within a small plug just above the pluton. Alteration associated with the Bertrand Lake pluton is much less extensive than for the other plutons.

McLeod Lake pluton

Only the northernmost portion of the pluton was mapped in detail. Alteration was not extensive, and consisted of albitization close to, and within intrusive contacts, and localized areas of MAA and pyrite (Fig. 6 and Plate 1).

Contact Lake pluton

Rocks above the Contact Lake pluton (Fig. 6) show the most spectacular example of alteration effects in the Echo Bay area. Most altered rocks are concentrated within a zone roughly parallel to the roof of the southeastern half of the pluton, although there is minor alteration both below and within the pluton. Above the pluton, alteration extends outward in a narrow zone which has a core of intensely albitized andesite overlapped by broader area of intense magnetite-apatite-actinolite alteration. Albitized andesitic lava flows pervasively replaced by MAA are cut by pods and veins of actinolite-magnetite-apatite which are generally 1 to 5 cm wide, but range up to 15 cm wide. This area of intensely altered rock may reflect the presence of an upward protrusion of the pluton below the surface, or an area of localized fluid flow. Locally MAA constitutes up to 20% of the rock, which also contains fine- to coarse-grained albite. Subhedral, mauve apatite crystals up to

5 mm comprise up to 5% of the rock. Pyritic alteration is also well-pronounced as gossans greater than 50 m in width, which overlap both the albite and MAA zones.

Glacier Lake pluton

Alteration near the Glacier Lake pluton (Figs. 7, 8) is manifested by large, irregular zones of intense pyritization above the pluton. Minor disseminated actinolite and veins less than 3 cm wide of actinolite occur within the pluton and in andesitic lava flows near the upper and lower contacts of the pluton. The MAA zone is restricted to a narrow U-shaped zone near the southern end of the pluton (Fig. 7), where large veins of coarse actinolite-magnetite-apatite up to 80 cm wide contain magnetite crystals to 8 cm. Directly below the pluton, pervasive albitization, magnetite-apatite-actinolite alteration and breccias are present in a narrow, elongate zone adjacent to a narrow extension of the pluton perpendicular to the lower contact (Fig. 7).

Tut pluton

The upper contact of the Tut pluton is not exposed, since the pluton crops out in the core of a syncline (Hildebrand, 1981; 1984a). At the southwestern contact, extensive albitized zones are present both within the pluton and the country rocks (Fig. 8). Near Glacier Lake, actinolite pods and veins up to 1.5 m thick are present within the pluton. In two locations, near plutonic contacts, zones of breccia up to 3 m across contain subrounded, very fine-grained pink fragments up to several centimeters in diameter in an actinolite- and magnetite-rich matrix. Discontinuous veins of specular hematite to 3 cm wide also occur locally within the pluton.

All three zones of altered rock are found southwest of the pluton, and extend west to the shore of Great Bear Lake and south to Port Radium. However, albitized rocks increase

westward toward Great Bear Lake, and MAA occurs east of the lake, about 500 m from the shore. The pyrite zone is present east of the MAA zone. This suggests the former presence of another pluton to the west, possibly an extension of the Bertrand Lake pluton. A small, fault-bounded portion of a pluton very similar in texture and composition to the Mystery Island intrusive suite occurs on Cobalt Island at Port Radium (Fig. 8) (Reardon, 1990), and may be a part of another pluton.

Whole-rock geochemical analyses

Sixty-four samples from the Labine Group and Mystery Island intrusive suite were analyzed for major, trace and rare earth elements at the Geological Survey of Canada (Appendix B). The data are given in Table 2. All data used in the plots were recalculated to 100% on a volatile-free basis. See Plate 1 for sample locations.

Andesite

The susceptibility of the andesitic lava flows to alteration is reflected in their volatile contents. Andesite lava flows of the Echo Bay Formation have variable water contents ranging from 0.9 to 4.8 wt.%. CO_2 contents are also variable, ranging from 0.1 to 4.7 wt.%. Elemental variation is greater in the andesites as compared to the plutons.

Major, minor, and trace elements for altered andesitic lava flows ranging from 58 to 60.6 wt.% SiO_2 within the alteration haloes of the Glacier Lake pluton and Bertrand Lake pluton, and for andesitic lava flows ranging from 54.5 to 56 wt.% SiO_2 within the alteration haloes of the Contact Lake pluton were plotted against K_2O and Na_2O (Figs. 24a and b). Samples with limited ranges of SiO_2 content were used to eliminate the effects of elemental variation due to magmatic differentiation. The samples with higher K_2O contents are enriched in Ba, Sr, Rb, Zr, and Al_2O_3 and depleted in FeO, MgO, MnO and REEs (Fig. 24a).

Table 2. Major, minor and trace element analyses for andesitic lava flows of the Echo Bay Formation and plutons of the Mystery Island intrusive suite. Major elements in weight % and trace elements in ppm.

	H-79-202	H-77-124	P-79-171	H-79-80	H-77-52	H-77-170	C-87-1	C-87-2	C-87-3	C-87-4	C-87-5	C-87-6	C-87-7
TYPE	P	P	P	P	P	P	P	P	P	P	P	P	P
SiO2	57.00	58.48	60.70	61.38	61.78	67.16	68.20	67.10	68.00	63.80	65.40	66.40	64.50
TiO2	0.99	0.79	0.53	0.62	0.60	0.37	0.47	0.48	0.49	0.55	0.52	0.52	0.50
Al2O3	17.60	16.98	17.68	17.24	14.79	14.69	14.30	14.60	14.40	15.10	14.60	14.40	15.00
Fe2O3	2.53	2.43	2.10	2.18	2.17	1.94	1.20	1.20	1.10	1.30	1.00	0.10	1.20
FeO	2.38	3.65	5.21	5.02	4.63	3.90	3.20	3.10	3.90	4.80	4.30	5.40	4.00
MnO	0.34	0.28	0.44	0.43	0.18	0.08	0.08	0.07	0.11	0.10	0.09	0.10	0.10
MgO	4.03	3.72	3.55	2.71	3.78	1.85	1.83	1.30	1.51	2.12	1.47	1.61	1.77
CaO	6.80	4.81	1.94	4.78	5.03	1.23	1.42	1.79	1.32	2.21	2.05	0.69	1.21
Na2O	5.07	5.91	4.32	2.74	2.67	1.24	2.10	1.80	1.20	2.40	2.20	1.80	1.50
K2O	2.56	2.78	3.12	2.63	4.37	7.42	6.25	6.38	6.98	4.98	5.62	6.24	6.81
P2O5	0.27	0.19	0.22	0.26	0.00	0.13	0.11	0.10	0.10	0.12	0.12	0.12	0.11
S							0.00	0.00	0.00	0.01	0.01	0.03	0.00
H2O	2.12	4.34	2.96	2.74	2.34	2.98	1.90	1.10	2.00	1.80	1.50	1.50	2.20
CO2							1.00	0.50	0.90	0.50	0.60	0.50	0.90
total	102.14	104.37	102.97	102.75	102.34	102.99	99.86	99.82	100.01	99.79	99.48	100.01	99.80
Nb	6	6	5	4	13	20	0	0	0	0	0	0	0
Zr	139	152	136	110	166	237	228	225	232	210	245	243	233
Y	28	27	18	20	29	16	7	8	0	9	8	32	8
Sr	271	185	296	438	299	125	126	181	106	181	178	111	84
Rb	97	92	95	93	162	281	230	291	254	215	258	258	257
Ba	864	714	1247	1098	896	1332	808	798	998	873	918	760	977
Pb	173	21	7	14	22	12	13	29	16	42	20	20	15
Zn	402	275	375	251	192	60	76	47	38	100	52	43	75
Cu	48		9	12	10	24	41	34	19	150	34	43	25
Ni	3	17	4		41	24	14	15	15	20	16	17	15
Co	0	0	0	0	0	0	16	13	13	21	17	13	14
Cr	9	84			122	23	43	40	47	58	39	36	47
V	155	195	104	98	124	60	88	61	65	90	72	68	66
Be							2.9	2.5	2.6	2.4	2.6	2.9	3.2
La	0.0	15.1	0.0	0.0	33.7	10.1	35.0	53.0	57.0	98.0	100.0	170.0	26.0
Yb		2.3			1.8	2.0	1.9	2.0	2.0	1.9	2.1	2.1	2.3

	C-87-8	C-87-9	C-87-10	C-87-11	C-87-12	C-87-13	C-87-14	C-87-15	C-87-16	C-87-17	C-87-18	C-87-19	C-87-20
TYPE	P	P	P	P	P	P	P	P	P	P	P	P	P
SiO2	65.70	64.10	64.40	64.30	63.00	62.90	62.60	61.40	59.30	63.00	62.40	63.00	66.10
TiO2	0.50	0.50	0.53	0.45	0.61	0.50	0.62	0.60	0.62	0.59	0.57	0.54	0.50
Al2O3	14.30	14.90	14.80	15.50	15.40	15.20	15.10	15.40	15.40	15.40	15.20	14.50	14.70
Fe2O3	1.20	1.30	3.30	1.40	2.40	1.40	2.60	2.00	3.10	1.10	1.10	1.90	0.80
FeO	4.20	5.60	2.10	3.80	3.50	4.00	4.00	4.10	3.40	4.10	5.00	4.80	4.30
MnO	0.10	0.22	0.25	0.26	0.18	0.22	0.23	0.25	0.24	0.23	0.19	0.15	0.08
MgO	1.90	2.20	1.94	2.05	2.43	1.50	2.07	2.73	2.32	2.68	2.97	2.60	1.39
CaO	0.61	2.05	1.31	3.05	2.91	3.30	2.95	3.64	4.92	2.99	2.86	3.43	1.62
Na2O	1.60	2.10	2.50	2.40	2.50	2.60	3.50	2.70	2.70	3.10	2.30	2.70	2.30
K2O	6.43	4.61	6.05	5.42	4.97	5.44	3.83	4.40	3.79	5.23	5.12	4.39	5.79
P2O5	0.12	0.14	0.14	0.14	0.15	0.13	0.16	0.14	0.17	0.14	0.16	0.14	0.12
S	0.00	0.00	0.02	0.01	0.03	0.00	0.00	0.00	0.00	0.00	0.04	0.00	0.00
H2O	2.20	2.50	1.60	1.50	1.30	1.60	1.70	1.90	1.60	1.30	1.60	1.50	1.40
CO2	0.40	0.40	0.60	0.20	0.20	0.70	0.50	0.90	1.60	0.20	0.20	0.20	0.40
total	99.27	100.62	99.98	100.48	99.58	99.49	99.87	100.17	99.18	100.07	100.32	99.86	99.70
Nb	0	0	0	0	0	0	0	0		0	0	0	0
Zr	254	210	209	225	179	209	265	185	6	202	267	231	238
Y	0	0	0	0	0	0	0	0		0	1	0	0
Sr	81	184	94	283	284	231	279	258		275	225	278	185
Rb	276	159	182	184	184	170	129	91	304	141	182	115	272
Ba	814	1036	1864	1335	1136	1067	1654	1586	1000	1444	1000	1103	825
Pb		17	17	24	14	27	16	30	129	21	13	18	22
Zn		160	210	110	130	91	110	140	171	75	93	86	43
Cu		36	19	80	16	14	26	22		24	76	21	38
Ni		12	7	9	15	12	14	15		22	24	18	16
Co		18	15	16	22	15	17	21		20	21	21	17
Cr		48	50	44	51	45	73	67		90	77	81	38
V		80	77	83	98	80	110	110	0	84	110	100	69
Be		2.5	2.2	2.0	1.9	2.2	2.0	1.8		1.6	1.8	1.8	2.7
La		26.0	53.0	47.0	61.0	25.0	45.0	40.0	0.0	43.0	55.0	31.0	58.0
Yb		1.8	1.9	1.9	1.9	1.7	2.0	1.8		1.5	1.7	2.0	1.9

* Recalculated to 100% P = pluton A = andesite D = dacite

Table 2. continued.

	88-R062	88-R065	88-R088	88-R093	88-R156	88-R302	89-R410	89-R512	H-77-53	H-77-53b	H-77-80	H-77-51	H-77-96
TYPE	P	P	P	P	P	P	P	P	A	A	A	A	A
SiO2	65.70	59.80	68.50	67.00	58.70	59.00	69.90	59.50	57.65	59.03	59.42	59.98	60.42
TiO2	0.53	0.69	0.66	0.46	0.67	0.77	0.38	0.67	0.66	0.48	0.73	0.74	0.79
Al2O3	14.50	15.90	16.50	14.60	14.80	15.70	14.30	15.30	17.43	15.52	15.90	16.19	17.94
Fe2O3	0.40	2.80	0.40	1.40	0.00	1.90	1.40	2.20	2.28	2.12	2.34	2.30	2.34
FeO	5.80	3.70	1.30	2.50	6.50	5.20	1.80	4.50	7.61	6.52	7.66	3.51	3.45
MnO	0.14	0.30	0.13	0.09	0.65	0.18	0.08	0.18	0.34	0.47	0.47	0.18	0.16
MgO	1.93	3.06	0.85	1.65	4.16	3.74	1.55	3.27	4.23	3.72	3.92	2.70	1.88
CaO	0.41	4.04	1.32	2.17	3.80	3.59	0.58	5.93	1.62	3.20	1.26	3.72	5.01
Na2O	2.10	2.40	5.30	2.20	2.90	2.30	2.30	2.70	4.08	4.06	3.81	2.97	3.69
K2O	3.74	3.74	3.71	5.65	4.15	4.40	6.15	3.63	3.81	2.59	4.20	5.37	4.03
P2O5	0.12	0.15	0.02	0.10	0.19	0.19	0.13	0.20	0.28	0.28	0.08	0.26	0.29
S	0.00	0.00	0.05	0.00	0.00	0.00	0.00	0.01	0.00	0.00	0.00	0.00	0.00
H2O	2.10	2.10	0.80	1.40	2.10	1.80	1.40	0.50					
CO2	0.30	0.90	0.30	0.60	0.30	0.60	0.30	0.60					
total	99.90	99.80	99.70	100.00	100.20	99.70	100.30	99.50	99.99	99.99	99.99	100.00	100.00
Nb	0	0	6	0	0	0	0	0	10	14	10	10	11
Zr	280	190	250	220	140	360	240	190	149	137	162	162	163
Y	18	19	13	20	18	19	19	26	18	45	24	27	25
Sr	76	270	96	230	290	380	140	350	129	62	64	555	553
Rb	220	120	120	210	150	130	300	20	119	48	89	124	120
Ba	800	1200	340	840	1500	1100	690	810	1028	511	1499	1624	1150
Pb	11	7	9	9	8	0	11	7	9	16	9	0	21
Zn	39	120	23	53	350	120	42	84	211	136	340	94	144
Cu	110	42	19	10	31	65	7	79	0	24	33	57	49
Ni	15	11	14	4	24	23	8	26	0	0	0	0	0
Co	9	17	10	9	19	16	6	18	88	250	54	17	15
Cr	130	76	97	130	150	130	76	140	173	112	182	107	110
V	56	100	27	49	110	100	35	120					
Be	1.9	2.0	1.6	2.3	1.8	2.0	3.1	2.0					
La	56.0	35.0	25.0	53.0	34.0	29.5	58.0	28.0					
Yb	1.9	1.9	1.5	2.1	1.7	1.8	1.9	2.0					

	H-77-50	H-77-15	H-77-140	88-R010	88-R016	88-R020	88-R024	88-R033a	88-R038	88-R041	88-R051	88-R056	88-R066
TYPE	A	A	D	A	A	A	A	A	A	A	A	A	A
SiO2	60.57	63.59	67.32	60.20	52.90	57.60	62.60	59.00	61.80	56.60	66.90	58.60	53.60
TiO2	0.69	0.49	0.42	0.66	0.76	0.71	0.60	0.67	0.58	0.73	0.54	0.62	0.74
Al2O3	15.30	17.10	17.33	17.30	14.10	15.70	13.60	15.90	11.90	14.60	15.50	13.60	9.60
Fe2O3	2.26	2.05	2.01	1.40	6.30	3.50	2.60	1.80	2.10	1.60	0.90	3.80	0.00
FeO	4.87	3.84	1.57	3.00	8.60	4.80	6.90	5.90	10.40	6.30	2.70	9.00	12.60
MnO	0.27	0.07	0.17	0.20	0.19	0.30	1.11	0.17	0.14	0.18	0.10	0.18	0.27
MgO	4.95	1.26	2.06	1.09	5.33	3.10	2.31	4.18	5.29	3.89	1.66	3.23	8.77
CaO	4.27	1.88	1.63	2.74	1.07	4.26	0.18	2.16	0.27	4.55	0.98	0.99	4.63
Na2O	2.30	3.99	1.85	7.90	3.10	2.00	0.00	2.70	0.00	2.70	4.70	4.00	4.10
K2O	4.31	5.59	5.58	1.37	3.08	4.19	5.30	4.40	1.99	4.39	3.41	2.89	0.57
P2O5	0.16	0.15	0.10	0.76	0.29	0.21	0.14	0.16	0.16	0.19	0.02	0.23	0.04
S	0.00	0.00	0.00	0.00	0.05	0.01	0.57	0.05	0.52	0.02	0.00	0.33	0.02
H2O				1.20	3.60	2.10	3.10	2.53	4.80	1.60	1.50	2.30	2.60
CO2				1.30	0.00	1.60	1.40	1.60	0.20	1.10	1.10	0.40	1.60
total	100.00	100.01	100.01	99.60	100.30	100.40	100.70	100.40	100.30	99.30	100.10	100.20	99.30
Nb	11	17	20	10	0	0	0	0	0	0	0	6	0
Zr	166	213	233	150	110	160	180	160	140	120	240	110	81
Y	29	30	32	32	13	20	18	18	15	19	4	24	52
Sr	305	216	107	130	89	360	55	340	18	340	80	45	59
Rb	125	183	210	36	76	140	190	170	100	200	99	80	46
Ba	880	1198	670	480	903	1400	1200	700	290	850	600	500	180
Pb	16	16	5	4	10	12	12	19	8	8	14	120	11
Zn	260	48	62	45	140	240	110	90	50	41	15	190	110
Cu	0	0	0	47	190	50	23	18	11	15	30	21	26
Ni	0	0	0	9	150	12	31	11	49	14	1	19	17
Co	197	10	3	5	34	18	14	4	15	17	4	14	8
Cr	147	85	33	89	420	110	180	63	240	89	140	110	330
V				46	160	130	82	100	110	140	1	200	160
Be				1.3	2.1	1.9	2.2	2.1	1.9	1.8	1.5	2.8	3.6
La				42.5	23.0	31.5	27.0	13.0	19.5	27.5	6.9	32.5	15.0
Yb				2.7	1.3	2.0	1.8	1.9	1.4	1.8	0.5	2.0	5.7

* Recalculated to 100% P = pluton A = andesite D = dacite

Table 2. continued.

	88-R063a	88-R148	88-R150	88-R177	88-R180	88-R182	88-R186	88-R222	88-R303	H-77-93	89-R404	88-R019
TYPE	A	A	A	A	A	A	A	A	A	A	A	A
SiO2	54.80	63.20	53.70	51.90	46.00	59.40	56.80	70.80	53.50	70.20	67.30	61.50
TiO2	0.66	0.62	0.73	0.59	0.98	0.59	0.72	0.27	0.90	0.51	0.54	0.71
Al2O3	13.10	15.50	15.00	13.60	15.70	16.50	16.50	7.80	16.90	13.20	17.40	15.00
Fe2O3	7.10	2.50	2.00	1.30	12.50	0.80	1.20	3.00	1.60	0.90	0.70	8.10
FeO	5.40	4.60	8.10	5.70	8.60	6.80	5.80	11.30	7.70	2.50	1.40	1.70
MnO	0.22	0.14	0.27	0.15	0.14	0.07	0.21	0.26	0.36	0.23	0.12	0.15
MgO	5.76	1.67	5.65	3.22	2.67	3.19	2.07	1.36	3.93	1.43	1.07	1.80
CaO	2.35	1.04	6.65	8.46	5.69	5.87	4.35	0.07	4.97	1.74	0.78	0.82
Na2O	5.00	3.80	2.50	4.50	5.60	2.50	6.60	0.00	4.20	4.10	6.50	0.30
K2O	1.48	4.62	3.20	1.57	0.52	1.91	1.39	0.33	2.86	2.72	0.70	7.19
P2O5	0.02	0.22	0.26	1.58	0.02	0.18	0.33	0.08	0.22	0.17	0.14	0.25
S	0.12	0.00	0.00	0.02	0.00	0.34	0.24	0.97	0.01	0.00	0.00	0.00
H2O	2.20	1.10	1.60	1.60	1.50	2.00	1.60	3.60	1.90	1.20	0.90	2.10
CO2	1.60	0.20	0.10	4.70	0.30	0.10	2.30	0.20	0.20	0.40	0.20	0.60
total	100.00	99.60	100.20	99.00	100.20	100.10	100.10	100.10	99.30	99.40	99.90	100.40
Nb	0	0	0	0	0	0	0	0	0	8	5	0
Zr	120	170	95	92	98	140	180	110	120	180	210	190
Y	31	24	17	54	17	18	25	10	19	16	13	25
Sr	180	210	480	380	380	300	150	7	380	53	110	64
Rb	44	160	100	63	11	98	31	16	110	96	39	220
Ba	440	1400	1100	520	60	410	800	270	820	370	150	1300
Pb	7	7	6	9	6	74	39	61	25	14	2	5
Zn	160	82	160	90	200	100	180	950	320	200	29	39
Cu	37	16	22	14	23	95	93	340	13	6	22	6
Ni	19	1	42	20	31	17	11	22	7	9	7	0
Co	10	11	25	12	15	20	14	110	17	8	4	6
Cr	97	70	180	80	66	83	54	65	32	150	42	64
V	330	74	160	140	580	110	100	43	150	36	26	97
Be	2.4	2.3	1.5	3.0	1.5	1.6	1.9	0.5	1.5	1.4	1.8	2.2
La	11.5	38.0	20.0	130.0	13.5	24.0	36.5	36.0	20.5	14.0	17.5	20.0
Yb	3.5	2.4	1.5	4.3	1.0	1.6	2.3	0.7	1.7	1.8	1.4	2.2

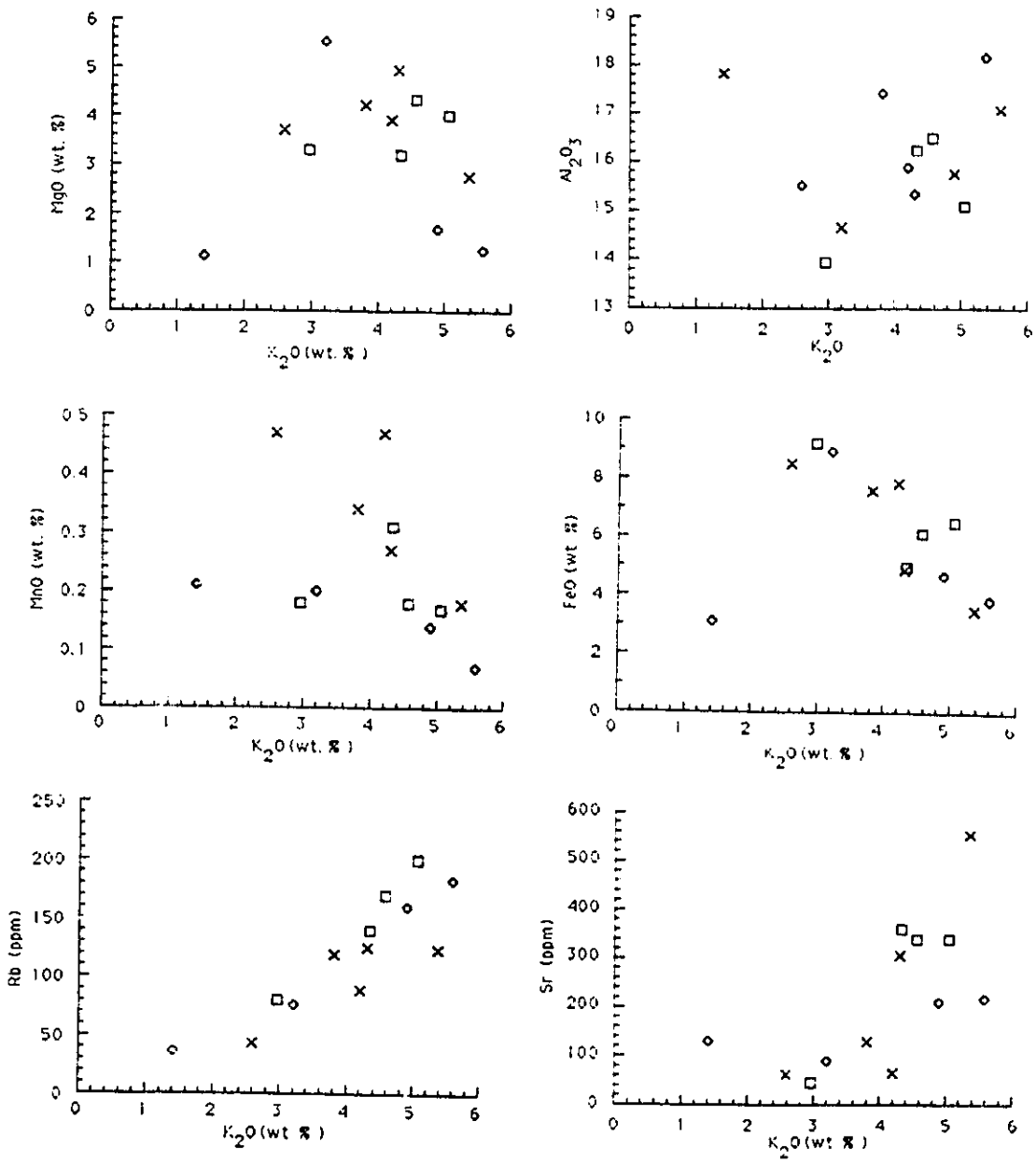

Figure 24. a) Plots of K_2O vs. MgO, Al_2O_3, MnO, FeO, Rb, Sr, Zr, Ba, Ce, Eu, Gd, and Dy for andesitic lava flows above the southern part of the Glacier Lake (squares), Contact Lake (diamonds) and Bertrand Lake (X) plutons. Samples with higher K_2O contents are enriched in Sr, Rb, Zr, Ba, and Al_2O_3 and depleted in FeO, MgO, MnO and REEs. The sample with a K_2O content of 1.5% is strongly albitized (Na_2O = 7.9%).

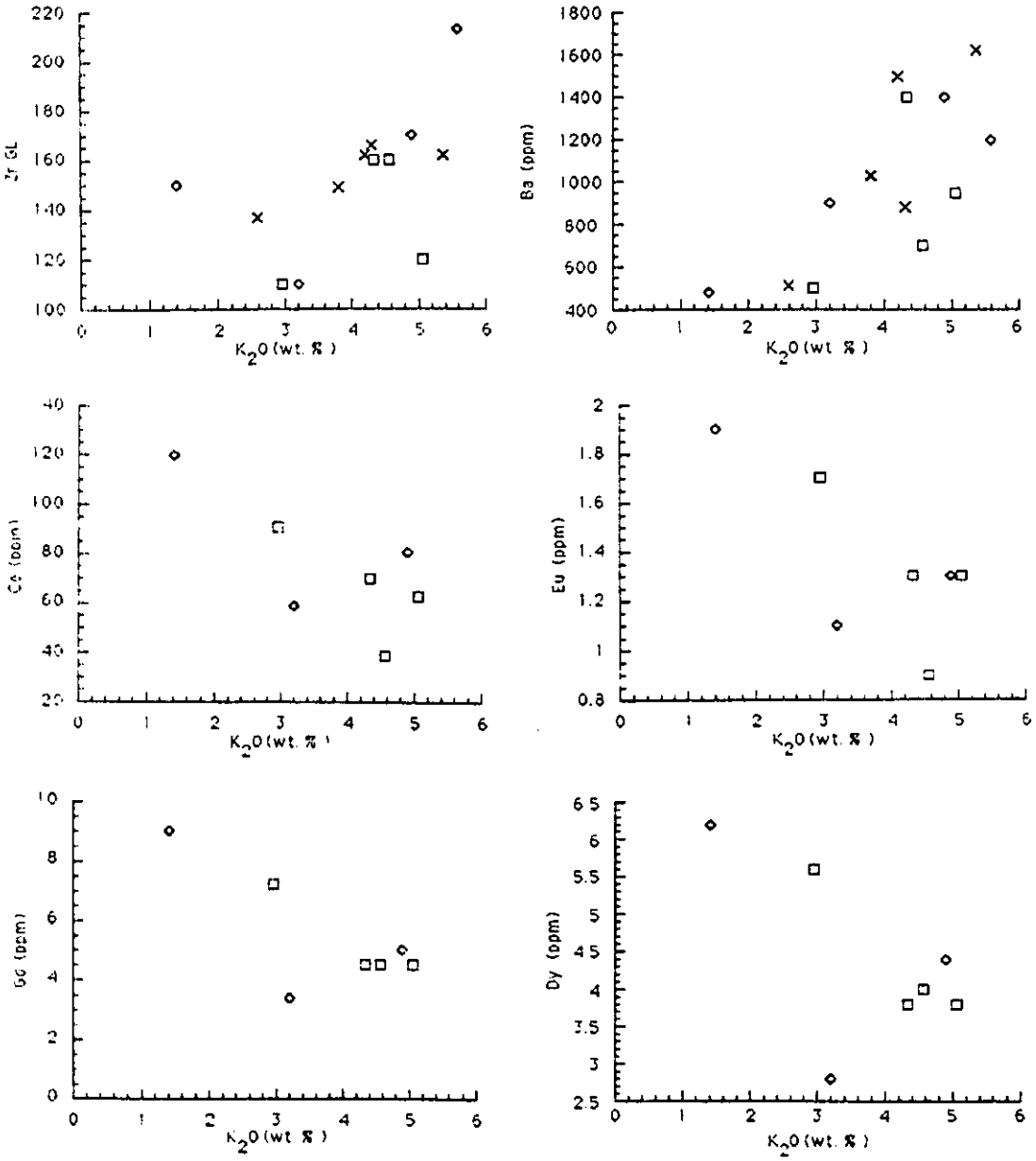

Figure 24. a) continued.

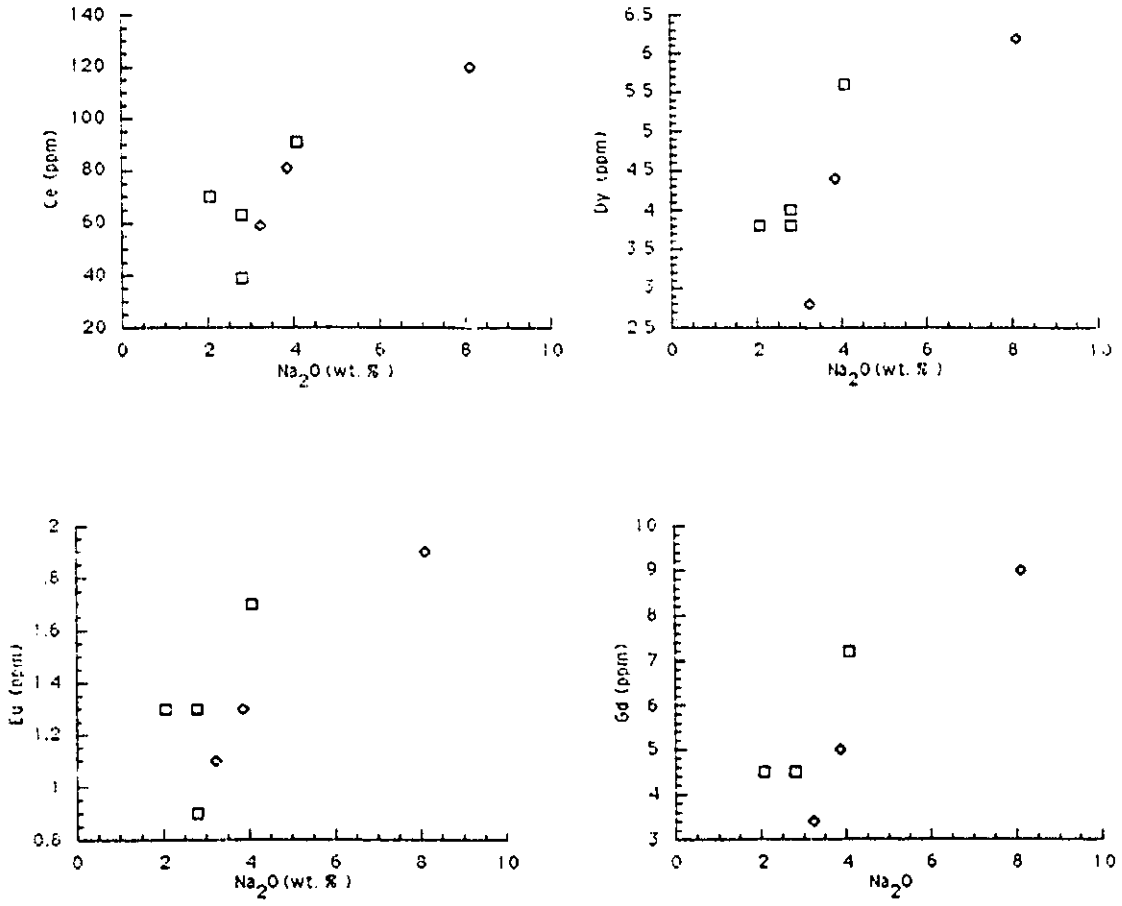

Figure 24. b) Plots of Na_2O vs. Ce, Eu, Gd, and Dy for andesitic lava flows above the southern part of the Glacier Lake and Contact Lake plutons.

One sample with a K_2O content of 1.5% is strongly albitized (Na_2O = 7.9%). Na-rich rocks are enriched in REEs (Fig. 24b), but Na_2O does not correlate with other elements. Na_2O and K_2O contents do not correlate. The strongly albitized sample has the highest P, Ti, Ca and REE contents, which is due to the presence of titanite and apatite in veinlets within this sample. Apatite may contain up to a few tenths of a percent of these elements (Koritnig, 1978), and titanite, has partition coefficients for the REEs similar to apatite or slightly greater (Henderson, 1980; Gromet and Silver, 1983). The positive correlation of K_2O with Ba, Sr, and Rb is probably due to the substitution of these elements in plagioclase and K-feldspar.

Plutons

Of the four plutons of the Mystery Island intrusive suite studied in detail (Tut, Glacier Lake, Contact Lake, Bertrand Lake), the Tut pluton is least altered, and shows a normal calc-alkaline magmatic trend of increasing K and decreasing Na with increasing SiO_2 content (Fig. 25). However, one sample from the Tut pluton is albitized, and contains 5.3 wt.% Na_2O (Fig. 25). The Bertrand Lake pluton is Na-metasomatized, as indicated by high Na contents for some of the samples. One sample from the Contact Lake pluton in Na-metasomatized, and has an elevated Na content and lower K content relative to other samples with similar Si contents. However, part of the Glacier Lake pluton is K-metasomatized, as indicated by elevated K_2O contents and decreased Na contents not correlative with an increase in SiO_2. The samples depleted in Na are also depleted in Ca. Four samples from the Contact Lake pluton, ranging in SiO_2 content from 64.1 to 65.1 wt.% SiO_2, and five samples from the Glacier Lake pluton ranging from 68.1 to 68.3 wt.% SiO_2 were used to evaluate the effects of Na- and K-metasomatism, respectively. In the Glacier Lake pluton, Na and K vary antithetically (Fig. 26a). No regular variation between these elements occurs in the Contact Lake pluton (Fig. 26a). K-metasomatism in the plutons has

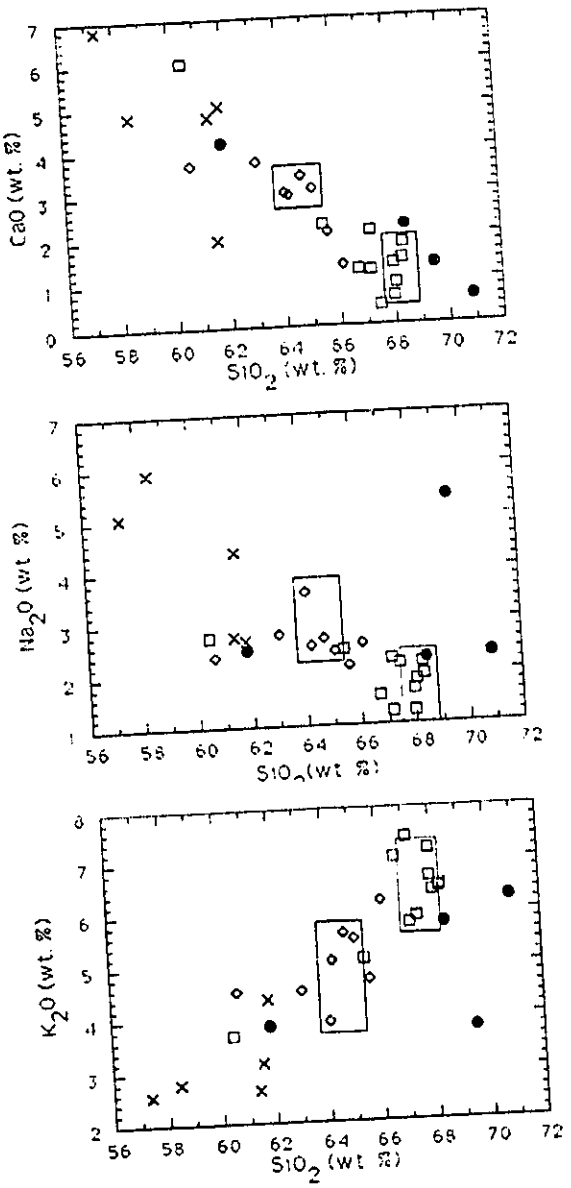

Figure 25. Plots of a) CaO vs. SiO_2 b) Na_2O vs. SiO_2; and c) K_2O vs. SiO_2 for the Tut (●), Bertrand Lake (X), Glacier Lake (squares), and Contact Lake (diamonds) plutons. Boxes indicate samples plotted in Figure 26. The Tut pluton is least altered, and shows a normal magmatic trend of increasing K and decreasing Na with increasing SiO_2 content. However, one sample is albitized. The Bertrand Lake and Contact Lake plutons are Na-matasomatized, as indicated by high Na contents which do not correlate with SiO_2 content. Part of the Glacier Lake pluton is K-metasomatized, as indicated by elevated K_2O contents not correlative with an increase in SiO_2.

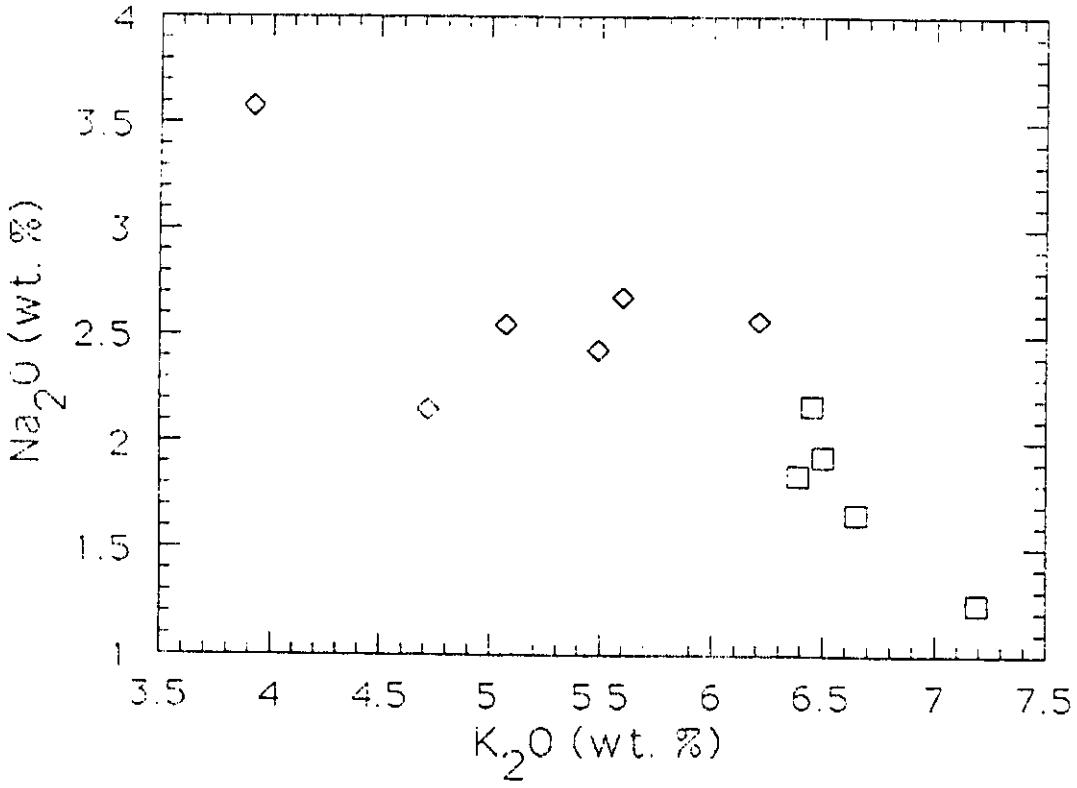

Figure 26. a) Plot of Na_2O vs. K_2O for samples with restricted ranges of SiO_2 content from the Glacier Lake (squares) and Contact Lake (diamonds) plutons. Na and K vary antithetically in the Glacier Lake pluton. No regular variation of Na_2O and K_2O is evident in the Contact Lake pluton.

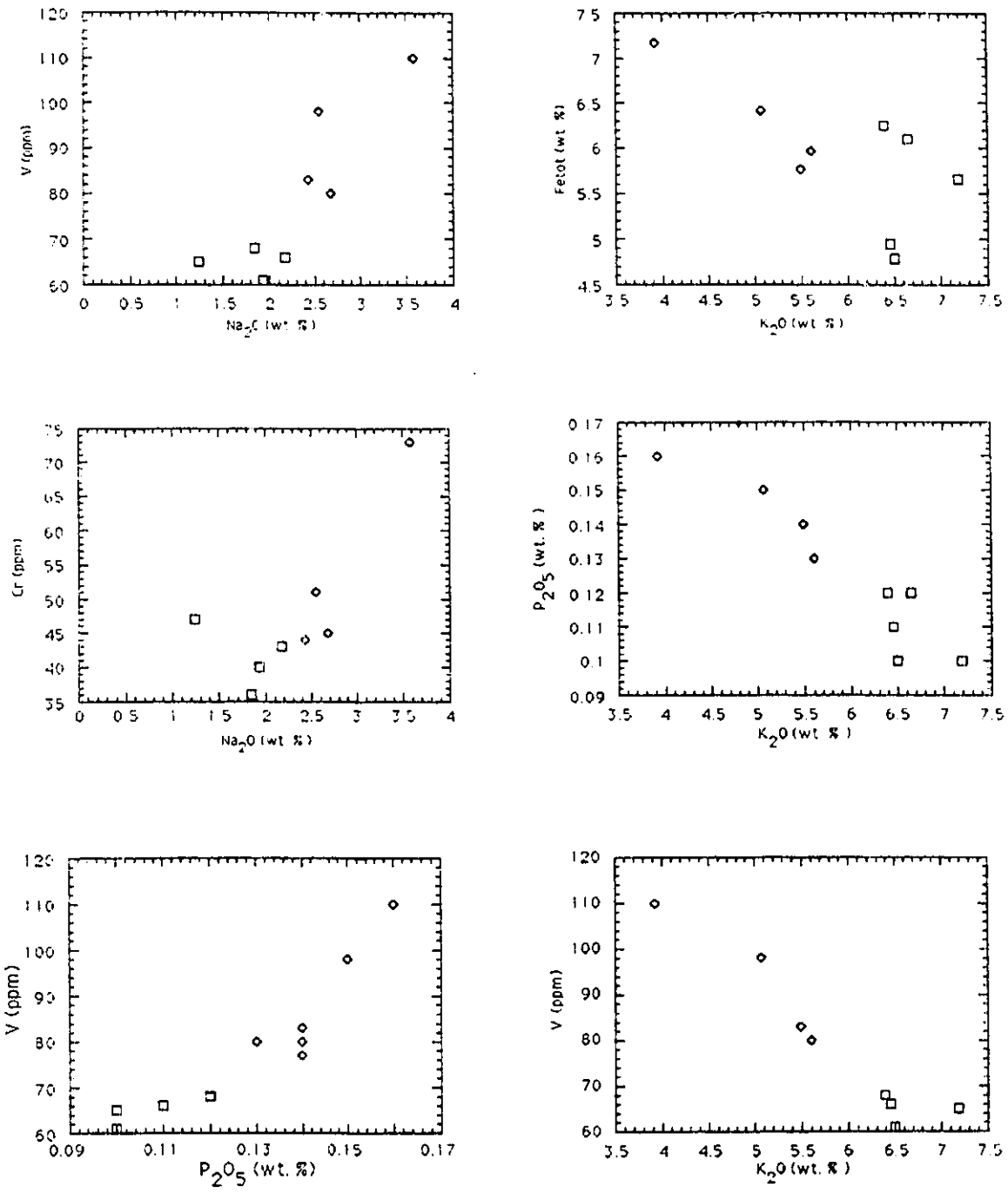

Figure 26. b) Plots of Na_2O vs. V and Cr; K_2O vs. Fe_{TOT}, P_2O_5, and V and V vs. P_2O_5 for the Glacier Lake (squares) and Contact Lake (diamonds) plutons. K-metasomatism in the plutons has caused depletion of Fe, P, and V; these elements vary antithetically with K_2O in both plutons. Cr and V increase with increasing Na_2O content.

caused depletion of Fe, P, and V; these elements vary antithetically with K_2O in both plutons (Fig. 26b). Cr and V increase with increasing Na_2O content (Fig. 26b).

Concentrations of SiO_2, Na_2O and K_2O (Fig. 27a) plotted vs. relative height in the pluton for the Glacier Lake pluton show a regular, antithetic variation of Na_2O and K_2O. SiO_2 is constant at 68 wt.% +/- 1 wt.%, except one sample from near the top of the pluton, which has slightly lower SiO_2 (65.5 wt.%) and K_2O (5 wt.%), and higher Na_2O (2.5 wt.%) relative to the other samples. In the Contact Lake pluton, K_2O and SiO_2 decrease with increasing height in the pluton (Fig. 27b). This may represent normal zoning of the pluton, from a more mafic rim to more silica-rich at the center. However, the bottom contact of the pluton is not exposed to confirm the distribution of this apparent zoning. Na_2O contents range from 2 to 3 wt.% and increase steadily with height in the pluton, except one albitized sample near the top of the pluton which has a slightly higher Na_2O content (3.6%) (Fig. 27b).

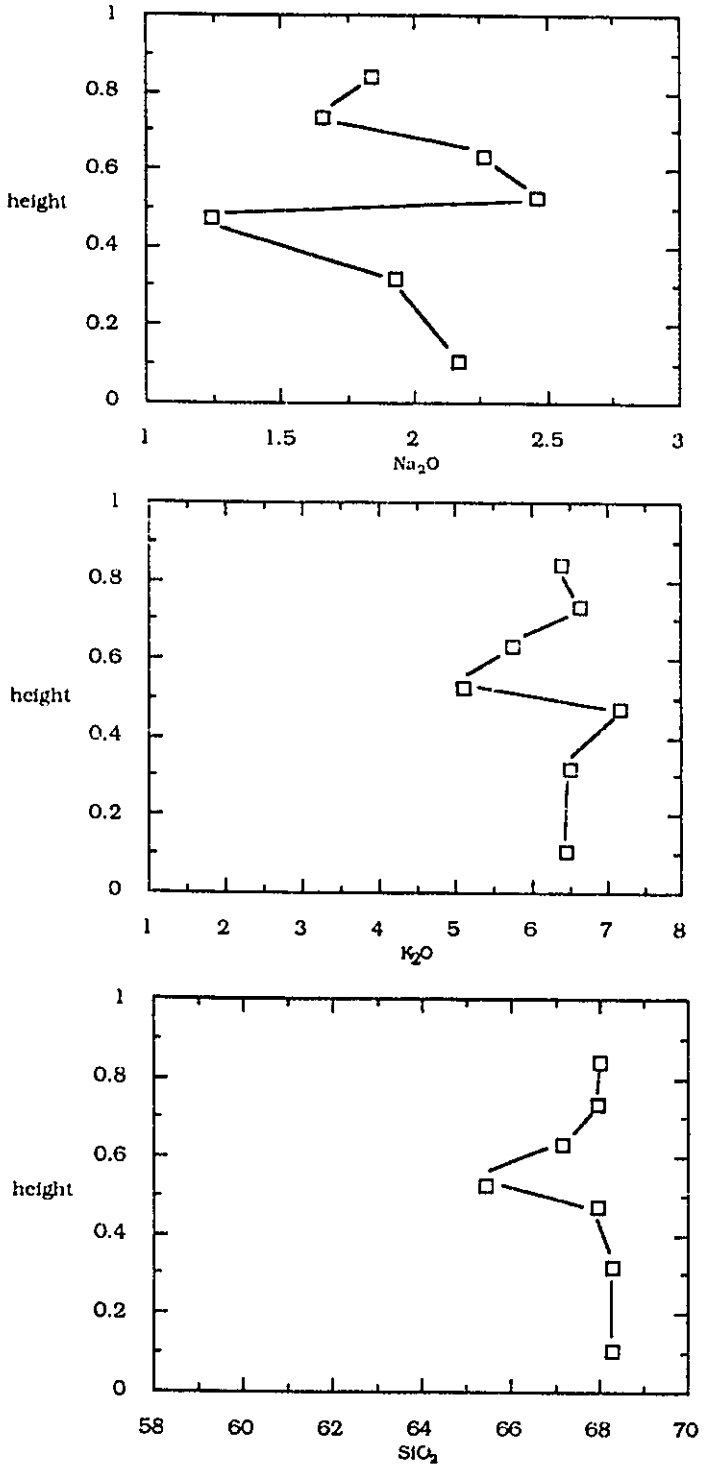

Figure 27. a) SiO_2, K_2O and Na_2O vs. relative height in the southern part of the Glacier Lake pluton. Na_2O and K_2O vary antithetically.

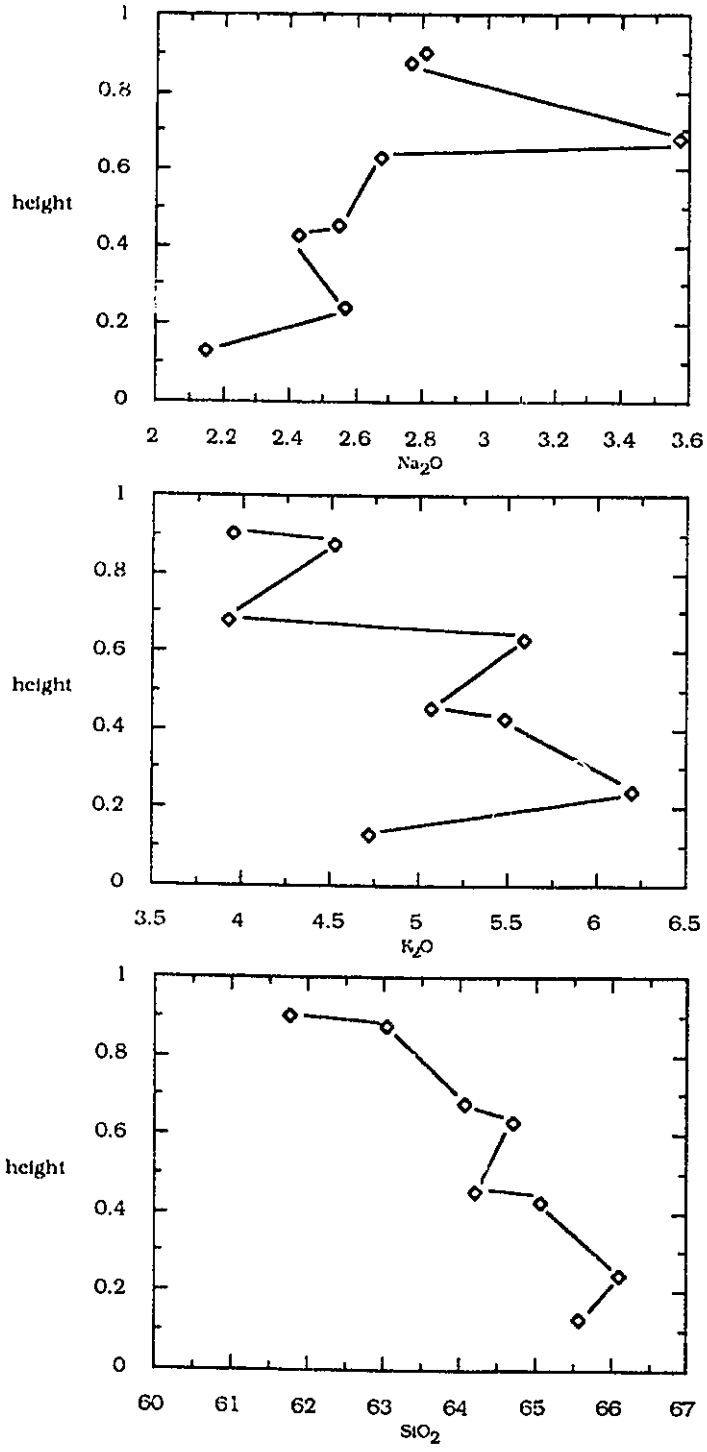

Figure 27. b) SiO_2, K_2O and Na_2O vs. relative height in the Contact Lake pluton. The pluton is reversely zoned, and K_2O and SiO_2 decrease towards the top of the pluton. Na_2O contents range from 2 to 3 wt.% and increase steadily with height in the pluton, except one albitized sample near the top of the pluton which has a slightly higher Na_2O content.

IV. STABLE ISOTOPE GEOCHEMISTRY

Stable isotope analyses of hydrogen, oxygen, carbon and sulphur were carried out on whole-rock samples, mineral separates and bulk fluid inclusions from the Port Radium and Echo Bay Formations, Mystery Island intrusive suite, and magnetite-apatite-actinolite veins and pervasively altered wall rocks. Sample locations are indicated on Plate 1. Isotopic compositions are reported in per mil deviation from SMOW (Standard Mean Ocean Water) for oxygen and hydrogen, PDB (Belemnitella americana, Peedee Formation) for carbon, and CDT (Cañon Diablo Troilite) for sulphur. Analytical methods are described in Appendix C.

Plutons and wall rocks

Oxygen and hydrogen

Whole-rock samples from the LaBine Group, Mystery Island intrusive suite and Richardson pluton were analyzed for their oxygen and hydrogen isotope ratios by standard techniques. Isotopic compositions and water contents of whole-rock samples are given in Table 3. Variation of $\delta^{18}O$ within the plutons and their altered wall rocks is small, and $\delta^{18}O$ ranges from +5.7 to +12.3‰ (Fig. 28). Seventy whole-rock hydrogen analyses were carried out on samples from the Port Radium Formation, Echo Bay Formation, the Mystery Island intrusive suite and the Richardson pluton. δD values for these rocks range from -92 to -56‰ (Fig. 29).

Port Radium Formation

Six samples of fine-grained sedimentary rocks of the Port Radium Formation, two carbonates and one siltstone at Port Radium, and two siltstones from above and below the Bertrand Lake pluton were analyzed. $\delta^{18}O$ values range from +7.8 to +11.4‰, and have a

Table 3. $\delta^{18}O$ and δD (‰, SMOW) and water content (wt.%) data for whole-rock samples.

ABBREVIATIONS:

AREA:

BTL	Bertrand Lake area
CBF	Cameron Bay Formation
CTL	Contact Lake area
MCL	McLeod Lake area
NGL	North Glacier Lake area
PR	Port Radium area
SGL	South Glacier Lake area
TUT	Tut pluton area

TYPE:

AND	andesite
BRC	breccia (volcanogenic)
CRB	sedimentary carbonate rock
DCT	dacite
DRT	diorite
DYK	dyke (granitic)
GRD	granodiorite
MNZ	monzonite
MZD	monzodiorite
MZG	monzogranite
POR	andesitic porphyry
QMD	quartz monzodiorite
QMZ	quartz monzonite
SLT	siltstone
SYT	syenite
TUF	tuff
VSS	volcanogenic sandstone

ZONE:

A	albite zone
M	magnetite-apatite-actinolite zone
P	pyrite zone

sample	area	type	zone	$\delta^{18}O$	δD	wt.% H_2O
77-015	CTL	and		10.2	-63	
77-019	CBF	sed		10.1	-63	1.2
77-022	CBF	tuf		11.1	-66	1.7
77-042	CBF	tuf		12.7	-73	1.1
77-051	BTL	and		9.6	-66	1.1
77-052	BTL	mnz		7.9	-79	
77-053	BTL	and		10.3	-65	
77-081	BTL	sed		11.4	-66	1.8
77-093	CTL	and		10.2	-70	0.9
77-095	PR	and			-70	
77-096	PR	and		8.8	-81	1.4
77-124	BTL	ptn		8.8	-58	
77-135	BTL	sed		8.6	-57	2.7
77-140	CTL	dct		12.1	-66	
77-154b	CBF	tuf		9.6	-60	1.2
77-170	NGL	mnz			-64	
77-172	CBF	sed		11.2	-75	1.1
77-239	CBF	drt			-60	1.9
77-226	CBF	tuf		10.9	-63	1.5
80-069	CTL	syt		10.4	-71	
87-009	CTL	ptn		11.2	-65	1.9
87-011	CTL	ptn		8.9	-72	1.1
87-013	CTL	ptn		8.6	-71	1.3
87-015	CTL	ptn		9.0	-65	1.2
88-001	CTL	and		8.7		
88-002	CTL	dyk	A	10.4		
88-003	CTL	and	P	8.2		
88-010	CTL	and	P	10.3		
88-013	CTL	and		11.7		
88-016	CTL	and	P	9.4		
88-019	CTL	and		10.5	-68	1.5
88-022	SGL	and	P	10.3		
88-023	SGL	and	P	9.5	-56	
88-024	SGL	and		9.5		
88-028	SGL	and	AP	9.0		
88-031	SGL	dyk	AP	10.7		
88-033a	SGL	and	P	9.9		
88-034	SGL	and	P	9.1		
88-035	SGL	and	P	8.6		
88-036	SGL	and	M	8.4		
88-037	SGL	and	M	7.1		
88-041	SGL	and	M	7.5		
88-042	SGL	and		9.2		
88-043	SGL	and		9.4		
88-044	SGL	mnz		8.8		
88-049	SGL	mnz	A	8.4		
88-050	SGL	and		8.0		
88-051	SGL	and	M	9.7		
88-052	SGL	mnz		8.9		
88-053	SGL	and		8.1		
88-056	SGL	and		8.5		

Table 3. continued.

sample	area	type	zone	$\delta^{18}O$	δD	wt.% H_2O
88-056	SGL	and	P	8.5	-67	
88-057	SGL	and	M	8.6		
88-062	SGL	mnz		9.0	-64	1.4
88-066	SGL	and	M	8.2		
88-068	SGL	and	M	8.9		
88-070	SGL	mzd		9.8		
88-075	BTL	qdt		12.3		
88-076	BTL	drt		8.1	-65	
88-081	BTL	mnz		8.8		
88-083a	SGL	and	MP	10.0	-65	1.5
88-085	TUT	drt		8.3	-60	
88-087	TUT	drt		8.7	-62	1.5
88-088	TUT	mzg		10.3	-75	0.6
88-089	TUT	mnz		9.4	-60	1.3
88-091	TUT	qmd		7.7		
88-099	TUT	mzd		9.5	-67	0.9
88-112	NCTL	and	P	8.5	-61	
88-124	NCTL	and	P	9.1		
88-128	NCTL	qmd		9.0		
88-130	NCTL	and	M	8.9	-70	
88-135	SCTL	and	MP	7.3		
88-141	SCTL	and	M	7.2	-68	1.2
88-142	SCTL	and	A	8.8		
88-148	SCTL	and		9.4		
88-150	SCTL	and	M	7.2	-80	
88-156	MCL	qmz		9.2	-70	1.5
88-162	SCTL	and	P	8.1	-78	
88-166	SCTL	and	A	7.4		
88-172	CTL	and	A	9.5		
88-174	CTL	and	AM	9.4		
88-176	CTL	and		9.2		
88-177	CTL	and	AM	9.6		
88-180	CTL	and	M	7.7	-85	1.0
88-182	CTL	and	AMP	6.3	-92	1.4
88-185	CTL	and	AM	7.8		
88-186	CTL	and	P	8.9		
88-188a	CTL	and	M		-72	0.7
88-188b	CTL	maa	M	7.0		
88-189	CTL	and	M	8.1		
88-196	CTL	and	M	8.2		
88-197	CTL	and		10.0	-65	
88-198	CTL	qmz		9.8	-77	0.9
88-204	BTL	drt		5.8	-83	1.5
88-207	BTL	and		5.3	-65	1.7
88-212	CTL	and?	M	6.9	-75	1.2
88-216	BTL	drt		7.8		
88-219	BTL	slt		7.8		
88-222	NGL	brc	P	8.8		
88-226	CTL	and		8.7		
88-227	CTL	and	AM	9.9		
88-231	CTL	and	M	6.5		

sample	area	type	zone	$\delta^{18}O$	δD	wt.% H_2O
88-234	SGL	and	M	8.4		
88-243	SGL	mzd		8.5	-61	1.4
88-257a	BTL	mzd		9.4	-72	0.8
88-263b	BTL	por		10.1	-60	1.8
88-269	BTL	mnz		8.5	-83	
88-302	SCTL	qmz		9.5		
88-303	SCTL	and		9.3	-74	1.3
88-305	SCTL	qmz		8.7		
88-306	SCTL	and		8.2		
88-308	NGL	and	P	9.5		
89-013	PR	sed	MP	8.1		
89-019	PR	ptn		9.9		
89-162	PR	sed	P	9.2		
89-173	PR	por	AM	7.8	-89	0.5
89-191	PR	por		10.5	-58	
89-226	PR	sed		8.7	-68	
89-234	PR	por		8.9		
89-291	PR	por?			-62	
89-294	PR	and		7.8		
89-313	PR	and		9.4	-70	
89-323	PR	and		9.0		
89-338	TUT	and		8.3		
89-352	TUT	grd		8.7		
89-404	TUT	and	A	8.6		
89-410	TUT	qmz		11.0	-62	1.0
89-423	TUT	and	AM	10.4		
89-432	TUT	and		10.4		
89-447	MCL	grd		9.7	-67	1.1
89-449	MCL	and	MP	9.0	-60	1.9
89-469	TUT	por		10.0	-68	0.9
89-506	NGL	and		9.2		
89-508	NGL	and		8.9	-57	2.7
89-512	NGL	qmz		7.8	-91	0.7
89-538	TUT	mzd		8.5	-68	1.5
89-548	TUT	and		8.7		
89-549	TUT	and		8.4		
89-576	SGL	and		9.9		
89-578	SGL	mnz	A	9.6		
89-580	SGL	mnz		9.7		
89-582	SGL	qmz		9.7		
89-584	SGL	mnz		8.7		
89-586	SGL	mnz		10.0		
89-588	SGL	qmz		9.8		
89-590	SGL	qmz		10.4		
89-592	SGL	mnz		9.0	-68	
89-594	SGL	dyk		9.9		
89-596	SGL	dyk		9.7		
89-598	SGL	and		8.7		
89-603	PR	crb	A	9.1	-84	0.6
89-604	PR	crb		6.7	-62	0.5
89-608	BTL	and		9.8	-57	
89-620	BTL			9.3		

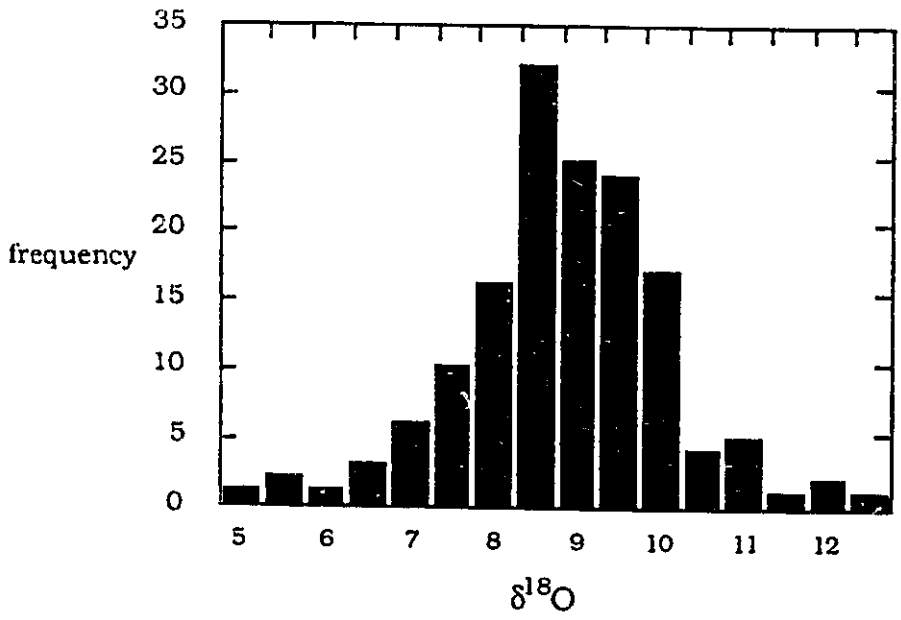

Figure 28. Histogram of $\delta^{18}O$ data for altered andesitic lava flows, cogenetic intrusive porphyritic andesite and plutons of the Mystery Island intrusive suite.

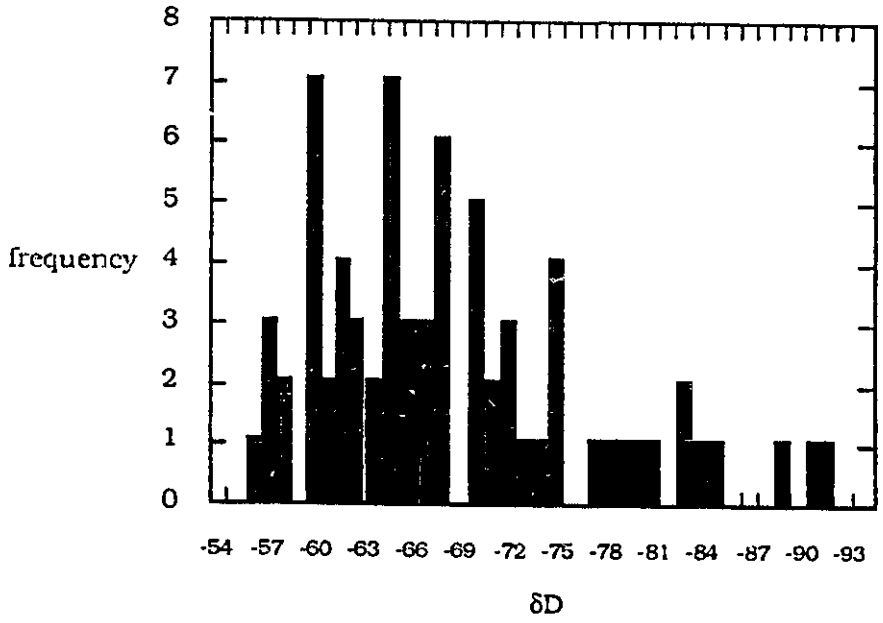

Figure 29. Histogram of δD data for altered andesitic lava flows, cogenetic intrusive porphyritic andesite and plutons of the Mystery Island intrusive suite.

mean value of +8.4‰. Sedimentary rocks from the Port Radium Formation have δD values ranging from -84 to -62‰.

Echo Bay Formation

Andesitic lava flows and cogenetic intrusive porphyries range in $\delta^{18}O$ from +6.9 to +11.7‰. The $\delta^{18}O$ of andesite typically is in the range +6.0 to +8.0‰ (Hoefs, 1980). Andesitic lavas, related porphyries and volcanogenic sandstone from the Echo Bay Formation range in δD from -92 to -56‰. Volcanogenic sandstone from the Echo Bay Formation have $\delta^{18}O$ values from +7.8 to +9.2‰.

Mystery Island intrusive suite

Plutons of the Mystery Island intrusive suite have $\delta^{18}O$ values ranging from +5.7 to +12.3‰. The mean value is +9.1‰. Five samples through the southern portion of the Glacier Lake pluton (Fig. 7) range in $\delta^{18}O$ from +10.7 to +12.7‰, and no trend is evident. Similarly, four samples through the Contact Lake pluton (Fig. 6a) show no trend for $\delta^{18}O$, and range from +8.6 to +11.2‰. The $\delta^{18}O$ of the plutons is slightly higher than for average, unaltered intermediate plutons, which have $\delta^{18}O$ from +8.0 to +9.0‰ (Hoefs, 1980). Plutons of the Mystery Island intrusive suite range in δD from -91 to -60‰.

Cameron Bay Formation

Sedimentary rocks and tuffs of the Cameron Bay Formation range in $\delta^{18}O$ from +10.1 to +12.7‰. The higher $\delta^{18}O$ values for these rocks, as compared to the plutons of the Mystery Island intrusive suite and altered andesitic lava flows, may reflect their original composition, since sedimentary rocks have higher average $\delta^{18}O$ values than igneous rocks. Alternatively, the higher values may be due to their greater susceptibility to alteration due

to greater permeability. Volcanic and sedimentary rocks of the Cameron Bay range in δD from -76 to -60‰.

Richardson pluton

One sample of the Richardson pluton was analyzed, and has a $\delta^{18}O$ of +10.4‰. This value is slightly higher than typical values for unaltered granitic plutons, which have $\delta^{18}O$ values between +6.0 and +10.0‰. (Hoefs, 1980). The pluton has a δD value of -71‰.

Carbon

Whole-rock $\delta^{13}C$ values of both the plutons of the Mystery Island intrusive suite and their wall rocks have a very limited range of -25.7 to -25.0‰. These values are much lighter than carbon from a magmatic source and are indicative of biogenically reduced carbon. Thus, the $\delta^{13}C$ values obtained indicate contamination, and are therefore not useful in interpreting the hydrothermal history of the rocks.

Magnetite-apatite-actinolite zone

Magnetite, apatite, actinolite, biotite, epidote and quartz from the MAA zone were analyzed for their oxygen and hydrogen isotopic compositions. Sample locations are shown on Plate 1. Analytical methods are described in Appendix C.

Oxygen

$\delta^{18}O$ data for actinolite, epidote, biotite, apatite, quartz and magnetite (in part martite) from 14 veins and pervasively altered rocks are presented in Tables 4a and b. Actinolite ranges in $\delta^{18}O$ from +6.4 to +9.6‰. Talc has a $\delta^{18}O$ of +12.3‰. Biotite has a $\delta^{18}O$

Table 4. $\delta^{18}O$ and δD (‰, SMOW) and water content (wt.%) data for minerals from magnetite-apatite-actinolite veins and pervasively altered rocks.

sample	type	mineral	$\delta^{18}O$	δD	$\delta^{18}OH_2O$		δDH_2O	
					300°C	400°C	300°C	400°C
89-193	pod	actinolite	+ 6.4	- 80	+ 6.9	+ 7.7	- 39.8	- 21.1
89-446	pod	actinolite	+ 6.6	- 53	+ 7.1	+ 7.9		
88-256	vein	actinolite	+ 6.9	- 72	+ 7.4	+ 8.2	- 39.4	- 20.6
88-115	vein	actinolite	+ 7.0	- 78	+ 7.5	+ 8.3	- 43.1	- 24.4
88-153	par	actinolite	+ 7.0	- 80	+ 7.5	+ 8.3	- 40.5	- 21.7
89-495	vein	actinolite	+ 7.1	- 80	+ 7.6	+ 8.4		
88-248	par	actinolite	+ 7.4	- 67	+ 7.9	+ 8.7	- 45.1	- 26.4
89-059b	brc	actinolite	+ 7.7	- 82	+ 8.2	+ 9.0	- 41.8	- 23.0
89-124	vein	actinolite	+ 7.9	- 78	+ 8.4	+ 9.2	- 39.7	- 20.9
89-126	pod	actinolite	+ 8.5	- 65	+ 9.0	+ 9.8	- 42.2	- 23.5
89-600b	vein	actinolite	+ 9.4	- 80	+ 9.9	+10.7		
89-445b	pod	actinolite	+ 9.6	- 74	+10.1	+10.9	- 40.4	- 21.6
88-153	par	epidote	+ 4.1		+ 4.1	+ 5.1		
88-256	vein	epidote	+ 5.4	- 93	+ 5.4	+ 6.4	- 42.9	- 18.5
89-059b	brc	biotite	+ 9.7	-112	+11.6	+ 11.9	- 44.3	- 67.8
88-083b	vein	talc	+ 12.3	- 55				
88-115	vein	apatite	+ 6.5		+ 3.7	+ 5.1		
88-248	par	apatite	+ 6.5		+ 3.7	+ 5.1		
88-256	vein	apatite	+ 6.9		+ 4.1	+ 5.0		
89-600b	vein	apatite	+ 7.3		+ 4.5	+ 5.4		
89-445b	pod	apatite	+ 7.5		+ 4.7	+ 5.6		
89-059b	brc	apatite	+ 8.0		+ 5.2	+ 6.1		
88-256	vein	quartz	+12.4		+ 3.6	+ 7.0		
89-124	vein	magnetite	- 3.1		+ 5.1	+ 3.9		
88-083b	vein	martite	- 2.2					
88-083b	vein	magnetite	- 0.5		+ 7.7	+ 6.5		
89-446	pod	magnetite	+ 1.0		+ 9.2	+ 8.0		
89-445b	pod	magnetite	+ 2.3		+10.5	+ 9.3		
89-193	pod	magnetite	+ 2.4		+10.6	+ 9.4		
89-059b	brc	magnetite	+ 3.6		+11.8	+10.6		
88-153	par	magnetite	+ 4.1		+12.3	+11.1		
89-600b	vein	magnetite	+ 4.2		+12.4	+11.2		
88-188b	pod	magnetite	+ 4.5		+12.7	+11.5		

References:

$\delta^{18}O$:

$10^3 \ln \alpha$ biotite-H_2O = 0.4 ($10^6/T^2$) - 3.1 (500-800°C) Bottinga and Javoy, 1973; 1975

$10^3 \ln \alpha$ quartz-H_2O = 4.1 ($10^6/T^2$) - 3.7 (500-800°C) Bottinga and Javoy, 1973

$10^3 \ln \alpha$ garnet-H_2O = 1.22 ($10^6/T^2$) - 3.7 (500-800°C) Bottinga and Javoy, 1973; 1975

$10^3 \ln \alpha$ magnetite-H_2O = -1.47 ($10^6/T^2$) - 3.7 (500-800°C) Bottinga and Javoy, 1973

$10^3 \ln \alpha$ chlorapatite-H_2O = 1.68 ($10^6/T^2$) - 2.29 (xxx°C) J.R. O'Neil, pers. comm. to B.E. Taylor, 1990

$10^3 \ln \alpha$ quartz-hornblende = 3.15 ($10^6/T^2$) - 0.3 (500-800°C) Bottinga and Javoy, 1975

δDH_2O:

$10^3 \ln \alpha$ garnet-H_2O = 29.2 ($10^6/T^2$) - 139 (<300°C) Graham et al., 1980

$10^3 \ln \alpha$ biotite-H_2O = -21.3 ($10^6/T^2$) - 2.8 (400-850°C) Suzuoki and Epstein, 1976

of +9.7‰ . Apatite ranges in $\delta^{18}O$ from +6.5 to +8.0‰. Epidote has $\delta^{18}O$ of +4.1‰ and +5.4‰; quartz from the same sample has a $\delta^{18}O$ of +12.4‰.

Nine samples of magnetite (partially replaced by martite) have $\delta^{18}O$ values from -3.1 to +4.5‰ (Table 4b), and are not in isotopic equilibrium with other minerals in the assemblage. Because of the finely-intergrown nature of the hematite in magnetite, some martite remained within the magnetite samples. The martitization of the magnetite may have occurred late in the formation of the veins at lower temperatures, as indicated by the occurrence of hematite as a late mineral in all samples. If the oxidation of the magnetite occurred at lower temperatures, the $\delta^{18}O$ of the hematite will be lower than that of the magnetite. Also, the fractionation of $\delta^{18}O$ between hematite and water is about 1.5‰ greater than the fractionation of $\delta^{18}O$ between magnetite and water at 400°C, and increases to about 5‰ at 100°C (Zheng, in press). One sample of martite was analyzed, and has a $\delta^{18}O$ of -2.2‰. Thus, the values obtained for the magnetites can only be considered as a minimum value.

Hydrogen

Hydrous minerals were analyzed for δD and water content (Table 4a). Twelve actinolites range in δD from -82 to -53‰. One biotite, which occurs with magnetite and actinolite, has a δD value of -112‰. Talc has a δD value of -55‰. Epidote, which occurs with actinolite and quartz, has a δD value of -93‰.

Fluid Inclusions

Water extracted from bulk crushing of two MAA samples was analyzed for δD. The method is outlined in Appendix C. The δD values for samples 88-256 and 88-083b are -122 and -154‰, respectively. The values obtained are much lighter than expected if the

inclusions are in isotopic equilibrium with the minerals in these veins. Thus, the fluid inclusions must have incorporated hydrogen and oxygen from groundwater, and are not useful in determining the δD of the mineralizing fluids. The δD of Great Bear Lake water is -148‰ (Chankakoti et al., 1986a).

Pyrite zone

Sulphur

Pyrite and chalcopyrite from gossans, pods and veins within the pyrite and chalcopyrite zones were analyzed for $\delta^{34}S$ (Table 6). Robinson and Ohmoto (1973) determined a $\delta^{34}S$ value of +4.1 to +5.1‰ for disseminated pyrite in the Port Radium Formation and and Robinson and Badham (1974) reported $\delta^{34}S$ values of +3.5 and +5.1‰ for pyrite and +4.0‰ for chalcopyrite in tuffs at the Terra Mine, in the Camsell River area (Fig. 3). Pyrite from within the magnetite-apatite-actinolite zone has similar $\delta^{34}S$ to those of sulphides in the pyrite zone (Table 6). Pyrite in a magnetite-hornblende vein at Port Radium has $\delta^{34}S$ of +2.15‰ (Robinson and Ohmoto, 1973). Massive sulphides at the Silver Bay Mine in the Camsell River area have distinctly lower $\delta^{34}S$ of -8.4 to -10.2‰ (Robinson and Badham, 1974).

The data are comparable to data from iron skarns worldwide, which have typical $\delta^{34}S$ of about -4.0 to +10.0 per mil (Taylor, 1987), and are similar to those for sulphides from the Yangtze valley iron deposits, which average +5.0 ‰ (Zhang, 1986). However, one value for chalcopyrite (+10.8‰) is unusually high. Therefore, the sulphides may actually have greater variation which is not evident due to the limited number of analyses.

Quartz-carbonate veins

Knowledge of the fluids which formed the quartz-carbonate veins in the Echo Bay area is necessary in order to assess the influence of these fluids on the isotopic composition of the rocks in the area. Calcite and siderite from unmineralized veins in the Port Radium area were analyzed for $\delta^{18}O$ and $\delta^{13}C$ (Table 7), and chalcopyrite from quartz- and calcite-chalcopyrite veins was analyzed for $\delta^{34}S$ to compare them with the results from the pitchblende-bearing veins.

Oxygen and carbon

Calcite from a calcite pod in andesitic porphyry has a $\delta^{18}O$ value of +9.1‰ (Table 7). $\delta^{18}O$ values for calcite from two chalcopyrite-bearing quartz-carbonate veins are +7.0 and +10.7‰. Siderite from a chalcopyrite-bearing quartz-carbonate vein has a $\delta^{18}O$ of +14.2‰. Siderite from a quartz-carbonate vein has a $\delta^{18}O$ of +16.6‰. These values are similar to those obtained by Robinson and Ohmoto (1973), Robinson and Badham (1974) and Changkakoti et al. (1986a) for carbonate minerals from pitchblende, native Ag, Ni-Co arsenide veins in the Echo Bay and Camsell River areas.

$\delta^{13}C$ data for calcite and siderite in quartz-carbonate ($^{+/-}$chalcopyrite) veins (Table 7) are also comparable to those of Robinson and Ohmoto (1973), Robinson and Badham (1974) and Changkakoti et al. (1986a). Calcite from a calcite pod in andesitic porphyry has a $\delta^{13}C$ of -5.7‰. Calcite from chalcopyrite-bearing quartz-carbonate veins have $\delta^{13}C$ of -5.6 and -4.2‰. Siderite from a similar vein has a $\delta^{13}C$ of -2.2‰. Siderite from a quartz-carbonate vein has a $\delta^{13}C$ of -2.9‰.

Sulphur

Chalcopyrite from a pyrite- and chalcopyrite-bearing quartz vein has a $\delta^{34}S$ value of +5.6‰ (Table 6), similar to values determined by Robinson and Ohmoto (1973) and Robinson and Badham (1974) for chalcopyrite from mineralized veins in the Echo Bay and Camsell River areas. Sulphides in the pitchblende, native Ag, Ni-Co arsenide veins at Echo Bay are reported (Robinson and Badham, 1974) to have a wide range of $\delta^{34}S$ from -26.0 to +26.9‰, but massive and banded chalcopyrite, which occurs with dolomite, has a limited range of +3.7 to +7.9‰; chalcopyrite which occurs with calcite has a value of +13.5‰.

Fluid Inclusions

Waters obtained by bulk crushing of four quartz-carbonate veins were analyzed for δD. Three of the samples are very light in δD and have values of -130‰ (88-106), -127‰ (88-301), and -103‰ (88-245). Quartz in these samples is cloudy, heavily fractured, and contains very small fluid inclusions. It is probable that the fluid inclusions in these veins were opened during fracturing and exchanged with meteoric water, either during or after faulting, or both. However, a fluorite-quartz-carbonate vein, in which quartz is not heavily fractured and contains large fluid inclusions, has a δD value of -65‰ (88-132). This value may probably be primary, and is consistent with data obtained from fluid inclusions by Changkakoti et al. (1986b) for mineralized veins at Port Radium and in the Camsell River area.

Whole-rock oxygen and hydrogen isotopic data were used to characterize the nature and origin of fluids responsible for the formation of the alteration haloes associated with the Mystery Island intrusive suite. The isotopic composition of fluids in equilibrium with these rocks was estimated at a temperature of 400° to 500°C using known mineral-water fractionations for feldspars (O'Neil and Taylor, 1967) with an average An content of 45.

Table 5. $\delta^{34}S$ (‰, CDT) of pyrite and chalcopyrite from the pyrite zone and chalcopyrite subzone.

sample	description	mineral	$\delta^{34}S$
89-429b	calcite-chalcopyrite pod	chalcopyrite	+ 4.2
89-483b	calcite-chalcopyrite pod	chalcopyrite	+ 10.3
89-373	gossan	pyrite	+ 0.8
89-360	pyrite pod in MAA zone	pyrite	+ 2.7
89-143	pyrite pod	pyrite	+ 4.4
89-276	gossan	pyrite	+ 4.8

Table 6. a) $\delta^{18}O$ (‰, SMOW) and $\delta^{13}C$ (‰, PDB) of calcite and siderite:

sample	description	mineral	$\delta^{18}O$	$\delta^{13}C$
88-245b	chalcopyrite-bearing quartz-carbonate vein	calcite	+ 7.0	- 5.6
88-263a	chalcopyrite-bearing quartz-carbonate vein	calcite	+ 10.7	- 4.2
89-008	calcite pod in andesitic porphyry	calcite	+ 9.1	- 5.7
89-021b	quartz-siderite vein	siderite	+ 16.6	- 2.9
89-188b	chalcopyrite-bearing quartz-carbonate vein	siderite	+ 14.2	- 2.2

b) $\delta^{34}S$ (‰, CDT) of chalcopyrite from quartz-carbonate-sulphide veins.

sample	description	mineral	$\delta^{34}S$
89-459	chalcopyrite and pyrite -bearing quartz vein	chalcopyrite	+ 5.6

assuming that the oxygen isotopic composition of the rocks is dominated by feldspar.The hydrogen isotopic composition of the rocks is represented by hornblende and chlorite (Taylor, 1974), which have similar mineral-water fractionations which do not vary significantly with temperature below about 700°C (Suzuoki and Epstein, 1976). The whole-rock isotopic compositions of these samples and their corresponding calculated waters are shown in Figure 30.

$\delta^{18}O$ and δD data for actinolite, epidote, biotite, apatite, quartz and magnetite were used to estimate the isotopic composition of the mineralizing fluids which formed the MAA zone, based on known isotopic fractionations between minerals and water for a range of temperatures (Table 4). For calculation of the δD of H_2O in equilibrium with actinolite, Al, Mg, and Fe were considered to occupy the octahedral sites. A temperature of 300° to 400°C was used based on temperature estimates for the formation of MAA in similar deposits determined by mineral assemblages and stable isotopic data (Research Group of Porphyrite Iron Ore of the Middle-lower Yangtze Valley, 1977; Ripley and Ohmoto, 1979).

The $\delta^{18}O$ of the fluids calculated from magnetite and actinolite range from +5.1 to +12.0‰ at 300°C, and from +3.9 to +11.5‰ at 400°C. Fluids in equilibrium with apatite, however, range from +3.7 to +5.2‰ (Table 4). These minerals occur together, and if in equilibrium should give the same values for $\delta^{18}O_{H2O}$. The values calculated for apatite were using fractionations between chlorapatite and water (J.R. O'Neil, pers. comm.), since no data for fluorapatite are available. The discrepancy may be due to this. Re-equilibration of the apatite is unlikely, due to the resistance of phosphate minerals to exchange (Kolodny, 1983; Shemesh et al., 1983).

$\delta^{18}O_{H2O}$ values calculated from other minerals are comparable to those calculated for magnetite, actinolite, and apatite. Epidote from an actinolite-epidote-quartz vein gives a $\delta^{18}O_{H2O}$ of +5.4 at 300°C, and +6.4‰ at 400°C. Quartz which replaces actinolite in this

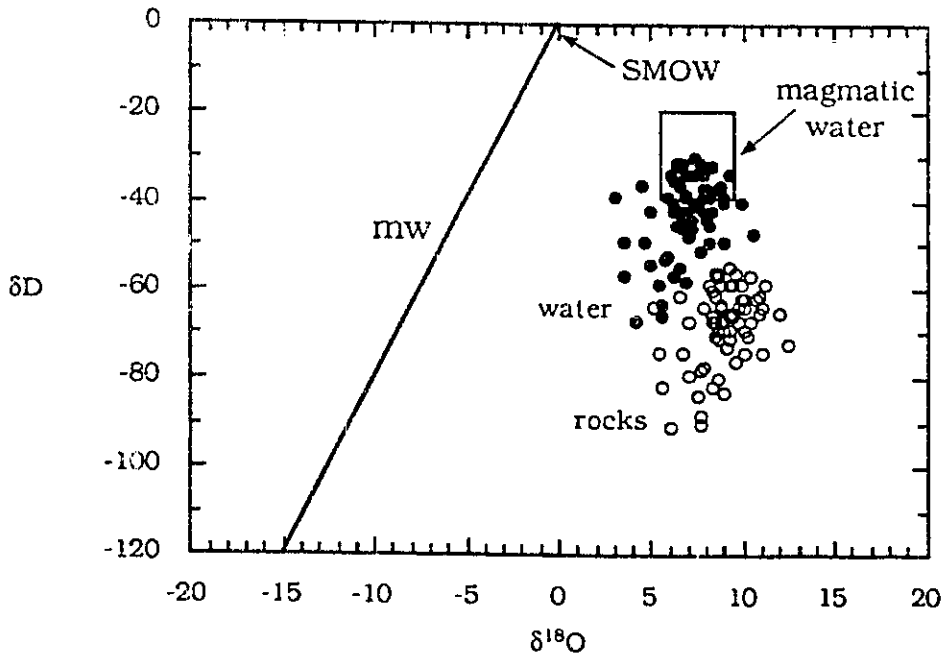

Figure 30. Plot of $\delta^{18}O$ vs. δD for altered andesitic lava flows, cogenetic intrusive porphyritic andesite and plutons of the Mystery Island intrusive suite and for waters in equilibrium with these rocks. The values for the waters were calculated using known mineral-water fractionations for feldspars (O'Neil and Taylor, 1967) with an average An content of 45, assuming that the oxygen isotopic composition of the rocks is represented by the feldspars, and a temperature of 400° to 500°C. The variation of $\delta^{18}O$ for feldspar-water fractionation for this temperature range is about 2‰. The hydrogen isotope composition is represented by hornblende and chlorite (Taylor, 1974), which have similar mineral-water fractionations which do not vary significantly with temperature below about 700°C (Suzuoki and Epstein, 1976).

vein gives $\delta^{18}O_{H2O}$ values of +3.6 (300°C) and +7.0‰ (400°C). Biotite from an MAA breccia gives a $\delta^{18}O_{H2O}$ of +11.6‰ (300°C) and +11.9‰ (400°C). Epidote from pervasively altered andesite gives similar values of +4.1 (300°C) and +5.1‰ (400°C) (Table 4). Overall, the data indicate that the fluids which deposited these minerals ranged from about +5.0 to +12.0‰ for $\delta^{18}O$ and from -60 to -80‰ for δD. Calculated $\delta^{18}O$ and δD values of waters in equilibrium with actinolites from the MAA zone are plotted in Figure 31.

The $\delta^{34}S$ of the fluids which formed the pyrite zone is more difficult to determine, since the $\delta^{34}S$ values of sulphide minerals may be dependant on the oxidation state of the fluids. If the sulphides were deposited by reduced fluids, their $\delta^{34}S$ composition would be very close to that of the fluids which deposited them. In relatively oxidized fluids, sulphur may be in solution as SO_2 or SO_4^{-2} having much higher $\delta^{34}S$ (Ohmoto and Rye, 1979). Above 400°C, SO_2 is the main oxidized species, and total sulphur in the fluid is about one per mil heavier than the H_2S. Magmatic fluids from arc volcanoes of andesitic composition typically have positive $\delta^{34}S$ (SO_2), from 0‰ up to +11.6‰ (Taylor, 1986). However, at lower temperatures under certain pH and fO_2 conditions, the $\delta^{34}S$ of the fluid may be as much as 20 per mil higher than the precipitated sulphides (Ohmoto and Rye, 1979). The oxidation state of the fluids which deposited the MAA was relatively high, as indicated by the presence of specularite within some of the veins. Since the sulphides were deposited relatively late, they were probably deposited at temperatures less than 400°C, and SO_4^{-2} would have predominated. Therefore, the fluids which deposited the veins may have had significantly higher $\delta^{34}S$ than that of the minerals.

Estimation of the effects of overprinting during the formation of later quartz veins on these results is difficult, since fluids responsible for formation of the quartz veins may have been slightly lighter (late meteoric input) or the same as those which formed the MAA zone alteration. Robinson and Ohmoto (1973) calculated a $\delta^{18}O$ of +1.0‰ for the fluids

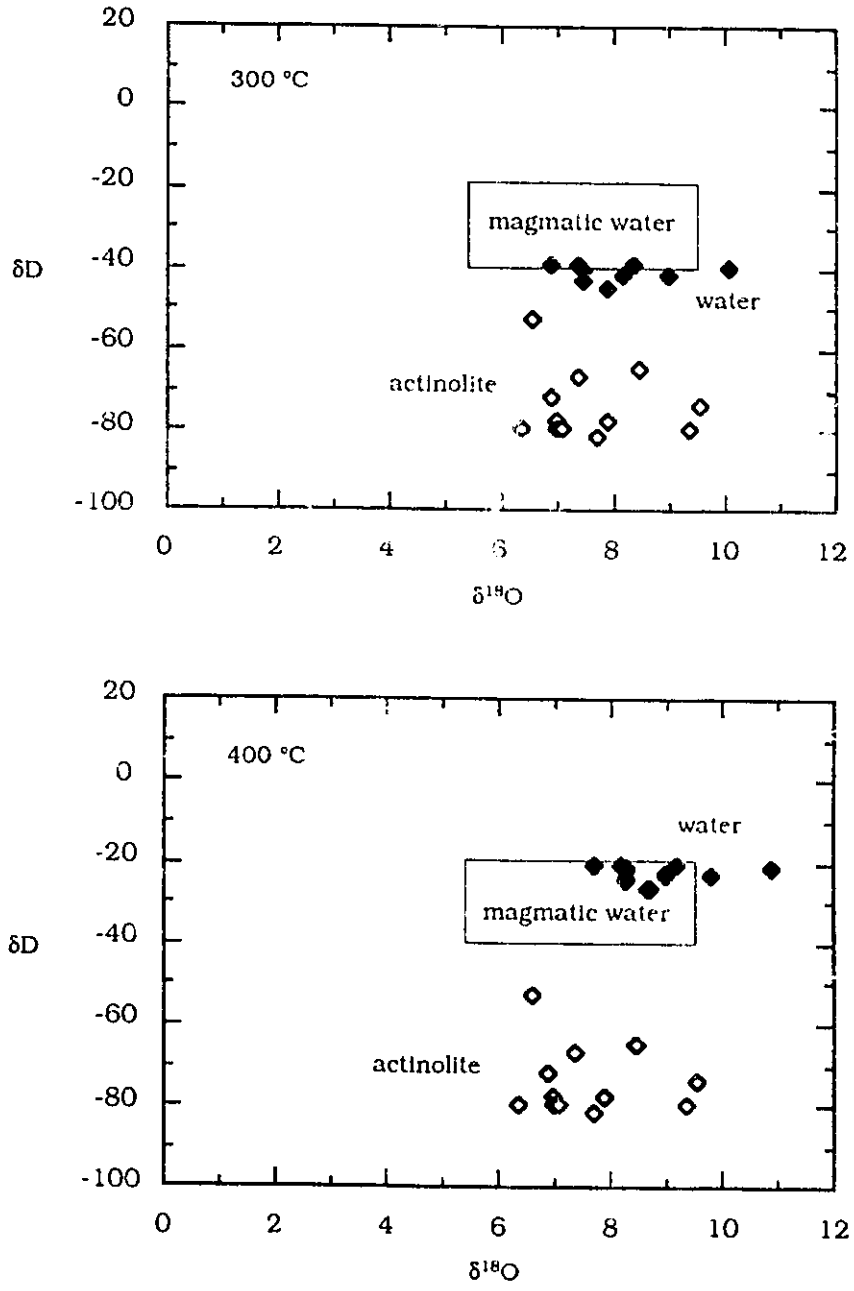

Figure 31. a) Plot of $\delta^{18}O$ vs. δD for actinolites from veins, pods and pervasively altered rocks in the magnetite-apatite-actinolite zone, and for waters in equilibrium with these minerals at 300°C; b) Plot of $\delta^{18}O$ vs. δD for actinolites from veins, pods and pervasively altered rocks in the magnetite-apatite-actinolite zone, and for waters in equilibrium with these minerals at 400°C.

which deposited the pitchblende-bearing veins at Port Radium, based on isotopic data from mineral separates of quartz, hematite, calcite and dolomite. Robinson and Badham (1974) calculated a $\delta^{18}O$ of +2.0‰ based on isotopic data for calcite and dolomite. However, Changkakoti et al. (1986a) calculated a range of $\delta^{18}O$ for the mineralizing fluids, from +9.12‰ (early fluids) to +0.47‰ (late fluids) from the $\delta^{18}O$ of quartz, calcite and dolomite. No zoning of $\delta^{18}O$ is evident in the wall rocks surrounding the veins.

V. DISCUSSION: EVIDENCE FOR A HYDROTHERMAL ORIGIN

The evolution of a fluid phase from a magma is controlled by the solubility of H_2O in the melt, which is in turn dependent on pressure, temperature and composition. The plutons of the Mystery Island intrusive suite were emplaced at a depth of about 2 km, based on stratigraphy and the hornblende geobarometer (Hildebrand, 1984; 1986). At 2 km, or about 550 bars, the solubility of H_2O in a melt of dioritic composition is 2.7 to 3.0% (Burnham, 1979). As sill-like intrusions cool, a rind of solidified material forms at the margins of the body; the last region to solidify is the center of the body (Marsh, 1990). Cooling and crystallization of the magma causes saturation, and the evolution of a H_2O-rich fluid.

As crystallization proceeds, the magma must expand, or internal pressure must increase. A body of granodioritic melt containing 2.7% H_2O at 2 km depth will expand 50% upon complete crystallization (Burnham and Ohmoto, 1980). Since the direction of least principal stress lies in the horizontal plane, fractures will tend to be vertical in orientation. Thermal cracking results in the opening of horizontal fractures (Wright and Okamura, 1977). These fractures serve as channelways for the escape of fluids evolved from the magma. The orientations of most of the MAA veins associated with the plutons of the Mystery Island intrusive suite are either parallel or perpendicular to the pluton contacts. The presence of veins demonstrates the high permeability of fractured rocks and the flow of fluids away from areas of high temperature, where mineral solubility is high, to areas of lower temperature, where mineral solubility is decreased (Labotka, 1990).

Metals, sulphur and chlorine are partitioned into the fluid phase which separates from the cooling magma. Chlorine is partitioned into the aqueous phase (Kilinc and Burnham, 1972), and forms highly stable, neutral chloride complexes with hydrogen, alkali metals, alkaline earths, and heavy metals at magmatic temperatures and low to

moderate pressures. Fluorine also forms stable neutral fluoride complexes in magmatic fluids, but is highly soluble in silicate melts, and tends to be partitioned into the condensed phases (biotite, hornblende)(Burnham and Ohmoto, 1980). In felsic magmas, sulphur is strongly partitioned into the magmatic fluid, as is CO_2. Increasing fO_2 at a given pressure increases the amount of sulphur partitioned into the fluid phase, since H_2S is much less soluble in hydrous magmas than SO_2 (Burnham and Ohmoto, 1980). The oxidation state of contact aureoles and associated metals typically reflects the oxidation state of the magma: oxidized skarns occur with oxidized, commonly S-rich magmatic systems (Einaudi, 1982; Burnham and Ohmoto, 1980). The presence of Mg-rich silicate minerals, Mn-rich ilmenite and pyrophanite, martite, specular hematite and titanite in the altered rocks at Echo Bay indicate that the fluids which caused the alteration were highly oxidized. Due to the oxidation of Fe^{2+} to Fe^{3+}, iron no longer substitutes in these minerals, but is replaced by Mg and Mn in silicate and oxide minerals, respectively. The presence of veins of specularite within one of the plutons indicates that oxidized fluids prevailed within the plutons as well, or were superimposed on earlier alteration minerals (hematite after magnetite).

Experimental work by Sakuyama and Kushiro (1979) demonstrated that a vapour phase separated from an andesitic melt at pressures between 5 and 15 kbar, and T= 1150°C moves upwards and transports significant amounts of Na and K. Na is more soluble in the vapour phase than K, and the degree of enrichment of K was smaller in the experiments than for Na. The ratio of K to Na in a fluid is very important in metsomatic processes. This ratio can change substantially during the evolution of a magmatic aqueous phase from a cooling magma. K/Na+K may be as low as 0.2 initially, but as cooling proceeds and hornblende becomes stable, this ratio may increase up to 0.75, due to the incorporation of Na into hornblende (Burnham, 1967). Therefore, the initial composition of the magma and the timing of vapour separation can influence the nature of the dominant alkali in the

magmatic fluid. Pressure also effects the relative concentrations of alkalis in the vapour phase, since Na is preferentially partitioned into the vapour phase at high pressures (Shinohara, 1992). If $\alpha_{K^+}/\alpha_{H^+}$ is below K-feldspar stability, chlorite and epidote are produced, rather than muscovite. In dioritic systems, early potassic alteration typical of many porphyry copper systems is absorbed by large percentages of magnesium-bearing minerals, so that it does not displace other cations so effectively. These cations, in turn, inhibit the development of later phyllic (quartz-sericite) alteration as solutions decrease in $\alpha_{K^+}/\alpha_{H^+}$ (Beane, 1982).

Alteration at Echo Bay is similar to that of the propylitic assemblage of Rose (1970) and Beane (1982) found associated with intermediate composition plutons in convergent margin related continental arcs, such as the southeastern Arizona Laramide (Einaudi, 1982; Beane, 1982), and in the Coastal Batholith of Peru (Bookstrom, 1977; Menard, 1986). Oxidation, sodic alteration and Fe, Cu, Au mineralization are typical processes in these alteration halos (Barton et al., 1991).

Propylitic alteration of primary plagioclase releases Ca which contributes to the formation of epidote and/or calcite. Propylitic alteration may also involve leaching of K, Mg, and Fe (Beane, 1982), and leaching is evident in the albite zone at Echo Bay, where andesitic rocks have been altered to varying degrees to albite. Leaching of elements by K-metasomatism and Na-metasomatism in the plutons, and by Na-metasomatism in the andesites, provides a source of the elements required to form the MAA and pyrite zones in addition to those carried with the magmatic fluid. Although Al_2O_3 is conventionally considered to be conserved among solid phases during alteration (Hemley et al., 1980), experimental work has found that even Al, Ti, and V are more mobile in a metasomatic environment than previously thought (Meineri, 1984). The mobility of REEs from K-metasomatized rocks to Na-metasomatized rocks is interesting, since other large

hydrothermal iron deposits are REE-enriched, such as Olympic Dam, Australia (Roberts and Hudson, 1983). Experimental data suggest that REEs form stable complexes with Cl and F (Humphris, 1984).

Apatite solubility in melts decreases with increasing SiO_2 content and temperature, and becomes saturated when melts reach intermediate composition (Watson, 1979). However, Mg is known to markedly inhibit the precipitation of hydroxyapatite, and high solubilities of apatite are recognized in highly alkaline, Cl-rich geyser and hot spring waters (Stauffer, 1982). Thus, Mg and Cl-rich fluids exsolved from intermediate composition plutons could be capable of transporting large amount of dissolved apatite. The presence of fluorapatite, rather then chlorapatite in these deposits is best explained by the much greater affinity of Cl for the vapour phase as compared to F, which prefers the liquid phase (Truesdell and Singers, 1974; Candela, 1986). The relative amounts of F and Cl in apatite from the MAA zone are comparable to fresh apatites from granitic rocks (Nedachi, 1980).

The evidence given above indicates that the alteration of the plutons and their wallrocks was by hydrothermal processes related to the solidification and cooling of epizonal plutons. However, the relative amount of magmatic water to other waters can only be resolved using stable isotopes. The dominance of magmatic fluids in extensive contact aureoles which extend hundreds of meters from intrusive contacts has been documented using stable isotopes (Lattanzi et al., 1980; Nabalek et al., 1984; 1990). The calculated values of most $\delta^{18}O$ and δD for waters from the altered zones at Echo Bay are D-enriched relative to the commonly accepted range of magmatic waters of -40 to -80‰ (Taylor, 1974). However, recent studies indicate that δD of magmatic waters is much lighter, and that the lower values reflect degassing which leaves the hydrous minerals in the rock (which are used to calculate δD of magmatic waters) depleted in δD (Taylor, 1986;

1991). Magmatic water from rhyolitic magma has a δD of +/-40‰, and values of -30 to -20‰ are found in high temperature fumaroles on dacite and andesite volcanoes (Taylor, 1986; Matsuhisha, in press). Thus, a range for magmatic water of +5.5 to +9.0‰ for $\delta^{18}O$, and from -20 to -40‰ for δD is assumed. Most of the samples fall within or just below this "magmatic water box". The samples which have lower $\delta^{18}O$ and δD probably represent local mixing of isotopically lighter surface waters. The lower δ–values occur within all rock types, throughout the area, and are not spatially related to faults, diabase dykes or gabbroic sills. Also, $\delta^{18}O$ and δD data for fluids in equilibrium with actinolites from the MAA zone fall near the range of magmatic fluids ($\delta^{18}O$ = +5.5 to +9.0‰, Sheppard, 1986; δD = -20 to -40‰, see discussion above), and are distinctly higher in $\delta^{18}O$ and δD than meteoric water or seawater (see Taylor, 1986).

Several lines of evidence preclude the formation of Kiruna-type deposits by injection or eruption of iron magmas. Experimental work indicates that the existence of a magnetite melt would require temperatures greater than 1000°C (Hildebrand, 1986; Philpotts, 1967). At such high temperatures, distinct thermal effects in the immediate wall rocks of these deposits would be expected for intrusions at shallow depths. The presence of magnetite veins and bodies with no chill margins and no distinct thermal effects in the immediate wall rocks indicate that the temperatures of emplacement were not high enough to have formed from an iron-rich melt. An iron-rich magma would sink in a silicic melt, due to the high density contrast. However, where spatial relationships can be demonstrated, Kiruna-type deposits occur above, or at the sides of the plutons (Mackin, 1968; Hildebrand, 1986; Ménard, 1986). If the "melts" carried enough volatiles to transport them upwards through a silicic melt, they would not be melts, but Fe-rich fluids. The low Ti content of magnetite and hematite in Kiruna-type deposits is also inconsistent with their deposition from an iron-rich melt separated from a silicic melt. Immiscible Fe-rich melts separated from

silicious melts are characteristically Mn-Ti-rich (Buddington et al., 1955; Silver et al.,1985). Therefore, an iron-rich melt in equilibrium with a silicate melt would be Ti-rich.

VI. SUMMARY AND CONCLUSIONS

Geologic, textural, mineralogic, and stable isotopic evidence indicate a magmatic - hydrothermal origin for the altered and mineralized rocks in the Echo Bay area. The close spatial association of the altered rocks to the plutons of the Mystery Island intrusive suite is demonstrated by: 1) the occurrence of altered rocks primarily above the plutons; 2) zonation of altered rocks around the plutons, and 3) the occurrence of alteration minerals within the plutons. The origin of these deposits by replacement is supported by pervasive replacement of the rocks, and selective replacement of sedimentary rocks which preserved sedimentary textures. Alteration also occurred along veins and in breccias. The abundance of hydroxyl-bearing minerals, and coarse-grained, zoned, pegmatitic MAA veins are consistent with deposition from a fluid phase along fractures which served as channelways for the escape of fluids evolved from the magma. The orientations of most of the MAA veins associated with the plutons of the Mystery Island intrusive suite are consistent with fracture development during the expansion of the cooling magma body. Breccias contain eroded, and sometimes rotated fragments, also typical of explosive hydrothermal brecciation.

Chemical compositions of the altered wall rocks show that the plutons are Na-metasomatized and K-metasomatized locally. The Tut pluton is relatively unaltered and shows a normal calc-alkaline magmatic trend of increasing K_2O and decreasing Na_2O with increasing SiO_2 content, however, this may be due to the lack of exposure of the roof of the pluton, since it is exposed in the core of a syncline, and not in oblique cross-section as the other plutons. Profiles of SiO_2, Na_2O, and K_2O with stratigraphic height in two of the the plutons show large variations of Na_2O and K_2O. The samples with higher K_2O contents are enriched in Ba, Sr, Rb, Zr, and Al_2O_3 and depleted in FeO, MgO, MnO and REEs (Fig. 24a). Na-rich rocks are depleted in FeO, MgO, MnO, Ba, and Rb, and enriched in REEs. Na_2O and

K_2O contents do not correlate. One albitized sample has the highest P, Ti, Ca and REE contents, which may be due to the presence of titanite and/or apatite. The positive correlation of K_2O with Ba, Sr, and Rb is probably due to the substitution of these elements in plagioclase and K-feldspar.

The presence of abundant Fe, P, and S in the alteration halos can be explained by separation of an Mg-rich, oxidized magmatic fluid containing alkali metals, alkaline earths, and iron as chloride complexes, and sulphur as SO_2. The highly-oxidized state of the fluid is reflected in the presence of Mg-rich silicate minerals, Mn-rich ilmenite and pyrophanite, martite, specular hematite and titanite in the altered rocks. Although intermediate magmas are near saturation with respect to apatite, the precipitation of apatite is inhibited by the presence of abundant Mg, and apatite is not precipitated until the precipitation of actinolite.

Although hydrothermal fluids produced both Na- and K- metasomatism within the plutons, extensive albitization of wall-rocks, and the presence of secondary riebeckite in the plutons, and within the wall rocks locally, indicates that the fluids were dominantly sodium-rich. The upward movement of alkalis, particularly Na, during separation of a vapour phase from an andesitic melt is consistent with the alteration observed within and above the plutons. The initial composition of the magma, pressure, and the timing of vapour separation during the crystallization of the magma influence which alkali (K or Na) will dominate in the fluid; such variations may explain why some of the plutons are K-metasomatized and others are Na-metasomatized. However, the dominance of Na over K may be related to the high Mg content of the system, since early potassic alteration can be absorbed by large percentages of magnesium-bearing minerals.

Stable isotopic data for the Mystery Island intrusive suite and altered wall rocks demonstrate that the alteration was produced by dominantly magmatic fluids. Most $\delta^{18}O$

and δD whole-rock values are higher than +6 and -70‰, respectively, consistent with alteration by magmatic fluids. Lower values suggest involvement of a minor component of evolved meteoric water or connate water. Calculated $\delta^{18}O$ and δD of fluids which formed the magnetite-apatite-actinolite deposits range from +5.0 to +12.0‰ and -60 to -30‰, respectively.

REFERENCES

Andrews, A. J., Owsiacki, L., Kerrich, R.W., Strong, D.,F.

1982: Petrology, stable isotopes, and fluid inclusions of the Ag-Co-Ni arsenide vein deposits near Cobalt and Gowganda, Ontario; in Summary of Field Work, 1982, Ontario Geol. Survey Misc. Paper 106, p. 207-209.

Badham, J.P.N.

1972: The Camsell River - Conjuror Bay area, Great Bear Lake, N.W.T.; Can. J. Earth Sci., v. 9, p.1460-1468.

Badham, J.P.N.

1973a: Calcalkaline volcanism and plutonism from the Great Bear batholith, N.W.T.; Can. J. Earth Sci., v. 10, p.1319-1328.

Badham, J.P.N.

1973b: Volcanogenesis, orogenesis and metallogenesis, Camsell River, N.W.T.; unpublished Ph.D. thesis, University of Alberta, Edmonton, Alberta, 334 p.

Eadham, J.P.N.

1975: Mineralogy, paragenesis and origin of the Ag-Ni, Co arsenide mineralisation, Camsell River, N.W.T., Canada; Mineral. Dep., v. 10, p. 153-175.

Badham, J.P.N., and Morton, R.D.

1976: Magnetite-apatite intrusions and calc-alkaline magmatism, Camsell River, N.W.T.; Can. J. of Earth Sci., v. 13, p. 348-354.

Barton, M.D., Battles, D.A., Debout, G.E., Capo, R.C., Christensen, J.N., Davis, S.R., Brooks Hanson, R., Michelson, C.J., and Trim, H.E.

1991: Mesozoic contact metamorphism in the western United States; in Metamorphism and crustal evolution of the western United States, W.G. Ernst, ed., p. 111-167.

Bastin, E.S.

1939: The nickel-cobalt-native silver ore type; Econ.Geol., v. 34, p. 1-40.

Beane, R.E.

1982: Hydrothermal alteration in silicate rocks; in S.R. Titley, ed., Advances in Geology of Porphyry Copper Deposits, University of Arizona Press, p. 117-137.

Bell. J.M.

1901: Report of the topography and geology of Great Bear Lake and a chain of lakes and streams thence to Great Slave Lake; Geol. Survey of Canada, Annual Report 1901, p. 5c-35c.

Bookström, A.A.

1977: The magnetite deposits of El Romeral, Chile; Econ. Geol., v. 72, p. 1101-1130.

Bottinga, Y. and Javoy, M.

1973: Comments on oxygen isotope geothermometry; Earth Planet. Sci. Lett., v. 20, p. 250-265.

Bottinga, Y. and Javoy, M.

1975: Oxygen isotope partitioning among the minerals in igneous and metamorphic rocks; Rev. Geophys. Space Phys. v. 13, p. 401-418.

Bowring, S. A.

1984: U-Pb zircon geochronology of Early Proterozoic Wopmay Orogen, N.W.T., Canada: an example of rapid crustal evolution; Ph.D. thesis, University of Kansas, Lawrence, 148 p.

Bowring, S.A. and Ross, G.M.

1985: Geochronology of the Narakay Volcanic Complex: Implications for the age of the Coppermine Homocline and Mackenzie igneous events; Can. J. Earth Sci., v. 22, p. 774-780.

Bowring, S.A. and Grotzinger, J.P.

1992: Implications of new chronostratigraphy for tectonic evolution of Wopmay orogen, northwest Canadian Shield; Amer. J. Sci., v. 292, p. 1-20.

Bowring, S.A., Housh, T. and Grotzinger, J.P.

1989: U-Pb isotopic analysis of carbonate cements, early Proterozoic Rocknest formation: Evidence for differential element mobility during diagenesis; Geol. Assoc. Canada/Mineral. Assoc. Canada, Program with Abstracts, v. 14, Montreal, 1989, p.A78.

Burnham, C.W. and Ohmoto, H.

1980: Late-stage processes of felsic magmatism in Granitic Magmatism and Related Mineralization, S. Ishihara and S. Takenouchi, eds., The Society of Mining Geologists of Japan, Mining Geology Special Issue 8, p. 1-12.

Campbell, D.D.

1955: Geology of the pitchblende deposit of Port Radium, Great Bear Lake, N.W.T.; unpublished Ph.D. thesis, California Institute of Technology, Pasadena, California.

Candela, P. A.

1986: Toward a thermodynamic model for the halogens in magmatic systems: an application to melt-vapor-apatite equilibria; Chem. Geol., v. 57, p. 289-301.

Changkakoti, A. and Morton, R.D.

1986: Electron microprobe analyses of native silver and associated arsenides from the Great Bear Lake silver deposits, Northwest Territories, Canada; Can. J. Earth Sci., v. 23, p. 1470-1479.

Changkakoti, A., Morton, R.D., Gray, J., and Yonge, C.J.,

1986a: Oxygen, hydrogen, and carbon isotopic studies of the Great Bear Lake silver deposits, Northwest Territories; Can. J. Earth Sci., v. 23, p. 1463-1469.

Changkakoti, A., Morton, R.D. and Gray, J.

1986b: Hydrothermal environments during the genesis of silver deposits in the Northwest Territories of Canada: evidence from fluid inclusions; Mineral. Dep., v. 21, p. 63-6[illegible].

Cherer, R.M.

1988: Petrology and geochemistry of three plutons of the Mystery Island intrusive suite, District of Mackenzie, Northwest Territories; unpublished B.Sc. thesis, University of Toronto, Toronto, 144 p.

Crane, G.W.

1912: The iron ores of Missouri; Missouri Bureau of Geology and Mines, v. 10, 2nd series, 434 p.

Crowell, J.C.

1984: Origin of late Cenozoic basins in southern California; in Tectonics in Sedimentation, Soc. Econ. Paleontol. Mineral., Spec. Publ. 22, p. 190-204.

Daly, R.A.

1915: Origin of the iron ores at Kiruna; Vetensk. O Prakt. Undersok. I Lappland, v. 5, 31 p.

Easton, R.M.

1981: Stratigraphy of the Akaitcho Group and development of an early Proterozoic continental margin, Wopmay orogen, Northwest Territories; in Campbell, F.H.A., ed., Proterozoic Basins of Canada, Geol. Survey of Canada Paper 81-10, p. 79-95.

Einaudi, M.T.

1982: General features and origin of skarns associated with porphyry copper plutons; in S.R. Titley, ed., Advances in Geology of Porphyry Copper Deposits, University of Arizona Press, p. 185-209.

Fcniak, M.

1947: The Geology of Dowdell Peninsula, Great Bear Lake, Northwest Territories; Geol. Survey of Canada, Central Technical File 86E/16-1.

Forsell, P.

1987: The stratigraphy of the Precambrian rocks of the Kiruna District northern Sweden; Sveriges Geol. Undersokning, Ser. C No. 812, p. 1-36.

Fortier, Y.O.,

1948: Geology of Glacier Lake areas, Great Bear Lake, Northwest Territories; Geol. Survey of Canada, Central Technical File 86E/16-1.

Frietsch, R.

1970: Trace elements in magnetite and hematite mainly from Northern Sweden; Sveriges geol. Undersokning, ser. C, no. 646, 136 p.

Frietsch, R.

1978: On the magmatic origin of iron ores of the Kiruna type; Econ. Geol., v. 73, p. 478-485.

Frutos, J.J. and Oyarzún, M.J.

1975: Tectonic and geochemical evidence concerning the genesis of El Laco magnetite lava flow deposits, Chile; Econ. Geol., v. 70, p. 988-990.

Furnival, G.M.

1935: The large quartz veins of Great Bear Lake, Canada. Econ. Geol., v. 30, p. 843-850.

1939a: Geology of the area north of Contact Lake, N.W.T., Canada; Amer. J. Sci., v. 237, p. 478-480.

1939b: A silver-pitchblende deposit at Contact Lake, Great Bear Lake, Canada; Econ. Geol., v. 34, p. 739-776.

Geijer, P.

1911: Studies on the geology of the iron ores of Lapland; Geol. Fören. Förh., v. 34, p. 727-789.

1915: Some problems in iron ore geology in Sweden and in America; Econ. Geol., v. 10, p. 299-329.

1980: The iron ores of the Kiruna type: Geographical distribution, geological characteristics, and origin; Sveriges Geol. Undersoking, ser. C, no. 367, 39 p.

Geijer, P. and Odman, O.H.

1974: The emplacement of the Kiruna iron ores and related deposits; Sveriges Geol. Undersoking, ser. C, no. 700, 48 p.

Graham, C.M., Sheppard, S.M.F., and Heaton, T.H.E.

1980: Experimental hydrogen isotope studies: I. Systematics of hydrogen isotope fractionation in the systems epidote-H_2O, zoisite-H_2O and AlO(OH)-H_2O; Geochim. Cosmochim. Acta, v. 44, p. 353-364.

Gromet, L.P. and Silver, L.T.

1983: Rare earth element distribution among minerals in a granodiorite and their petrogenetic implications; Geochim. Cosmochim. Acta, v. 47, p. 925-939.

Grotzinger, J.P.

1986: Evolution of early Proterozoic passive-margin carbonate platform, Rocknest Formation, Northwest Territories; Can. J. Sedimentary Petrol., v. 56, p.831-847.

Harland, W.B., Cox, A.V., Llewellyn, P.G., Pickton, C..G., Smith, A.G. and Walters, R.

1982: A geologic time scale; A.H. Cook, W.B. Harland, N.F. Hughes, A. Putnis, J.G. Sclater, and M.R.A. Thomson, eds., Cambridge University Press, Cambridge, 131 p.

Hegemann, F. and Albrecht, F.

1954: Zur geochemie oxydischer; Eisenerze Chemie der Erde, v. 17, p. 81-103.

Hemley, J.J., Montoya, J., Marinenko, J.W. and Luce, R.W.

1980: Mineral equilibria in the system Al_2O_3-SiO_2-H_2O and some implications of alteration/mineralization processes; Econ. Geol., v. 75, p. 210-228.

Henderson, P.

1980: Rare earth element partition between sphene, apatite and other coexisting minerals of the Kangerdlugssuaq intrusion, East Greenland; Contrib. Mineral. Petrol., v. 72, p. 81-85.

Hildebrand, R.S.

1981: Early Proterozoic LaBine Group of Wopmay orogen: Remnant of a continental volcanic arc developed during oblique convergence; in Proterozoic Basins of Canada, ed. F.H.A. Campbell, Geol. Survey of Canada Paper 81-10, p. 133-156.

1982: An early Proterozoic continental volcanic arc at Great Bear Lake, Northwest Territories; Ph.D. thesis, Memorial University of Newfoundland, St. John's, 237 p.

1983a: Geology, Echo Bay - MacAlpine Channel area. Geol. Survey of Canada Map, 1546A, 1:50 000 scale.

1983b: Geology, Rainy Lake - White Eagle Falls, District of Mackenzie; Geol. Survey of Canada, Map 1589A. 1:50 000 scale.

1984a: Geology of the Rainy Lake and White Eagle Falls map areas, District of Mackenzie: Early Proterozoic cauldrons, stratovolcanoes and subvolcanic plutons; Geol. Survey of Canada Paper 83-20, 42 p.

1984b: Folded cauldrons of the early Proterozoic LaBine Group, northwestern Canadian Shield; Jour. Geophys. Res., v. 89, p. 8429-8440.

1986: Kiruna-type deposits: their origin and relationship to intermediate subvolcanic plutons in the Great Bear Magmatic Zone, Northwest Canada; Econ. Geol., v. 81, p. 640-659.

1988a: Implications of ash dispersal for tectonic models with an example from Wopmay orogen; Geology, v. 16, p. 1089-1091.

1988b: Ore deposits in the Great Bear magmatic zone, an early Proterozoic arc terrane in Wopmay orogen, northwestern Canadian shield; in International Field Conference on the Tectonic Setting of Proterozoic Volcanism and Associated Ore Deposits, Turku, Finland, abstract volume, p. 12.

Hildebrand, R.S. and Bowring, S.A.

1984: Continental intra-arc depressions: a nonextensional model for their origin, with an example from Wopmay Orogen; Geology, v. 12, p. 73-77.

Hildebrand, R.S. and Bowring, S.A.

1991: Two periods of transpressive deformation in Wopmay orogen, northwestern Canadian Shield; Geol. Society of America, Programs with Abstracts, v. 23, p. A309.

Hildebrand, R.S. and Roots, C.F.

1985: Geology of the Riviere Grandin map area (Great Bear magmatic zone and western Great Bear magmatic zone), District of Mackenzie; in Current Research, Part A, Geol. Survey of Canada, Paper 85-1A, p. 373-383.

Hildebrand, R.S., Bowring, S.A., Steer, M.E. and Van Schmus, W.R.

1983: Geology and U-Pb geochronology of parts of the Leith Peninsula and Riviere Grandin map areas, District of Mackenzie; in Current Research, Part A, Geol. Survey of Canada Paper 83-1A, p. 329-342.

Hildebrand, R.S., Hoffman, P.F. and Bowring, S.A.

1987: Tectono-magmatic evolution of the 1.9 Ga Great Bear magmatic zone, Wopmay orogen, Northwestern Canada; J. Volc. Geothermal Res., v. 32, p. 99-118.

Hildebrand, R.S., Bowring, S.A. and Housh, T.

1990: The medial zone of Wopmay orogen, District of Mackenzie; in Current Research, Part C, Geol. Survey of Canada Paper 90-1C, p. 167-176.

Hildebrand, R.S., Paul, D., Pietikainen, P., Hoffman, P.F., Bowring, S.A. and Housh, T.

1991: New geological developments in the internal zone of Wopmay orogen, District of Mackenzie; in Current Research, Part C, Geol. Survey of Canada Paper 91-1C, p. 157-164.

Hoefs, J .

1980: Stable Isotope Geochemistry; Springer-Verlag, Berlin, 208 p.

Hoffman, P.F.

1972: Cross-section of the Coronation Geosyncline (Aphebian), Tree River to Great Bear Lake, District of Mackenzie (86 J, K, O, P); in Report of Activities, April to October 1971, Geol. Survey of Canada Paper 72-1, Part A, p. 119-125.

1978: Geology of the Sloan River map area (86K), District of Mackenzie; Geol. Survey of Canada, Open File Map 535.

1980: Wopmay orogen: A Wilson cycle of early Proterozoic age in the northwest of the Canadian Shield; Geol. Assoc. Canada Spec. Paper 16, p. 523-549.

1982: The Northern Internides of Wopmay Orogen; Geol. Survey of Canada Map 832, scale 1:250 000.

1984: Geology of the northern internides of Wopmay orogen, District of Mackenzie, Northwest Territories; Geol. Survey of Canada Map 1576A, scale 1:250 000.

1987: Early Proterozoic foredeeps, foredeep magmatism, and Superior-type formations of the Canadian Shield in Proterozoic Lithospheric Evolution, ed. A. Kroner, Geodyn. Ser., v. 17, Washington, DC, Amer. Geophys. Union, p. 85-98.

1988: United plates of America, the birth of a craton: Early Proterozoic assembly and growth of Laurentia; Ann. Rev. Earth Planet. Sci., v. 16, p. 543-603.

1989: Precambrian geology and tectonic history of North America; in The Geology of North America, Vol. A, The Geology of North America - An Overview, Geol. Soc. Amer., p. 447-512.

Hoffman, P.F. and Bell, I.

1975: Volcanism and plutonism, Sloan River Map Area (86K), Great Bear Lake, District of Mackenzie; Geol. Survey Canada Paper 75-1, Part A, p. 331-337.

Hoffman, P.F., and Bowring, S.A.

1984: Short-lived 1.9 Ga continental margin and its destruction, Wopmay orogen, northwest Canada; Geology, v. 12, p. 68-72.

Hoffman, P.F., and McGlynn, J.C.

1977: Great Bear batholith: A volcano-plutonic depression; Geol. Assoc. Canada Spec. Paper 16, p. 170-192.

Hoffman, P.F., Bell, I.R. and Tirrul, R.

1976: Sloan River Map Area (86K), Great Bear Lake, District of Mackenzie; Geol. Survey of Canada Paper 76-1A, p.353-358.

Hoffman, P.F., Tirrul, R., King, J.E., St. Onge, M.R. and Lucas, S.B.

1988: Axial projections and modes of crustal thickening, eastern Wopmay Orogen, northwest Canadian Shield; in Processes in Continental Lithospheric Deformation, eds. S.P. Clark, Jr., C. Burchfiel, and J. Suppe, Geol. Soc. Amer., Spec. Paper 218.

Humphris, S.

1984: Mobility of rare earth elements in the crust; in Henderson, ed., Rare earth element geochemistry, Elsevier, Amsterdam, p.317-340.

Joliffe, A.W. and Bateman, J.D.

1944: Map of the Eldorado map-area; Geol. Survey of Canada, Central Technical File 86E/16-1.

Jory, J.T.

1964: Mineralogical and isotopic relations in the Port Radium pitchblende deposit, Great Bear Lake, Canada; unpublished Ph.D. thesis, California Institute of Technology, Pasadena, California.

Kerans, C., Ross, G.M., Donaldson, J.A. and Geldsetzer, H.J.

1981: Tectonism and depositional history of the Helikian Hornby Bay and Dismal Lakes groups, District of Mackenzie; in Proterozoic Basins of Canada, ed. F.H.A. Campbell, Geol. Survey of Canada Paper 81-10, p. 157-182.

Kidd, D.F.

1932: A pitchblende-silver deposit, Great Bear Lake, Canada; Econ. Geol., v. 27, p. 145-159.

1933: Great Bear Lake area, Northwest Territories; Geol. Survey of Canada Summer Report, 1932, Pt. C, p. 1-36.

Kilinc, I.A. and Burnham, C. W.

1972: Partitioning of chloride between a silicate melt and coexisting aqueous phase from 2 to 8 kilobars; Econ. Geol., v. 67, p. 231-235.

King, J.E.

1986: The metamorphic internal zone of Wopmay orogen, Canada: 30 km of structural relief in a composite section based on plunge projection; Tectonics, v. 5, p. 973-994.

Kolodny, Y. Luz, B. and Navon, O.

1983: Oxygen isotope variations in phosphate of biogenic apatites: I. Fish bone apatite - rechecking the rules of the game; Earth Planet. Sci. Lett., v. 64, p. 398-404.

Koritnig, S.

1978: Phosphorus in Handbook of Geochemistry, v. II-2, ed. K.H. Wedepohl. Springer-Verlag, New York.

Kroutov, G.A.

1972: Le gisement de minerais Ag-Ni-Co au Khovou-Axy; 24th Int. Geol. Conf. Proc., Section 4, p. 527.

Labotka, T.C.

1990: Chemical and Physical Properties of Fluids; in Contact Metamorphism, Mineral. Soc. Amer. , Rev. Mineral., v. 26, p. 43-104.

Landergren, S.

1948: On the geochemistry of Swedish iron ores and associated rocks; Sveriges Geol. Undersokning, ser. C, no. 496, 182 p.

Lattanzi, P., Rye, D., and Rice, J.M.

1980: Behavior of ^{13}C and ^{18}O in carbonates during contact metamorphism at Marysville, Montana: Implications for isotope systematics in impure dolomitic limestones; Amer. J. Sci., v. 280, p. 890-906.

Leake, B.E.

1968: A catalogue of analyzed calciferous and subcalciferous amphiboles together with their nomenclature and associated minerals; Geol. Soc. Amer. Spec. Paper 98, 210 p.

Leake, B.E.

1978: Nomenclature of amphiboles; Can. Mineral., v. 16, p. 501-520.

Lord, C.S. and Parsons, W.H.

1947: Camsell River map-area; Geol. Survey of Canada Map 1014A (with descriptive notes by C.S. Lord).

Lundberg, B. and Smellie, J.A.T.

1979: Painirova and Mertainen iron ores: Two deposits of the Kiruna iron ore type in northern Sweden; Econ. Geol., v. 74, p. 1131-1152.

Mackin, J.H.

1968: Iron ore deposits of the Iron Springs district, southwestern Utah; in Ore Deposits in the United States, ed. J.D. Ridge, 1933-1967 (Graton-Sales vol.) New York, Amer. Inst. Mining Metall. Petr. Eng., v. 2, p. 992-1019.

Marsh, B.D.

1990: Igneous processes in sills; The Australian Institute of Mining and Metallurgy, Pacific Rim Congress 1990.

Matsuhisha, M.

in press Origin of magmatic waters in subduction zones: stable isotope constraints; in Extended Abstracts, U.S. - Japan Seminar on Magmatic Contributions to Hydrothermal Systems, J. Hedenquist, S. Kesler, E. Izawa and P. Muffler, eds., Geol. Survey Japan Report 279.

McGlynn, J.C.

1976: Geology of the Calder River (86F) and Leith Peninsula (86E) map-areas, District of Mackenzie; Geol. Survey of Canada Paper 76-1A, p. 359-366.

McGrath, P.H. and Hildebrand, R.S.

1984: An estimate, based on magnetic interpretation, of the minimum thickness of the Hornby Bay Group, Leith Peninsula, District of Mackenzie; in Current Research, Part A, Geol. Survey orf Canada, Paper 84-1A, p. 223-228.

McNiven, J.G.

1967: History of the Eldorado Mine, Port Radium (Part 2); Can. Inst. Mining Metall. Bulletin, v. 60, p. 1387-1395.

Meinert, L.D.

1984: Mineralogy and petrology of iron skarns in western British Columbia, Canada; Econ. Geol. 79, p. 869-882.

Ménard, J.J.

1986: Un modele metasomatique pour les gisements de la ceinture de fer du Chili; C.R. Acad. Sc. Paris, t. 302, Serie II, no. 12, 775-778.

Miller, R.G.

1982: The geochronology of uranium deposits in the Great Bear batholith, Northwest Territories; Can. J. Earth Sci., v. 19, p. 1428-1448.

Mrna, F.

1963: Deposit of Ag-Bi-Co-Ni ores in Jáchymov; Symposium, Problems of postmagmatic ore deposition - some ores of the Bohemian Massif; Guide to Excursion, Czech. Acad. Sci., Prague, p. 43-54.

Mursky, G.

1973: Geology of the Port Radium map area, District of Mackenzie; Geol. Survey of Canada, Memoir 374, 40 p.

Nabelek, P.I., Labotka, T.C., O'Neil, J.R., and Papike, J.J.

1984: Contrasting fluid/rock interaction between the Notch Peak granitic intrusion and argillites and limestones in western Utah: Evidence from stable isotopes anf phase assemblages; Contrib. Mineral. Petrol., v. 86, p. 25-34.

Nabelek, P.I.

1990: Stable Isotope Monitors; in Contact Metamorphism, D.M. Kerrick, ed., Rev. Mineral., v. 26, p.395-435.

Nedachi, M.

1980: Chlorine and fluorine contents of rock-forming minerals of the Neogene granitic rocks in Kyushu, Japan; in Late-stage processes of felsic magmatism in Granitic Magmatism and Related Mineralization, S. Ishihara and S. Takenouchi, eds., The Society of Mining Geologists of Japan, Mining Geology Special Issue 8, p. 39-48.

Neumann, H.

1944: Silver deposits at Kongsberg; Norges Geol. Unders., no. 162.

Ohmoto, H. and Rye, R.O.

1979: Isotopes of sulfur and carbon; in Geochemistry of hydrothermal ore deposits, H.L. Barnes, ed., Wiley, New York, p.509-567.

O'Neil, J.R. and Taylor, H.P., H.P., Jr.

1967: The oxygen isotope and cation exchange chemistry of feldspars; Amer. Mineral., v. 52, p. 1414-1437.

Oyarzún, J. and Frutos, J.

1984: Tectonic and petrological frame of the Cretaceous iron deposits of north Chili; Mining Geol., v. 34, p. 21-31.

Padgham, W.A., Shegelski, R.J. and Jefferson, C.W.

1974: Geology of the White Eagle Falls area (86F/12); Department of Indian Affairs and Northern Development, Yellowknife, N.W.T., Open File 199.

Panno, S.V. and Hood, S.V.

1983: Volcanic stratigraphy of the Pilot Knob iron deposits, Iron County, Missouri; Econ. Geol., v. 78, p. 972-982.

Parák, T.

1973: Rare Earths in the apatite iron ores of Lappland together with some data about the Sr, Th and U content of these ores; Econ. Geol., v. 68, p. 210-221.

1975: Kiruna iron ores are not "intrusive-magmatic ores of the Kiruna type"; Econ. Geol., v. 70, p. 1242-1258.

1985: Phosphorous in different types of ore, sulfides in the iron deposits, and the type and origin of ores at Kiruna; Econ. Geol., v. 80, p. 646-665.

Park, C.F. Jr.

1961: A magnetite flow in northern Chile: Econ. Geol., v. 56, p. 431-441.

Park, C.F. Jr.

1972: The iron ore deposits of the Pacific Basin; Econ. Geol., v. 76, p. 339-349.

Philpotts, A.R.

1967: Origin of certain iron-titanium oxide and apatite rocks; Econ. Geol., v. 62, p. 303-315.

Reardon, N.C.

1989: The Mystery Island Intrusive Suite and associated alteration haloes, Great Bear Lake, District of Mackenzie, N.W.T. ; in Current Research, Part C, Geol. Survey of Canada Paper 89-1C, p. 37-42.

Reardon, N.C.

1990: Altered and mineralized rocks at Echo Bay, N.W.T., and their relationship to the Mystery Island intrusive suite; in Current Research, Part C, Geol. Survey of Canada, Paper 90-1C, p. 143-150.

Reichenbach, I.G.

1986: An ensialic marginal basin in Wopmay orogen, northwestern Canadian Shield; M. Sc. thesis, Carleton University, Ottawa, Ontario, 120 p.

Reichenbach, I.G.

1991: The Bell Island Bay Group, remnant of an early Proterozoic ensialic marginal basin in Wopmay orogen, District of Mackenzie; Geol. Survey of Canada Paper 88-28, 43p.

Research Group of Porphyrite Iron Ore of the Middle-lower Yangtze Valley

1977: Porphyrite iron ore - a genetic model of a group of iron ore deposits in andesitic volcanite area: Acta Geologica Sinica, v. 60, p. 1-23.

Ripley, E.M. and Ohmoto, H.

1979: Oxygen and hydrogen isotopic studies of ore deposition and metamorphism at the Raul mine, Peru; Geochim. Cosmochim. Acta, v. 43, p. 1633-1643.

Riley, C.S.

1935: Some mineral relationships in the Great Bear Lake area; Can. Mining J., v. 54, p. 146-147.

Roberts, D.E. and Hudson, G.R.T.

1983: The Olympic Dam copper-uranium-gold deposit, Roxby Downs, South Australia; Econ. Geol., v. 78, p. 799-822.

Robinson, B.W.

1971: Studies on the Echo Bay silver deposit, N.W.T., Canada; unpublished Ph.D. thesis, University of Alberta, Edmonton, Alberta.

Robinson, B.W. and Badham, J.P.N.

1974: Stable isotope geochemistry and the origin of the Great Bear Lake silver deposits, Northwest Territories, Canada; Can. J. of Earth Sci., v. 11, p. 698-711.

Robinson, B.W. and Morton, R.D.

1972: The geology and geochronology of the Echo Bay area, Northwest Territories, Canada; Can. J. of Earth Sci., v. 9, p. 158-171.

Robinson, B.W. and Ohmoto, H.

1973: Mineralogy, fluid inclusions, and stable isotopes of the Echo Bay U-Ni-Ag-Cu deposits, Northwest Territories, Canada; Econ. Geol., v. 68, p. 635-656.

Robinson, H.S.

1933: Notes on the Echo Bay District, Great Bear Lake, Northwest Territories; Can. Inst. Mining Metall. Bull., v. 26, p. 609-628.

Rose, A.W.

1970: Zonal relations of wallrock alteration and sulphide distribution at porphyry copper deposits; Econ. Geol., v. 65, p. 920-936.

Rosler, H.J. and Bauman, L.

1970: On the different origin of Varsican and post-Varsican mineralisations in central Europe; Int. Union of Geol. Sci., Series A, #2, p. 72-77.

Ross, G.M. and Kerans, C.

1989: Geology, Hornby and Dismal Lakes groups, Coppermine Homocline, District of Mackenzie, Northwest Territories; Geol. Survey of Canada, Map 1663A, scale 1:250 000 (with descriptive notes).

Ruiz, C., Ortiz, A., Moraga, A. and Aguilar, A.

1968: Genesis of the Chilean iron ore deposits; 23rd Internat. Geol. Congr. Czechoslovakia, v. 7, 328-338.

Sakuyama, M. and Kushiro, I.

1979: Vesiculation of hydrous andesitic melt and transport of alkalies by separated vapor phase; Contrib. Mineral. Petrol., v. 71, p. 61-66.

Shegelski, R.J.

1973: Geology and mineralogy of the Terra Silver mine, Camsell River, N.W.T.; M.Sc. thesis, University of Toronto, Toronto, 169 p.

Shegelski, R.J. and Murphy, J.D.

1973: Preliminary geologic map of the Camsell River silver district; Department of Indian Affairs and Northern Development, Yellowknife, N.W.T., Open File 135, 18 p.

Shegelski, R.J. and Scott, S.D.

1975: Geology and mineralogy of the silver-uranium-arsenide veins of the Camsell River District, Great Bear Lake, N.W.T.; in Abstracts with Programs, Geol. Soc. Amer., v. 7, no. 6, p. 857-858.

Sheppard, S.M.F.

1986: Characterization and isotopic variations in natural waters in Stable isotopes in high temperature geological processes; Valley, J.W., Taylor, H.P., Jr. and O'Neil, J.R. (eds.), Rev. Mineral. Min. Soc. Amer., v. 16, p. 165-181.

Shemesh, A., Kolodny, Y. and Luz, B.

1983: Oxygen isotope variations in phosphate of biogenic apatites: Phosphorite rocks; Earth Planet. Sci. Lett., v. 64, p. 405-416.

Shinhara, H.

1992: Does acid volcanic gas represent magmatic discharge at depth?; in Magmatic contributions to hydrothermal systems and the behavior of volatiles in magma, J. W. Hedenquist, (ed.), Rept. Geol. Survey Japan, 279, p. 152-155.

Smellie, J.A.T.

1980: Kiruna-type iron ores from Mertainen and Painirova; [abs.]. Geol. Foren. Stockholm Forh., v. 102, p. 280-281.

Snyder, F.G.

1969: Precambrian iron deposits in Missouri; Econ. Geol. , Mon. 4, p. 231-238.

Stauffer, R.E.

1982: Fluorapatite and fluorite solubility controls on geothermal waters in Yellowstone National Park; Geochim. Cosmochim. Acta, v. 46, p. 465-474.

Strekeisen, A.L.

1973: Plutonic rocks. Classification and nomenclature recommended by the IUGS subcommission on the systematics of igneous rocks; Geotimes, October, 1973, p.26-30.

Steiger, R.H. and Jager, E.

1978: Subcommission on Geochronology: convention on the use of decay constants in geo- and cosmochronology; Earth Planet. Sci. Lett., v. 36, p. 359-362.

Suzuoki, T. and Epstein, S.

1976: Hydrogen isotope fractionation between OH-bearing minerals and water; Geochim. Cosmochim. Acta, v. 40, p. 1229-1240.

Taylor, B.E.

1986: Magmatic volatiles: Isotopic variation of C, H, and S; in Stable Isotopes in High Temperature Geological Processes, eds. J.W. Valley, H.P. Taylor, Jr., J.R. O'Neil, Reviews in Mineralogy, v. 16, p. 185-225.

1991: Degassing of obsidian Dome rhyolite, Inyo volcanic chain, California in Stable Isotope Geochemistry: A Tribute to Samuel Epstein; The Geochemical Society, Spec. Publ. 3, H.P. Taylor, Jr., J.R. O'Neil and R. Kaplan, eds., p. 339-353.

in press: Degassing of H_2O from rhyolite magma during eruption and shallow intrusion, and the isotopic composition of magmatic water in hydrothermal systems; in Extended Abstracts, U.S. - Japan Seminar on Magmatic Contributions to Hydrothermal Systems, J. Hedenquist, S. Kesler, E. Izawa and P. Muffler, eds., Geol. Survey Japan Report 279.

Taylor, H.P., Jr.

1974: The application of oxygen and hydrogen isotope studies to problems of hydrothermal alteration and ore deposition; Econ. Geol., v. 69, p. 843-883.

The Staff, Eldorado.

1946: The Eldorado Enterprise; Can. Inst. Mining Metall., Transactions, vol. XLIX, p. 423-428.

Thorpe, R.

1971: Lead isotopic evidence on the age of mineralization, Great Bear Lake, District of Mackenzie, Canada; Geol. Survey of Canada Paper 71-1, Part B, p. 72-75.

Thorpe, R.

1974: Lead isotope evidence on the genesis of the silver arsenide vein deposits of the Cobalt and Great Bear Lake areas, Canada; Econ. Geol., v. 69, p. 777-791.

Thurber, J.B.

1946: Glacier Bay - Cameron Bay area, Great Bear Lake, N.W.T.; Geol. Survey of Canada, Central Technical File 86E/16-1.

Tirrul, R.

1976: The geology of the Rainy Lake Igneous Complex, District of Mackenzie, Northwest Territories; B.Sc. thesis, Queen's University, Kingston, 115 p.

Tirrul, R.

1983: Structure cross-sections across Asiak foreland thrust and fold belt, Wopmay orogen, District of Mackenzie; in Current Research, Part B, Geol. Survey of Canada Paper 83-1B, p. 253-260.

Truesdell, A.H. and Singers, W.

1974: The calculation of aquifer chemistry in hot-water geothermal systems; Jour. Res. U.S. Geol. Surv., v.2, p. 271-278.

Vidal, C.E., Injoque-Espinoza, J., Sidder, G.B. and Mukasa, S.B.

1990: Amphibolitic Cu-Fe skarn deposits in the central coast of Peru; Econ. Geol., v. 85, p. 1447-1461.

Wanless, R.K., Stevens, R.D., Lachance, G.R. and Delabio, R.N.

1970: Age determinations and geologic studies; K-Ar isotopic ages, Report 8, Canada Geol. Survey Paper 67-2A.

Watson, E.B.

1979: Apatite saturation in basic to intermediate magmas; Geophys. Res. Lett., v. 6, p. 937-940.

Wright, T.L. and Okamura, R.T.

1977: Cooling and crystallization of tholeiitic basalt, 1965 Makaopuhi lava lake, Hawaii; U.S. Geol. Surv. Prof. Paper 1004, 78 p.

Ypma, P.J.M.

1972: The multistage emplacement of the Chalanches (France) Ni-Co-Bi-As-Sb-Ag deposits and the nature of the mineralizing solutions; 24th Int. Geol. Cong. Proc., Section 4, p. 525.

Zhang, R.

1986: Sulphur isotopes and pyrite-anhydrite equilibria in a volcanic basin hydrothermal system of the middle to lower Yangtze River valley; Econ. Geol., v. 81, p. 32-45.

Zheng, Y.

in press: Calculation of oxygen isotope fractionation in metal oxides; Geochim. Cosmochim. Acta.

APPENDIX A - Electron Microprobe Analyses

Quantitative mineral analyses were carried out by the author at McGill University, Montréal with the Cameca Camebax electron microprobe using an accelerating voltage of 15 kV, a beam current of 8 nA and a beam diameter of approximately 1 micron. Analyses were obtained from standard polished thin sections carbon coated before analysis. Standards used were andradite or SWOL for Fe; diopside or SWOL for Mg; SWOL for Ca; SWOL for Si; Amelia albite for Na; orthoclase for Al; olivine for Mn; fluorite for F; vanadanite [$(PbCl)(Pb_4)(VO_4)$] for V and Cl; apatite for P; wilemite for Zn; chalcopyrite for Cu; NiO for Ni; and synthetic Mn-ilmenite for Ti. Data were acquired for until a standard deviation of less than 2 wt.% was achieved. The ZAF correction technique was used for data correction.

Appendix A-1: Magnetite, hematite, ilmenite and pyrophanite electron microprobe analyses

Sample	88-256-1 hematite	88-256-2 hematite	88-256-3 hematite pt 1	88-256-3 hematite pt 2	88-256-4 magnetite pt 1	88-256-4 hematite pt 2	89-193-1 magnetite core	89-193-1 magnetite	89-193-1 magnetite	89-193-1 hematite rim
Fe2O3	99.46	100.72	94.78	99.90	103.34	98.94	101.91	103.73	104.28	99.89
MnO	0.09	0.01	0.06	0.00	0.17	0.11	0.14	0.03	0.06	0.06
ZnO	0.00	0.01	0.00	0.03	0.01	0.03	0.03	0.07	0.00	0.00
Al2O3	0.13	0.20	0.06	0.00	0.04	0.48	0.38	0.16	0.17	0.22
MgO	0.00	0.00	0.02	0.01	0.00	0.04	0.05	0.04	0.02	0.05
SiO2	0.33	0.03	0.11	0.05	0.34	0.48	0.08	0.05	0.04	0.12
CaO	0.00	0.03	0.07	0.01	0.03	0.15	0.01	0.03	0.16	0.22
CuO	0.06	0.02	5.73	0.00	0.00	0.03	0.00	0.06	0.07	0.03
TiO2	0.03	0.00	0.09	0.01	0.03	0.22	0.58	0.16	0.08	0.19
Cr2O3	0.14	0.14	0.00	0.00	0.00	0.00	0.00	0.08	0.00	0.00
V2O5	0.00	0.01	0.01	0.00	0.07	0.06	0.61	0.54	0.55	0.59
NiO	0.00	0.04	0.03	0.01	0.01	0.00	0.00	0.02	0.03	0.00
Total	100.24	101.21	100.96	100.02	104.04	100.54	103.79	104.97	105.46	101.04

Sample	89-193-2 magnetite core	89-193-2 hematite rim	89-193-3 magnetite core	89-193-3 magnetite rim	89-193-5 magnetite pt 1	89-193-5 magnetite pt 2	89-193-5 magnetite pt 3	89-193-5 hematite pt 4	89-193-5 hematite pt 5	89-193-5 magnetite pt 6
Fe2O3	103.35	99.91	101.98	103.23	103.72	101.50	100.75	96.98	97.11	98.97
MnO	0.08	0.02	0.12	0.16	0.03	0.17	0.18	0.04	0.06	0.08
ZnO	0.11	0.05	0.00	0.05	0.09	0.13	0.00	0.01	0.08	0.04
Al2O3	0.18	0.18	0.23	0.35	0.19	0.25	0.36	0.25	0.25	0.19
MgO	0.02	0.04	0.06	0.01	0.01	0.00	0.04	0.00	0.00	0.05
SiO2	0.06	0.07	0.07	0.06	0.06	0.04	0.10	0.09	0.05	0.75
CaO	0.02	0.09	0.02	0.04	0.02	0.00	0.00	0.04	0.02	0.28
CuO	0.03	0.00	0.00	0.00	0.00	0.03	0.00	0.00	0.02	0.09
TiO2	0.11	0.13	0.15	0.32	0.25	0.58	0.57	0.40	0.30	0.52
Cr2O3	0.18	0.00	0.00	0.00	0.01	0.29	0.14	0.00	0.00	0.00
V2O5	0.51	0.55	0.58	0.45	0.49	0.47	0.52	0.52	0.58	0.52
NiO	0.02	0.00	0.05	0.00	0.05	0.00	0.08	0.20	0.19	0.00
Total	104.67	101.04	103.26	104.67	104.92	103.46	102.74	98.53	98.66	101.49

Sample	89-193-6 magnetite	89-59b-1 magnetite pt 1	89-59b-1 hematite pt 3	89-59b-2 magnetite pt 1	89-59b-2 magnetite pt 2	89-59b-3 magnetite pt 1	89-59b-3 hematite pt 2	88-248-5 hematite pt 1	88-248-1 magnetite pt 1	88-248-1 hematite pt 2
Fe2O3	100.43	100.13	99.20	101.12	100.79	101.14	99.21	97.15	100.65	97.27
MnO	0.03	0.03	0.02	0.03	0.09	0.04	0.09	0.04	0.07	0.06
ZnO	0.00	0.01	0.09	0.04	0.09	0.00	0.09	0.00	0.04	0.00
Al2O3	0.10	0.32	0.27	0.22	0.28	0.32	0.24	0.05	0.08	0.12
MgO	0.02	0.09	0.07	0.04	0.09	0.07	0.07	0.01	0.02	0.00
SiO2	0.06	0.02	0.04	0.05	0.04	0.03	0.24	0.08	0.04	0.11
CaO	0.02	0.00	0.00	0.05	0.00	0.01	0.07	0.04	0.04	0.12
CuO	0.00	0.00	0.01	0.00	0.00	0.00	0.00	0.01	0.00	0.00
TiO2	0.09	0.20	0.23	0.26	0.24	0.29	0.20	0.15	0.18	0.70
Cr2O3	0.00	0.00	0.00	0.00	0.02	0.18	0.08	0.05	0.07	0.00
V2O5	0.55	0.48	0.41	0.43	0.48	0.45	0.46	0.66	1.18	1.16
NiO	0.03	0.03	0.00	0.05	0.04	0.06	0.05	0.08	0.10	0.01
Total	101.33	101.31	100.34	102.29	102.16	102.59	100.80	98.32	102.47	99.54

Sample	88-248-6 magnetite pt 1	88-248-6 hematite pt 2	89-495-5 hematite pt 1	89-495-5 hematite pt 2	89-495-2 hematite	89-495-4 hematite pt 1	89-495-4 hematite pt 2	89-495-4 hematite pt 3	88-124-1 hematite pt 1	88-124-1 magnetite pt 2
Fe2O3	99.89	96.81	96.99	96.50	99.20	98.78	97.72	96.90	99.28	99.24
MnO	0.40	0.06	0.25	0.18	0.05	0.13	0.03	0.03	0.03	0.26
ZnO	0.00	0.21	0.04	0.05	0.00	0.00	0.11	0.09	0.00	0.07
Al2O3	0.07	0.12	0.22	0.32	0.02	0.39	0.05	1.12	0.06	0.40
MgO	0.02	0.02	0.02	0.11	0.02	0.02	0.01	0.21	0.00	0.48
SiO2	0.13	0.10	0.06	0.06	0.15	0.06	0.07	0.04	0.02	1.52
CaO	0.01	0.06	0.00	0.01	0.02	0.02	0.01	0.01	0.02	0.13
CuO	0.01	0.01	0.03	0.06	0.05	0.10	0.00	0.00	0.00	0.00
TiO2	1.48	0.15	0.79	0.66	0.03	0.46	0.15	0.75	0.11	0.15
Cr2O3	0.00	0.35	0.00	0.00	0.19	0.00	0.00	0.01	0.00	0.00
V2O5	0.91	0.73	0.74	0.72	0.31	0.85	1.32	0.78	0.50	0.60
NiO	0.00	0.00	0.02	0.00	0.00	0.01	0.06	0.00	0.05	0.00
Total	102.92	98.62	99.16	98.67	100.04	100.82	99.53	99.94	100.07	102.85

Appendix A-1 continued.

Sample	88-124-1 hematite pt 3	88-124-1 magnetite pt 4	88-124-1 hematite pt 5	88-124-1 magnetite pt 6	88-124-1 magnetite pt 7	88-124-1 magnetite pt 8	88-124-1 magnetite pt 9	88-124-1 magnetite pt 10	88-124-1 magnetite pt 11	88-124-1 hematite pt 12
Fe2O3	98.22	101.24	99.92	98.75	98.90	101.07	100.58	100.26	99.80	99.23
MnO	0.02	0.27	0.05	0.20	0.29	0.28	0.27	0.18	0.24	0.10
ZnO	0.03	0.00	0.00	0.07	0.00	0.00	0.00	0.05	0.02	0.01
Al2O3	0.13	0.19	0.03	0.53	0.49	0.32	0.23	0.30	0.31	0.14
MgO	0.03	0.26	0.00	1.02	0.80	0.40	0.35	0.43	0.55	0.05
SiO2	0.09	0.64	0.03	2.06	1.58	0.88	1.04	1.06	1.39	0.09
CaO	0.01	0.07	0.03	0.23	0.23	0.13	0.13	0.15	0.16	0.00
CuO	0.02	0.08	0.01	0.00	0.00	0.06	0.00	0.00	0.02	0.00
TiO2	0.12	0.10	0.23	0.29	0.32	0.13	0.09	0.08	0.03	0.11
Cr2O3	0.00	0.00	0.22	0.00	0.00	0.00	0.00	0.00	0.00	0.00
V2O5	0.61	0.61	0.53	0.60	0.66	0.48	0.52	0.53	0.46	0.38
NiO	0.02	0.00	0.00	0.02	0.00	0.01	0.01	0.01	0.00	0.12
Total	99.30	103.46	101.05	103.77	103.27	103.75	103.20	103.04	102.98	100.22

Sample	88-124-4 magnetite core	88-124-4 hematite rim	88-153-2 magnetite core	88-153-2 hematite rim	88-153-3 magnetite core	89-445b-1 magnetite core	89-445b-1 hematite rim	89-445b-4 hematite core	89-445b-4 magnetite core	89-445b-4 hematite rim
Fe2O3	99.30	98.80	102.46	98.50	102.12	100.51	96.01	98.12	100.80	98.08
MnO	0.23	0.13	0.08	0.16	0.17	0.18	0.04	0.13	0.17	0.08
ZnO	0.05	0.02	0.02	0.00	0.02	0.14	0.19	0.00	0.00	0.00
Al2O3	0.33	0.09	0.03	0.04	0.13	0.05	0.03	0.13	0.05	0.06
MgO	0.85	0.12	0.01	0.02	0.02	0.00	0.02	0.18	0.00	0.01
SiO2	1.39	0.39	0.10	0.07	0.06	0.11	0.02	0.36	0.08	0.11
CaO	0.17	0.02	0.00	0.05	0.00	0.02	0.02	0.00	0.00	0.00
CuO	0.00	0.04	0.00	0.00	0.00	0.04	0.08	0.00	0.00	0.00
TiO2	0.11	0.08	0.02	0.03	0.07	0.13	0.00	0.00	0.03	0.00
Cr2O3	0.00	0.00	0.03	0.00	0.00	0.03	0.30	0.25	0.35	0.53
V2O5	0.59	0.63	0.40	0.32	0.38	0.48	0.28	0.37	0.43	0.29
NiO	0.04	0.11	0.05	0.00	0.02	0.07	0.00	0.07	0.07	0.00
Total	103.05	100.41	103.20	99.18	102.99	101.76	96.98	99.61	101.96	99.15

Sample	89-445b-4 hematite rim	89-445b-3 magnetite core	89-445b-3 hematite rim	89-445b-5 magnetite core	89-445b-5 hematite rim	88-248-5 hematite	88-248-1 hematite
Fe2O3	98.16	101.00	97.00	99.05	97.17	97.28	96.78
MnO	0.06	0.08	0.09	0.11	0.08	0.04	0.04
ZnO	0.00	0.03	0.00	0.07	0.01	0.00	0.01
Al2O3	0.08	0.07	0.05	0.02	0.03	0.07	0.01
MgO	0.01	0.00	0.00	0.00	0.00	0.00	0.00
SiO2	0.05	0.07	0.05	0.08	0.09	0.03	0.08
CaO	0.01	0.00	0.01	0.01	0.00	0.06	0.09
CuO	0.00	0.00	0.04	0.00	0.00	0.00	0.00
TiO2	0.01	0.04	0.03	0.00	0.00	0.12	0.25
Cr2O3	0.39	0.44	0.63	2.02	0.11	0.00	0.00
V2O5	0.46	0.00	0.46	0.26	0.23	0.67	1.23
NiO	0.00	0.04	0.00	0.02	0.01	0.07	0.00
Total	99.23	101.77	98.36	101.65	97.71	98.34	98.48

Sample	88-115-2 ilmenite pt 1	88-115-2 ilmenite pt 2	88-115-1 pyrophanite	88-124-3 pyrophanite pt 2	88-124-3 pyrophanite pt 3	89-426-2 ilmenite	89-426-3 ilmenite
Fe2O3	44.77	44.56	11.61	14.78	18.05	47.07	46.51
MnO	8.68	0.08	37.73	34.95	32.50	8.42	8.69
ZnO	0.12	0.03	0.22	0.00	0.02	0.00	0.00
Al2O3	0.01	0.01	0.00	0.01	0.03	0.01	0.00
MgO	1.28	0.02	0.09	0.03	0.04	0.02	0.03
SiO2	0.01	0.05	0.05	0.07	4.15	0.02	0.03
CaO	0.00	0.08	0.00	0.39	0.76	0.05	0.03
CuO	0.05	0.00	0.00	0.00	0.07	0.04	0.00
TiO2	49.26	54.00	48.24	46.99	47.15	43.81	44.61
Cr2O3	0.00	0.00	0.00	0.00	0.00	0.00	0.00
V2O5	0.26	0.31	0.25	0.24	0.28	0.25	0.28
NiO	0.00	0.04	0.16	0.00	0.00	0.00	0.00
Total	104.44	99.14	98.35	97.45	103.03	99.68	100.18

Appendix A-2: Apatite electron microprobe analyses

Sample	89-193-1 core	89-193-1 rim	89-193-2 core	89-193-2 rim	89-59b-1	89-59b-2	89-59b-3 core	89-59b-4 core	89-124-2 core	89-124-3 core
CaO	55.65	55.50	55.31	55.49	54.69	55.45	55.49	55.83	55.55	54.64
MgO	0.00	0.00	0.00	0.00	0.00	0.00	0.00	0.00	0.00	0.00
Fe2O3(T)	0.06	0.08	0.00	0.00	0.15	0.00	0.10	0.07	0.06	0.06
MnO	0.04	0.01	0.05	0.08	0.00	0.00	0.00	0.02	0.04	0.04
SrO	0.00	0.00	0.00	0.00	0.01	0.01	0.00	0.03	0.01	0.05
P2O5	41.51	42.36	41.58	42.02	41.34	41.74	42.43	41.75	41.85	40.93
F	4.82	3.87	4.79	4.29	6.11	4.61	4.89	5.06	5.24	3.99
Cl	0.26	0.19	0.29	0.20	0.25	0.15	0.15	0.17	0.11	0.10
	102.35	102.01	102.02	102.08	102.55	101.96	103.06	102.93	102.86	99.81
O=F	2.03	1.63	2.02	1.81	2.57	1.94	2.06	2.13	2.21	1.68
O=Cl	0.06	0.04	0.06	0.46	0.06	0.03	0.03	0.04	0.02	0.02
Total	100.26	100.34	99.94	99.81	99.92	99.99	100.97	100.76	100.63	98.11

Sample	88-248-1 core
CaO	53.33
MgO	0.00
Fe2O3(T)	0.04
MnO	0.01
SrO	0.10
P2O5	39.85
F	4.05
Cl	0.86
	98.24
O=F	1.70
O=Cl	0.19
Total	96.35

Appendix A-3: Actinolite electron microprobe analyses

Sample	88-115-1 actinolite pt 1	88-115-1 actinolite pt 2	88-115-1 actinolite pt 3	88-115-2 actinolite pt 1	88-115-2 actinolite pt 2	88-115-2 actinolite pt 3	88-115-3 actinolite	88-115-4 actinolite	88-115-5 actinolite	88-153-1 actinolite rim
SiO2	53.89	53.99	55.17	52.99	53.44	55.96	56.63	58.29	55.16	53.83
TiO2	0.66	0.48	0.28	1.01	0.86	0.32	0.22	0.24	0.26	0.07
Al2O3	2.43	2.32	1.36	3.19	3.03	1.29	1.10	1.28	1.74	1.64
FeOT	8.00	8.19	6.85	7.27	7.44	5.87	5.17	8.11	6.24	12.73
MnO	0.13	0.05	0.09	0.09	0.14	0.10	0.16	0.61	0.06	0.07
MgO	18.75	18.58	19.26	19.38	19.09	20.83	21.57	16.31	20.28	15.98
CaO	11.54	11.56	12.09	10.80	11.12	11.36	11.81	12.14	11.55	12.39
Na2O	1.20	1.29	0.87	1.57	1.26	0.90	0.69	0.50	1.02	0.31
K2O	0.35	0.31	0.21	0.42	0.43	0.30	0.17	0.07	0.32	0.10
F	1.08	1.25	1.09	1.19	1.11	1.22	0.84	0.32	1.35	0.22
Cl	0.12	0.12	0.10	0.07	0.10	0.06	0.06	0.05	0.06	0.08
H2O	1.57	1.49	1.61	1.53	1.56	1.55	1.75	1.99	1.48	1.96
	99.72	99.63	98.89	99.51	99.58	99.76	100.17	99.91	99.52	99.38
O=F	0.46	0.53	0.42	0.50	0.47	0.51	0.35	0.13	0.57	0.09
O=Cl	0.03	0.03	0.02	0.02	0.02	0.01	0.01	0.01	0.01	0.02
Total	99.23	99.07	98.45	98.99	99.09	99.24	99.81	99.77	98.94	99.27

Sample	88-153-1 actinolite core	88-153-2 actinolite core	88-153-2 actinolite rim	88-153-3 actinolite pt 1	88-153-3 actinolite pt 2	89-59b-1 actinolite core	89-59b-2 actinolite core	89-59b-3 actinolite core	88-256-1 actinolite pt 1	88-256-2 actinolite pt 2
SiO2	56.43	54.72	54.81	53.89	54.90	54.74	54.82	55.32	51.45	51.94
TiO2	0.02	0.12	0.07	0.34	0.55	0.21	0.02	0.06	0.08	0.00
Al2O3	0.68	1.29	1.15	1.95	1.92	2.05	1.70	1.28	2.50	2.19
FeOT	10.24	13.54	12.41	9.89	8.11	10.53	10.32	9.75	23.26	20.14
MnO	0.31	0.56	0.50	0.52	0.15	0.04	0.03	0.10	0.89	0.75
MgO	18.51	15.46	15.55	17.32	19.32	17.85	17.78	18.47	9.49	9.50
CaO	12.33	12.04	12.14	11.65	11.84	11.93	12.15	12.14	11.74	11.94
Na2O	0.16	0.21	0.11	0.73	0.91	0.75	0.61	0.52	0.34	0.25
K2O	0.03	0.06	0.09	0.32	0.38	0.29	0.18	0.19	0.17	0.15
F	0.21	0.15	0.17	0.27	0.53	0.85	0.80	0.87	0.12	0.14
Cl	0.02	0.02	0.02	0.06	0.07	0.06	0.06	0.04	0.14	0.06
H2O	2.04	2.02	1.99	1.94	1.87	*1.34	*1.34	*1.34	*2.6	*2.6
	100.98	100.19	98.99	98.88	100.55	100.64	99.81	100.08	102.78	99.66
O=F	0.09	0.06	0.07	0.12	0.22	0.36	0.34	0.37	0.06	0.07
O=Cl	0.00	0.00	0.01	0.01	0.02	0.01	0.01	0.01	0.01	0.03
Total	100.89	100.13	98.91	98.75	100.31	100.27	99.46	99.70	102.71	99.56

Sample	88-256-2 actinolite pt 1	88-256-2 actinolite pt 2	88-256-2 actinolite pt 3	88-248-1 actinolite	88-248-2 actinolite	89-193-1 actinolite	89-193-2 actinolite	89-426-1 actinolite	89-426-2 actinolite	89-124-1 actinolite
SiO2	49.36	51.51	53.78	56.73	57.29	55.51	56.51	54.70	55.26	48.75
TiO2	0.03	0.08	0.11	0.05	0.11	0.09	0.10	0.74	0.50	0.14
Al2O3	6.74	1.94	0.95	1.07	1.06	1.46	0.57	2.10	1.94	8.27
FeOT	16.03	22.89	21.15	9.48	5.68	9.93	10.64	8.42	8.34	9.64
MnO	1.40	1.13	0.86	0.38	0.18	0.18	0.18	0.11	0.17	0.14
MgO	16.94	7.87	9.64	18.98	22.09	18.17	16.89	18.90	18.38	15.40
CaO	6.19	11.87	11.75	12.59	12.20	12.37	12.44	11.43	11.50	11.96
Na2O	0.12	0.27	0.12	0.59	0.21	0.50	0.21	0.91	0.81	1.37
K2O	0.02	0.18	0.07	0.01	0.12	0.24	0.12	0.29	0.23	0.73
F	0.20	0.16	0.02	0.32	0.24	0.71	0.49	0.27	0.24	0.72
Cl	0.03	0.14	0.06	0.02	0.03	0.06	0.12	0.12	0.11	0.14
H2O	*2.6	*2.6	*2.6	*2.3	*2.3	1.78	1.85	1.97	1.98	1.69
	99.66	100.64	101.11	102.52	101.51	101.00	100.12	99.96	99.46	98.95
O=F	0.08	0.07	0.01	0.13	0.10	0.30	0.21	0.11	0.10	0.30
O=Cl	0.01	0.03	0.01	0.00	0.01	0.01	0.03	0.03	0.03	0.03
Total	99.57	100.54	101.09	102.39	101.40	100.69	99.88	99.82	99.33	98.62

Appendix A-3 continued.

Sample	89-124-2 actinolite	89-445b-1 actinolite pt 1	89-445b-1 actinolite pt 2	89-445b-2 actinolite	89-193-3 actinolite	89-193-4 actinolite
SiO2	55.75	54.64	55.59	55.20	57.06	54.00
TiO2	0.15	0.03	0.09	0.10	0.05	0.14
Al2O3	1.43	2.28	1.70	1.55	0.40	2.43
FeOT	9.21	12.32	11.14	12.78	10.66	10.82
MnO	0.09	0.03	0.19	0.10	0.19	0.17
MgO	18.33	16.81	16.51	14.87	17.54	16.24
CaO	12.48	12.21	12.08	12.08	12.49	12.02
Na2O	0.55	0.47	0.27	0.30	0.18	0.44
K2O	0.20	0.16	0.21	0.18	0.07	0.27
F	0.71	0.44	0.22	0.20	0.58	0.56
Cl	0.04	0.06	0.05	0.08	0.07	0.10
H2O	1.79	1.90	2.00	1.98	1.85	1.80
	43.40	44.40	42.67	42.57	43.63	42.42
O=F	0.30	0.19	0.09	0.08	0.24	0.23
O=Cl	0.01	0.01	0.01	0.02	0.02	0.02
Total	43.09	44.20	42.57	42.47	43.37	42.17

pt = point
*H2O calculated from volumetric measurements of hydrogen released by fusion.
H2O calculated on the basis of 24 (O, OH, F, Cl).

Appendix A-4: Biotite, chlorite and talc electron microprobe analyses

Sample	89-59b-1 biotite	89-59b-2 biotite	89-426-3 biotite	89-495-1 talc pt 1	89-495-1 talc pt 2	89-495-2 talc	89-495-3 talc	88-248-1 chlorite	88-248-2 chlorite
SiO2	42.65	41.94	40.15	62.50	62.31	62.17	62.82	28.09	27.75
TiO2	0.88	0.96	4.32	0.01	0.00	0.00	0.00	0.03	0.10
Al2O3	11.41	11.96	12.32	0.46	0.44	0.44	0.45	19.10	18.72
FeOT	11.25	10.35	13.08	2.84	2.73	2.66	2.31	23.79	25.99
MnO	0.06	0.01	0.02	0.05	0.06	0.03	0.04	0.58	0.70
MgO	20.45	20.81	16.59	29.10	28.10	28.26	28.30	17.41	15.53
CaO	0.04	0.00	0.03	0.02	0.02	0.05	0.02	0.09	0.10
Na2O	0.26	0.24	0.14	0.24	0.14	0.10	0.13	0.00	0.03
K2O	6.96	7.26	9.37	0.04	0.05	0.03	0.02	0.01	0.03
F	2.88	2.64	0.56	0.43	0.35	0.27	0.39	0.16	0.12
Cl	0.28	0.25	0.41	0.02	0.02	0.01	0.01	0.01	0.01
H2O	*2.6	*2.6	2.50					11.61	11.51
	99.72	99.02	99.49	95.71	94.22	94.02	94.49	100.89	100.58
O=F	1.21	1.11	0.24	0.08	0.08	0.04	0.08	0.07	0.05
O=Cl	0.06	0.06	0.09	0.00	0.00	0.00	0.00	0	0
Total	98.45	97.85	99.16	95.63	94.14	93.98	94.41	100.82	100.53

pt = point
H2O calculated on the basis of 24 (O, OH, F) for biotite; 18(O, OH, F, Cl) for chlorite.
*H2O calculated from volumetric measurement of hydrogen released by fusion.

APPENDIX B - Whole-Rock Geochemistry Methods

Major and minor elements (SiO_2, TiO_2, Al_2O_3, Cr_2O_3, Fe_2O_3, MnO, MgO, CaO, Na_2O, K_2O, P_2O_5) were obtained by X-ray fluorescence wavelength dispersive analysis on fused disks, except FeO, which was obtained by modified Wilson method (potentiometric titration following cold acid decomposition). H_2O, CO_2, and S were obtained by infra-red spectrometry. Fe_2O_3 was calculated using Fe_2O_3T (XRF) - 1.11134 (volumetric). Be, Co, Cr, Cu, Ni, Sc, V, and Zn by Induced Coupled Plasma Emmission Spectrometry. Pb by flame atomic absorption. Ce, Dy, Er, Eu, Gd, Ho, La, Nd, Sm, Tm, Y, and Yb were determined by Induced Coupled Plasma Mass Spectrometry, Induced Coupled Plasma Emmission Spectrometry, and Graphite Furnace Atomic Absorption.

APPENDIX C - Stable Isotope Analyses

Stable isotope analyses were completed for whole-rock samples by the author and John Sekerka at the Geological Survey of Canada in Ottawa. Mineral separate analyses were completed by the author. Bulk fluid inclusion analyses were carried out by Bruce Taylor (Geological Survey of Canada) and the author at the GSC, Ottawa. Mass spectrometer analyses were carried out by John Sekerka at the Geological Survey of Canada for deuterium, and by Gilles St. Jean and Margaret McLaren at the University of Ottawa for oxygen, carbon and sulphur.

Whole-rock samples were trimmed to remove all weathered surfaces, split to less than 2 cm size, and crushed in either a cyclone crusher or jaw crusher. This material was then split into two fractions, one of which was pulverized in a tungsten puck pulverizer for three to five minutes, depending on sample hardness.

Oxygen for isotopic analysis was liberated from approximately 10 mg of powdered sample by reaction with BrF_5. The oxygen was converted to CO_2 by passing it over a hot carbon rod. To liberate hydrogen, eighty to 120 mg of powdered sample was heated incrementally under vacuum until fused. Hydrogen was produced by passing the H_2O over hot uranium metal. Volumetric measurements of the hydrogen yield were recorded to determine water content. CO_2 from calcite was liberated by reaction with H_3PO_4 at 25°C for 24 hours; siderite was reacted for 72 hours. $\delta^{34}S$ Routine precision for whole-rock samples is approximately 0.2 ‰ (1σ) for $\delta^{18}O$, 1.0‰ (1σ) for δD and 0.1‰ for $\delta^{13}C$.

Water was extracted from fluid inclusions in MAA material by crushing samples in evacuated stainless steel tubes. Water was collected and converted to hydrogen as described above.

APPENDIX D- Sample descriptions and petrographic summaries

All percentages are approximate. Minor = 1 to 5%. Trace = <1%. NTS = no thin section.

H-77: (collected by R.S. Hildebrand, 1977)

015 Porphyritic andesite with 15% partially to extensively sericitized, subhedral plagioclase phenocrysts to 5 mm and rare chloritized relict amphibole phenocrysts to 3 mm; clusters of carbonate, chlorite, opaque minerals. Strongly hematized groundmass of very fine feldspar and quartz, chlorite and iron oxide.

019 Fine-grained volcanogenic sandstone. (NTS)

022 Eutaxitic dacite tuff. (NTS)

042 Eutaxitic dacite tuff. (NTS)

051 Strongly porphyritic andesite with extensively sericitized plagioclase phenocrysts from 0.5 to 6 mm which are also altered to chlorite and epidote. Subhedral relict clinopyroxene replaced by epidote. Abundant clumps to 4 mm of epidote, chlorite and opaque minerals. Reddish hematized groundmass contains coarse patches of very fine-grained chlorite, magnetite, epidote, plagioclase and brown alteration mineral (iron oxide?). Also minor magnetite up to 0.5 mm. Chlorite + epidote veinlets cut both groundmass and phenocrysts.

052 Medium-grained hypidiomorphic monzonite. Extensively sericitized plagioclase laths to 5 mm with relatively fresh rims and minor replacement by amphibole. Lesser quartz and potassium feldspar interstitial to plagioclase. Amphibole, clinopyroxene, biotite, magnetite. Trace apatite.

053 Porphyritic andesite with weakly to extensively sericitized plagioclase phenocrysts to 4 mm. Chlorite aggregates, minor quartz aggregates and chlorite-rimmed quartz amygdules to 3 mm. Groundmass of chlorite, plagioclase, magnetite and carbonate.

081 Fine-grained volcanogenic sandstone. (NTS)

093 Porphyritic andesite. (NTS)

095 Porphyritic andesite with 30% partially sericitized sieve-textured subhedral plagioclase phenocrysts to 4 mm, many of which are fractured. Lithic fragments of quartzo-feldspathic material to 5 mm. Few quartz-chlorite amygdules. Very fine-grained anhedral magnetite.

096 Porphyritic andesite with completely sericitized and epidotized subhedral plagioclase phenocrysts from 2 to 4 mm. Minor chloritized amphibole phenocrysts to 2 mm. Clots of chlorite, epidote, carbonate and magnetite. Groundmass of plagioclase, chlorite, magnetite and carbonate. Veinlets of amphibole less than 0.25 mm. wide

124 Fine-grained monzodiorite. (NTS)

135 Fine-grained sandstone. (NTS)

140 Dacite. (NTS)

154b Tuff. (NTS)

170 Fine-grained monzonite. (NTS)

172 Fine-grained sandstone. (NTS)

226 Fine-grained sandstone. (NTS)

239 Altered medium-grained diorite. (NTS)

HWA-80-J:

069 Coarse-grained biotite syenite (Richardson pluton).

HWA-87-C: (collected by R. Cherer, 1987)

009 Moderately altered, fine- to medium-grained granodiorite comprised of 40% strongly sericitized plagioclase, 25% anhedral quartz, 20% hornblende, and 15% potassium feldspar. Trace calcite, apatite and granophyre.

011 Moderately altered, medium-grained quartz monzonite comprised of 35% strongly sericitized plagioclase to 5 mm, 15% anhedral quartz, 30% hornblende, and 30% potassium feldspar. Minor magnetite. Trace calcite, apatite, titanite and granophyre. Calcite veinlets.

013 Strongly altered, medium-grained quartz monzonite comprised of 40% strongly sericitized plagioclase, 15% anhedral quartz, 15% hornblende, and 25% potassium feldspar. Minor epidote. Trace calcite, apatite, titanite and granophyre. Calcite veinlets.

015 Weakly altered, medium-grained quartz monzonite comprised of 40% weakly sericitized plagioclase, 15 to 20% anhedral quartz, 30% hornblende to 9 mm, and 25% potassium feldspar. Minor biotite and magnetite. Trace calcite, titanite, and apatite.

HWA-88-R: (collected by N. Reardon, 1988)

001 Strongly altered porphyritic andesite with 15% phenocrysts of corroded plagioclase to 3 mm altered to chlorite, epidote and quartz and relict clinopyroxene? 1 to 2 mm completely replaced by epidote and chlorite. Irregular quartz-filled amygdules to 4 mm. Groundmass of granular epidote, chlorite, quartz, feldspars, magnetite. Iron stained chlorite veinlets < 1 mm throughout.

002 Moderately altered, fine-grained xenomorphic quartz-potassium feldspar dyke. 50% cloudy, hematized, potassium feldspar, <10% strongly sericitized plagioclase to 3 mm and 20 to 25% quartz to 2 mm. 15% relict hornblende and biotite altered to chlorite and epidote. Minor fine grained ragged magnetite <0.5 mm. Trace zircon.

003 Strongly altered, weakly trachytic, porphyritic andesite with 35% phenocrysts of subhedral sericitized and chloritized plagioclase to 5 mm, some of which show regrowth and relict hornblende and/or clinopyroxene 1 to 3 mm replaced by chlorite and quartz, with magnetite rims, in a groundmass of chlorite, epidote and magnetite. 15% quartz-chlorite-quartz zoned amygdules to 5 mm with rare euhedral apatite and hematite, some of which have granular magnetite rims. Minor fine-grained magnetite and trace apatite.

010 Strongly altered andesite with 10% corroded chloritized plagioclase phenocrysts to 4 mm with calcite and sericite in a granular groundmass of feldspar to 1 mm and very fine grained chlorite and minor chlorite. four veinlets: 1) 2 mm apatite veinlet with chlorite, magnetite, hematite, titanite, calcite and unidentified yellow-brown mineral; 2) 0.5mm quartz-chlorite veinlet; 3) 1mm magnetite/chlorite/calcite/apatite veinlet. These three veinlets are parallel. 4) calcite veinlet with titanite which cuts the apatite vein at about 45 degrees.

013 Very strongly altered andesite?, completely replaced and recrystallized. Comprised primarily of anhedral patches of bright orange-red hematite to 8 mm (60%) and lesser specularite (10%). 20% fine-grained granular quartz and quartz veinlets which cut the hematite. 5% pods and veinlets of fan-like pale yellow mineral (natrolite?). Minor chlorite, some patches to 2 mm.

016 Very strongly altered plagioclase-amphibole-clinopyroxene porphyritic andesite with <10% anhedral to subhedral, very strongly sericitized (+ chlorite, epidote and calcite) plagioclase phenocrysts to 4 mm, minor relict subhedral amphibole to 4 mm altered to feldspar and chlorite with magnetite on fractures and rims, and relict subhedral clinopyroxene phenocrysts 2 to 5 mm altered to feldspar, quartz, chlorite and magnetite with granular magnetite concentrated at the rims or outlining relict zoning, in a groundmass of feldspar, chlorite, magnetite (15%) and trace calcite.

Trace pyrite. Feldspar-yellow-green chlorite filled fractures less than 0.5 mm wide cut and offset some phenocrysts.

019 Very strongly altered plagioclase-amphibole-clinopyroxene glomeroporphyritic andesite with 15 to 20% anhedral to subhedral, strongly sericitized (+ epidote and calcite) plagioclase phenocrysts to 4 mm, <10% relict subhedral amphibole to 4 mm altered to feldspar, chlorite and magnetite or hematite, and rare relict subhedral clinopyroxene phenocrysts 2 to 5 mm altered to epidote, feldspar, chlorite and magnetite in a hematized groundmass of feldspar, epidote, patchy disseminated or blebs to 1 mm of magnetite and hematite, and chlorite. Trace pyrite. Quartz-calite veinlets in two directions at 90 degrees.

022 Strongly altered plagioclase - amphibole - clinopyroxene glomeroporphyritic andesite with 15% to 20% anhedral to subhedral, strongly sericitized (+ epidote and calcite) plagioclase phenocrysts to 4 mm, 10 to 15% relict subhedral amphibole to 4 mm altered chlorite with epidote and calcite blebs, in a hematized groundmass of feldspar, epidote, chlorite and magnetite. Trace euhedral apatite. Quartz-calcite of fractures in at least two directions and irregular, discontinuous fractures with rusty brown stain.

023 Moderately altered plagioclase - amphibole - clinopyroxene glomeroporphyritic andesite with 20 to 25% subhedral to euhedral, moderately to strongly sericitized (+ epidote and calcite) plagioclase phenocrysts to 4 mm, 10 to 15% relict subhedral to euhedral amphibole 0.5 to 3 mm altered to chlorite with lesser calcite and epidote and magnetite rims, relict subhedral clinopyroxene phenocrysts 2 to 5 mm altered to epidote, calcite and chlorite, and minor anhedral magnetite <0.5 mm, in a hematized groundmass of feldspar, disseminated (20%) magnetite and hematite, epidote and chlorite.

024 Very strongly altered plagioclase-hornblende porphyritic, amygdular andesite with 15% completely sericitized, anhedral to subhedral plagioclase phenocrysts to 5 mm, 15% relict hornblende phenocrysts altered to feldspar and sericite with magnetite rims, and 5% irregular pods to 8 mm of granular subhedral to euhedral quartz with lesser epidote, chlorite and pyrite in a groundmass of granular sericitized feldspar

less than 0.1 mm with minor opaque as ragged patches, and minor anhedral to subhedral pyrite with rims of brown alteration mineral.

028 Very strongly altered plagioclase-hornblende porphyritic, amygdular andesite with 15% anhedral to subhedral plagioclase phenocrysts to 2 mm altered to epidote and sericite, 15% chloritized anhedral to subhedral hornblende phenocrysts to 2 mm and xx% quartz amygdules to 5 mm with chlorite, titanite <0.5 mm and hematite in a groundmass of granular feldspar and epidote and trace subhedral to euhedral magnetite and pyrite less than 0.1 mm.

031 Moderately altered, fine-grained xenomorphic quartz-potassium feldspar dyke. 50% cloudy, hematized, potassium feldspar, 5% strongly sericitized plagioclase to 1.5 mm and 35% quartz to 0.5 mm 5% relict chloritized hornblende and 5% anhedral to subhedral zoned riebeckite to 1 mm. Minor fine grained ragged hematite less than 0.1 mm. Trace zircon.

033a Very strongly altered plagioclase-(hornblende?) porphyritic andesite with 30 to 40% irregular felty patches of sericite and chlotite (plagioclase phenocrysts?), 5% irregular clusters of magnetite to 7 mm and irregular pods of chlorite to 1 mm (phenocryst remnants?) in a groundmass of granular feldspar with minor actinolite, chlorite, epidote, subhedral magnetite to 0,75 mm and pyrite cubes <0.1 mm. Rare biotite with hematite on cleavage.

034 Very strongly altered plagioclase-(hornblende?) porphyritic andesite with 15% chlorite/epidote clots to 5 mm and <5% irregular calcite blebs to 1 cm in a groundmass of granular feldspar with lesser chlorite, epidote and minor magnetite, hematite, pyrite and titanite clusters less than 0.2 mm. Chlorite-lined quartz veinlet with platy hematite.

035 Very strongly altered andesite (?) comprised of equal amounts of feldspar and completely chloritized actinolite with minor blue riebeckite sheaths and zoned, euhedral apatite <0.5 mm. Trace titanite, pyrite and zircon. Quartz-veinlet with magnetite and titanite and rusty alteration product.

036 Very strongly altered plagioclase-hornblende-(clinopyroxene?) porphyritic, amygdular andesite comprised of 10% anhedral to subhedral plagioclase phenocrysts to 6 mm altered to sericite, epidote feldspar and quartz, 15% chloritized anhedral to subhedral hornblende phenocrysts to 4 mm, <0.5% subhedral clinopyroxene? altered to yellow-brown amorphous mineral and calcite, and <5% quartz amygdules to 6 mm in a groundmass of granular feldspar, fibrous actinolite and chlorite with trace subhedral apatite <0.5 mm, titanite, hematite, riebeckite and pyrite.

037 Very strongly altered plagioclase-hornblende porphyritic, amygdular andesite comprised of 35% anhedral to subhedral completely sericitized plagioclase phenocrysts to 3 mm, 20% completely chloritized (+ calcite) hornblende < 1 mm in a groundmass of plagioclase microlites, very fine-grained feldspar, magnetite, epidote, chlorite, titanite, euhedral apatite and pyrite. Irregular quartz amygdules less than 1 mm.

041 Weakly altered plagioclase - hornblende - clinopyroxene glomeroporphyritic andesite comprised of 15 to 20% anhedral to subhedral strongly sericitized plagioclase phenocrysts to 3 mm, 5 to 10% anhedral to subhedral clinopyroxene to 3 mm altered to epidote and magnetite, and 5% chloritized and actinolitized hornblende up to 1 mm in a groundmass of very fine-grained feldspar, epidote and magnetite. Trace actinolite and apatite. Calcite-hematite veinlet less than 0.1 mm in width.

042 Very strongly altered plagioclase-hornblende porphyritic andesite comprised of 10% anhedral to subhedral weakly to moderately sericitized plagioclase phenocrysts to 4 mm and 10% ragged actinolite-chlorite patches to 3 mm in a groundmass of granular feldspar, actinolite, epidote and opaque minerals. Trace calcite. Calcite veinlets, <0.1 mm.

043 Very strongly altered plagioclase-hornblende porphyritic andesite comprised of less than10% ragged clinopyroxene to 2 mm, 5% very strongly sericitized, anhedral to subhedral plagioclase phenocrysts to 3 mm and minor chloritized amphibole in a

groundmass of fine-grained granular feldspar (albite?), actinolite and lesser magnetite, and epidote-rich bands. Trace quartz, calcite and biotite.

044 Strongly altered, medium-grained, seriate monzonite comprised of 35% moderately to strongly sericitized, subhedral plagioclase phenocrysts to 4 mm, 30% cloudy, anhedral potassium feldspar to 4 mm, 15% anhedral quartz less than 2 mm. 5% anhedral to subhedral, chloritized hornblende to 1 mm and 10% anhedral to subhedral, chloritized biotite to 2 mm. Minor magnetite associated with biotite. Trace granophyre, riebeckite, apatite, calcite and zircon. Quartz-calcite veinlets.

049 Weakly altered, medium- to coarse-grained monzonite comprised of 35% weakly sericitized, subhedral plagioclase phenocrysts to 6 mm, 25% anhedral potassium feldspar to 2mm, and 15% anhedral quartz less than 2 mm. 10% anhedral to subhedral, chloritized hornblende to 1 mm and 10% anhedral to subhedral, chloritized biotite to 2 mm. Minor magnetite associated with biotite. Trace riebeckite, apatite and zircon. Chlorite and chlorite-calcite veinlets.

050 Very strongly altered amygdular andesite comprised of 40% granular, relict plagioclase phenocrysts to 1 mm and rare moderately altered phenocrysts. 35% fibrous, pale green actinolite and 10% relict hornblende to 3 mm altered to chlorite, actinolite, magnetite and lesser quartz (cores), epidote and biotite. <5% quartz patches to 1 mm. Minor magnetite. Trace apatite.

051 Altered andesite in albite zone. (NTS)

052 Weakly to moderately altered, medium--grained monzodiorite comprised of 40% weakly to moderately sericitized, subhedral plagioclase phenocrysts to 5 mm, 30% subhedral to anhedral potassium feldspar to 5 mm, some of which are zoned, and 10% anhedral quartz. 15% subhedral chloritized and epidotized hornblende to 4 mm with biotite overgrowths. Minor biotite, granophyre, magnetite and unidentified pale brown amphibole. Trace titanite and apatite. Chlorite-calcite veinlets.

053 Very strongly altered plagioclase-hornblende-clinopyroxene porphyritic andesite comprised of <10% very strongly sericitized, anhedral to subhedral plagioclase phenocrysts to 3 mm, some with actinolite rims, 10% subhedral relict hornblende altered to chlorite, epidote and feldspar, and 5% anhedral to subhedral clinopyroxene to 2 mm altered to epidote, calcite and magnetite, in a groundmass of granular feldspar, actinolite and lesser magnetite. Trace calcite. Actinolite-titanite-calcite-chlorite veinlet cut by quartz-calcite veinlet.

056 Very strongly altered amygdular plagioclase - hornblende - clinopyroxene porphyritic andesite comprised of 20% weakly to moderately sericitized anhedral to subhedral seriate plagioclase phenocrysts to 2 mm and minor chloritized hornblende and quartz in a groundmass of granular feldspar and lesser epidote and magnetite. Trace calcite. Abundant rounded, magnetite-rich cognate xenoliths.

057 Very strongly altered, plagioclase - hornblende - clinopyroxene glomeroporphyritic, moderately trachytic andesite comprised of 10% moderately to strongly sericitized, subhedral plagioclase phenocrysts to 3 mm and 15% strongly altered clinopyroxene and hornblende to 1 mm in a groundmass of granular feldspar and microlites, and lesser epidote and actinolite. Trace apatite and magnetite. quartz-calcite veinlet.

062 Fine-grained hornblende-biotite monzonite. (NTS)

066 Altered andesite in MAA zone. (NTS)

068 Altered andesite in MAA zone. (NTS)

070 Fine-grained hornblende-biotite monzodiorite. (NTS)

075 Strongly altered, medium-grained quartz diorite comprised of 50% moderately to strongly sericitized, subhedral plagioclase phenocrysts to 3 mm, 15% anhedral potassium feldspar and 10% anhedral quartz. 25 to 30% of chloritized hornblende and biotite. Minor magnetite. Trace riebeckite, apatite, zircon and pyrite. Hematization along fractures. Quartz-chlorite veinlet.

076 Strongly altered, fine-grained diorite comprised of 50% strongly sericitized, zoned, subhedral plagioclase phenocrysts to 1 mm, 15% anhedral potassium feldspar and <5% anhedral quartz. 25% of chloritized hornblende and biotite. Minor magnetite. Trace apatite and zircon.

081 Fine-grained hornblende-biotite monzonite. (NTS)

083a Altered andesite with trace pyrite and specularite. (NTS)

083b 80 cm MAA vein in pyrite zone. (NTS)

085 Weakly to moderately altered, medium-grained quartz diorite comprised of 50% weakly to moderately sericitized, subhedral plagioclase phenocrysts to 4 mm, 10% anhedral potassium feldspar to 2 mm, less than10% anhedral quartz to 1 mm and 10% granophyre. 15% of chloritized hornblende and biotite. Minor magnetite. Trace apatite, zircon and calcite. Quartz-chlorite-calcite veinlet.

087 Medium-grained diorite. (NTS)

088 Weakly altered, fine-grained monzogranite (dyke?) comprised of 30% anhedral, granular quartz to 2 mm, 25 strongly sericitized subhedral plagioclase phenocrysts to 3 mm, 15% fresh, fine-grained, granular plagioclase and 25% fine-grained, granular potassium feldspar. Minor chloritized biotite and associated magnetite and titanite. Trace riebeckite, titanite, calcite and zircon.

089 Medium-grained quartz monzonite. (NTS)

091 Very strongly altered quartz monzodiorite comprised of 30% strongly sericitized and epidotized subhedral plagioclase phenocrysts to 3 mm and subhedral potassium feldspar to 3 mm, and 25% weakly chloritized hornblende to 3 mm in a groundmass of fine-grained granular, strongly sericitized plagioclase (30%) and quartz (15%). Minor magnetite. Trace calcite.

099 Medium-grained monzodiorite. (NTS)

106 Sulfide-bearing quartz vein. Anhedral to subhedral, cloudy, highly fractured quartz with abundant, very fine fluid inclusions. Some euhedral cross-sections to 8 mm, also fine-grained granular quartz.

112 Very strongly altered andesite comprised of 35% strongly sericitized subhedral plagioclase phenocrysts to 2 mm and 10% mafic clots of chlorite, actinolite, magnetite and calcite less than 2 mm in a groundmass of very fine-grained granular feldspar, chlorite, epidote, magnetite and trace calcite.

115 MAA vein in monzonite. (NTS)

124 Strongly altered amygdular andesite comprised of 25% moderately to strongly sericitized, subhedral plagioclase phenocrysts and 15% anhedral to subhedral hornblende, altered to chlorite, quartz and magnetite, and relict subhedral clinopyroxene in a opaque-rich groundmass of very fine-grained granular feldspar, chlorite, epidote, and trace calcite. Magnetite-rich patches to 3 mm around phenocrysts. Quartz veinlet.

128 Strongly altered, medium-grained quartz monzodiorite comprised of 50% weakly to strongly sericitized and epidotized subhedral plagioclase phenocrysts to 5 mm, 10 to 15% cloudy, anhedral potassium feldspar to 5 mm and 10% anhedral quartz. 10% an- subhedral chloritized amphibole <2 mm. Minor an- subhedral epidotized clinopyroxene to 2 mm, opaque minerals and granophyre. Trace chlorite and apatite.

130 Very strongly altered porphyritic andesite comprised of 15% moderately to strongly sericitized and epidotized subhedral plagioclase phenocrysts to 4 mm, 10% irregular patches of chlorite <1 mm, and minor clinopyroxene to 1 mm altered to chlorite, feldspar, epidote and magnetite in a groundmass of fine-grained, granular feldspar, epidote and magnetite.

132 Quartz-fluorite vein. Subhedral to euhedral quartz containing abundant fluid inclusions (trails), some of which contain liquid+vapour+crystal, most contain liquid+vapour only. Colourless, highly fractured fluorite with few inclusions, minor very fine hematite inclusions; rare, fine-grained pale purple fluorite. Minor chlorite sheaths in quartz, associated with unidentified white micaceous mineral.

135 Very strongly altered andesite comprised of relict plagioclase, hornblende and clinopyroxene phenocrysts to 4 mm in a groundmass of fine-grained, granular feldspar with lesser patchy actinolite and minor finely-disseminated magnetite and pyrite. Secondary patch of medium-grained magnetite to 4 mm, apatite to 0.5 mm, actinolite to 3 mm, pyrite replacing magnetite and cloudy feldspar to 1 mm. 5% magnetite, 2% pyrite total.

141 Albitized andesite in MAA zone. (NTS)

142 Very strongly altered andesite comprised of 80% granular plagioclase to 4 mm, 10% ragged patches of granular epidote and actinolite to 2 mm, some with quartz. Minor ragged, corroded crystals of magnetite altered to chlorite, epidote, calcite and quartz. Minor chlorite. Streaky hematization of groundmass.

148 Moderately to strongly altered andesite comprised of 20% subhedral to euhedral plagioclase phenocrysts to 3 mm and 5% relict chloritized hornblende phenocrysts to 2 mm with magnetite rims in a groundmass of fine-grained, granular plagioclase microlites with lesser chlorite, epidote, and opaque minerals. Trace apatite and zircon.

150 Moderately to strongly altered andesite comprised of 15 to 20% subhedral to euhedral, strongly sericitized and epidotized plagioclase phenocrysts to 3 mm and 10% strongly chloritized hornblende phenocrysts to 2 mm with actinolite cores, granular epidote concentrated in the rims and quartz coronas. 5% subhedral to euhedral epidotized (+chlorite and magnetite) clinopyroxene to 3 mm with quartz coronas. Groundmass of plagioclase microlites with lesser epidote, chlorite, magnetite and trace calcite. Chlorite and quartz veinlets.

153 MAA breccia in strongly altered andesite. (NTS)

156 Moderately altered, medium-grained quartz monzonite comprised of 35 to 40% subhedral, moderately to strongly chloritized actinolite and minor clinopyroxene altered to epidote, calcite and quartz, in a groundmass of very fine-grained granular feldspar and lesser epidote, chlorite and opaque minerals. Trace pyrite. 15 mm bleb of subhedral actinolite to 9 mm, calcite to 4 mm and magnetite with a rim of epidote, apatite and quartz. epidote veinlet.

166 Very strongly altered andesite comprised of 10 to 15% an- to subhedral, strongly sericitized plagioclase phenocrysts to 3 mm, minor relict hornblende altered to chlorite, actinolite and calcite, and minor clinopyroxene altered to epidote, calcite and quartz, in a groundmass of very fine-grained granular feldspar and lesser actinolite, epidote, chlorite and opaque minerals. Trace titanite associated with magnetite. Discontinuous magnetite and actinolite veinlets and quartz veinlet.

172 Altered,plagioclase porphyritic andesite in albite zone. (NTS)

174 Altered plagioclase porphyritic andesite in MAA zone. (NTS)

176 Plagioclase porphyritic andesite. (NTS)

177 Altered plagioclase porphyritic andesite in MAA zone. (NTS)

180 Very strongly altered andesite comprised of 55% slightly hematized, granular plagioclase to 0.5 mm, 25% blebs of granular epidote to 5 mm. 20% ragged patches of finely disseminated magnetite (martite) to 15 mm.

182 Strongly altered andesite comprised of 25% subhedral, strongly epidotized plagioclase phenocrysts to 3 mm, 15% hornblende to 3 mm altered to actinolite, biotite, epidote, magnetite and quartz and 5% subhedral to euhedral clinopyroxene to 1 mm altered to actinolite and epidote in a groundmass of fine-grained plagioclase (some microlites), epidote and lesser opaque minerals. Trace apatite and pyrite. Chlorite and actinolite veinlets.

185 Very strongly altered andesite comprised of minor anhedral, relict plagioclase phenocrysts to 4 mm, 5% an- to subhedral, chloritized hornblende phenocrysts to 2 mm and rare relict epidotized clinopyroxene phenocrysts in a groundmass of fine-grained, granular feldspar, epidote, actinolite and lesser chlorite and opaque minerals.

186 Very strongly altered andesite comprised of 20% subhedral, strongly sericitized (+ chlorite, epidote and calcite) plagioclase phenocrysts to 4 mm, and minor completely chloritized subhedral hornblende to 1 mm in a hematized groundmass of fine-grained plagioclase and lesser epidote, chlorite, calcite and opaque minerals. chlorite-calcite veinlets. Hand sample has magnetite veinlets with brecciated wall rock.

188 Massive magnetite-apatite-actinolite rock in andesitic lava with magnetite to 1 cm. Pyrite pods.

189 Very strongly altered andesite comprised of 10% anbhedral, strongly sericitized (+ chlorite, epidote and calcite) plagioclase phenocrysts to 3 mm in a weakly hematized groundmass of fine-grained plagioclase and lesser chlorite (relict hornblende?) and magnetite. Trace pyrite.

196 Altered andesite in MAA zone. (NTS)

197 Moderately to strongly altered, weakly trachytic andesite comprised of 15% subhedral to euhedral, strongly sericitized plagioclase phenocrysts to 4 mm, and less than10% completely chloritized (+ calcite and magnetite) an- to eubhedral hornblende to 2 mm in a very strongly hematized groundmass of fine-grained plagioclase microlites and lesser epidote, chlorite and opaque minerals.

198 Moderately to strongly altered, fine-grained, plagioclase porphyritic quartz monzonite comprised of 40% subhedral strongly sericitized plagioclase phenocrysts, 20% subhedral potassium feldspar, 15% anhedral quartz, and 10 to 15% relict hornblende altered to chlorite, magnetite and calcite, and 10%

magnetite. Minor biotite with chlorite rims and magnetite on cleavage planes, and relict subhedral clinopyroxene to 2 mm altered to epidote, magnetite and calcite. Trace apatite and titanite. Chlorite-hematite veinlets.

204 Strongly altered fine-grained monzodiorite comprised of 80% subhedral strongly epidotized and sericitized plagioclase phenocrysts, 20% subhedral chloritized and actinolitized hornblende to 3 mm and 105 anhedral potassium feldspar to 2 mm. Minor magnetite to 0.25 mm with associated titanite. Trace quartz.

207 Weakly altered plagioclase-hornblende porphyritic, pilotaxitic andesite comprised of 15% subhedral to eubhedral, weakly sericitized plagioclase phenocrysts to 2 mm and 15% completely chloritized (+ epidote, quartz, magnetite), subhedral hornblende to 2 mm in a felty groundmass of 90% plagioclase microlites to 0.1 mm and minor epidote, chlorite and hematized magnetite.

212 Strongly altered andesite in MAA zone. 30% magnetite and actinolite. (NTS)

216 Weakly altered porphyritic diorite comprised of 50% an- to subhedral, weakly sericitized plagioclase phenocrysts, 15% potassium feldspar, 15% fresh, subhedral hornblende and 15% subhedral, stubby epidote less than0.2 mm. Minor anhedral quartz less than0.2 mm and subhedral apatite to 1 mm. quartz veinlets.

219 Altered, actinolitized siltstone, 50% mafic minerals. (NTS)

222 andesitic flow breccia comprised of 50% rock fine-grained fragments. The fragments are bimodal, being either quartz-chlorite-magnetite or very fine-grained granular feldspar. The groundmass is comprised of very fine grained feldspar and epidotized phenocrysts to 2 mm, angular to rounded quartz to 2 mm, epidote and minor pyrite and calcite.

226 Porphyritic andesite. (NTS)

227 Very strongly altered andesite comprised of 50% strongly sericitized, granular plagioclase, 20% irregular patches of calcite to 1 mm associated with 5% magnetite.

15% chlorite and minor patches of chlorite, magnetite and quartz. 2-3% subhedral to euhedral apatite to 1 mm.

231 Very strongly altered andesite comprised of 35% strongly sericitized, anhedral plagioclase laths less than 1 mm, 20% anhedral quartz to 1 mm 20% anhedral, granular epidote, 10% chlorite to 0.5 mm, and 15% very finely disseminated and granular magnetite to 2 mm. 1 to 2% finely disseminated calcite and calcite blebs to 3 mm. Trace zircon. quartz-calcite veinlets.

234 Altered andesite in magnetite-apatite-actinolite zone. (NTS)

243 Very strongly altered, medium-grained monzodiorite comprised of 20% strongly sericitized, subhedral plagioclase laths to 4 mm and 10% mafic clots to 3 mm of chlorite, magnetite and epidote in a groundmass of very fine, granular plagioclase and potassium feldspar (65%), epidote, chlorite, quartz, and magnetite. Trace riebeckite. quartz-chlorite veinlets.

245b Quartz vein with abundant chloritized and epidotized wall rock fragments to > 1 cm. An- to euhedral quartz less than0.1 mm to 4 mm with abundant brown streaks of minute inclusions which cross crystal boundaries.

248 Magnetite-apatite-actinolite pod in fine-grained monzodiorite. (NTS)

256 Actinolite-epidote-quartz vein with hematite-lined vesicles less than1 mm. (NTS)

257a Moderately altered, fine-grained, plagioclase porphyritic monzodiorite comprised of 75% moderately to strongly sericitized subhedral plagioclase phenocrysts to 0.5 mm, 10% subhedral, partially chloritized hornblende to 0.5 mm and 10% ragged patches of chlorite and epidote. 1% andhedral quartz less than0.1 mm. Minor magnetite associated with trace titanite. Moderately hematized and 0.5 mm quartz veinlet.

263a 60 cm chalcopyrite-bearing quartz-carbonate vein. (NTS)

263b Andesitic porphyry (wall rock of 263a). (NTS)

269 Moderately to strongly altered, fine- to medium-grained monzonite comprised of 40% moderately to strongly sericitized and epidotized, subhedral plagioclase to 2 mm, 35% anhedral potassium feldspar to 1 mm intergrown with 10% andhedral quartz to 1 mm. 15% subhedral, partially chloritized hornblende and actinolite to 3 mm and 5% chloritized biotite. Minor granophyre. Trace apatite.

301 Sulfide-bearing quartz vein. An- to subhedral, granular quartz crystals less than 1 mm and coarse crystals to 5 mm, some of which have truncated zoning and overgrowth. Minor green chlorite and pyrite cubes less than 1 mm. Rusty alteration of pyrite.

302 Weakly altered, medium-grained quartz monzonite comprised of 40% weakly sericitized, subhedral plagioclase to 5 mm, 35% anhedral potassium feldspar to 4 mm, 10% andhedral quartz to 3 mm and 10% subhedral, partially chloritized hornblende to 3 mm. Minor biotite associated with magnetite. Trace apatite, riebeckite, 10% subhedral, chloritized hornblende to 2 mm and 5% an- to subhedral, fine-grained, fresh biotite. 1% opaque minerals, associated with biotite. Trace riebeckite, titanite, apatite and zircon.

306 Very strongly altered, heterogeneous andesite breccia comprised of 30 to 75% granular feldspar, 10 to 60% fine-grained, granular epidote and chlorite, up to 10% biotite associated with magnetite. 5 to 15% magnetite, trace riebeckite, pyrite, and zircon. chlorite veinlet.

308 Altered plagioclase porphyritic andesite. Calcite veinlets. (NTS)

HWA-89-R: (collected by N. Reardon, 1989)

008 Calcite pod in andesitic porphyry. (NTS)

013 Strongly altered, finely-bedded, fine-grained volcanogenic sandstone with 5 to 45% secondary, chloritized amphibole, the proportion of which varies with individual

beds. Also significant but variable amounts of chlorite, altered biotite (?), turbid plagioclase, incusion-rich quartz pods and an- to euhedral poikilitic magnetite. less than5% minor granular epidote in feldspar. Trace titanite, apatite and pyrite. chlorite veinlets.

019 Fine-grained monzonite, 40% mafic minerals. Hematized. (NTS)

021b Quartz-siderite vein. (NTS)

059b Magnetite-apatite-actinolite breccia in siltstone. Minor pyrite. (NTS)

124 8 cm magnetite-actinolite vein in andesitic porphyry. (NTS)

143 Pyrite pod in strongly albitized andesitic porphyry. (NTS)

162 Strongly altered, finely-bedded, fine-grained volcanogenic sandstone comprised of 50% fine-grained, moderately altered, granular feldspar, 30% amphibole, and 10% finely disseminated calcite, some of which is associated with anhedral ragged magnetite. Minor chlorite and epidote, lesser quartz, ragged magnetite, pyrite and garnet (?) Trace zircon.

173 Altered andesitic porphyry in magnetite-apatite-actinolite zone. Trace pyrite. (NTS)

188b 60 cm quartz-siderite-chalcopyrite-pyrite vein. (NTS)

191 Strongly altered, plagioclase porphyritic, amygdular andesite with 30% strongly altered, subhedral plagioclase phenocrysts to 4 mm, some of which have amphibole-chlorite cores, in a hematized groundmass of 40% granular feldspar, 10% chlorite, 10% of an unidentified colourless mineral, minor calcite and pyrite. Minor irregular quartz amygdules less than3 mm with chlorite rims. Trace pyrite.

193 Magnetite-apatite-actinolite pod in andesitic porphyry. (NTS)

226 Fine- to medium-grained volcanogenic sandstone comprised of 40% very fine-grained to medium-grained anhedral feldspar, 25% angular to sub-rounded monocrystalline to granular quartz to 2 mm, and 20% very fine-grained, granular, partially chloritized amphibole. Less than10% disseminated chlorite. Less than 5% biotite associated with fine-grained, anhedral magnetite. Rare pyrite cubes.

234 Moderately altered plagioclase - hornblende - clinopyroxene porphyritic andesite with 15% an- to euhedral, strongly sericitized plagioclase phenocrysts to 3 mm; 20% subhedral, twinned, chloritized hornblende; and 5% an- to subhedral, twinned, chloritized clinopyroxene in a hematized groundmass of feldspar, epidote, anhedral magnetite, amphibole (?) and rare quartz. Trace pyrite.

251 Strongly altered, fine-grained andesitic porphyry with 50% strongly sericitized stubby plagioclase laths with epidotized rims, some with overgrowths; 25% dark green-brown biotite associated with chlorite and epidote; 20% relict chloritized amphibole; and less than 5% anhedral fine-grained quartz. One blob of chlorite with sericite halo. Minor granophyre. Trace very fine-grained magnetite and hematite, and pyrite.

276 Pyrite pod in strongly altered andesite with 5% disseminated pyrite up to 3 mm. (NTS)

291 Strongly altered plagioclase porphyritic andesite with 15% subhedral strongly sericitized plagioclase laths up to 4 mm. 40% chloritized, irregular masses of amphibole and lesser calcite with quartz rims throughout the groundmass, some with remnants of clinopyroxene (?), in a groundmass comprised of mostly plagioclase with lesser calcite and chlorite. Trace magnetite and quartz-rimmed titanite associated with relict clinopyroxene.

294 Strongly altered plagioclase porphyritic, amygdular andesite with 25% strongly sericitized (+amphibole) subhedral plagioclase laths 1 to 3 mm and less than 1 mm, and less than10% relict clinopyroxene phenocrysts up to 3 mm, altered to chlorite and magnetite, in a groundmass of feldspar and 50% chloritized, irregular masses of amphibole. 10% irregular quartz-filled amygdules up to 2 mm. Large quartz-rich

xenolith (sedimentary rock?) with rounded plagioclase comprises 30% of the thin section

313 Strongly altered plagioclase - clinopyroxene glomeroporphyritic andesite with 20% strongly sericitized (+quartz) subhedral plagioclase laths up to 3 mm and 20% relict clinopyroxene, altered to amphibole, epidote, chlorite and magnetite, in a hematized groundmass of feldspar, epidote, amphibole with associated magnetite, chlorite, and magnetite. Trace pyrite.

323 Moderately altered plagioclase porphyritic andesite with 15% weakly sericitized plagioclase laths up to 4 mm in a hematized groundmass of plagioclase and chlorite with lesser quartz, an- to subhedral magnetite up to 3 mm, anhedral to euhedral calcite less than0.1 mm, and fine-grained, granular epidote. Patchy chlorite and epidote in groundmass may be relict clinopyroxene or amphibole. Quartz-calcite veinlets less than0.5 mm.

338 Moderately altered plagioclase - clinopyroxene porphyritic andesite or andesitic porphyry with 25% strongly sericitized anhedral plagioclase laths up to 4 mm and 20% relict clinopyroxene altered to amphibole, chlorite and quartz in a groundmass of feldspar, biotite, chlorite, epidote and magnetite. Trace pyrite and zircon.

352 Weakly altered, medium-grained, equigranular granodiorite with 40% moderately sericitized subhedral, stubby plagioclase laths up to 4 mm, 20% anhedral, perthitic potassium feldspar up to 4 mm, and 15 to 20% anhedral quartz 1 to 3 mm with unidentified needle-like inclusions. 10% anhedral, pleochroic golden-brown/red-brown biotite with magnetite on cleavage planes. 10% pleochroic, partially to completely chloritized amphibole. Less than 2% anhedral magnetite associated with biotite. Rare myrmekite and trace apatite and titanite. Fine chlorite veinlets.

360 Coarse actinolite-apatite pod with disseminated pyrite up to 3 mm. (NTS)

373 Massive pyrite with silica blebs and veinlets from gossan. (NTS)

404 Strongly altered plagioclase porphyritic andesite with 15% strongly sericitized plagioclase phenocrysts up to 3 mm, some with chlorite cores, in a fine-grained recrystallized groundmass of plagioclase (albite?) with minor chlorite, magnetite, quartz and trace finely disseminated anhedral to euhedral calcite.

410 Moderately altered, fine- to medium-grained quartz monzonite comprised of 40% cloudy potassium feldspar up to 3 mm, 30% completely sericitized subhedral plagioclase up to 2 mm and 15 to 20% anhedral, irregular to granular quartz up to 2 mm with unidentified needle-like inclusions. Some potassium feldspar-quartz intergrowths. 10% chlorite-magnetite patches. Trace apatite and Riebeckite.

423 Strongly albitized andesite in magnetite-apatite-actinolite zone. (NTS)

426 15 cm actinolite pod with biotite, in volcanogenic sandstone. (NTS)

429b massive chalcopyrite from calcite pod in andesite. (NTS)

432 Moderately altered plagioclase porphyritic, amygdular andesite with 15 to 20% an- to subhedral moderately sericitized plagioclase phenocrysts, 25% irregular quartz-filled amygdules up to 6 mm, some with chlorite or chlorite + calcite cores, and having increased concentrations of disseminated magnetite in the groundmass surrounding them. Hematized groundmass comprised principally of feldspar and epidote with minor calcite, chlorite, magnetite and specularite. Quartz-calcite veinlets.

445b Actinolite-apatite pod in andesite. (NTS)

446 One meter actinolite vein with minor pyrite, in andesite. (NTS)

447 Medium-grained hornblende granodiorite. (NTS)

449 Altered , magnetite-rich andesite with 3 to 4% pyrite. (NTS)

459 Moderately altered andesite which contains 1 cm chalcopyrite vein, chalcopyrite blebs and 2 cm vuggy quartz-chalcopyrite vein. (NTS)

469 Altered andesitic porphyry. Trace pyrite. Calcite veinlets. (NTS)

483b massive chalcopyrite from 80 cm cacite pod in andesite. (NTS)

495 Coarse, 70 cm actinolite-hornblende pod with malachite stain. (NTS)

506 Altered plagioclase porphyritic andesite. Trace pyrite. (NTS)

508 Moderately altered andesitic breccia, 45% very fine- to coarse-grained angular to sub-rounded fragments and 15% subhedral, sericitized, chloritized plagioclase phenocrysts in a chlorite-rich matrix with 15% 1 to 2 mm anhedral quartz. Trace titanite.

512 Weakly altered, medium-grained monzonite comprised of: 35% weakly sericitized, subhedral plagioclase laths 1 to 3 mm; 30% potassium feldspar; 15% hornblende strongly altered to biotite and iron oxide; 15% augite partially altered to amphibole and biotite along cleavage planes; 5% biotite as overgrowths on amphibole, and having magnetite and bright red mineral on cleavage planes. Minor granophyre and magnetite.

538 Medium-grained hornblende-biotite monzodiorite. (NTS)

548 Strongly altered plagioclase porphyritic andesite with 10 to 15% completely sericitized (+ quartz + chlorite) subhedral plagioclase laths 1 to 5 mm and 5% relict blocky, subhedral clinopyroxene? phenocrysts up to 3 mm, completely altered to chlorite in a groundmass of unidentified dark green-brown, granular material with less than1% magnetite. Trace pyrite. Quartz-chlorite veinlets and very fine fractures with rusty alteration product.

549 Strongly altered plagioclase porphyritic amygdular andesite with 10 to 15% completely sericitized subhedral plagioclase phenocrysts 1 to 6 mm, less than10%

relict subhedral to euhedral chloritized hornblende phenocrysts up to 2 mm, and 10% irregular quatrz-filled amygdules up to 4 mm in a groundmass of feldspar, epidote, chlorite and magnetite. Minor magnetite, trace very fine-grained titanite and riebeckite. Quartz-chlorite veinlets and very fine fractures with rusty alteration product.

576 Strongly altered plagioclase porphyritic andesite with 15 to 20% strongly sericitized (+ epidote), subhedral, corroded plagioclase phenocrysts up to 4 mm in a groundmass comprised primarily of granular feldspar with lesser epidote and chlorite. Minor magnetite and trace calcite. Chlorite veinlets cut by quartz-chlorite veinlets with adjacent calcite.

577 Strongly altered plagioclase porphyritic andesite with 20 to 25 % strongly sericitized, subhedral plagioclase phenocrysts up to 6 mm in a groundmass composed primarily of granular feldspar with lesser epidote (15 to 20% of rock), minor calcite and magnetite, and trace chlorite which is associated with the magnetite. Chlorite veinlets and quartz-chlorite veinlets with adjacent calcite.

578 Strongly altered plagioclase porphyritic andesite with moderately sericitized plagioclase phenocrysts up to 5 mm with abundant inclusions of stubby, prismatic, colourless mineral and prismatic birefringent mineral and 15% relict amphibole or biotite replaced by chlorite and carbonate in a groundmass of granular feldspar with lesser chlorite and minor magnetite and carbonate. Rare fine-grained anhedral quartz.

579 Strongly altered plagioclase porphyritic andesite with 15 to 20% sericitized subhedral plagioclase phenocrysts up to 2 mm and minor relict mafic mineral altered to epidote and chlorite in a groundmass of granular feldspar with lesser epidote and minor anhedral quartz, magnetite, calcite and chlorite. Calcite and quartz veinlets.

580 Strongly altered medium-grained monzonite comprised of 30% strongly sericitized subhedral plagioclase phenocrysts up to 3 mm, 25% irregular, anhedral, relatively fresh potassium feldspar up to 2 mm, 15% anhedral quartz up to 3 mm, 20% relict

an- to subhedral biotite and amphibole altered to chlorite + magnetite, carbonate, titanite, riebeckite.

581 Moderately altered, fine-grained quartz monzonite comprised of: 15% completely sericitized zoned, subhedral plagioclase phenocrysts 1 to 4 mm with very fine apatite and riebeckite (?) inclusions; 15% strongly sericitized plagioclase less than1 mm; 25% cloudy, brown, an to subhedral potassium feldspar 1 to 3 mm; 20% anhedral quartz up to 3 mm with abundant fluid inclusion (some with liquid and vapour) trails.; and 15% subhedral chloritized (with magnetite on cleavage planes) biotite up to 2 mm. Minor granophyre, magnetite, trace carbonate and rare relict epidotized amphibole up to 4 mm. Trace riebeckite and zircon. Calcite veinlets.

582 Moderately altered, fine-grained, seriate, plagioclase porphyritic quartz monzonite comprised of: 35% Strongly sericitized, an- to subhedral, zoned plagioclase phenocrysts 2 to 3 mm; 30% cloudy, brown, anhedral potassium feldspar up to 3 mm; 20% anhedral quartz up to 2 mm with riebeckite inclusions; 10 to 15% an to subhedral, partially chloritized, dark brown biotite with magnetite on cleavage planes. Minor granophyre, magnetite, and relict mafic mineral replaced by calcite, biotite, quartz and magnetite. Trace riebeckite?, apatite and zircon. Cacite and chlorite veinlets.

583 Moderately altered, fine-grained, seriate, plagioclase porphyritic monzonite comprised of: 35% anhedral, fresh potassium feldspar 1 to 2 mm, some of which are zoned; 30% moderately to strongly sericitized subhedral plagioclase up to 4 mm, some of which arte zoned; 20% anhedral quartz less than1 mm; and less than10% subhedral, dark brown, chloritized biotite less than1 mm with magnetite on cleavage planes. Minor amphibole altered to biotite, chlorite and calcite. Minor finely-disseminated an- to subhedral magnetite. Trace epidote, subhedral to euhedral apatite and zircon.

584 Moderately altered, fine- to medium-grained, seriate, plagioclase porphyritic quartz monzonite comprised of: 35% strongly sericitized subhedral plagioclase phenocrysts up to 3 mm; 30% weakly altered (cloudy) irregular, anhedral, potassium feldspar up to 2 mm; less than20% irregular, anhedral quartz less than1

mm; and 10% chloritized biotite. Minor chloritized (+ calcite) relict hornblende up to 2 mm and lesser magnetite. Trace riebeckite up to 1 mm (some patches up to 10 mm), apatite and zircon. Calcite veinlets.

585 Moderately altered, fine-grained, seriate, plagioclase porphyritic quartz monzonite comprised of: 35% strongly sericitized subhedral plagioclase phenocrysts to 3 mm some of which show regrowth; 35% weakly altered (cloudy) irregular, anhedral, potassium feldspar to 2 mm; less than15% irregular, anhedral quartz less than1 mm; and 10% chloritized biotite. 5% chloritized (+ calcite) relict hornblende to 2 mm and lesser magnetite. Trace riebeckite to 1 mm(some patches to 1 cm), apatite and zircon.

586 Moderately altered, fine-grained, seriate, plagioclase porphyritic monzonite comprised of: 40% strongly sericitized subhedral plagioclase phenocrysts up to 5 mm; weakly altered (cloudy) irregular, anhedral, potassium feldspar up to 2 mm; less than10% anhedral quartz; 10% dark red-brown fresh and chloritized biotite up to 2 mm. 8 mm pod of graghically intergrown quartz-riebeckite (schorlite). Trace riebeckite growing on feldspar and as inclusions in quartz.

587 Moderately altered, fine-grained, plagioclase - clinopyroxene glomeroporphyritic monzonite comprised of: 35% subhedral moderately sericitized plagioclase laths up to 3 mm; 35% anhedral to subhedral potassium feldspar up to 3 mm; less than10% anhedral quartz up to 6 mm and 10% chloritized (+mt) biotite less than 1 mm. 5% chloritized (+biotite, calcite, hematite) amphibole. Trace apatite, magnetite up to 2 mm and zircon.

588 Weakly altered, fine-grained, seriate, plagioclase porphyritic quartz monzonite comprised of: 35% zoned, subhedral, moderately to strongly sericitized plagioclase laths up to 4 mm; fresh 35% anhedral potassium feldspar up to 2 mm; 10 to 15% irregular, anhedral quartz less than 2 mm; and 15% chloritized biotite less than 1 mm with magnetite on cleavage planes, some fresh biotite. Minor chloritized amphibole and epidotized clinopyroxene. Trace apatite, very fine-grained an- to subhedral magnetite, calcite and zircon.

589 Weakly altered, fine-grained, seriate, plagioclase porphyritic quartz monzonite comprised of: 35% zoned, subhedral strongly sericitized plagioclase laths up to 5 mm; 35% anhedral potassium feldspar up to 2 mm; 15% irregular, anhedral quartz less than 2 mm; and 10% an- to subhedral, chloritized (+mt) biotite less than 1 mm. Minor anhedral, chloritized amphibole and granophyre. Trace magnetite, subhedral to euhedral apatite, subhedral riebeckite up to 4 mm, and zircon.

590 Weakly altered, hematized, fine-grained, seriate, plagioclase porphyritic quartz monzonite comprised of: 35% very cloudy, anhedral potassium feldspar; 30% weakly to strongly sericitized plagioclase, fine-grained and phenocrysts up to 5 mm; 15 to 20% anhedral quartz less than2 mm; and 12% chloritized biotite. Minor chloritized amphibole and magnetite. Trace apatite, calcite and zircon.

591 Moderately altered, hematized, coarse-grained monzodiorite comprised of: 50% weakly sericitized plagioclase up to 4 mm; 25% cloudy, reddish anhedral potassium feldspar; less than10% irregular, anhedral quartz less than1mm; 10% amphibole altered to biotite.; and 5% chloritized (+calcite and magnetite) amphibole. Minor magnetite. Trace apatite, calcite and zircon.

592 Medium-grained monzonite comprised of 40% strongly sericitized plagioclase up to 4 mm; 25% cloudy, brown anhedral potassium feldspar less than2 mm; 10 to 15% fine-grained, anhedral quartz; less than10% chloritized biotite; and 5% partially chloritized hornblende up to 4 mm. Minor granophyre and an- to subhedral magnetite less than1 mm. Trace calcite and zircon.

593 Weakly to moderately altered medium-grained diorite comprised of 50% weakly to moderately sericitized plagioclase up to 4 mm; 15 to 20% strongly epidotized (+ magnetite) an- to euhedral clinopyroxene up to 1 mm; and less than10% red-brown to green, chloritized biotite. Minor strongly chloritized (+ magnetite) amphibole up to 3 mm. Less than 5% of anhedral, interstitial quartz. Minor interstitial chlorite and an- to euhedral magnetite less than1 mm. Trace apatite and subhedral riebeckite up to 2 mm.

594 Strongly altered quartz-potassium feldspar dyke comprised of: 50% subhedral to euhedral, cloudy red-brown potassium feldspar laths up to 1 mm; 40% anhedral quartz up to 1 mm, interstitial to potassium feldspar; and 10% chloritized biotite up to 1 mm. Minor relict clinopyroxene (?), now mostly chlorite and epidote. Less than 5% fine-grained, anhedral to subhedral magnetite associated with chlorite. Minor granophyre. Trace titanite, calcite, apatite, and zircon. Vug less than 1 mm filled with magnetite, inward-growing titanite growing on the magnetite, and chlorite.

595 Moderately altered plagioclase - clinopyroxene porphyritic andesite comprised of: 15% plagioclase phenocrysts up to 3 mm and 15% strongly epidotized clinopyroxene phenocrysts in a groundmass of epidote, very fine-grained, anhedral magnetite, quartz, and chloritized biotite. Green epidote-rich streaks 1 to 2 mm wide cut by quartz-calcite veinlets.

596 Quartz-potassium feldspar dyke comprised of: 50% subhedral to euhedral, cloudy red-brown potassium feldspar laths less than 1 mm; 35% anhedral quartz interstitial to potassium feldspar. 10% chloritized biotite. Relict clinopyroxene (?) altered to chlorite and epidote. Minor anhedral plagioclase. Trace calcite, apatite, titanite and zircon. One cm quartz bleb with chlorite corona.

597 Very strongly altered, plagioclase porphyritic andesite or monzonite border phase with 30 to 35% subhedral, corroded, moderately sericitized plagioclase phenocrysts up to 2 mm with granular feldspar rims in a groundmass of granular feldspar and epidote. Minor quartz, chlorite and anhedral to subhedral magnetite. Trace zircon.

598 Very strongly altered clinopyroxene - plagioclase - hornblende glomeroporphyritic andesite with 15 to 20% anhedral epidotized (+ calcite and magnetite) clinopyroxene phenocrysts up to 2 mm; 10 to 15% strongly sericitized plagioclase phenocrysts up to 2 mm; and 5 to 10% anhedral, chloritized hornblende phenocrysts up to 1 mm in a groundmass comprised primarily of granular feldspar and epidote. Minor very fine-grained anhedral to subhedral magnetite. Trace calcite.

599 Very strongly altered plagioclase - amphibole porphyritic andesite with 20% subhedral plagioclase phenocrysts up to 3 mm and relict amphibole phenocrysts up

to 2 mm in a groundmass of granular feldspar and epidote with minor quartz and ragged magnetite less than1 mm. Quartz-chlorite-calcite veinlets and actinolite-chloritized biotite veinlet.

600 Strongly altered, finely-bedded, hematized volcanogenic sandstone comprised of 60% chloritized actinolite, 30% anhedral, red-brown feldspar and less than10% ragged to euhedral magnetite. Minor epidote, but up to 15% in some beds. Trace zircon.

600b Magnetite-apatite-actinolite pod in volcanogenic sandstone. (NTS)

603 Chlorite-rich carbonate rock. (NTS)

604 Chlorite-rich carbonate rock. (NTS)

619 Strongly altered plagioclase - amphibole porphyritic andesite with 30% moderately to strongly sericitized subhedral plagioclase phenocrysts up to 5 mm and 5% chloritized (+calcite and magnetite) anhedral amphibole phenocrysts up to 2 mm in a hematized groundmass of feldspar, finely-divided opaque minerals, chlorite and epidote. Trace apatite.

620 Strongly altered plagioclase glomeroporphyritic, amygdular andesite with 35% moderately to strongly sericitized subhedral sieve-textured plagioclase phenocrysts up to 5 mm; minor relict amphibole (?), altered to chlorite, up to 2 mm, and minor quartz-chlorite filled amygdules less than1 mm in a groundmass of feldspar and epidote with minor magnetite and chlorite. Trace apatite.

Energy, Mines and Resources Canada | Énergie, Mines et Ressources Canada
Geological Survey of Canada | Commission géologique du Canada

August 25, 1992

Nancy C. Reardon
Geological Survey of Canada
188-601 Booth St.
Ottawa , Ontario
K1A 0E8

Dear Ms. Reardon:

As scientific authority for Project C1.1.5 of the Canada - Northwest Territories Mineral Development Agreement and Geological Survey of Canada Project 86002, I give you permission to use data and materials produced by you during these projects as part of your Master of Science thesis at the University of Ottawa.

Yours truly,

Robert S. Hildebrand

10'

05'

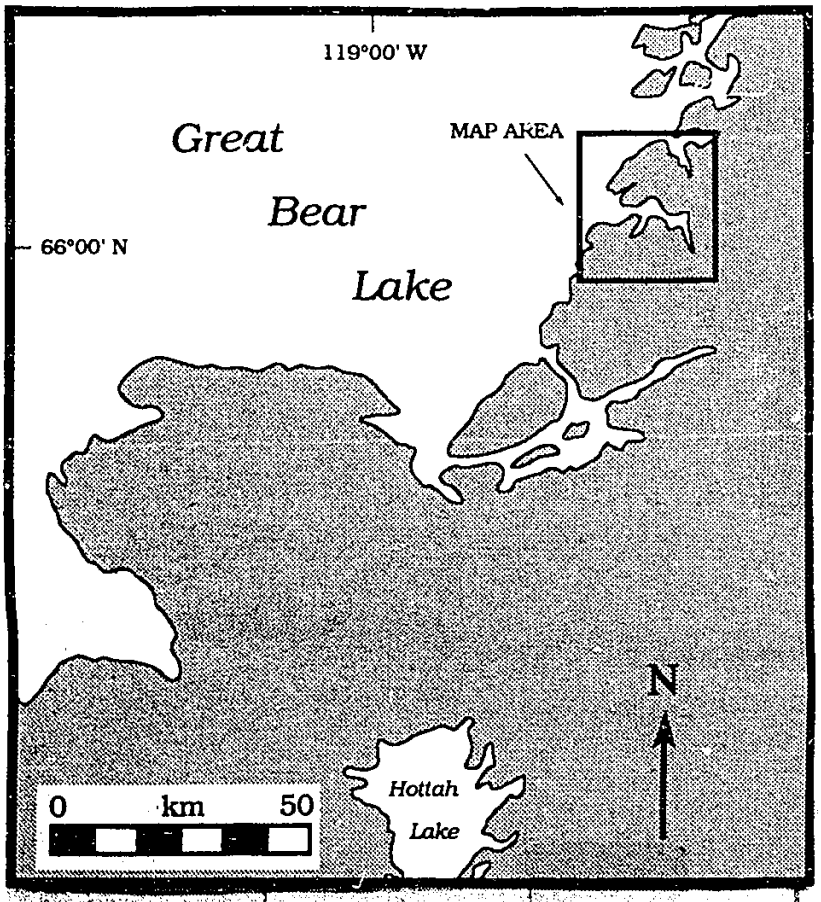

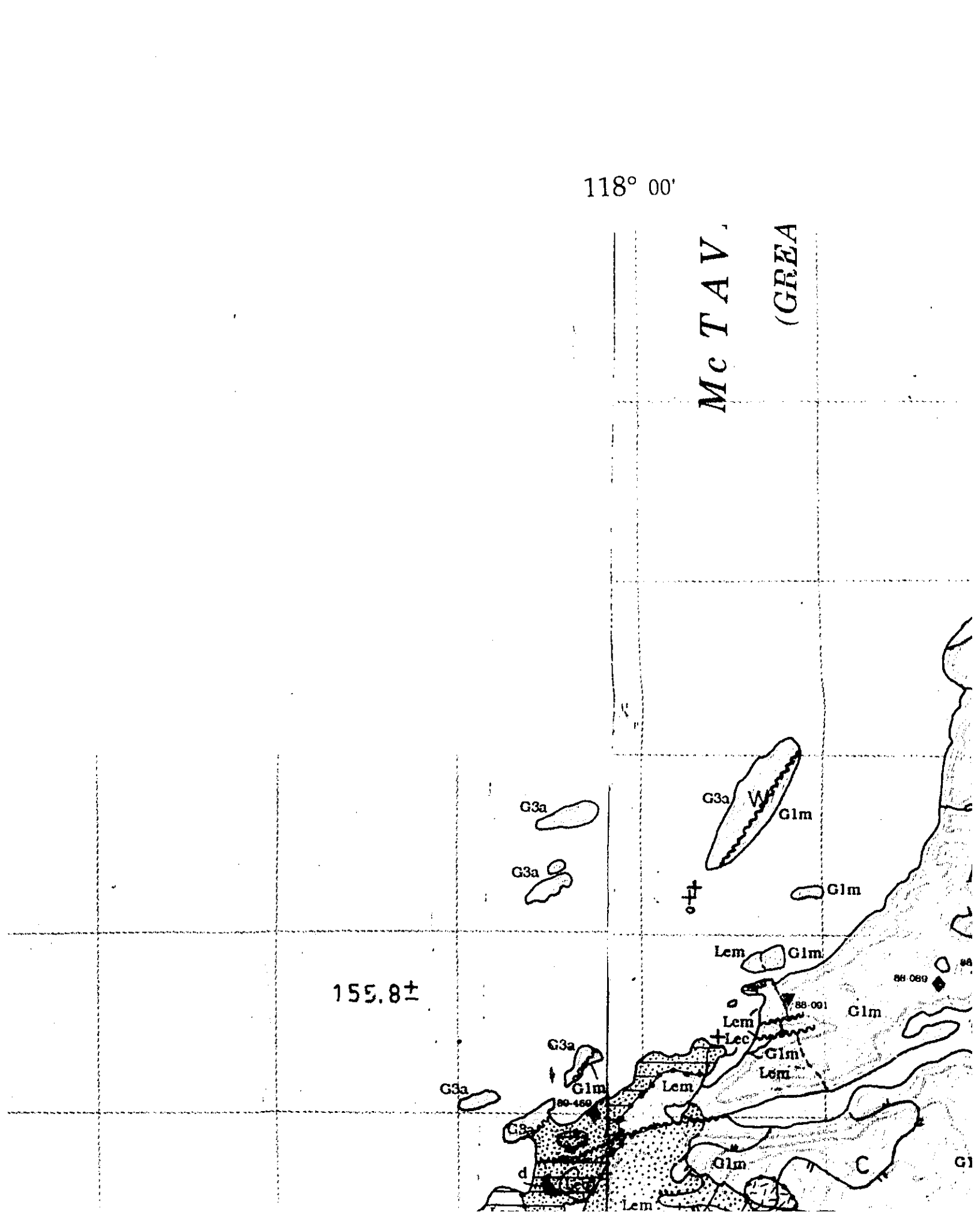
118° 00'
Mc TAV
(GREA
G3a
G3a
G3a
W
G1m
G1m
Lem
G1m
155.8±
88-089
88-091
G1m
Lem
Lec
G1m
Lem
G3a
G3a
G1m
Lem
88-469
G3a
G1m
C
d
Lem

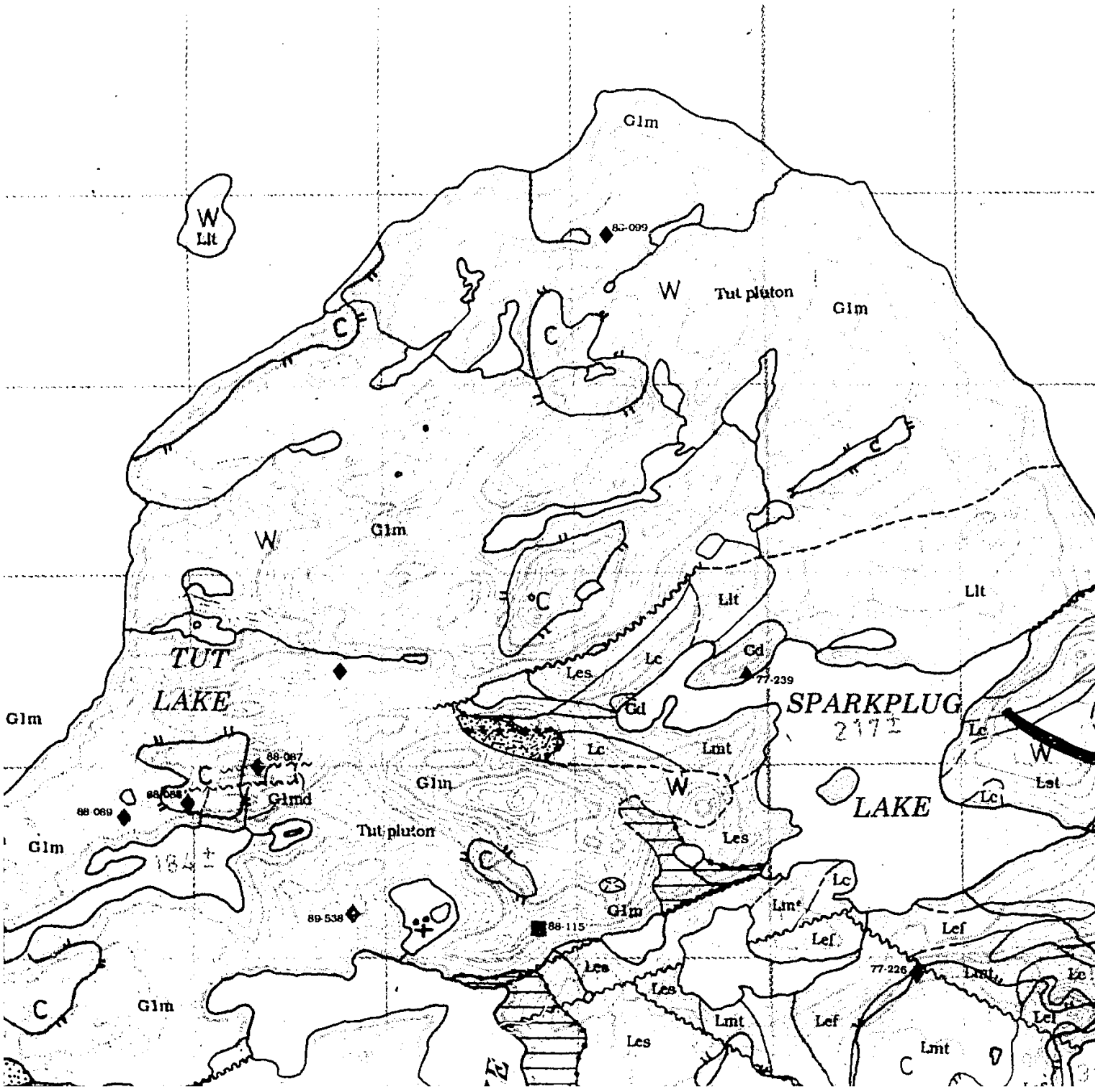
Glm
W
Llt
88-099
W
Tut pluton
Glm
C
C
C
W
Glm
°C
Llt
Llt
TUT
LAKE
Les
Lc
Gd
77-239
SPARKPLUG
217±
Glm
Gd
Lc
Lmt
Lc
W
Lst
88-087
88-088
88-089
Glmd
Glm
W
LAKE
Lc
Glm
184±
Tut pluton
Les
C
89-538
88-115
Glm
Lmt
Lc
Lef
Lef
Les
Les
77-226
Lmt
Lc
C
Glm
Lmt
Lef
Les
Lmt
C

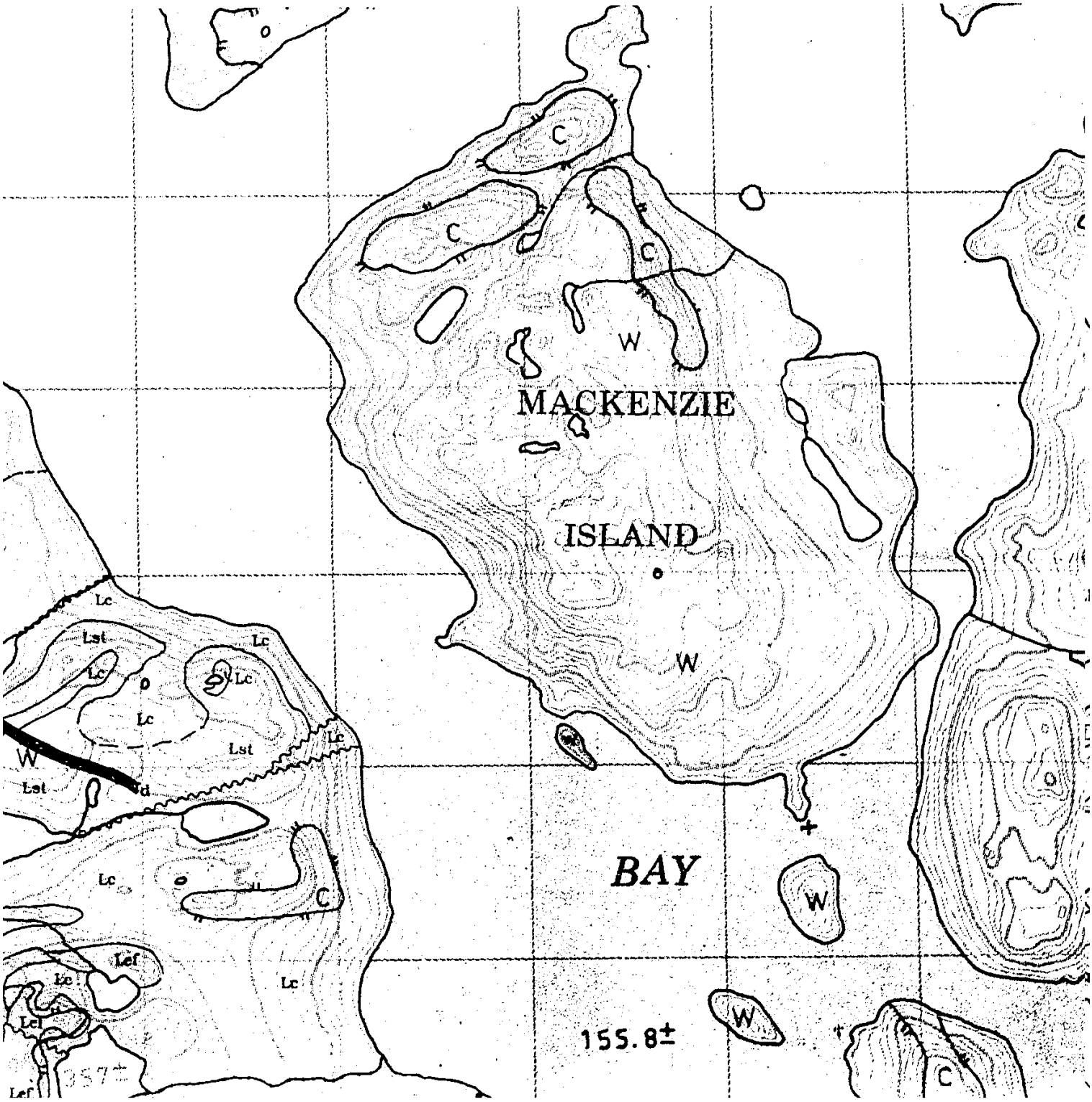
50'
45'
MACKENZIE
ISLAND
BAY
155.8±
Lc
Lst
Lef
W
C

45'

117°40'

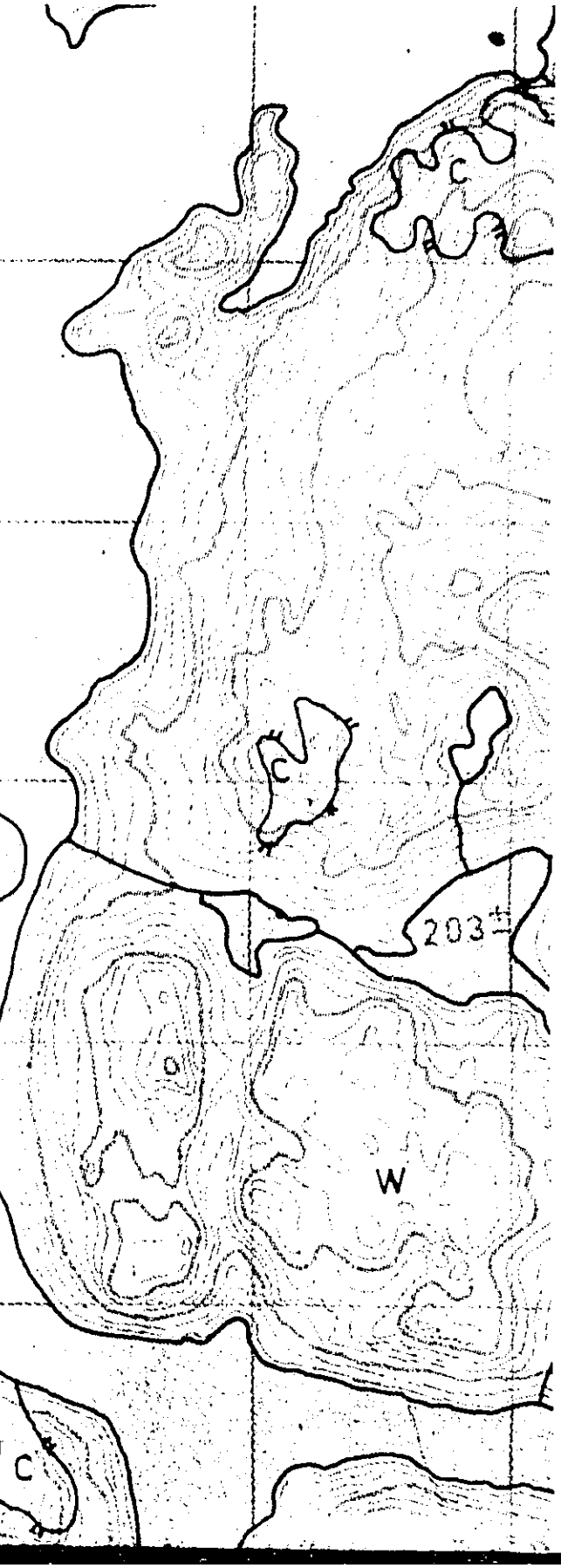

Altered Rocks Associated wi
Island Intrusive Suite,
Northwest Territ

Nancy C. Reardon

LEGEND

LITHOLOGIES

Middle Proterozoic

d — Gabbro and diabase: near vertical north-south an and sub-horizontal sheets

Early Proterozoic

GREAT BEAR BATHOLITH

G3dk | G3a | G3ga — Monzogranite (a), syenogranite (k), ar hornblende-biotite (chlorite-epidote) b

Gd — Diorite, fine-grained, altered; age uncertain, how suggests that it is older than G3 plutons

Gm — Monzonite and quartz monzonite, fine- to mediu uncertain, but found only within the LaBine Gro

ALTERED ROCKS ASSOCIATED WITH PLUTONS OF THE MY

Albite zone

Characterized by pervasive replacement of the host r red-brown to pale pink to white; veins and pods of albi overlaps with the magnetite-apatite-actinolite and pyri

Magnetite-apatite-actinolite zone (MAA)

Defined by the presence of at least two of the three r actinolite which occur as disseminated crystals, veins,

Pyrite zone

Characterized by the presence of disseminated pyrit

117°40'

ltered Rocks Associated with the Mystery Island Intrusive Suite, Echo Bay, Northwest Territories

Nancy C. Reardon

LEGEND

THOLOGIES

ddle Proterozoic

d — Gabbro and diabase: near vertical north-south and east-west trending dykes and sub-horizontal sheets

'ly Proterozoic

REAT BEAR BATHOLITH

idk | G3a | G3ga — Monzogranite (a), syenogranite (k), and granodiorite (g); coarse-grained, hornblende-biotite (chlorite-epidote) bearing; G3d, Dowdell Pluton

d — Diorite, fine-grained, altered; age uncertain, however, the degree of alteration suggests that it is older than G3 plutons

m — Monzonite and quartz monzonite, fine- to medium-grained, leucocratic; age uncertain, but found only within the LaBine Group

.TERED ROCKS ASSOCIATED WITH PLUTONS OF THE MYSTERY ISLAND INTRUSIVE SUITE

Albite zone

Characterized by pervasive replacement of the host rock by albite; altered rocks are red-brown to pale pink to white; veins and pods of albite are present locally; commonly overlaps with the magnetite-apatite-actinolite and pyrite zones

Magnetite-apatite-actinolite zone (MAA)

Defined by the presence of at least two of the three minerals magnetite, apatite or actinolite which occur as disseminated crystals, veins, pods, and breccias

Pyrite zone

Characterized by the presence of disseminated pyrite crystals or pods up to several

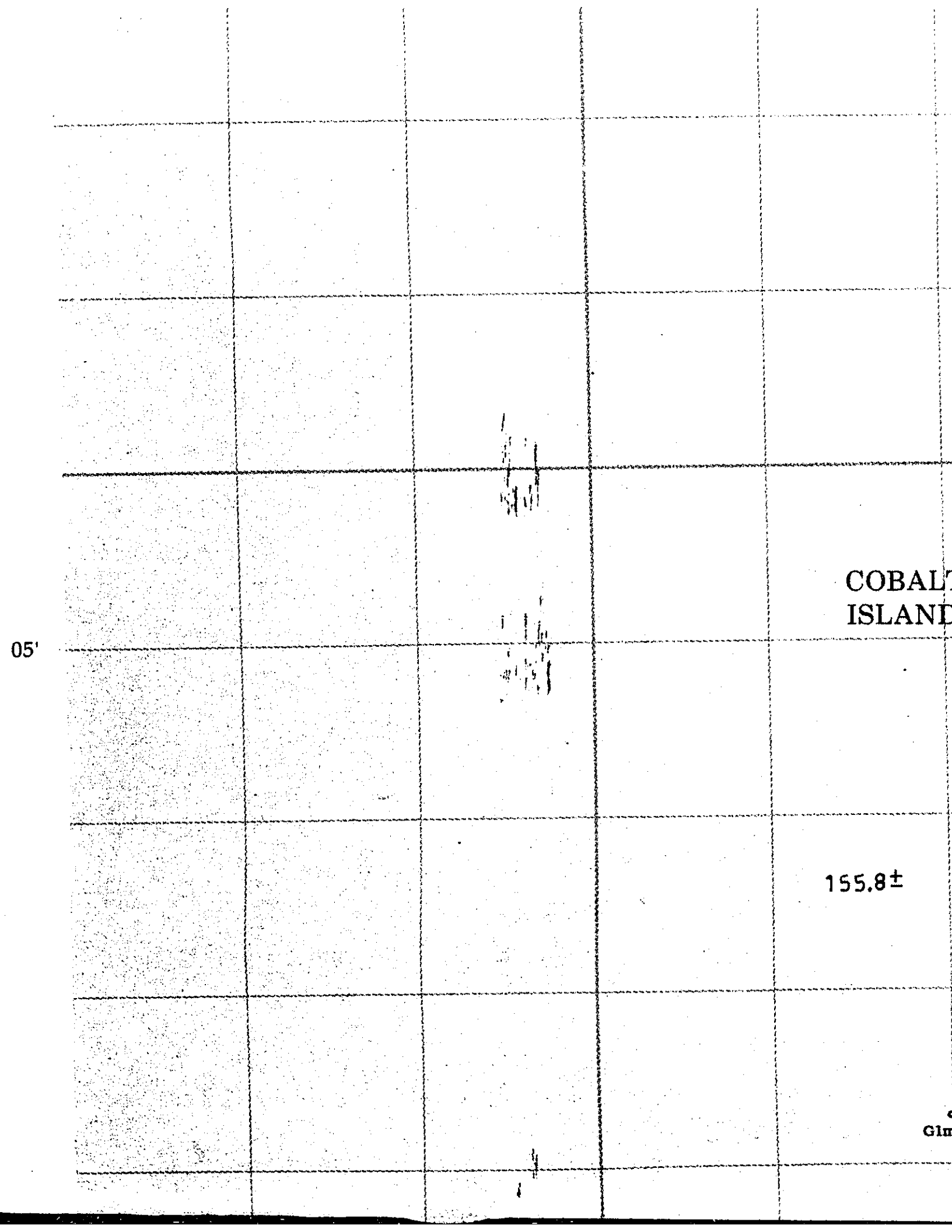
COBAL
ISLAND
05'
155.8±

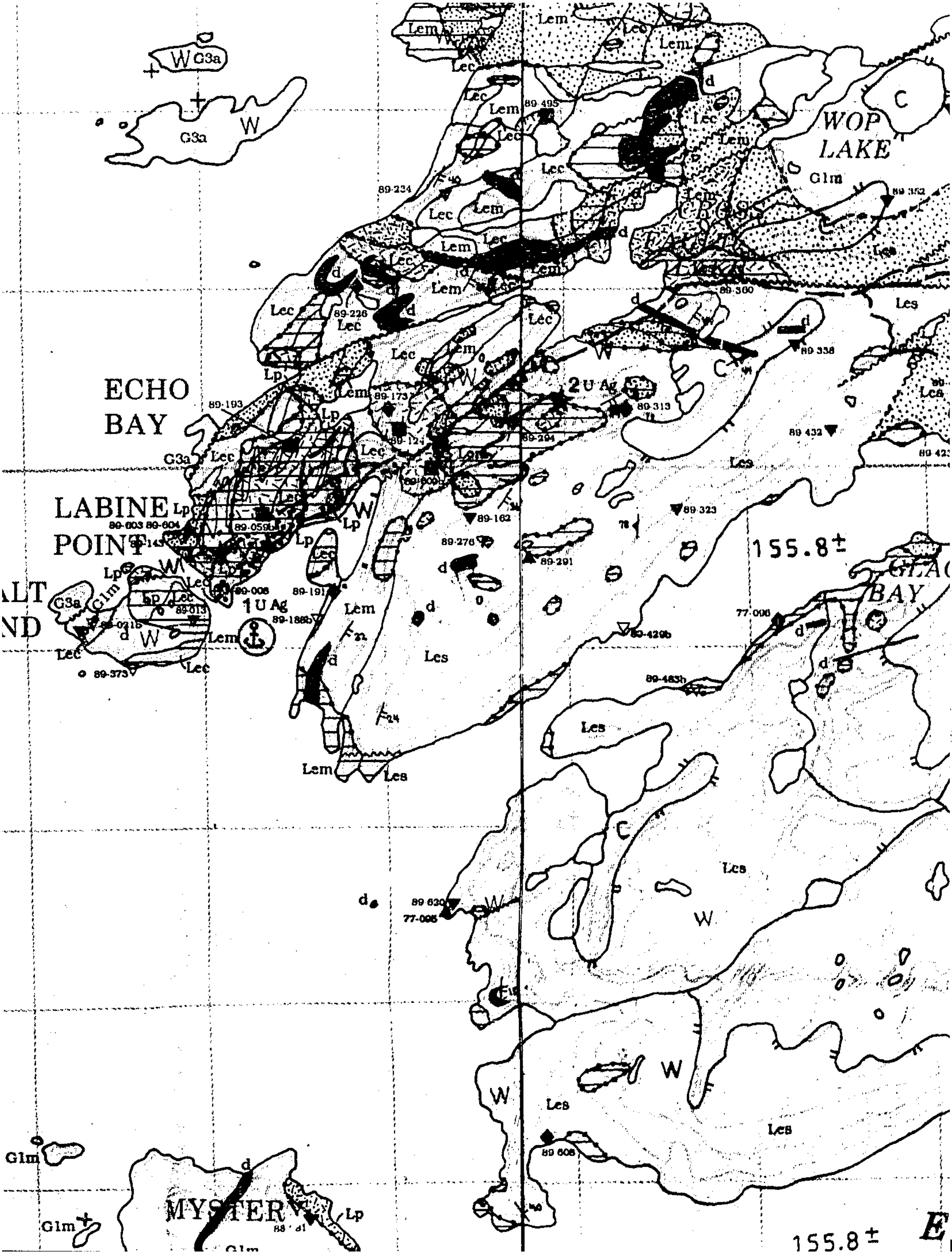
ECHO
BAY
LABINE
POINT
WOP
LAKE
CROSS
FAULT
GLAC
BAY
ALT
ND
MYSTER
1 U Ag
2 U Ag
155.8±
155.8±
E
Lem
Lec
Les
Lp
G3a
Glm
W
C
d
89-234
89-495
89-226
89-193
89-173
89-124
89-294
89-313
89-300
89-338
89-352
89-432
89-323
89-162
89-276
89-291
89-191
89-188b
89-008
89-013
89-603
89-604
89-059b
89-373
89-429b
89-483b
77-006
89-630
77-095
89-606

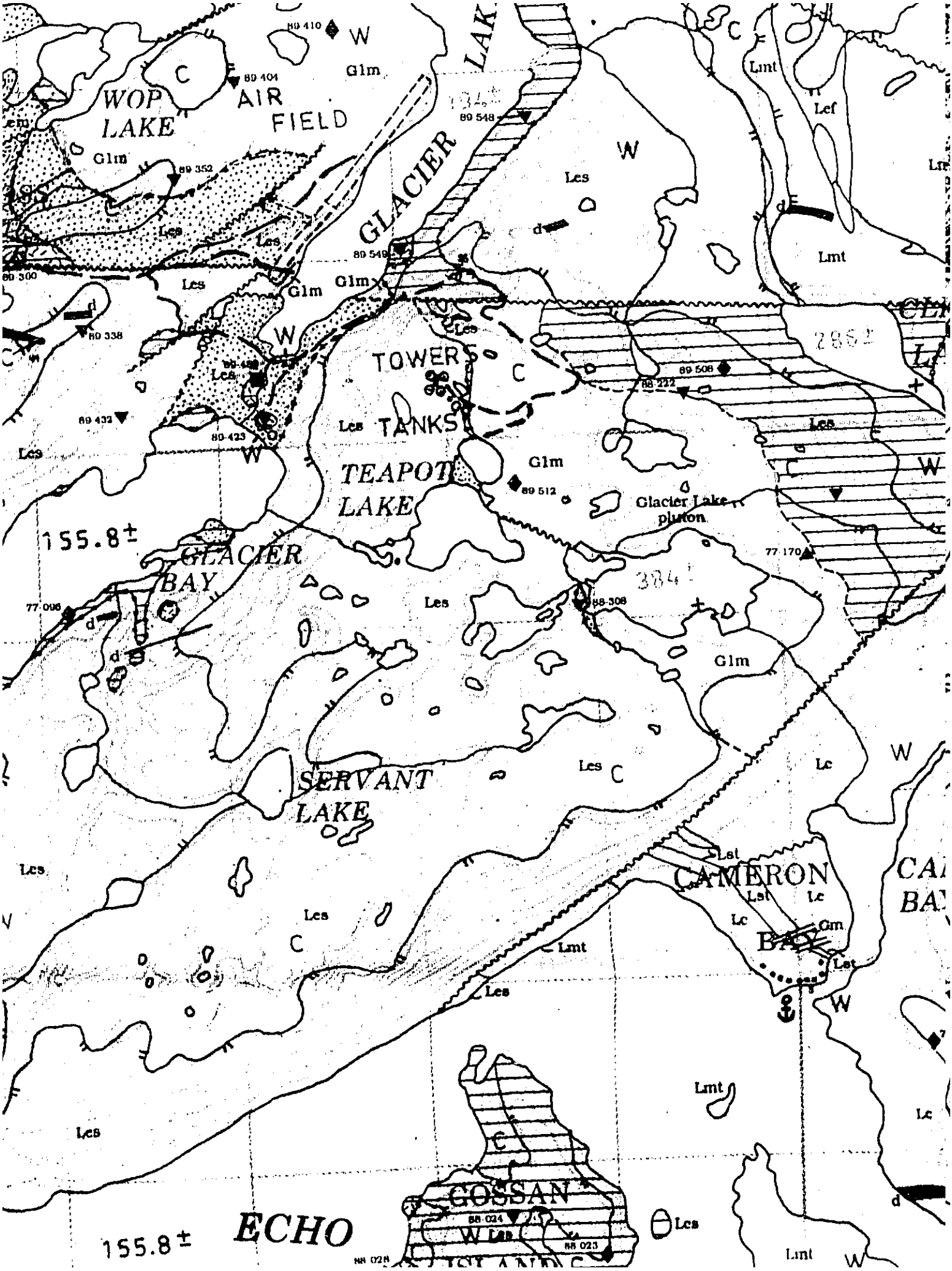
WOP LAKE
AIR FIELD
GLACIER LAKE
TOWERS
TANKS
TEAPOT LAKE
Glacier Lake pluton
GLACIER BAY
SERVANT LAKE
CAMERON BAY
GOSSAN
ECHO
155.8±
155.8±
Glm
Les
Lmt
Lef
Lst
Lc
W
C
89 410
89 404
89 548
89 352
89 549
89 300
89 338
89 432
89 423
89 512
89 508
88 222
77 170
77 006
88 308
88 024
88 023
88 028

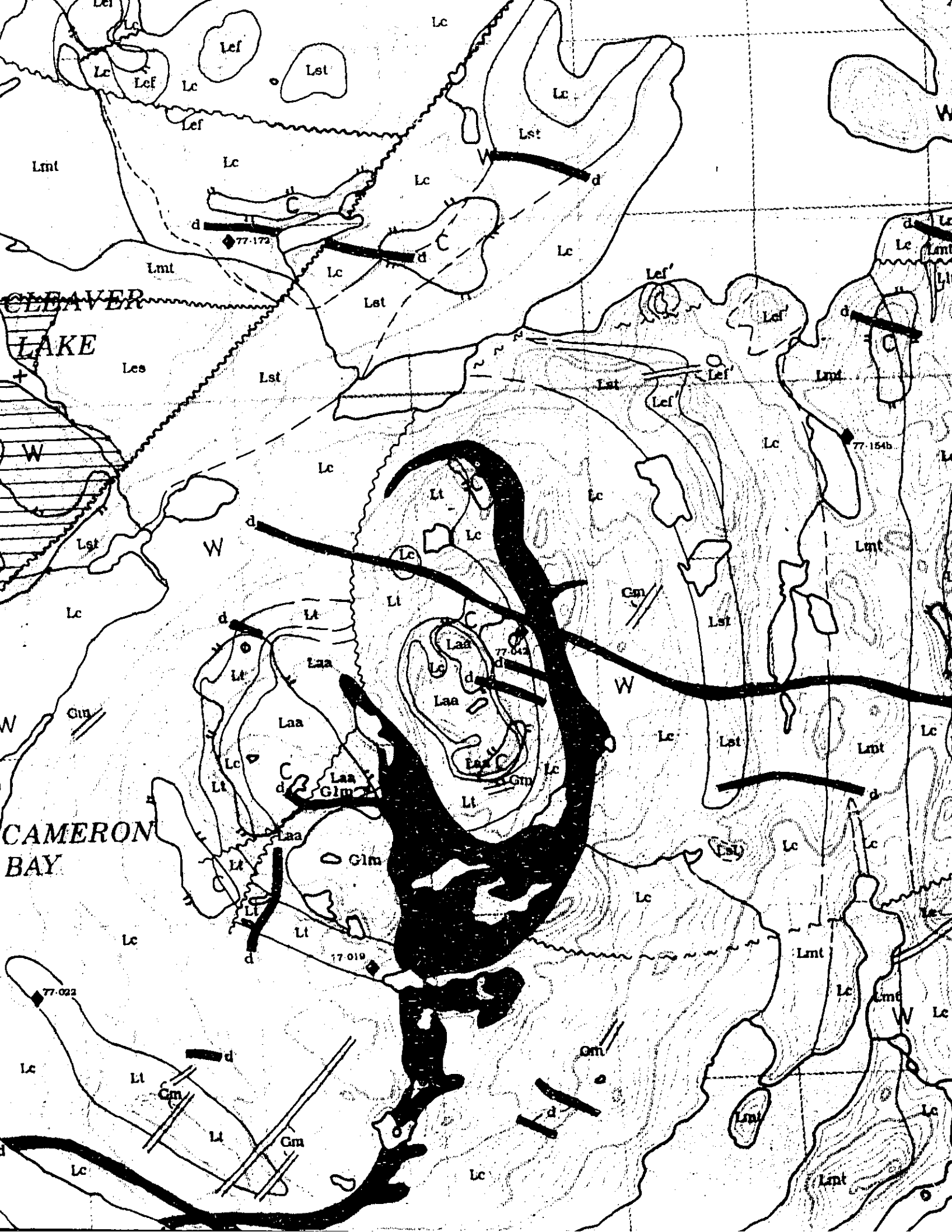
CLEAVER
LAKE
CAMERON
BAY
Lc
Lef
Lst
Lmt
Les
Lt
Laa
Glm
Gm
W
d
C
77-172
77-154b
77-019
77-022

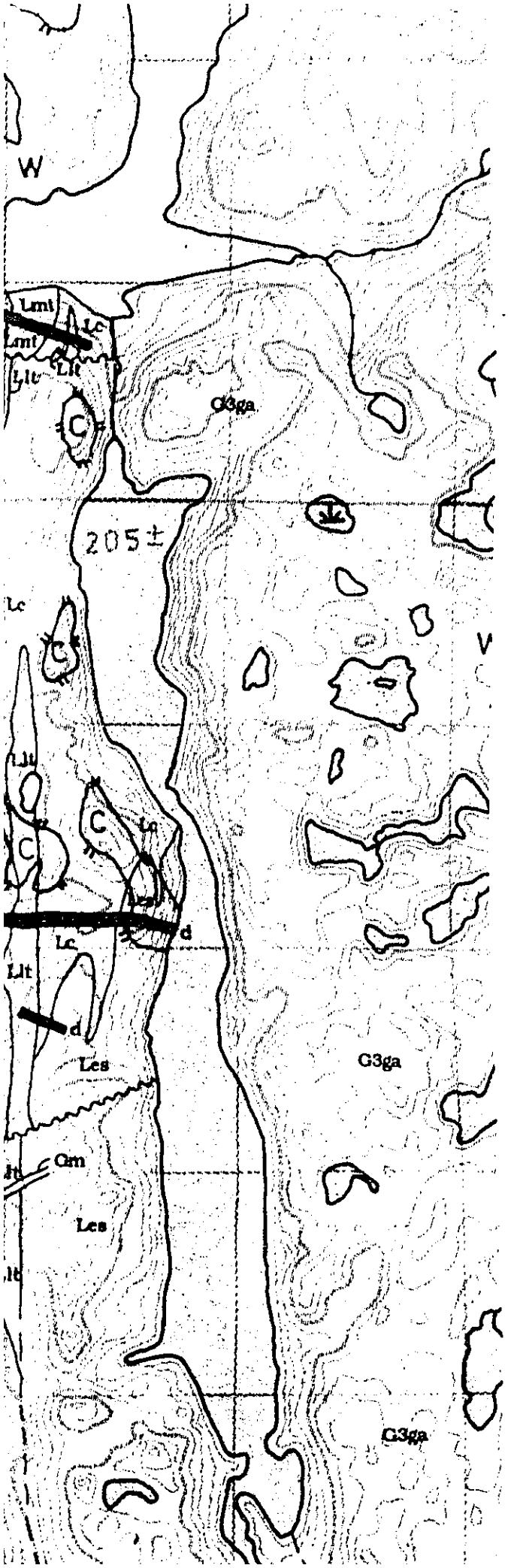

Characterized by the presence of disseminated p
cemtimeters in diameter which form visible rusty p
surfaces, or extensive gossans where pyrite is locall
occur locally; commonly overlaps the MAA zone.
Radium is characterized by the presence of finely-c
groundmass and within amygdules in andesitic lav

G1md **Mystery Island intrusive suite:** medium-gra
sharp contact with the Tut pluton

G1m **Mystery Island intrusive suite:** diorite - mo
monzodiorite - quartz monzonite - granodio
seriate; biotite-hornblende-bearing. An augi
locally

LABINE GROUP

Lc **CAMERON BAY FORMATION:** sandstone, p
volcanic-lithic and feldspathic; ripple-laminatec
mud cracks; hematitic polymictic conglomerate
provenance; thin beds and erosional remnants c
and explosion breccias near volcanic flow dome
designated as informal members (Lt); cauldron
with ash flow tuff members. The Cameron Bay
altered (MAA) rock locally, and is cut by a plut
Includes the following members in the map are

Laa **Achook andesite:** andesite; flows and explos
aphanitic to porphyritic; dominant phenocry
intercalated with several ash flow tuff memb
porphyritic than andesite in the Echo Bay Fo

Lmt **Mackenzie tuff:** tuff; composite ash flow she
crystals of plagioclase, quartz and potassium

Llt **Lindsley tuff:** tuff; ash flow sheet containing
from mostly quartz near the base to mostly p
moderately to densely welded

The Echo Bay Formation interfingers with the Camerc

ECHO BAY FORMATION

Lef **Sparkplug Lake member:** andesite; porphy
only by their stratagraphic position above th
cone and vent complex south of Lindsley Ba

Les **Surprise Lake member:** andesite; porphyri
flows and breccia; many flows are trachytic;
colour; includes thin sedimentary interbeds

Lec **Cobalt Porphyry member:** porphyry; intrus
porphyry and microdiorite

Lem **Mile Lake member:** andesite; porphyritic flc
volcanogenic sandstone and conglomerate, a
and ashstone

Lp **PORT RADIUM FORMATION:** siltstone and
fine-grained with at least

naracterized by the presence of disseminated pyrite crystals or pods up to several timeters in diameter which form visible rusty patches on weathered outcrop aces, or extensive gossans where pyrite is locally abundant. Veins of pyrite to 1 cm ır locally; commonly overlaps the MAA zone. A chalcopyrite zone east of Port ium is characterized by the presence of finely-disseminated chalcopyrite within the ındmass and within amygdules in andesitic lava flows

Mystery Island intrusive suite: medium-grained dioritic phase; occurs in sharp contact with the Tut pluton

Mystery Island intrusive suite: diorite - monzodiorite - monzonite - quartz monzodiorite - quartz monzonite - granodiorite; fine- to medium-grained, seriate; biotite-hornblende-bearing. An augite-bearing border phase occurs locally

GROUP

CAMERON BAY FORMATION: sandstone, planar and cross-bedded, volcanic-lithic and feldspathic; ripple-laminated siltstone and mudstone with mud cracks; hematitic polymictic conglomerate mainly of volcano-plutonic provenance; thin beds and erosional remnants of devitrified ashstone; local talus and explosion breccias near volcanic flow domes; ash flow tuff units not designated as informal members (Lt); cauldron collapse breccias interfingered with ash flow tuff members. The Cameron Bay Formation contains clasts of altered (MAA) rock locally, and is cut by a pluton of the Mystery Island suite. Includes the following members in the map area:

Achook andesite: andesite; flows and explosion breccias, amygdaloidal, aphanitic to porphyritic; dominant phenocrysts are plagioclase and hornblende; intercalated with several ash flow tuff members; more amygdaloidal and less porphyritic than andesite in the Echo Bay Formation

05'

Mackenzie tuff: tuff; composite ash flow sheet containing less than 10 per cent crystals of plagioclase, quartz and potassium feldspar

Lindsley tuff: tuff; ash flow sheet containing up to 25 per cent crystals, zoned from mostly quartz near the base to mostly plagioclase near the top; moderately to densely welded

ıo Bay Formation interfingers with the Cameron Bay Formation

ECHO BAY FORMATION

Sparkplug Lake member: andesite; porphyritic flows and breccia, distinguished only by their stratagraphic position above the Mackenzie Tuff; includes a small cone and vent complex south of Lindsley Bay (Lef)

Surprise Lake member: andesite; porphyritic (hornblende-augite-plagioclase) flows and breccia; many flows are trachytic; some flows oxidized to a brick-red colour; includes thin sedimentary interbeds (Les') and minor laharic breccia

Cobalt Porphyry member: porphyry; intrusive hornblende-plagioclase porphyry and microdiorite

Mile Lake member: andesite; porphyritic flows interbedded with volcanogenic sandstone and conglomerate, and andesitic lapilli tuff and ashstone

PORT RADIUM FORMATION: siltstone and sandstone; thinly bedded, fine-grained with at least two carbonate

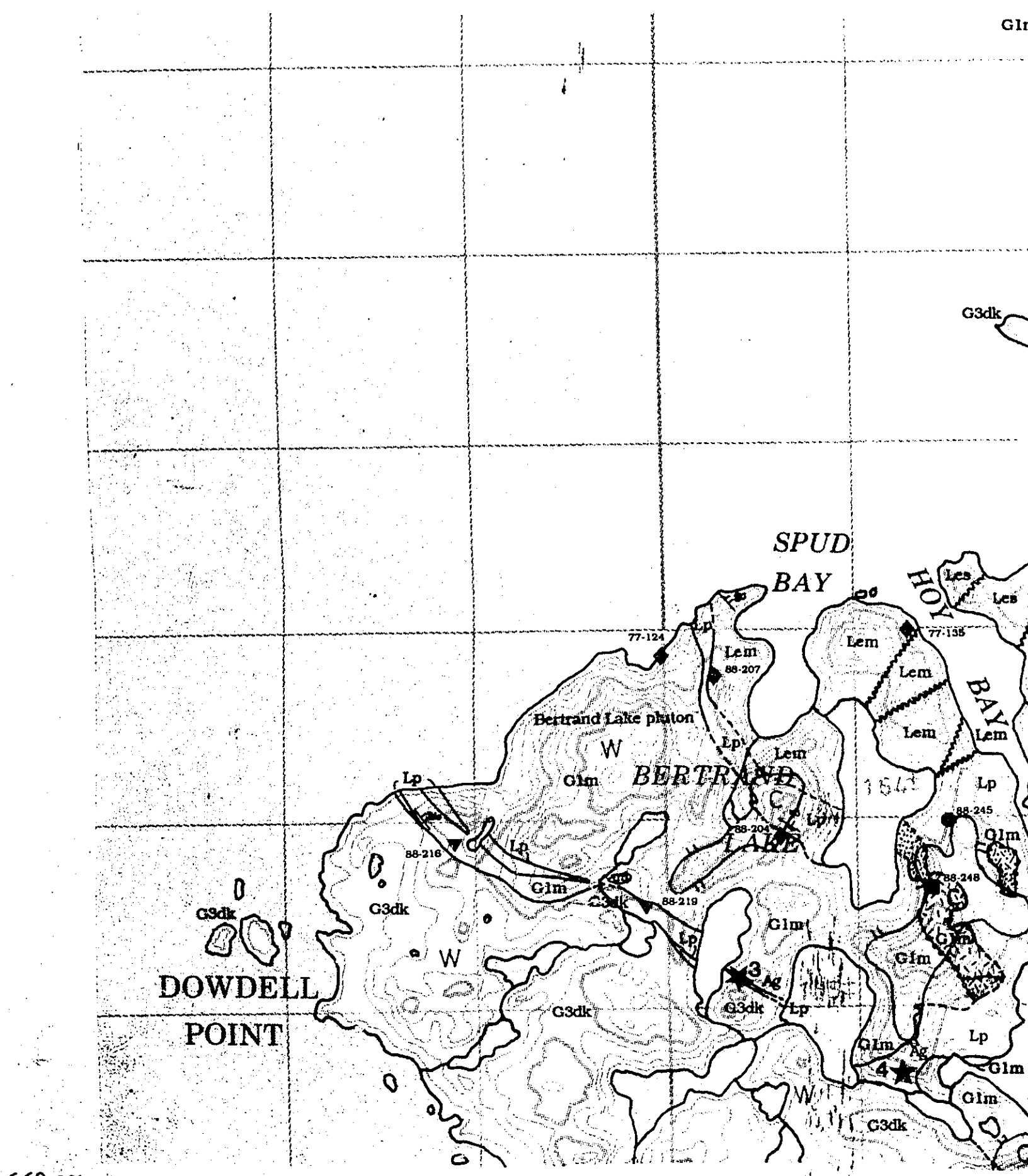

ALTERED ROCKS AND MAGNETITE-APATITE-ACTINOLITE DEPOSITS

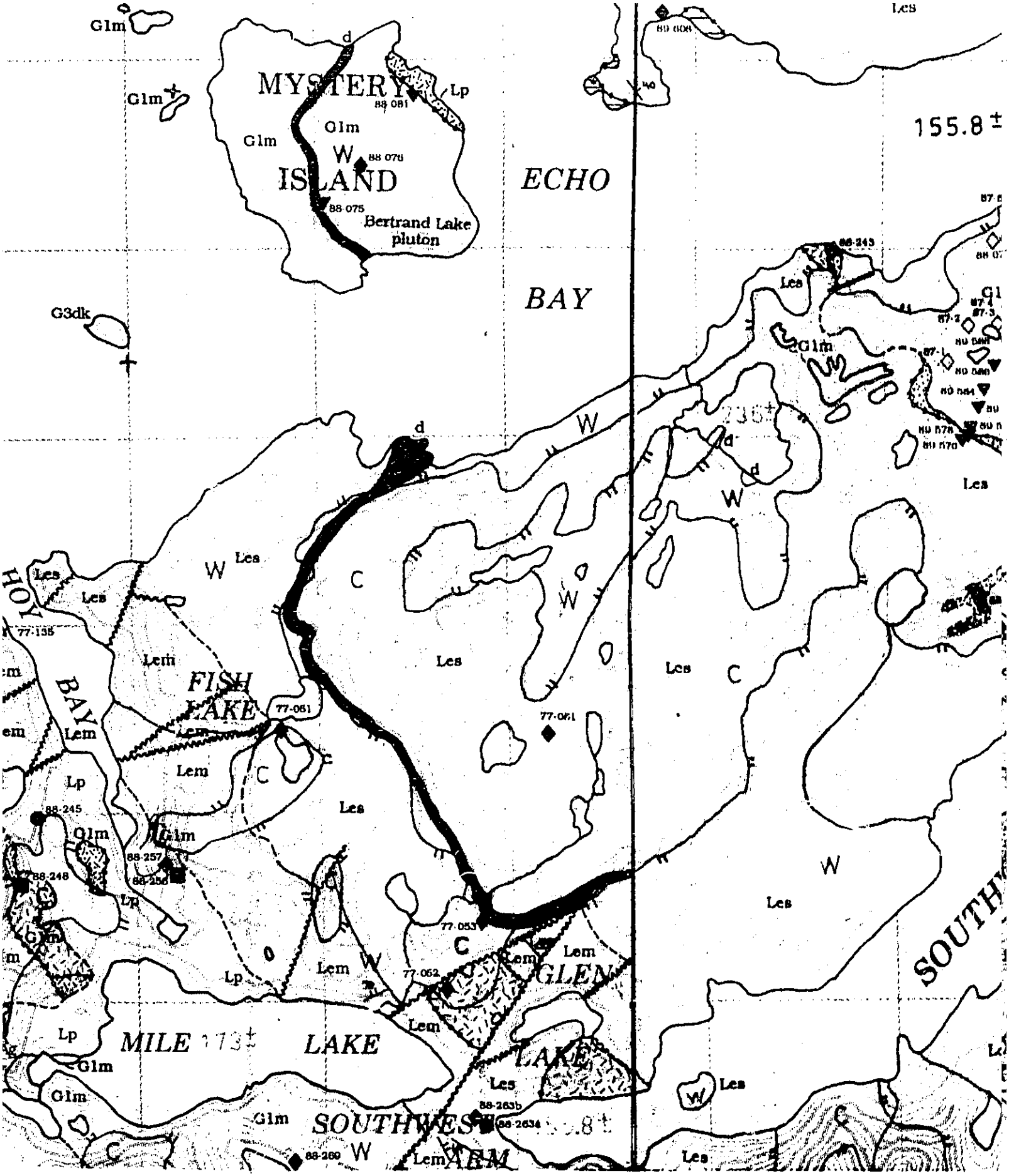
MYSTERY ISLAND
ECHO BAY
Bertrand Lake pluton
FISH LAKE
MILE LAKE
GLEN LAKE
SOUTHWEST ARM
SOUTH
BAY
HOY
155.8±
Glm
Lp
Lem
Les
W
C
d
88-081
88-076
88-075
88-245
88-248
88-257
88-258
88-260
88-263b
88-263d
88-263
77-061
77-052
77-053
77-135
G3dk

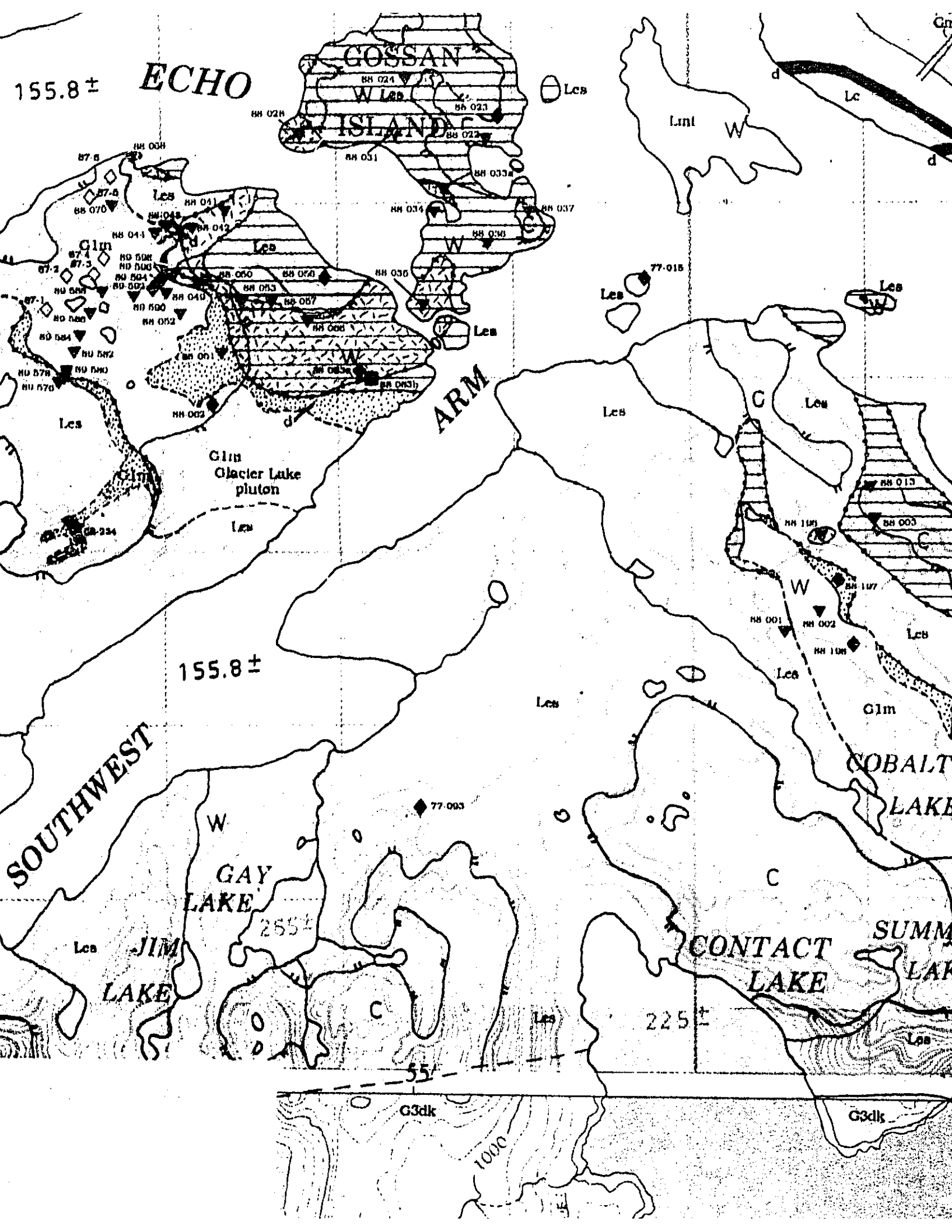
155.8±
ECHO
GOSSAN
ISLAND
W
Les
Glm
Glacier Lake
pluton
ARM
SOUTHWEST
GAY
LAKE
JIM
LAKE
CONTACT
LAKE
COBALT
LAKE
SUMM
LAK
225±
255±
77-003
77-015
G3dk
1000
55

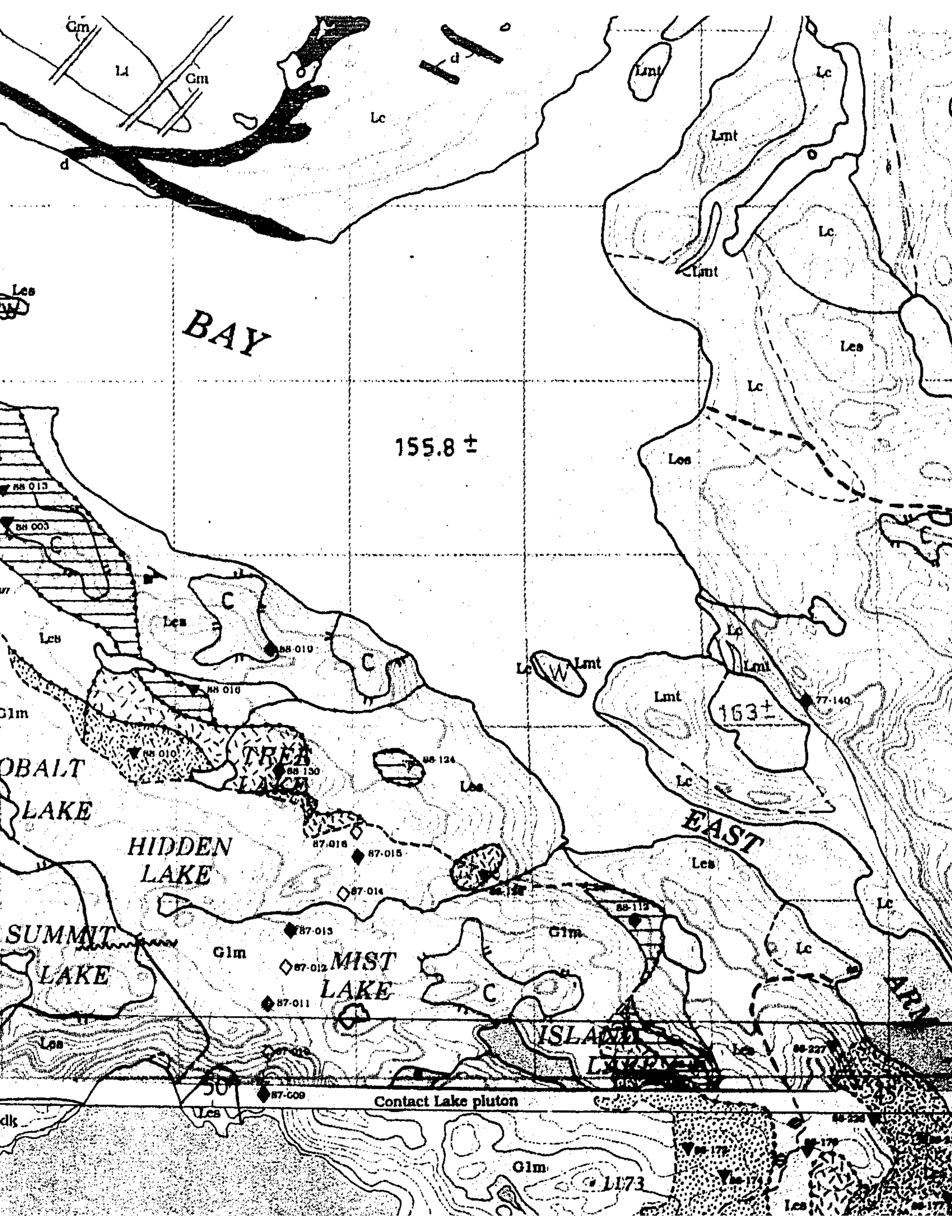

Gm
Li
Gm
d
d
Lc
Lmt
Lc
Lmt
Lmt
Lc
Les
BAY
Les
Lc
155.8 ±
Les
88 013
88 003
C
C
Les
Les
88 019
C
Lc
W
Lmt
Lmt
Lc
Lmt
163 ±
77-140
88 016
Glm
88 010
OBALT
LAKE
TREE
LAKE
88 130
88 124
Les
Lc
EAST
HIDDEN
LAKE
87-016
87-015
87-014
Les
Lc
SUMMIT
LAKE
87-013
Glm
Glm
88-112
87-012
MIST
LAKE
C
Lc
87-011
ISLAND
LAKE
Les
88-227
Les
87-010
87-009
Contact Lake pluton
dk
Les
Glm
1173
Les

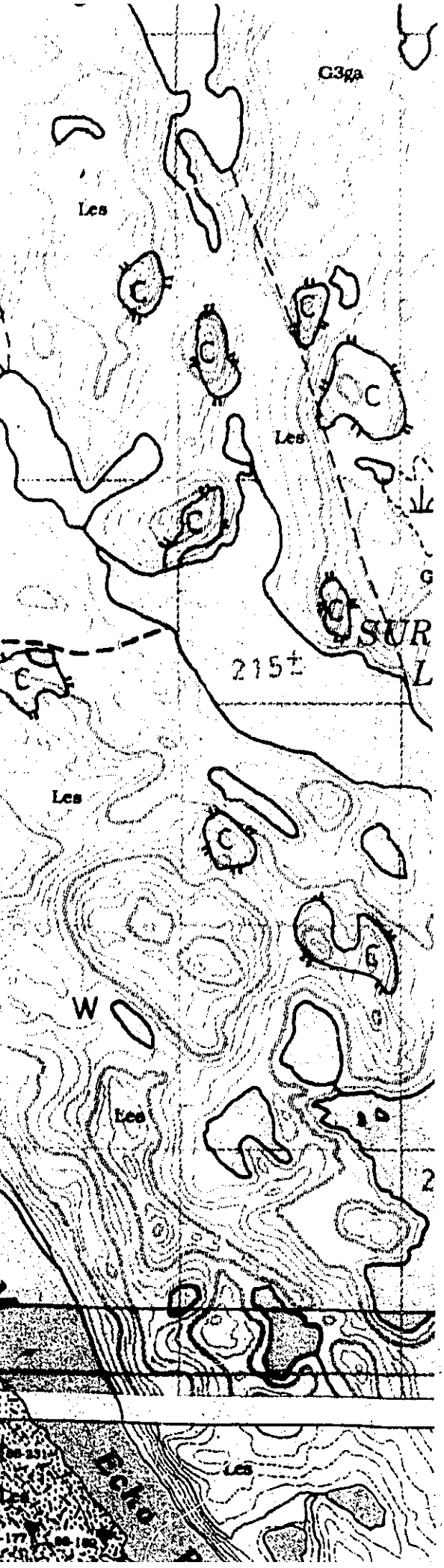

porphyry and microdiorite

Lcm — **Mile Lake member:** andesite; porphyritic flows inte
volcanogenic sandstone and conglomerate, and ande
and ashstone

Lp — **PORT RADIUM FORMATION:** siltstone and sandsto
fine-grained with at least two carbonate interbeds less t
exposures lie within alteration halos of the Mystery Isla

clear area .....

wooded area .....

geologic contact (defined, approximate) .....

unconformity .....

fault (defined, approximate) .....

limit of alteration zone .....

chalcopyrite subzone.....

bedding, tops known (inclined).....

bedding, tops unknown (inclined).....

flow banding (inclined).....

mine (abandoned) .....

1. Port Radium; 2. Echo Bay; 3. Bonanza; 4. El Bonanza; 5

Sample locations:

Whole-rock geochemistry only.....

D/H whole rock analys .....

$^{18}O/^{16}O$ whole rock analysis.....

D/H and $^{18}O/^{16}O$ whole rock analyses.....

magnetite-apatite-actinolite (mineral isotope analyses).....

$^{34}S/^{32}S$ mineral analysis.....

quartz-carbonate vein (mineral isotope analyses).....

Plutonic rock names after Streckeisen, 1973. Geology fro
Canada Map 1546A (Hildebrand, 1980). Revisions and alte
Reardon, 1988-89. Mapping (1988-89) was assisted by S. M.
data by N. C. Reardon, 1989-90. Field work was supported
Territories - Canada Mineral Development Agreement and
Canada, project 860002 (R. S. Hildebrand). Critical review o
greatly improved its content and form.

Scale 1:25 000

ɪrphyritic flows interbedded with
glomerate, and andesitic lapilli tuff

ltstone and sandstone; thinly bedded,
ɪnate interbeds less than 1 m thick; all
s of the Mystery Island intrusive suite

..... W

).....

..... 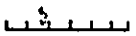

..... 

.....

..... 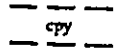

.....

.....

..... 

..... 

nza; 4. El Bonanza; 5. Contact Lake

..... ◇

..... ▲

..... ▼

..... ◆

ɔtope analyses)..... ■

..... ▽

analyses)..... ●

ı, 1973. Geology from Geological Survey of
Revisions and alteration zones by N.C.
ras assisted by S. M. Lagacé. Stable isotope
work was supported by the Northwest
ent Agreement and the Geological Survey of
d). Critical review of the map by J.B. Henderson

66° 00'

e 1:25 000

66° 00'

ALTERED ROCKS AND MAGNETITE-APATITE-ACTINOLITE DEPOSITS ASSOCIATED WITH THE MYSTERY ISLAND INTRUSIVE SUITE, ECHO BAY, NORTHWEST TERRITORIES

Marginal Notes

Introduction

Magnetite-apatite-actinolite deposits occur as pervasive replacement, veins, pods and breccias within wall rocks to the plutons of the Mystery Island intrusive suite at Echo Bay, District of Mackenzie, Northwest Territories. The plutons and their altered wall rocks host previously-mined pitchblende, native Ag, Ni-Co arsenide veins. Although numerous studies were carried out on the pitchblende, native Ag, Ni-Co arsenide veins (see Reardon 1992a,b for references), the origin of the altered rocks which host them remains uncertain. Hildebrand (1986) mapped two of the plutons and associated altered and mineralized rocks in the Camsell River area and recognized zoned alteration haloes within, and adjacent to, the plutons. He concluded that the alteration was the result of replacement and brecciation of the country rocks by high-temperature, highly acidic, chlorine-dominated fluids derived from the plutons of the Mystery Island intrusive suite.

The plutons of the Mystery Island intrusive suite intrude a complex of andesitic stratovolcanoes of the LaBine Group, within the 1.87 Ga Great Bear magmatic zone of Wopmay orogen (Hildebrand, 1984, 1986). The plutons are compositionally heterogeneous, sheet-like bodies of intermediate composition. The plutons are synvolcanic and were emplaced at a depth of 2 to 3 km at two distinct stratigraphic levels within the LaBine Group: within the Port Radium Formation and the lowermost part of the conformably overlying Echo Bay Formation, and within andesitic lava flows of the Echo Bay Formation (Hildebrand, 1986). At 1.84 Ga the stratovolcanoes and plutons were folded such that the tops and bottoms of the plutons are exposed (Bowring, 1984). After 1.84 Ga, the area was cut by northeast-trending transcurrent faults and diabase dykes and sills (Hoffman, 1984). Pitchblende, native Ag, Ni-Co arsenide mineralization probably occurred during a period of reactivation of the faults at 1.667 Ga (Bowring et al., 1989).

Altered rocks

All plutons of the Mystery Island intrusive suite have associated zoned alteration haloes, although the zones are somewhat irregular and discontinuous. Three zones of altered rocks were mapped in the Echo Bay area: 1) an inner zone of albite; 2) an intermediate zone of magnetite-apatite-actinolite (MAA); and 3) an outer zone of disseminated sulphides. The zones overlap spatially, and geologic and petrographic evidence show that temporally, the albite zone was formed first, followed by MAA and finally pyrite.

Albite zone

The albite zone is characterized by pervasive replacement of the host rock by very fine- to coarse-grained albite; albitized rocks are red-brown to pale pink. Extensively altered rocks, found in close proximity to the plutons, are white both on the fresh and weathered surfaces. Albitized rocks generally occur within 100 m of the pluton roofs, but extend up to 1 km above the plutons locally. Altered rocks also occur locally within and below the plutons. Veins and pods of albite are present in some highly altered areas. The albite zone commonly overlaps with the magnetite-apatite-actinolite and pyrite zones.

Magnetite-apatite-actinolite zone

The magnetite-apatite-actinolite (MAA) zone is defined by the presence of at least two of the

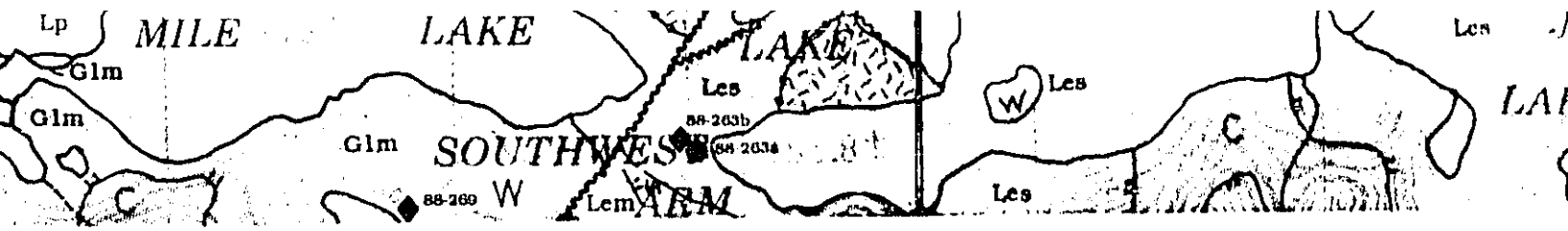

SITS
E,

and breccias
y, District of
previously-
e carried out
erences), the
apped two of
er area and
ded that the
ks by high-
the Mystery

of andesitic
e of Wopmay
ıs, sheet-like
at a depth of
Port Radium
rmation, and
1.84 Ga the
ıs are exposed
ent faults and
nineralization
t al., 1989).

ration haloes,
ed rocks were
of magnetite-
zones overlap
bite zone was

y very fine- to
altered rocks,
ered surfaces.
1 km above the
ns and pods of
rlaps with the

least two of the
s disseminated

Whole-rock Geochemistry

Whole-rock geochemistry of the altered wall rocks above the plutons shows tha correlates negatively with SiO_2, K_2O, Ba, and Rb for altered andesitic lava flows wit alteration haloes of some of the plutons (Reardon, 1992a,b). Gd, Dy, Be, Yb, Y, Sm, MgO a correlate negatively with K_2O; Ba and Rb correlate positively with K_2O. Na and antithetically in the plutons, but other elements do not show regular variations with Na or Tut pluton is relatively unaltered and shows a normal magmatic trend of increasing decreasing Na with increasing SiO_2 content. The Contact Lake and Bertrand Lake plutons metasomatized locally, as indicated by high Na contents. Part of the Glacier Lake pluto metasomatized, as indicated by elevated K_2O not correlative with an increase in SiO_2. Pr SiO_2, Na_2O and K_2O with height in the Contact Lake and Glacier Lake plutons show a antithetic variation of Na_2O and K_2O. The Contact Lake pluton is reversely zoned, and SiO_2 decrease with increasing height in the pluton.

Stable Isotope Geochemistry

Wall rocks

Whole rock oxygen and hydrogen isotopic data were used to map the aerial extent of al and to characterize the nature and origin of the fluids responsible for the alteration. Roc LaBine Group and Mystery Island intrusive suite were analyzed for their hydrogen and isotope ratios. Isotopic data are reported by Reardon (1992a,b). Variation of $\delta^{18}O$ wi plutons and their altered zones is limited. Most whole-rock $\delta^{18}O$ and δD are higher than + -70‰, respectively, consistent with alteration under low water to rock ratios by dor magmatic fluids. Lower values suggest involvement of a minor component of seawater, water, or evolved meteoric water, and some input of surficial waters is probable.

MAA and pyrite zones

Stable isotopic data for actinolite, epidote, biotite, apatite, quartz and magnetite w to calculate a range of isotopic compositions ($\delta^{18}O$ and δD) of the fluids which depos minerals, based on known mineral - water isotopic fractionations for a range of temp The data indicate that the fluids which deposited these minerals ranged from about + +12.0‰ for $\delta^{18}O$ and from -60‰ to -30‰ for δD, assuming a temperature of 400°C. The fall within the range of magmatic fluids, and $\delta^{18}O$ and δD are distinctly higher than exp meteoric water or seawater (see Taylor, 1986). A minor component of seawater, connate evolved meteoric water cannot be ruled out. Pyrite and chalcopyrite from gossans, pods within the pyrite and chalcopyrite zones were analyzed for $\delta^{34}S$. Most of the $\delta^{34}S$ data and chalcopyrite at Echo Bay are typical for igneous rocks and are consistent with a source for the sulphur.

Quartz-carbonate veins

Knowledge of the fluids which formed the mineralized (pitchblende, native A arsenide) and unmineralized quartz-carbonate veins in the Echo Bay area is necessary i assess the influence of these fluids on the rocks in the area. Estimation of the overprinting during the formation of quartz-carbonate veins is difficult, since fluids re for formation of the quartz veins ranged from lighter than, to the same in $\delta^{18}O$ (from + +0.47‰; Changkakoti et al., 1986) as the fluids which formed the MAA zone a However, no large-scale zoning of $\delta^{18}O$ is evident in the wall rocks surrounding the ve and $\delta^{13}C$ of carbonate minerals from unmineralized quartz-carbonate veins in the Echo are similar to those of carbonate minerals from the mineralized veins.

Summary

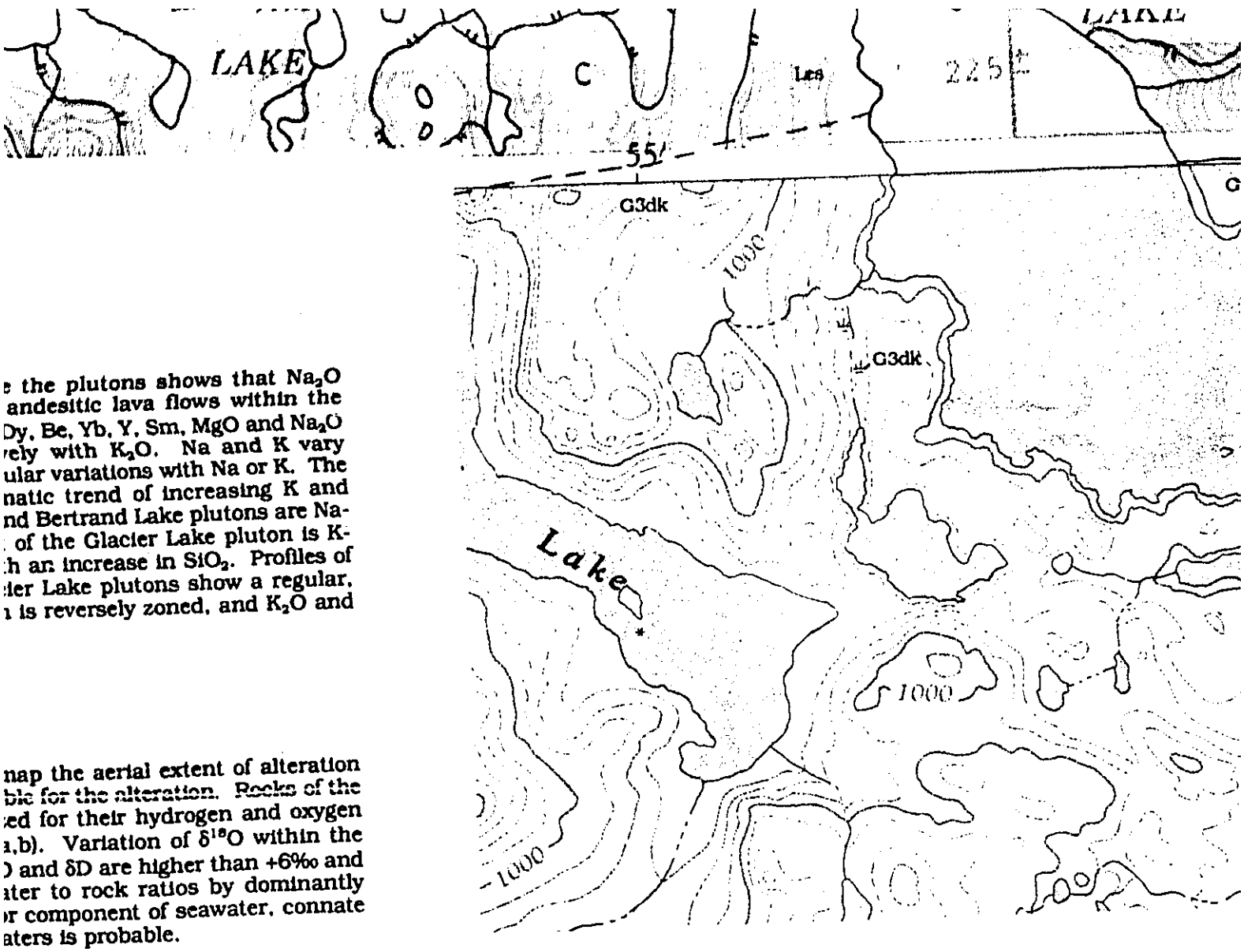

e the plutons shows that Na_2O andesitic lava flows within the Dy, Be, Yb, Y, Sm, MgO and Na_2O ely with K_2O. Na and K vary ular variations with Na or K. The natic trend of increasing K and nd Bertrand Lake plutons are Na- of the Glacier Lake pluton is K- h an increase in SiO_2. Profiles of ier Lake plutons show a regular, ı is reversely zoned, and K_2O and

nap the aerial extent of alteration ble for the alteration. Rocks of the ed for their hydrogen and oxygen a,b). Variation of $\delta^{18}O$ within the) and δD are higher than +6‰ and ater to rock ratios by dominantly r component of seawater, connate aters is probable.

e, quartz and magnetite were used of the fluids which deposited the tions for a range of temperatures. erals ranged from about +5.0‰ to emperature of 400°C. These values distinctly higher than expected for ment of seawater, connate water, or pyrite from gossans, pods and veins ^{34}S. Most of the $\delta^{34}S$ data for pyrite nd are consistent with a magmatic

zed (pitchblende, native Ag, Ni-Co cho Bay area is necessary in order to area. Estimation of the effects of is difficult, since fluids responsible o the same in $\delta^{18}O$ (from +9.12‰ to formed the MAA zone alteration. l rocks surrounding the veins. $\delta^{18}O$ arbonate veins in the Echo Bay area zed veins.

alteration haloes comprised of three

REFERENCES

Bowring, S. A.
1984: U-Pb zircon geochronology of Early Proterozoic example of rapid crustal evolution; Ph.D. thesis, U

Bowring, S.A., Housh, T. and Grotzinger, J.P.
1989: U-Pb isotopic analysis of carbonate cements. Evidence for differential element mobility Canada/Mineral. Assoc. of Canada Program w p.A78.

Changkakoti, A., Morton, R.D. and Gray, J.
1986: Hydrothermal environments during the genes Territories of Canada: evidence from fluid inclus 69.

Hildebrand, R.S.
1984: Geology, Echo Bay - MacAlpine Channel area: (

Hildebrand, R.S.
1986: Kiruna-type deposits: their origin and relations in the Great Bear Magmatic Zone, Northwest C

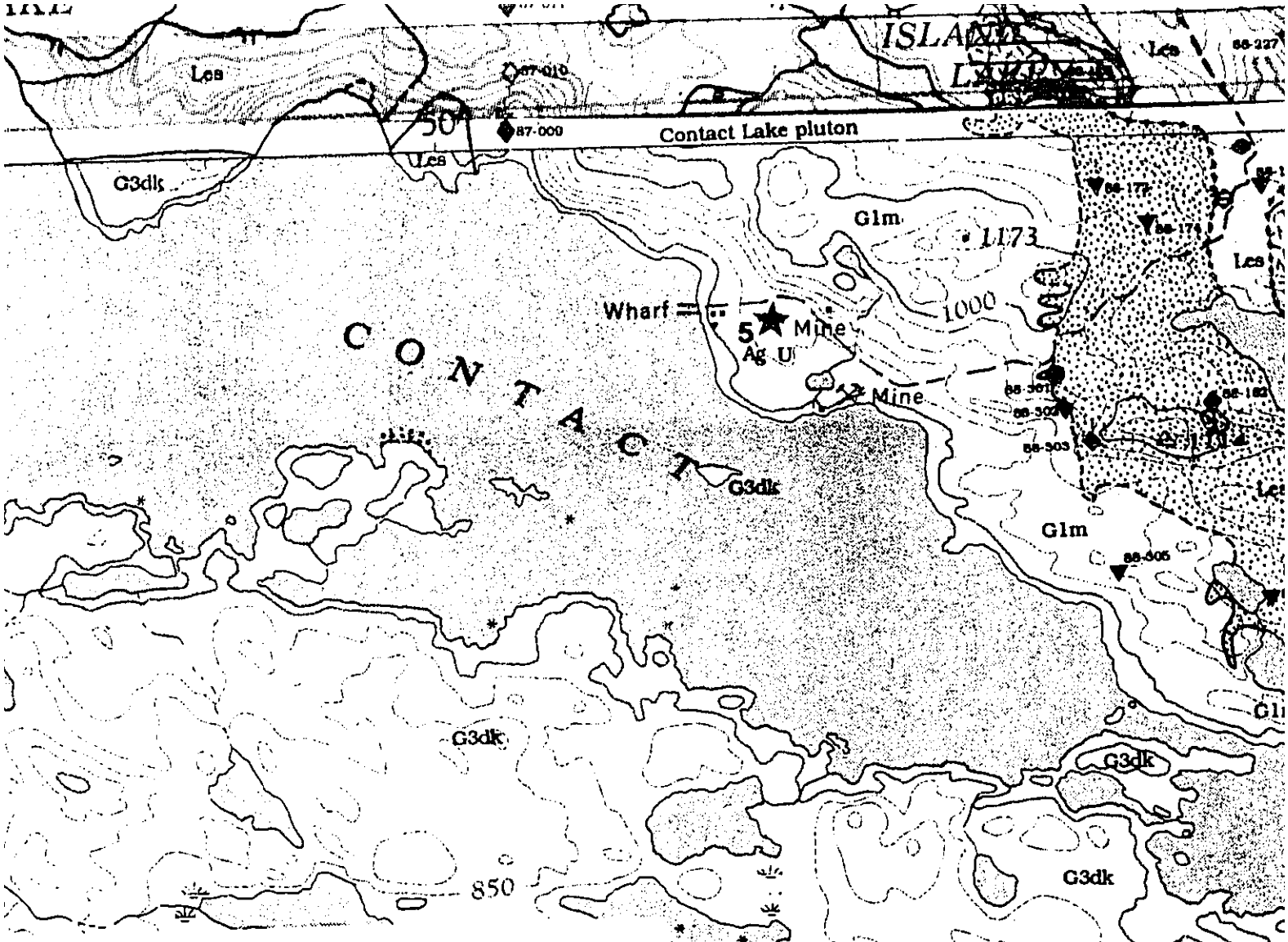

ERENCES

Proterozoic Wopmay Orogen, N.W.T., Canada: an .D. thesis, University of Kansas, Lawrence, 148 p.

cements, early Proterozoic Rocknest formation: mobility during diagenesis; Geol. Assoc. of Program with Abstracts, v. 14, Montreal, 1989,

the genesis of silver deposits in the Northwest fluid inclusions; Mineralium Deposita, v. 21, p. 63-

nnel area: Geological Survey of Canada, Map 1546A.

nd relationship to intermediate subvolcanic plutons Northwest Canada; Economic Geology, v. 81, p. 640-

data by N. C. Reardon, 1989-90. Field work wa
Territories - Canada Mineral Development Agr
Canada, project 860002 (R. S. Hildebrand). Crit
greatly improved its content and form.

Scale 1:25 0

1 0 1

Kilometers

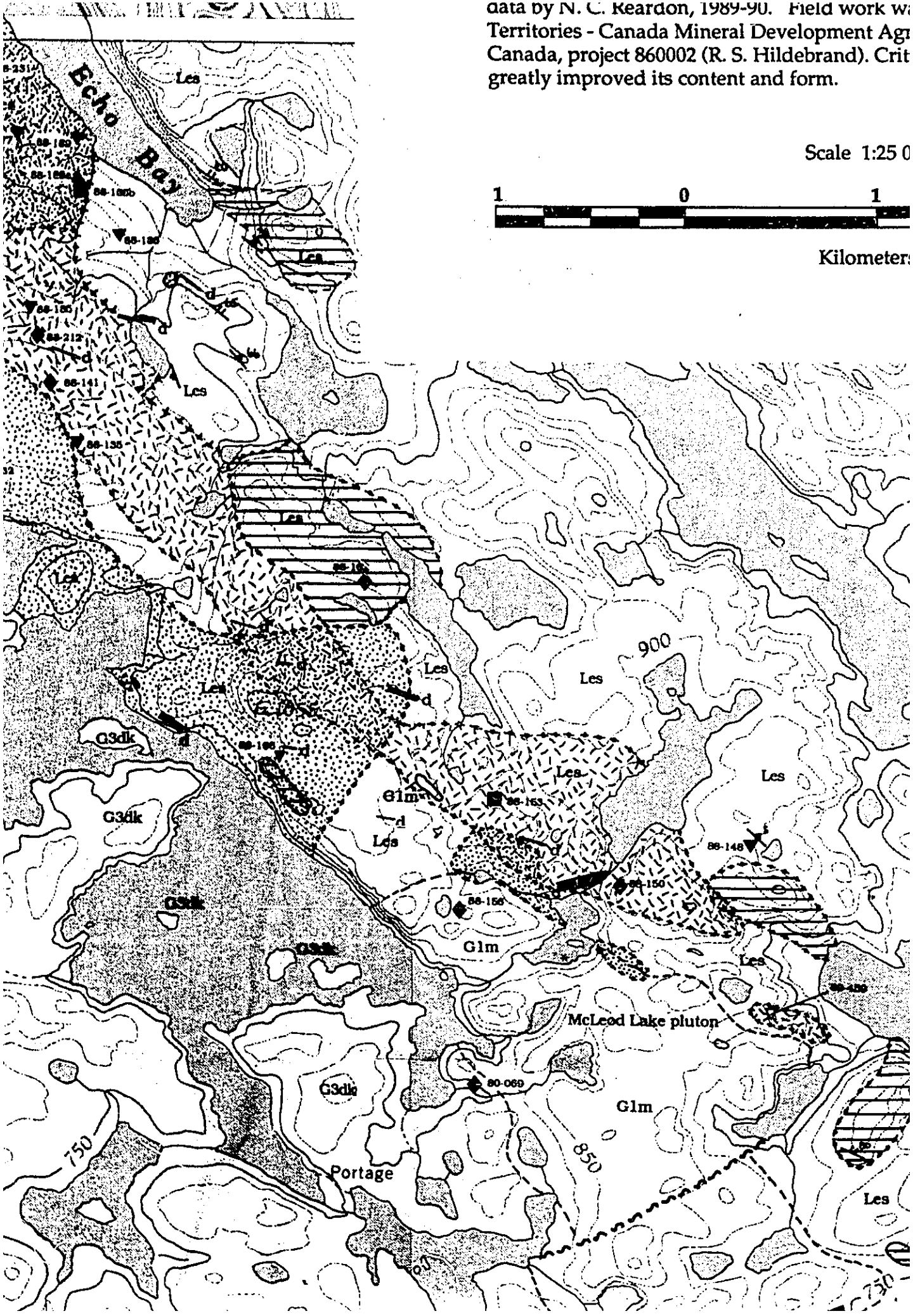

Reardon, 1989-90. Field work was supported by the Northwest Canada Mineral Development Agreement and the Geological Survey of ect 860002 (R. S. Hildebrand). Critical review of the map by J.B. Henderson oved its content and form.

66° 00'

Scale 1:25 000

0 1 2 3

Kilometers

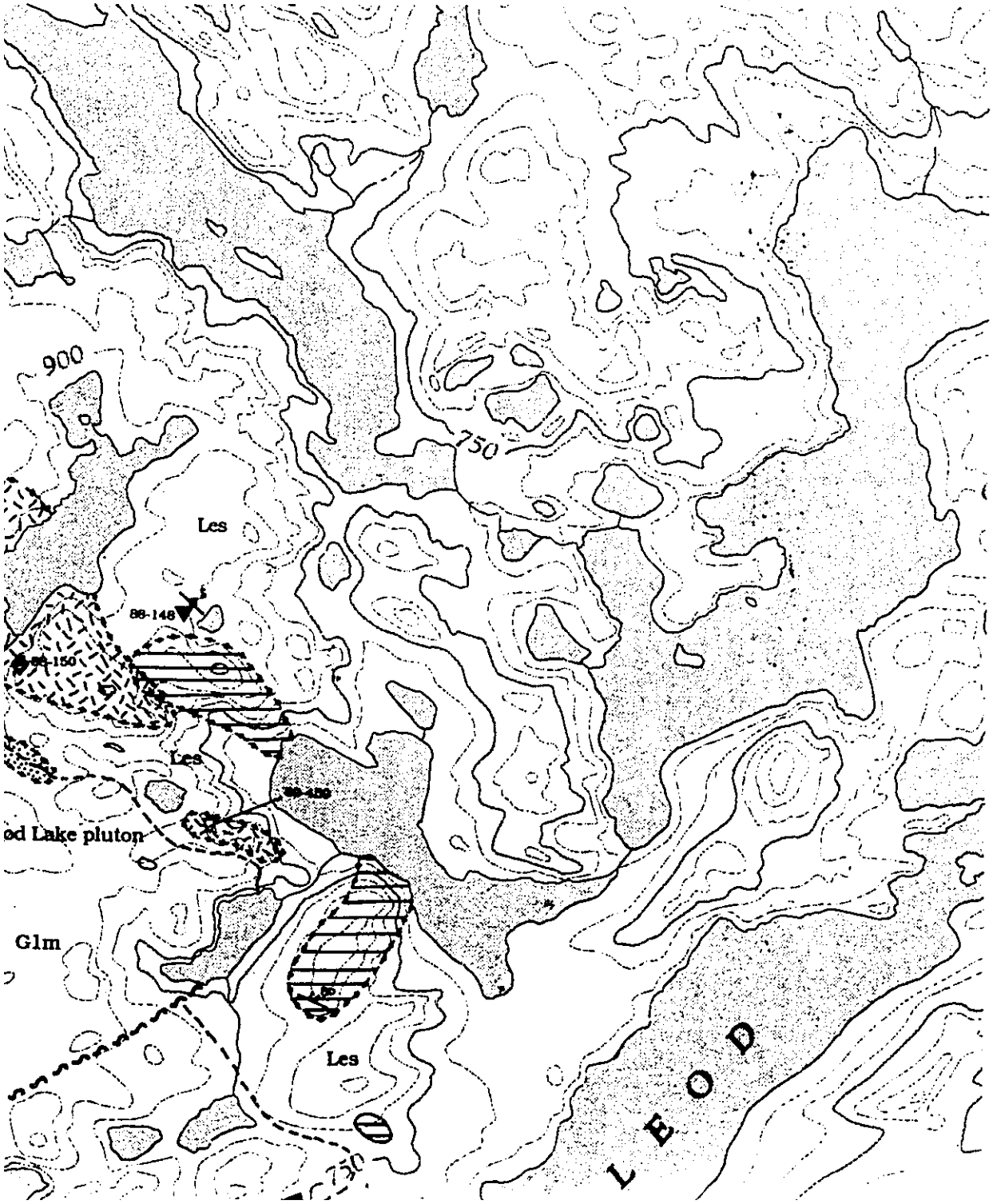

apatite-actinolite (MAA), and 3) an outer zone of disseminated sulphides. The zones overlap spatially, and geologic and petrographic evidence show that temporally, the albite zone was formed first, followed by MAA and finally pyrite.

Albite zone

The albite zone is characterized by pervasive replacement of the host rock by very fine- to coarse-grained albite; albitized rocks are red-brown to pale pink. Extensively altered rocks, found in close proximity to the plutons, are white both on the fresh and weathered surfaces. Albitized rocks generally occur within 100 m of the pluton roofs, but extend up to 1 km above the plutons locally. Altered rocks also occur locally within and below the plutons. Veins and pods of albite are present in some highly altered areas. The albite zone commonly overlaps with the magnetite-apatite-actinolite and pyrite zones.

Magnetite-apatite-actinolite zone

The magnetite-apatite-actinolite (MAA) zone is defined by the presence of at least two of the three minerals: magnetite, apatite or actinolite. These minerals also occur as disseminated crystals, veins, pods, and breccias above the plutons, and locally, within and below them.

The mode of occurrence of magnetite, apatite and actinolite varies with original lithology. In andesitic lava flows, these minerals are present disseminated throughout the rock, and constitute up to 35% of the rock. In sedimentary rocks, beds are preferentially replaced by albite, actinolite, or magnetite. Limy beds at Port Radium are replaced by massive magnetite. Locally, pervasively altered andesite flows and sedimentary rocks are cut by veins of magnetite-apatite-actinolite or magnetite-actinolite. The most common assemblages of these alteration minerals in both replacement and veins/pods, in order of abundance, are: 1) actinolite + magnetite; 2) actinolite + apatite; and 3) magnetite + apatite + actinolite. Locally, near their contacts, the plutons are cut by veins of actinolite or actinolite-apatite.

Veins of MAA up to 80 cm wide are discontinuous and generally exposed along strike for less than 2 m. The veins have various orientations, but generally strike E-W and N-S and are steeply dipping. Pods are generally less than 1 cm in diameter, but many are up to several decimetres across. Actinolite is the most abundant mineral and occurs as laths to 5 cm in length. Magnetite occurs as sub- to euhedral crystals up to 8 cm across, but generally less than 1 cm.

Hydrothermal breccias, typically present near pluton contacts, comprise angular to sub-rounded fragments of country rock up to 1 m in diameter in a matrix of medium- to coarse-grained magnetite (± pyrite, chalcopyrite), actinolite, apatite, epidote and albite. Actinolite-rich breccias, which occur as pink (albitized?) fragments in a dark, actinolite-magnetite matrix, are found near pluton contacts locally.

Pyrite zone

The pyrite zone is characterized by the presence of disseminated pyrite crystals or pods up to several centimeters in diameter which form visible rusty patches on weathered outcrop surfaces, or extensive gossans where pyrite is locally abundant. Veins of pyrite to 1 cm wide occur locally. The pyrite zone occurs principally above the plutons, but locally within and below them. The zone is irregular and discontinuous, and is generally found at some distance above the roofs of the plutons. However, one gossan, more than 1 km across, is present directly above the northern portion of the Glacier Lake pluton. The pyrite zone commonly overlaps the MAA zone.

55'

A chalcopyrite zone east of Port Radium is characterized by the presence of finely-disseminated chalcopyrite within the groundmass and within amygdules in andesitic lava flows. The zone may represent a subzone of the pyrite zone, and is subparallel to stratigraphy. Within both zones, higher concentrations of pyrite and chalcopyrite are present in sedimentary rocks than in andesites.

118° 10'

05'

Contribution to Canada-Northwest Territories Mineral Development Subsidiary Agreement 1987-91, under the Economic Development Agreement.

evolved meteoric water cannot be ruled out. Pyrite and chalcopyrite from gossans, pods and within the pyrite and chalcopyrite zones were analyzed for $\delta^{34}S$. Most of the $\delta^{34}S$ data for and chalcopyrite at Echo Bay are typical for igneous rocks and are consistent with a mag source for the sulphur.

Quartz-carbonate veins

Knowledge of the fluids which formed the mineralized (pitchblende, native Ag, arsenide) and unmineralized quartz-carbonate veins in the Echo Bay area is necessary in or assess the influence of these fluids on the rocks in the area. Estimation of the effe overprinting during the formation of quartz-carbonate veins is difficult, since fluids respo for formation of the quartz veins ranged from lighter than, to the same in $\delta^{18}O$ (from +9.1 +0.47‰; Changkakoti et al., 1986) as the fluids which formed the MAA zone alter However, no large-scale zoning of $\delta^{18}O$ is evident in the wall rocks surrounding the veins, and $\delta^{13}C$ of carbonate minerals from unmineralized quartz-carbonate veins in the Echo Ba are similar to those of carbonate minerals from the mineralized veins.

Summary

All of the Mystery Island intrusive suite have zoned alteration haloes comprised of zones: 1) an inner zone of albite; 2) an intermediate zone of magnetite-apatite-actinolite; a an outer zone of disseminated sulphides. The zones overlap spatially, and geologic petrographic evidence show that temporally, the albite zone was formed first, followed by and finally pyrite.

Whole-rock geochemistry of the altered wall rocks above the plutons shows that correlates negatively with SiO_2, K_2O, Ba, and Rb for altered andesitic lava flows withi alteration haloes of some of the plutons. Gd, Dy, Be, Yb, Y, Sm, MgO and Na_2O con negatively with K_2O; Ba and Rb correlate positively with K_2O. Na and K vary antithetically i plutons, but other elements do not show regular variations with Na or K. The plutons ar metasomatized and K-metasomatized locally.

Whole-rock $\delta^{18}O$ and δD of altered rocks associated with the plutons of the Mystery I intrusive suite are not zoned, and range from +5.7‰ to +12.3‰ and -70‰ to -57‰ respec for the plutons; and from +5.3‰ to +11.7‰ and -92‰ to -56‰ respectively for altered and lavas and their cogenetic andesitic porphyries and volcaniclastic rocks. Most $\delta^{18}O$ and δ higher than +6‰ and -70‰, respectively, consistent with alteration under low water to ratios by magmatic fluids. Lower values suggest involvement of a minor component of ev surface water. Based on stable isotopic data from whole-rock samples and mineral separate magnetite-apatite-actinolite deposits formed from fluids of a dominantly magmatic o having $\delta^{18}O$ of about +5.0‰ to +12.0‰ and δD of -60‰ to -30‰.

Overall, the formation of magnetite-apatite-actinolite veins, pervasive replacement of by albite and magnetite-apatite-actinolite, and hydrothermal brecciation by magmatic flu consistent with geologic and isotopic data. Thus, it is inferred that these deposits form replacement in a hydrothermal system dominated by magmatic fluids exsolved by co epizonal plutons of the Mystery Island intrusive suite.

hblende, native Ag, Ni-Co
area is necessary in order to
stimation of the effects of
ilt, since fluids responsible
ne in $\delta^{18}O$ (from +9.12‰ to
the MAA zone alteration.
urrounding the veins. $\delta^{18}O$
veins in the Echo Bay area

haloes comprised of three
te-apatite-actinolite; and 3)
patially, and geologic and
med first, followed by MAA

plutons shows that Na_2O
sitic lava flows within the
, MgO and Na_2O correlate
K vary antithetically in the
or K. The plutons are Na-

itons of the Mystery Island
-70‰ to -57‰ respectively
ectively for altered andesitic
cks. Most $\delta^{18}O$ and δD are
n under low water to rock
inor component of evolved
and mineral separates, the
ninantly magmatic origin,

asive replacement of rocks
ition by magmatic fluids is
t these deposits formed by
fluids exsolved by cooling

example of rapid crustal evolution; Ph.D. thesis, University of Kansas

Bowring, S.A., Housh, T. and Grotzinger, J.P.
1989: U-Pb isotopic analysis of carbonate cements, early Proterozoic F Evidence for differential element mobility during diagenesis Canada/Mineral. Assoc. of Canada Program with Abstracts, v. 1 p.A78.

Changkakoti, A., Morton, R.D. and Gray, J.
1986: Hydrothermal environments during the genesis of silver deposit Territories of Canada: evidence from fluid inclusions; Mineralium De 69.

Hildebrand, R.S.
1984: Geology, Echo Bay - MacAlpine Channel area: Geological Survey of (

Hildebrand, R.S.
1986: Kiruna-type deposits: their origin and relationship to intermediate in the Great Bear Magmatic Zone, Northwest Canada; Economic Ge 659.

Hoffman, P.F.
1984: Geology of the northern internides of Wopmay orogen, District of M Territories; Geological Survey of Canada Map 1576A, scale 1:250 000

Reardon, N.C.
1992a: Altered rocks and magnetite-apatite-actinolite deposits associate Island intrusive suite, Echo Bay, Northwest Territories; Canada - N Mineral Development Agreement Final Report, Project C1.1.5.

Reardon, N.C.
1992b: Magmatic - hydrothermal alteration and magnetite-apatite-actin Bay, Northwset Territories; M.Sc. thesis, University of Ottawa, Ottaw

Streckeisen, A.L.
1973: Plutonic rocks. Classification and nomenclature recommer subcommission on the systematics of igneous rocks; Geotimes, Octob

Taylor, B.E.
1986: Magmatic volatiles: Isotopic variation of C, H, and S; in Stabl Temperature Geological Processes, eds. J.W. Valley, H.P. Taylor, Jr., in Mineralogy, v. 16, p. 185-225.

y of Kansas, Lawrence, 148 p.

roterozoic Rocknest formation:
diagenesis; Geol. Assoc. of
stracts, v. 14, Montreal, 1989,

ver deposits in the Northwest
neralium Deposita, v. 21, p. 63-

l Survey of Canada, Map 1546A.

termediate subvolcanic plutons
conomic Geology, v. 81, p. 640-

District of Mackenzie, Northwest
e 1:250 000.

s associated with the Mystery
Canada - Northewest Territories
1.1.5.

patite-actinolite deposits, Echo
tawa, Ottawa.

recommended by the IUGS
mes, October, 1973, p.26-30.

S; in Stable Isotopes in High
Taylor, Jr., J.R. O'Neil, Reviews

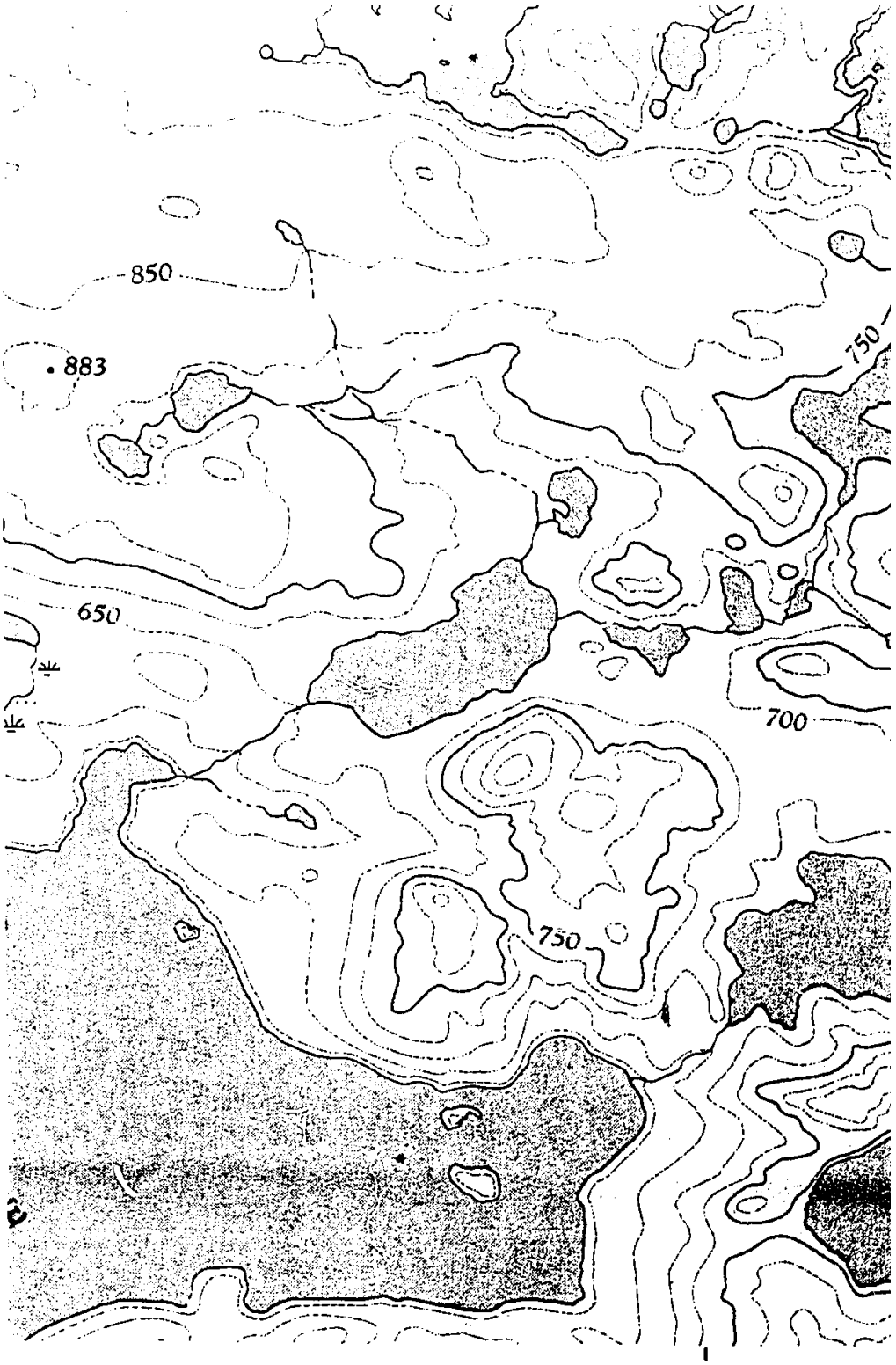

50'

45'


G3dk
G3dk
G1m
McLeod Lake pluton
80-069
G3dk
G1m
750
850
Portage
G1m
G3dk
G3dk
Portage
700
800
Portage
750
Les
G1m
G3dk
650

45'

40'

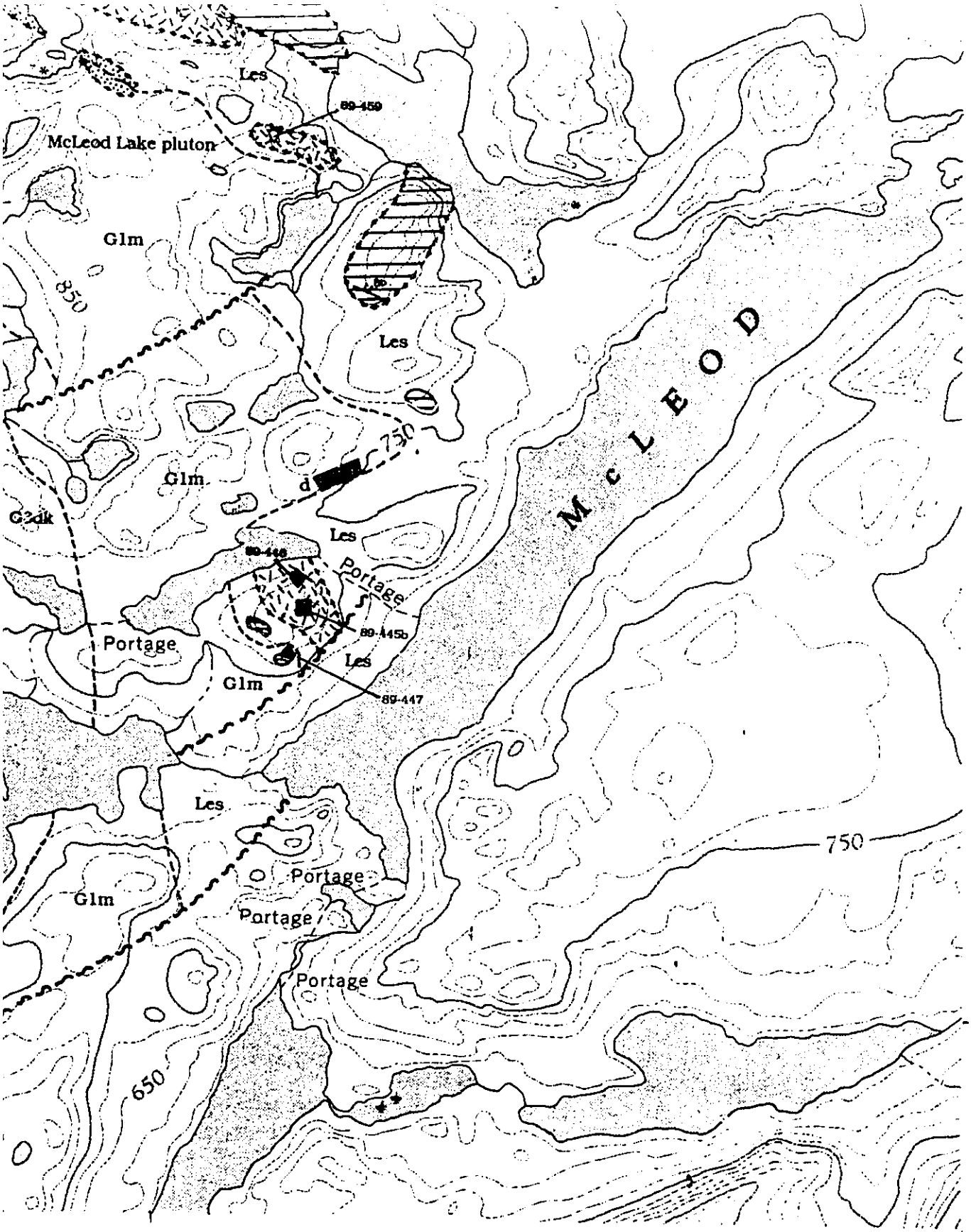
Les
89-459
McLeod Lake pluton
Glm
850
Les
750
Glm
d
Les
89-446
Portage
89-445b
Portage
Les
Glm
89-447
Les
Portage
Glm
Portage
Portage
650
M c L E O D
750
55'
40'
117°35'

A chalcopyrite zone east of Port Radium is characterized by the preser disseminated chalcopyrite within the groundmass and within amygdules in andesi The zone may represent a subzone of the pyrite zone, and is subparallel to stratigr both zones, higher concentrations of pyrite and chalcopyrite are present in sedin than in andesites.

118° 10'

05'

Contribution to Canada-Northwest Territories Mineral Development Subsidiary Agreement 1987-91, under the Economic Development Agreement. Project funded by the Geological Survey of Canada

Contribution à l'Entente auxiliaire Canada-Territoires du Nord-Ouest d'exploitation minérale 1987-1991, dans le cadre de l'Entente de développement économique. Projet subventionné par la Commission géologique du Canada

Northwest Territories Energy, Mines and Petroleum Resources

Energy, Mines and Resources Canada

Énergie, Mines et Ressources Canada

Canada

he presence of finely-
in andesitic lava flows.
to stratigraphy. Within
it in sedimentary rocks

05'

118° 00'

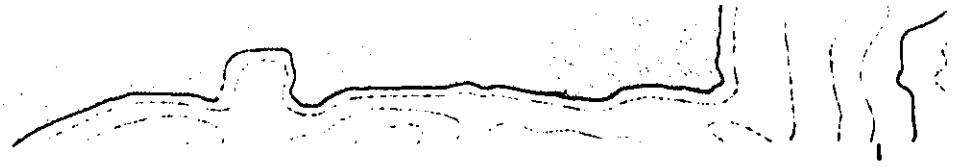

50'

45'

45'

40'

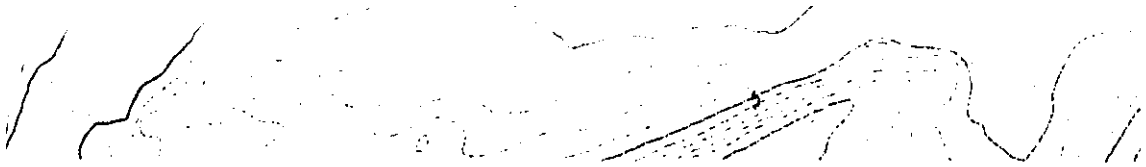

)'

117°35'

OPEN FILE
DOSSIER PUBLIC

2507

GEOLOGICAL SURVEY OF CANADA
COMMISSION GEOLOGIQUE DU CANADA
OTTAWA

1992